2025년
대한수부외과학회
추계학술대회

역경에도 손을 맞잡고
Against All Odds, Hand in Hand

일시: 2025년 11월 1일 (토)

장소: 연세대학교 세브란스병원 6층 은명대강당
및 종합관 보건대학원 강의실 331호, 337호

평점: 6점

Abstract book

대한수부외과학회
KOREAN SOCIETY FOR SURGERY OF THE HAND

Johnson&Johnson
MedTech

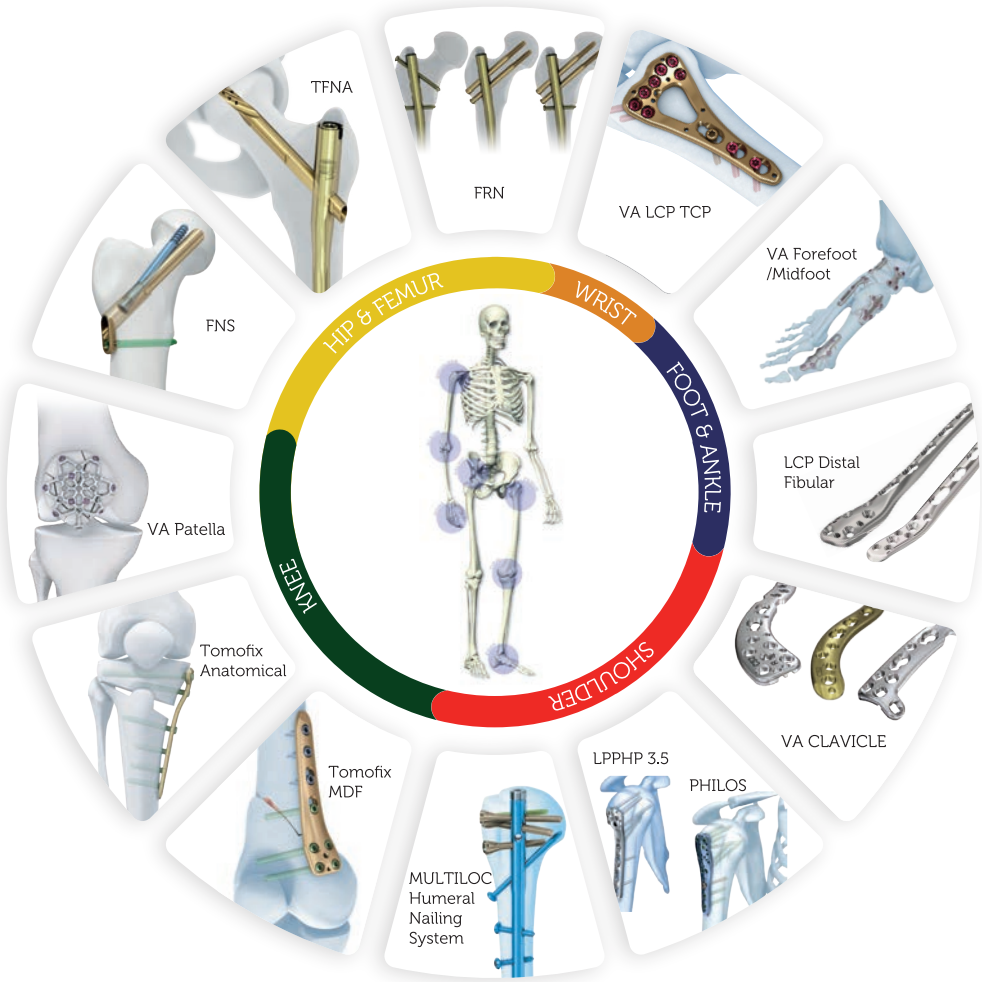

DISCOVER J&J MedTech **TOTAL TRAUMA** SOLUTIONS

Bone Substitution Material

HA rhBMP-2

Synergistic Effect of rhBMP-2+HA

A synthetic bone graft composed of hydroxyapatite ceramic and recombinant human BMP-2 (Bone Morphogenetic Protein), a genetically engineered protein that stimulates bone formation.

COPY-25005-S1

SK 케미칼
Life Science Biz.

beyond the Best

조인스®

연골보호효과 확인 [1, i]

장기투여 효과 확인 [1,2, ii]

안전성 프로파일 확인 [1,2]

제품요약정보[3]

전문의약품

【제품명】 조인스정200mg **【원료약품 및 그 분량】** 이 약 1정 중 조인스정 유효성분: 위령선·괄루근·하고초30%에탄올건조엑스(40→1)(별규) …200mg **【효능·효과】** 골관절증(퇴행관절질환), 류마티스관절염의 증상 완화 **【용법·용량】** 성인 : 1회 1정을 1일 3회 경구투여한다. 증상에 따라 적절히 증감한다. **【사용상의 주의사항】** 1. 다음 환자에는 신중히 투여할 것. 1) 감염상태 또는 감염의 원인이 있는 환자(감염에 대한 자체 저항력이 감소될 가능성이 있음을 고려해야 하며, 이런 경우에는 감염의 진행을 억제하는 처치를 취해야 한다.) 2) 임부 또는 임신하고 있을 가능성이 있는 여성 및 수유부 (후략) **【제조자】** 에스케이케미칼(주) 충청북도 청주시 흥덕구 산단로 149 **【판매자】** 에스케이케미칼㈜ 경기도 성남시 분당구 판교로 310

2011. 3. 21. 개정

※처방하시기 전 제품설명서 전문을 참고하십시오. 최신 허가사항에 대한 정보는 '식품의약품 안전처 의약품안전나라 (https://nedrug.mfds.go.kr/index)'에서 확인할 수 있습니다.

References 1. Joong Il Kim et al, Efficacy of JOINS on Cartilage Protection in Knee Osteoarthritis: Prospective Randomized Controlled Trial, knee surg relat res, 2017 sep 1;29(3):217–224. **2.** 조인스정 의약품 재심사 보고서 (2001.7.10~2005.7.9), Data on file SK 케미칼, [Updated 2005.10.07] **3.** 조인스정 허가정보, 의약품안전나라 [Cited 2023.01.20] Available from: https://nedrug.mfds.go.kr/

i) [조인스정의 4상 임상연구] 1년(시험 연장 참여 동의자의 경우 2년)의 RCT 연구에서 무릎 골관절염 환자 76명을 대상으로 MRI를 이용하여 조인스정과 위약의 연골보호효과를 비교하였음.
ii) 조인스정의 4상 임상 결과 상 2년 장기투여 대상자를, 4년간의 시판후 조사결과 상 6개월 이상 장기투여(184명, 전체의 3.09%) 대상자 포함하였음.

JNS-HA11-202301-01

SK 케미칼
Life Science Biz. 경기도 성남시 분당구 판교로 310(삼평동) Tel 080-021-3131 www.skchemicals.com/ls

JOINS®

나은필병원

THE NAEUN PIL HOSPITAL

나은필병원 전문센터 수부·정형·관절 중점 진료 병원

- 척추센터
- 어깨·상지센터
- 무릎관절센터
- 족부·족관절센터
- 수부·미세재건센터
- 골절·외상센터
- 통증·재활센터

보건복지부 인증 의료기관

보건복지부 인증 수지접합 전문병원

"신뢰와 더 나은 내일을 약속하는 나은필병원 입니다."

- 170병상 규모
- 24시간 **응급실** 운영

오시는 길

천안 고속터미널(신세계백화점) 앞

충남 천안시 동남구 만남로 64 나은필병원

대표번호 041-417-0001

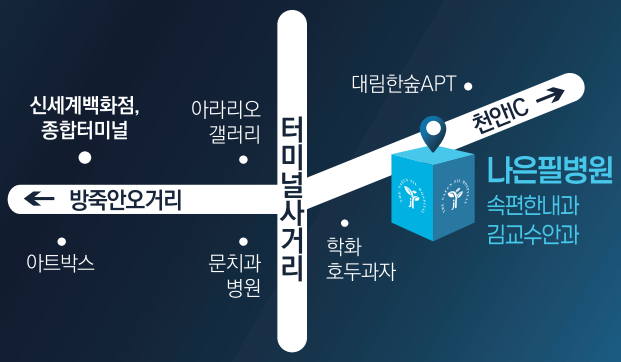

Globally renowned cohesive conforming bandage products

Mollelast® haft latex-free & Haftelast® latex-free.

- easy to apply, comfortable to wear
- air permeable
- reliably stays in place
- high quality, stable selvedges
- free of natural rubber latex

www.Lohmann-Rauscher.com

건강:사랑

한결같이 지켜온 믿음과 신뢰!
변함없는 사랑으로 지역민의 건강에
최선을 다하겠습니다.

건강재건, 행복재건, 미래재건

건강재건, 행복재건, 미래재건

MS재건병원

손 | 발 | 어깨 | 목 | 허리 | 골절 | 외상

개원 18주년
지역민의 건강과 함께 합니다!

24시간 응급진료

053.653.0119
대구시 중구 동덕로 194

동인네거리

We Have The Answer

114, Seonbugwangjang 1-ro, Danwon-gu, Ansan-si, Gyeonggi-do, Korea | Tel : +82-31-402-0114 | Fax:+82-31-414-1903
http://www.du-son.com

Certified Hand Surgery Specialist Training Hospital

STAFF

Jong-Ick Whang
MD-PhD
Hospital Director
Department of
Plastic Surgery2

Hyeung Gyo Seo

Chief of Medical Staff
Department of
Plastic Surgery1

Won Gyu Yang

Deputy Chief of Medical Staff
Department of
Orthopedic Surgery1

Yun Seop Kim

Department of
Plastic Surgery3

Hye Jung Jeon
MD-PhD
Director
Center for Radiology

SERVICES

Hand Surgery & Plastic Surgery

<Reconstructive Surgery >
Institute of Micro & Hand Surgery

◎ Hand reconstructive surgery and micro surgery
Hand replantation, Hand trauma, Post-traumatic deformity
Contracture and scar, Carpal tunnel Syndrom, tenosynovitis

◎ Congenital Hand
Syndactyly, polydactyly, Constriction band syndrome
Symphalangism, Hypoplastic hand

◎ Facial reconstructive surgery
Facial contouring, Facial bone fracture, Facial rejuvcnation

<Cosmetic Surgery Clinic>

◎ Cosmetic surgery
◎ Laser Clinic

Orthopedic Surgery

◎ Joint Clinic
Arthroscopy and Arthroplasty
Degenerative arthritis and Rheumatoid arthritis
◎ Musculoskeletal and spine Clinic
◎ Fracture, dislocation and traumatology

Radiology

Health screening program
Diagnostic medicine

DUSON offers a warm touch that heals even the wounded heart

Institute of Micro & Hand Surgery

DUSON HOSPITAL

수지접합전문병원

서부산센텀병원

부산·울산·경남 유일 **수지접합전문병원 지정**

진료과 소개

정형외과	신경외과	내과	가정의학과
재활의학과	영상의학과	마취통증의학과	

전문진료센터

수부미세수술연구소	인공관절센터	골절외상센터	척추센터
소화기센터	종합건강증진센터	응급실 ☎ 051-329-3119	

- 간병부담을 줄이는 **간호·간병 통합서비스**
- 편의성을 높이는 **원스톱 시스템**
- 만족도 높이는 **전문진료센터**
- 감염을 줄이는 **무균 수술실**
- 정확한 진단을 위한 **최첨단 의료장비**

지역주민들이 믿고 의지할 수 있는 **든든한 버팀목!**

센텀종합병원

진료과 소개

정형외과	간담도췌장외과	대장항문외과	신경외과	신경과
유방외과	간내과	소화기내과	심장내과	신장내과
소아청소년과	치과	비뇨의학과	정신건강의학과	호흡기내과
마취통증의학과	재활의학과	영상의학과	진단검사의학과	응급의학과
성형외과	류마티스내과	산부인과	핵의학과	
인터벤션 영상의학과				

전문진료센터

관절센터	척추센터	간담췌외과 및 이식수술센터	
뇌신경/뇌혈관센터	심혈관센터	간센터	인공신장실
소화기내시경센터	종합건강증진센터	복강경수술센터	
췌장담도센터	응급실 ☎ 051-750-5119		

정확한 진단과 질환별·부위별 **진료, 수술 원스톱 시스템**

서부산센텀병원
WEST BUSAN CENTUM HOSPITAL
☎ 대표전화 1644-5520
지하철 2·3호선 수영역 6번, 8 번 출구

센텀종합병원
CENTUM GENERAL HOSPITAL
☎ 대표전화 1644-5520
지하철 2·3호선 수영역 6번, 8 번 출구

의료법인 센텀의료재단
CENTUM MEDICAL FOUNDATION

센텀종합병원 CENTUM GENERAL HOSPITAL | 서부산센텀병원 WEST BUSAN CENTUM HOSPITAL

바른생각을 가진 사람들의 바른병원

서울대정병원

무릎, 어깨 척추, 수부, 족부

서울대출신 정형외과전문의 분과별 진료

철저한 **감염예방 시스템**

외상 관절 척추

대학병원급 최첨단 시설 (클린룸, MRI CT, 수술현미경)

수지접합, 수부전문의 상주

세계최고를 지향 연구하는 병원 (SCI 논문 저자)

365일, 정형외과 전문의 분과별 진료

무릎 / 어깨 / 척추 / 수부 / 족부 / 재활

NAVER 서울대정병원 검색

주 소 : 충남 천안시 서북구 불당33길 18 (불당동 1620)

대표번호 : 041) 415 - 0001 **팩 스** : 041) 415 - 0049

손, 발이 아프면

튼튼한 관절을
위한다면

허리, 목이 아프면

전주 정형외과는

실력있고 경험많은
병원을 찾는다면

오랜시간 쌓아온 신뢰, 역시 수병원 입니다

- 수부외과 세부전문의 맞춤진료
- 수부, 족부, 모든 관절
- 150만건 이상 외래진료
- 10만건 이상 수술
- 3.0T MRI, 128slice CT

전북 100병상 이상 병원급 의료기관 최초
보건복지부 인증의료기관

수병원
SOO HOSPITAL

전주 신시가지(서원로 63)

홈페이지 : www.soohospital.com

진료 문의 063)251-7200

Smith+Nephew

START
+ LIFE CARE
DRESSING

ALLEVYN◇ LIFE

Foam Dressing

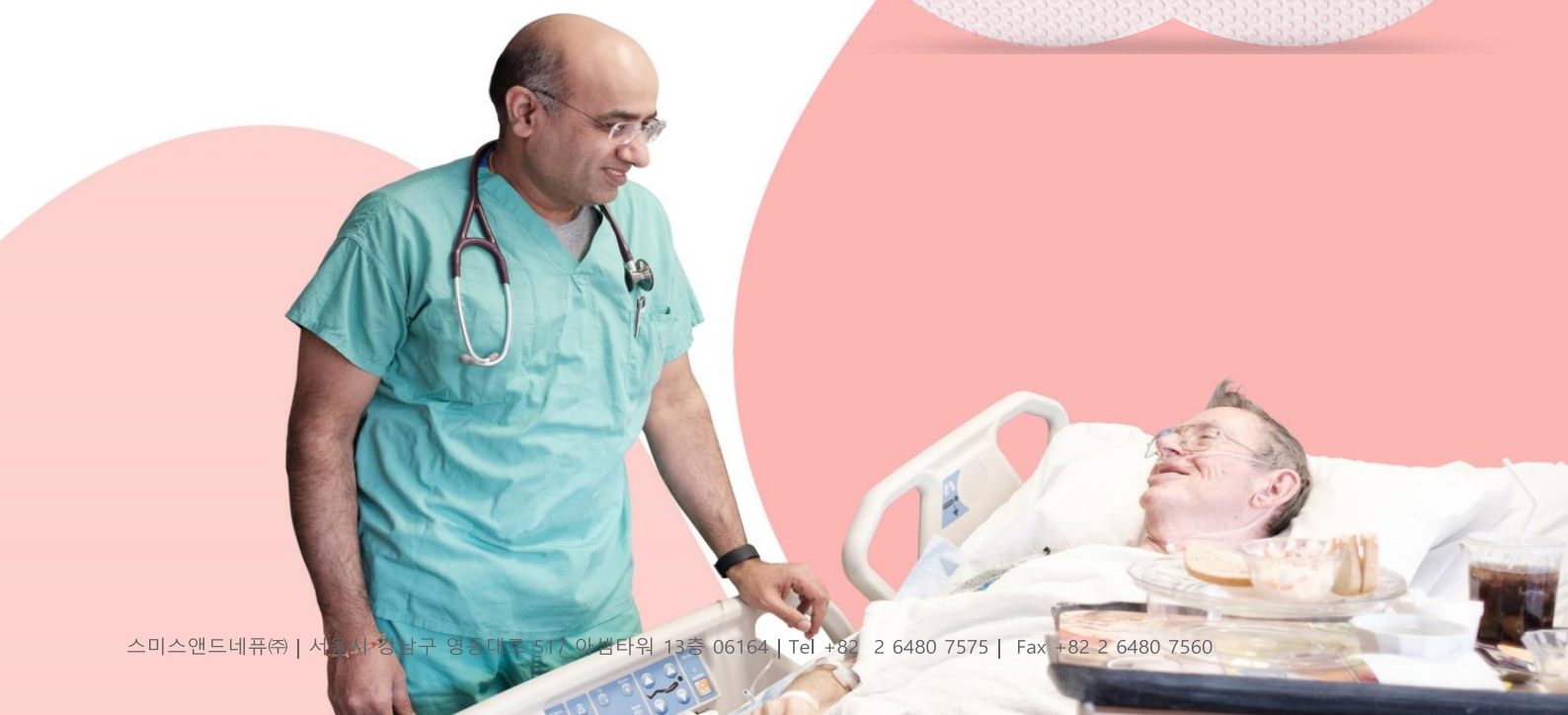

스미스앤드네퓨㈜ | 서울시 강남구 영동대로 517, 아셈타워 13층 06164 | Tel +82 2 6480 7575 | Fax +82 2 6480 7560

YEIN 예인메딕스

고보습 식물성의 부드러운 제모크림

BYE.MO

치오글리콜산 80%

쉐어버터
수분성 지질 성분으로
가벼운 발림성

코코넛오일
고보습으로
부드러운 촉감

알로에베라
피부자극을 최소화

쉽고 빠른 제모 | 자극을 최소화한 제모

세균 감염으로부터 보호가 가능한 제모

∴ 수술 전에 바이모크림

보건복지부지정 관절전문병원 SPECIALTY HOSPITAL OF KOREA

보건복지부지정 수지접합 전문병원 SPECIALTY HOSPITAL OF KOREA

보건복지부 지정
관절·수지접합 전문병원 제5기 지정

수부에서 시작하여 정형외과 세분화를 추구합니다

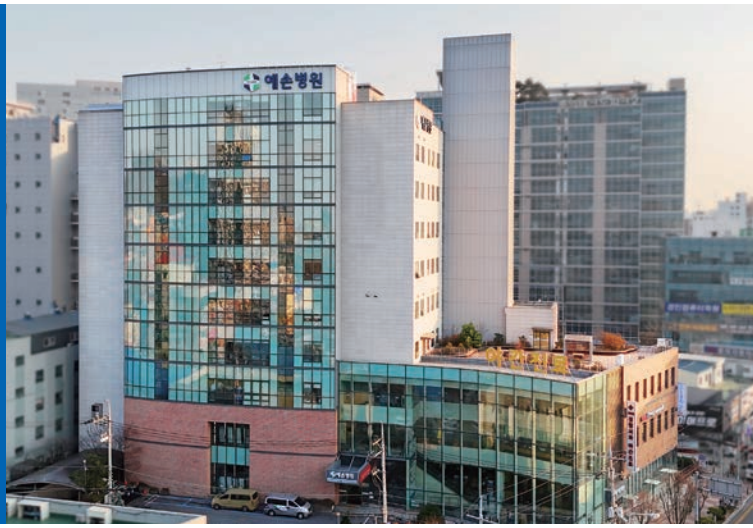

수부센터


수부세부전문의 **백구현 명예원장**


수부세부전문의 **김진호 대표원장**


수부세부전문의 **이충훈 원장**


수부세부전문의 **이재훈 원장**


수부세부전문의 **김홍균 원장**


수부세부전문의 **박진성 원장**


수부세부전문의 **이정석 원장**


수부세부전문의 **이준하 원장**


정형외과전문의 **마상범 원장**

전문 의료진 36명의 진료협진 시스템

[정형외과 · 신경외과 24명]

수부 **9명** 관절 **8명**

척추 **4명** 족부 **3명**

첨단의료장비

MRI 3대(3.0T 2대, 1.5T 1대) / 64채널 CT
C-arm / Microscope / 혈류검사기
고압산소 치료 멀티 챔버 / 뇌혈류초음파(TCD)
로봇인공관절(MAKO) / 플라즈마소독기
무균수술시스템 / PACS / DITI / BMD 등

홈페이지 QR 유튜브 QR 카카오플러스 QR

내과 | 재활의학과 | 신경과 | 영상의학과 | 마취통증의학과

365일, 24시간 정형외과 전문의 상주

1666-7582 | 경기도 부천시 원미구 부천로 206

www.yesonhospital.com

STRENGTHEN BONES WITH PROLIA®

10년 간의 골절 위험 감소와 골밀도 증가를 입증한 프롤리아®로 지속 치료해 주세요![1-3]

우수한 골밀도 증가 효과[4,5]

주요 부위에서 BP 대비 우수한 골밀도 증가 효과를 보였습니다.

골절 위험 감소 효과[3]

10년까지 지속 치료 시 추가적인 척추 및 비척추 골절 감소 효과를 보였습니다.

prolia® (denosumab) injection

BP, bisphosphonate.

References 1. Kendler DL, et al. *Adv Ther*. 2022;39(1):58-74. **2.** Ferrari S, et al. *Bone*. 2020 May;134:115287. **3.** Bone HG, et al. *Lancet Diabetes Endocrinol*. 2017;5(7):513-523. **4.** Miller PD, et al. *J Clin Endocrinol Metab*. 2016;101(8):3163-70. **5.** Kendler DL, et al. *J Bone Miner Res*. 2010;25(1):72-81.

Product Information

처방하시기 전 QR 코드 또는 식품의약품안전처 의약품통합정보시스템(https://nedrug.mfds.go.kr)을 통해 상세 제품정보를 참조하시기 바랍니다.

AMGEN 암젠코리아유한회사
서울특별시 중구 을지로5길 19, 20층 Tel. 02-3434-4899

종근당
공동판매원 종근당주식회사
서울특별시 서대문구 충정로 8 (충정로 3가) TEL 02-2194-0300 FAX 02-2194-0369
소비자상담실 : 080-6776-080 (수신자부담) 제품상세정보 : www.ckdpharm.com 참조

KOR-162-0225-80005

Coloplast

Biatain® Silicone 3DFit™ Technology

Biatain® Silicone with its unique 3DFit™ Technology conforms to the wound bed to fill the gap and prevent exudate pooling for optimal healing conditions.

3DFit® Technology

Conform to the Wound Bed

Absorb Vertically

Retain Exudate

NEW

Biatain® Silicone Sacral

Size (cm)	Item no.	EDI CODE
15x19	33404	M3032914

NEW

Biatain® Silicone Multishape

Size (cm)	Item no.	EDI CODE
14x19.5	33408	M3032939

Biatain® Silicone Surgical

Size (cm)	Item no.	EDI CODE
10x20	33400	M3032939
10x30	33401	M3032915

Biatain® Silicone (Standard)

Size (cm)	Item no.	EDI CODE
7.5x7.5	33434	M3032913
10x10	33435	M3032917
12.5x12.5	33436	M3032916
15x15	33437	M3032915
17.5x17.5	33438	M3032914

Biatain® Silicone Lite

Size (cm)	Item no.	EDI CODE
7.5x7.5	33444	M3032918
10x10	33445	M3032919
12.5x12.5	33446	M3032920

Hanmi 한미약품

국내 최초 2g 발매

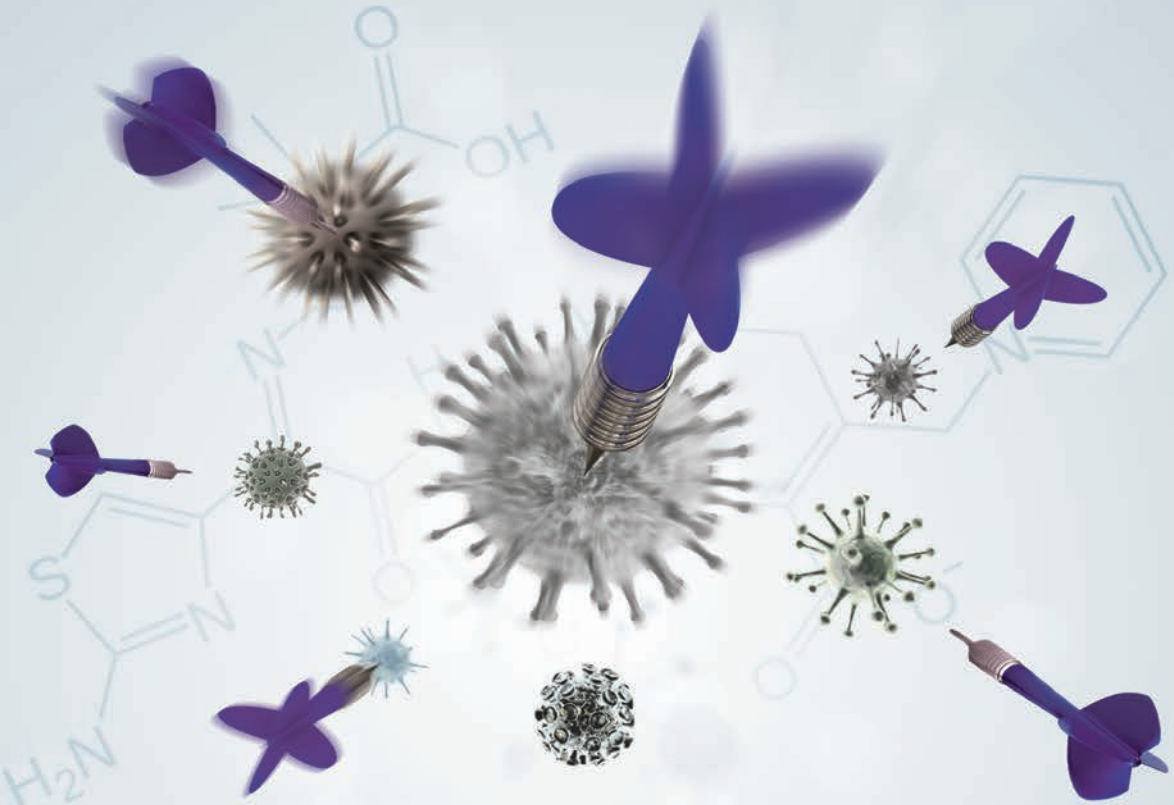

타짐® 주 1g 2g

(Ceftazidime)

- **국내 최초 2g** 규격 추가로 **조제 및 투여 용이성** 향상
- G(+) 및 다제내성균을 포함한 G(−)에도 효과적인 **광범위한 향균스펙트럼**[1)]
- 다른 3세대 세파 항생제에 비해 **유사하거나 낮은 이상반응 발현**[2)]

HM-Design 2102_01

Reference 1) Wust et al. Clin Microbiol Infect. 1999;5:262–269. 2) Gentry LO et al. Pharmacotherapy. Sep–Oct 1985;5(5):254–67.

TAZ-II-2102-01

새손병원

미세접합수술 병원

새손병원은 **환자중심**의
미세접합수술 병원입니다.
지역과 사회에 **환원**하는
새손병원이 되겠습니다.

수부외과·미세수술센터

- 수지접합, 미세현미경수술
- 안면외상 및 골절
- 소아외상 및 골절
- 응급 개방 복합 골절
- 미용수술

진 / 료 / 과 / 목

정형외과
- 팔·다리골절
- 소아 골절
- 골절 외상
- 팔꿈치, 수부 질환
- 족부 질환

성형외과
- 얼굴 상처 봉합
- 코뼈 골절
- 흉터 치료
- 흉터 성형
- 미용 성형
- 미용 부작용 치료

카카오톡채널 연결

홈페이지 연결

전화 문의 042) 535-1900

대전광역시 중구 계룡로 858 (오류동, 서대전사거리)

ONCE A WOUND IS INFECTED,
IT'S TOO LATE TO PREVENT IT

sorbact®
green wound healing

Juthis 서울시 서초구 서운로 8 J TOWER 4층 Tel.02-3461-1002 Fax.02-571-7617

국내 유일, 급여 가능한* 창상 세정제

메디터치®운드 솔루션

- 창상에 형성된 오염 제거
- 창상 보호
- 습윤환경 조성

- 차아염소산 나트륨
- 코카미도프로필 베타인
- 히알루론산
- 알로에 베라

제품 정보

* 2024년 4월 기준

[제품명] 메디터치 운드 솔루션
[품목허가번호] 제인23-4094호
[분류] 2등급 의료기기
[품목명] 국소 하이드로겔 창상피복재 [용량] 250g
[모델명] WCGA-250 (Foam type), WCGB-250 (Spray type)
[EDI code] M3010497

[사용목적] 창상을 보호하고 습윤환경을 조성하며 창상에 형성된 오염 제거를 위해 사용하는 창상피복재
[사용방법] 가) 포장을 개봉하여 제품을 꺼낸 후 보호캡(잠금장치)을 제거합니다. 나) 용기의 노즐을 누르거나 잡아당겨 적용 부위에 겔을 도포합니다. 다) 하루에 1~4번 적용합니다. 라) 필요시 거즈등의 다른 드레싱제와 함께 사용할 수 있습니다.

[사용기한] 제조일로부터 24개월(개봉 후 6개월)
[저장방법] 건조하고 습기가 낮은 곳에 직사광선을 피하여 실온(1~ 30℃에 보관
[판매업자] 일동제약㈜ 경기도 안성시 공단1로 25 www.ildong.com
소비자상담실 080-022-1010
※ 자세한 제품 정보는 식약처 의료기기안심책방(https://emedi.mfds.go.kr) - 알기 쉬운 의료기기 - 정보검색에서 확인할 수 있습니다.

INVITATION

존경하는 대한수부외과학회 회원 여러분

안녕하십니까. 대한수부외과학회 이사장 기세휘 입니다.
최장 기간의 의정 사태로 그 동안 우리가 적응하였던 의료시스템에 많은 변화가 진행 중이며 변화를 앞두고 있습니다. 많은 정보와 새로운 적응이 필요한 시기 입니다.

오는 2025년 11월 1일 제43차 추계학술대회를 개최하게 되었습니다. 깊어가는 가을, 수부외과의 발전을 향한 열정과 지혜를 나누기 위하여 다시 한자리에 모시게 되어 매우 기쁘고 뜻깊게 생각합니다.

이번 학회는 여러 해외의 저명한 수부외과 전문가들을 초청하였고 앞으로는 필수가 되리라고 생각되는 AI를 이용한 연구 및 분석, ROBOT 수술의 수부외과 적용, 수부외과 분야의 최신 지견과 술기, 그리고 연구 성과를 활발히 공유하는 뜻 깊은 자리가 될 것입니다. 학문적인 심화뿐 아니라 임상 현장에서의 다양한 도전과 경험을 함께 나눌 수 있는 교류의 장이 되기를 기대합니다.

우리 학회는 매년 다양한 심포지엄과 워크숍, 전공의 및 세부전문의 교육프로그램, 각 지역의 여러 모임을 지원하고 공유하여 실질적인 학습과 토론을 통하여 교육 기능을 강화하고 학문적 성취를 위하여 노력하여 왔습니다. 또한 해외 travelling fellowship 프로그램과 다양한 해외국가와 교환 프로그램을 통하여 국외 교류의 폭을 넓히고 최신 지식, 기법을 도입하는데 많은 노력을 하였습니다. 항상 그래 왔듯이 이번 학회도 학술적 업적의 증진과 국제적 협력을 강화하고 회원간의 교류를 증진할 기회가 될것입니다.

바쁘신 일정 중에도 많은 선생님들께서 자리를 함께 해 주시어 학술적 논의와 친목의 장을 더욱 풍성하게 만들어 주시기를 바랍니다.

깊어가는 가을, 여러분을 직접 만나 뵙고 뜻깊은 시간을 나눌 수 있기를 고대합니다.

감사합니다.

대한수부외과학회 이사장 **기 세 휘**

존경하는 대한수부외과학회 회원 여러분,

한해의 노력이 결실로 이어지는 가을에 제43차 대한수부외과학회 추계학술대회를 개최하게 되어 진심으로 기쁘게 생각합니다.

이번 추계학술대회는 국내외 저명한 연자들의 강연과 패널 토론을 통해 수부외과 영역의 다양한 질환 및 수부 외상을 학습하고 실제 임상에 적용할 수 있도록 준비 하였습니다.

프로그램에 외국 초청 연자의 강연 및 Traveling Fellow 발표가 포함되어 있으며, 주어진 임상 상황에 접근하는 다양한 의견을 보고 들을 수 있을 것으로 예상 됩니다.

나아가 최근 소개되고 있는 Human–Robot Collaboration 을 주제로 휴머노이드 연구단, 기계공학과, 전자공학과 등 다양한 분야의 연자를 초청하여 현재의 의료 술기 뿐만 아니라 미래의 과학 분야를 앞서 경험할 수 있겠습니다.

바쁘신 일정 가운데 참석해 주신 모든 회원님 그리고 관계자 여러분께 깊은 감사의 말씀을 드리며, 이번 추계학술대회가 학문적 교류와 친목 도모의 장으로 이어질 수 있기를 기원합니다.

마지막으로, 이번 추계학술대회를 준비하기 위해 수고해 주신 학회 임원진과 관계자 여러분께 깊은 감사의 말씀을 드리며, 참석하신 모든 분들의 건강과 발전을 기원 합니다.

감사합니다.

대한수부외과학회 회장 **권 봉 철**

INVITED SPEAKERS

Jeffrey B Friedrich
University of Washington

Chung-Chen Hsu
Chang Gung Memorial Hospital

Osamu Soejima
Fukuoka University

Satoshi Ichihara
Juntendo University

James Chang
Stanford University

Lam Wee Leon
Singapore General Hospital

Yuan-Kun Tu
E-Da Hospital

TRAVELLING FELLOWS

Marvin Man Ting Chung
University of Hong Kong

Cheng-Yu Yin
Taipei Veterans General Hospital

Takuya Tsumura
Kurashiki Central Hospital

Hidemasa Yoneda
Nagoya University Hospital

Eleni Karagergou
Papanikolaou Hospital

Yu-Huan Hsueh (Oscar)
E-Da Hospital / I-Shou University

PROGRAM AT A GLANCE

Time	Room A 6F, Main Building, Eun-myung Grand Auditorium	Room B 3F, Graduate School of Public Health, Room 337	Room C 3F, Graduate School of Public Health, Room 331	Room D 6F, Main Building, Seminar Room 2	VIP Lounge 6F, Main Building, Seminar Room 1
-08:10	Registration				
08:10-08:20	Opening Remarks				
08:20-09:20	**Symposium 1** Toward Human-Robot Collaboration in Microsurgery	**Free Paper 1** (Nationwide Study)	**Free Paper 2** (Arthritis: Hand)		
09:20-09:40	Coffee Break				
09:40-10:10	**Special Invited Lecture 1** Jeffrey B Friedrich	**Free Paper 3** (Elbow)	**Free Paper 4** (TFCC, UIS: Wrist)	**Hands-on Workshop 1** Ethicon Tenorrhaphy	
10:10-10:40	**TSSH Invitation Lecture** Chung-Chen Hsu				
10:40-11:40	**Special Invited Lecture 2** Osamu Soejima Satoshi Ichihara	**Free Paper 5** (Microsurgery)	**Free Paper 6** (DRF, Carpal Bone Fracture: Wrist)		
11:40-12:10	**Keynote Speech** Room A James Chang				
12:10-13:10	Group Photo & Lunch				
13:10-14:10	**KSSH 'W Grand Lecture'** Lam Wee Leon Yuan-Kun Tu	**ICL: Wrist Instability**	**Free Paper 7** (Hand)	**Hands-on Workshop 2** UCT medical Fracture (Distal Radius, Metacarpal)	VIP Lounge
14:10-15:10	**Symposium 2** Special Humanities Lecture	**Free Paper 8** (Peripheral Nerve)	**Free Paper 9** (Wrist)		
15:10-15:30	Coffee Break				
15:30-16:45	**Free Paper 10** (English Session: Basic Study)	**Travelling Fellows' Session**	**Symposium 3** AI Strategies for Clinical Research and Presentation		
16:45-17:15	**Industrial Session** NOVOSIS Trauma (rh BMP-2), JNJ MedTech	**Symposium 4** Flexor Tendon Surgery: Expert Techniques & Interactive Discussion	**Symposium 5** Mastering Scaphoid Nonunion Surgery: Expert Talks and Open Q&A		
17:15-17:45	**Travelling Fellowship Report** HKSSH, TSSH, JSSH, ASSH				
17:50-18:20	General Assembly & Award Ceremony				

PROGRAM

Room A
(6F Main Building, Eun-myung Grand Auditorium)

08:00-08:10	Registration		
08:10-08:20	Opening remarks	Chairman, KSSH **Sae Hwi Ki** President, KSSH **Bong Cheol Kwon**	
08:20-09:20	**Symposium 1. Toward Human-Robot Collaboration in Microsurgery**	Orthop Surg. Korea Univ. **Jong Woong Park** Plast Reconstr Surg. DongGuk Univ. **Su Rak Eo**	
08:20- 08:30	Why Microsurgeons Need Robots?	Plast Reconstr Surg. Korea Univ. **Jae-Ho Chung**	23
08:30-08:47	사람-로봇 협업을 위한 초미세수술 로봇 시스템 (Supermicrosurgical Robotic System for Human -Robot Collaboration)	Center for Humanoid Research, KIST **Yong Suk Ihn**	24
08:47-09:04	수술로봇을 위한 다축 힘센싱 기술 연구 (Multi-axis force sensing technology for surgical robots)	Ajou Univ. **Uikyum Kim**	25
09:04-09:20	초미세수술 자동화를 위한 인공지능 기반 요소기술 소개 (Toward Autonomous Microsurgical Robotics : Calibration, Pose Estimation, and Visual Servoing)	DGIST **Minho Hwang**	26
09:20-09:40	Coffee break		
09:40-10:10	**Special Invited Lecture 1**	Orthop Surg. Yonsei Wonju Univ. **Jin Rok Oh** Plast Reconstr Surg. Gwangmyeong Sungae General Hosp. **Jin Soo Kim**	
	Multidisciplinary Management of the Mangled Hand	University of Washington **Jeffrey B Friedrich**	28
10:10-10:40	**TSSH Invitation Lecture**	Orthop Surg. SM Christianity Hosp. **In Hyeok Rhyou** Orthop Surg. Seoul National Univ. **Hyun Sik Gong**	
	Medial Femoral Condyle Flap for Extremity Reconstruction	Chang Gung Memorial Hospital **Chung-Chen Hsu**	30
10:40-11:40	**Special Invited Lecture 2**	Orthop Surg. Kosin Univ. **Young Ho Kwon** Orthop Surg. Chung-Ang Univ. **Jae Sung Lee**	
	Treatment of Thumb CMC Arthritis: LRSA – From Concept to Clinical Excellence	Fukuoka University **Osamu Soejima**	32
	For the Development of Hand Surgery - From Europe to Asia-Pacific	Juntendo University **Satoshi Ichihara**	33

Room A
(6F Main Building, Eun-myung Grand Auditorium)

11:40-12:10 **Keynote Speech**
Orthop Surg. Yeson Hosp. **Goo Hyun Baek**
Plast Reconstr Surg. Inha Univ. **Sae Hwi Ki**

10 Recurring Lessons in Hand Reconstruction — Stanford University **James Chang** — 35

12:10-13:10 Group Photo & Lunch

13:10-14:10 **KSSH 'W Grand Lecture'**
W General Hosp. **Sang Hyun Woo**
Orthop Surg. Soonchunhyang Univ. **Byung Sung Kim**

10 questions I always have about congenital hand differences
Singapore General Hospital **Lam Wee Leon** — 37

The Current Trends in the Treatment for Brachial Plexus Injury and Spinal Cord Reconstructions
E-Da Hospital **Yuan-Kun Tu** — 38

14:10-15:10 **Symposium 2. Special Humanities Lecture**
Plast Reconstr Surg. Chonnam National Univ. **Kwang Seog Kim**
Orthop Surg. Hallym Univ. **Bong Cheol Kwon**

Cultural Codes of Hands in Ancient China (손으로 보는 문명의 몇 가지 코드들)
Chonnam National Univ. **Sung Won Lee** — 40

15:10-15:30 Coffee break

15:30-16:45 **Free Paper 10 (English Session: Basic Study)**
Orthop Surg. Inje Univ. **Hyun Il Lee**
Plast Reconstr Surg. Seoul National Univ. **Byung Jun Kim**

Biomechanical Analysis of Intramedullary Nailing and Cerclage Wiring for the Oblique Metacarpal Shaft Fractures — Orthop Surg. Yeson Hosp. **Joonha Lee, Chung Hoon Lee** — 42

Clinical Impact of Radiographic Severity and Anatomical Location of Heterotopic Ossification on Elbow Flexion-Extension in Post-Traumatic Stiffness: A CT-Based Muscle-Guided Classification Study — Asan Medical Center **Jia Guo** — 44

Hyperflexion After Olecranon Osteotomy Enhances Visualization of the Distal Humerus in Coronal Shear Fractures: A 3D Simulation Study — W General Hosp. **신동주** — 49

Biomechanical evaluation of the wrist after arthroscopic transosseous triangular fibrocartilage complex foveal repair using Biodex System 4 Isokinetic Dynamometer
[1]Orthop Surg. Korea Univ., [2]Sports Medical Center Korea Univ.,
[3]Christine M. Kleinert Institute for Hand and Microsurgery, University of Louisville, Louisville, Kentucky, USA
Yeongyoon Koh[1], Jinhyuk Lee[2], Kyubin Lee[2], Jae Jun Nam[1, 3], Jong Woong Park[1], In Cheul Choi[1, 2] — 51

PROGRAM

Room A
(6F Main Building, Eun-myung Grand Auditorium)

Rapidly dissolving microneedles incorporating lidocaine hydrochloride: a PVP/PVA-based approach for local anesthesia
[1]Orthop Surg. Chung-Ang Univ., [2]Spine Center, Bogang Hosp., [3]Neurosurg. Keimyung Univ., [4]College of Pharmacy and Research Institute of Pharmaceutical Sciences, Kyungpook National Univ.
Hyoung-Seok Jung[1], Eugene Jae-Jin Park[2], Sae Min Kwon[3], Dong Wuk Kim[4] 53

Deep learning-based ankle angle and gait-phase estimation in a rat sciatic nerve injury model
[1]Biomedical Engineering, AMIST, Asan Medical Center, [2]Orthop Surg, Asan Medical Center, [3]Convergence Medicine, Asan Medical Institute of Convergence Science and Technology, Asan Medical Center, [4]Center for Cell Therapy, Asan Medical Center, [5]Bigdata Research Center, Asan Institute for Life Science, Asan Medical Center
Youngjae Kim[1,3], Won Sun Lee[2], Min-Young Jo[2], Chae–Min Ryu[4], Hyunna Lee[5], Jae Kwang Kim[2] 54

Effect of Decellularized Amniotic Membrane Hydrogels on Enhanced Wound Healing in a UVB-Induced Burn Model in Rats
[1]Center for Biomaterials, Biomedical Research Institute, Korea Institute of Science and Technology (KIST), [2]Orthop Surg. Korea Univ. 3Applied Bioengineering, Graduate School of Convergence Science and Technology, Seoul National Univ.
Seongryeol Ye[1,3], Yu-Jin Kim[1], Jin Yoo[1], Kangwon Lee[3], Jae Jun Nam[2], Yeungyoon Ko[2], In Cheul Choi[2], Youngmee Jung[1], Jong Woong Park[2] 65

Strategy for Donor Nerve Selection in Nerve Transfers with an Emphasis on Functional Preservation
E-Da Hospital / I-Shou University **Yu-Huan Hsueh (Oscar)** 67

16:45-17:15 **NOVOSIS Trauma (rh BMP-2), JNJ MedTech [Industrial Session]**
W General Hosp. **Kyung-Chul Kim**
Orthop Surg. Konkuk Univ. **Seoung Joon Lee**

Bone Graft Option in Orthopedic Trauma, Challenging the Orthopedic Dogma
Orthop Surg. Korea Univ. **Jong-Keon Oh** 69

17:15-17:45 **Travelling Fellowship Report**
Plast Reconstr Surg. Wonkwang Univ. **Young Cheon Na**
Plast Reconstr Surg. Ewha Womans Univ. **Bo Young Park**

Remarkable Moments in HKSSH 2025 — Orthop Surg. Eulji Univ. **Seong Ju Choi** 71

Remarkable Moments in TSSH 2025 — Orthop Surg. Chung-Ang Univ. **Hyoung-Seok Jung** 72

Remarkable Moments in JSSH 2025 — Orthop Surg. Yonsei Univ. **Yun Rak Choi** 73

Remarkable Moments in ASSH 2025 — Orthop Surg. Ulsan Univ. **Young Ho Shin** 74

17:50-18:20 General Assembly & Award Ceremony

Room B
(3F Graduate School of Public Health, Room 337)

08:00-08:10 Registration

08:10-08:20 Opening remarks

Chairman, KSSH **Sae Hwi Ki**
President, KSSH **Bong Cheol Kwon**

08:20-09:20 **Free Paper 1 (Nationwide Study)**

Orthop Surg. CHA Univ. **Soo-Hong Han**
Plast Reconstr Surg. Yonsei Univ. **Hii-Sun Jeong**

Trends in mean hand grip strength, cutoff value, and prevalence of low hand grip strength : An analysis of 2014–2019 Korea National Health and Nutrition Examination Survey (KNHANES) data
Orthop Surg. Chungnam National Univ. **Yun Ki Kim** 77

What was different before and in COVID-19 pandemic in management of distal radius fracture aged over fifty: South Korea Nationwide Analysis Using Korea Health Insurance Dataset
Orthop Surg. Eulji Univ. **Seong Ju Choi** 78

Diagnostic Coding and Conservative Treatment Duration for Traumatic Triangular Fibrocartilage Complex Tears: A Survey of Korean Society for Surgery of the Hand
Orthop Surg. Yonsei Univ. **Yong Hyun Yoon** 79

Wrist Arthroscopy in South Korea: Utilization, Disparities, and Complications from an 11-Year Nationwide Cohort
[1]Orthop Surg. National Health Insurance Service Ilsan Hosp., [2]Orthop Surg. Korea Univ., [3]Orthop Surg. Eulji Univ.
Hyun Tak Kang[1], Chi-Hoon Oh[2], SeongJu Choi[3], Jun-Ku Lee[1] 80

An 11-Year Nationwide Analysis of Infection related Complications After Wrist Arthroscopy : A Nationwide Population-Based Study in South Korea (2013–2023)
[1]Orthop Surg. Yonsei Wonju Univ., [2]Orthop Surg. Eulji Univ.,
[3]Orthop Surg. National Health Insurance Service Ilsan Hosp., [4]Orthop Surg. Yonsei Univ.
Jisu Park[1], Jun-Ku Lee[3,4], SeongJu Choi[2], Jin Rok Oh[1] 81

Wrist Arthroscopic Management of Triangular Fibrous Cartilage Complex and Ligament Injury – South Korea Nationwide Study
[1]Orthop Surg. Korea Univ., [2]Orthop Surg. Eulji Univ.,
[3]Orthop Surg. National Health Insurance Service Ilsan Hosp., [4]Orthop Surg. Yonsei Univ.
Chi-Hoon Oh[1] , SeongJu Choi[2], Hyun Tak Kang[3], Jun-Ku Lee[3,4] 83

09:20-09:40 Coffee break

09:40-10:40 **Free Paper 3 (Elbow)**

Orthop Surg. Yeungnam Univ. **Sam Guk Park**
Orthop Surg. Hanyang Univ. **Joo Hak Kim**

Clinical outcomes and risk factors for platelet-rich plasma injections in lateral epicondylitis
[1]Orthop Surg. Chung-Ang Univ., [2]Radiology. Chung-Ang Univ.
Min Su Chu[1], Jae-Sung Lee[1] , Guen Young Lee[2], Hyoung-Seok Jung[1] 85

Long term outcomes of Kudo type total elbow arthroplasty in rheumatoid arthritis
[1]Orthop Surg. Hanyang Univ., [2]Orthop Surg. Ajou Univ., [3]MS Reconstruction Hosp.
이창훈[1], 이영석[1], 최완선[2], Jin Sik Park[3], Joo Hak Kim[1] 86

Room B
(3F Graduate School of Public Health, Room 337)

10:40-11:40 **Free Paper 5 (Microsurgery)**
Plast Reconstr Surg. Kyung Hee Univ. **Sang Yoon Kang**
Orthop Surg. Pusan National Univ. **Sang Hyun Lee**

Room B
(3F Graduate School of Public Health, Room 337)

Risk factors of flap reduction after free tissue transfer
Plast Reconstr Surg. Inha Univ. **Sae Hwi Ki, Do Hyuk Chung, Jee Hyun Moon, Min Ki Hong** 119

11:40-12:10 **Keynote Speech** Room A

12:10-13:10 Group Photo & Lunch

13:10-14:10 **ICL: Wrist Instability**
Orthop Surg. Yeson Hosp. **Jae Hoon Lee**
Orthop Surg. Jeju National Univ. **Kyu Bum Seo**

DRUJ Instability — Orthop Surg. Korea Univ. **Jong Woo Kang** 124

Scapholunate Instability — Orthop Surg. The Catholic Univ. of Korea **Il-Jung Park** 129

Midcarpal Instability — Orthop Surg. The Catholic Univ. of Korea **Joo Yup Lee** 134

14:10-15:10 **Free Paper 8 (Peripheral Nerve)**
Plast Reconstr Surg. Hanyang Univ. **Seung Suk Choi**
Orthop Surg. Ulsan Univ. **Jae Kwang Kim**

Simultaneous transfer of spinal accessory and intercostal nerves to suprascapular, axillary, musculocutaneous, median, and ulnar nerves in preganglionic whole-arm type injuries of brachial plexus
Orthop Surg. Seoul National Univ. **Ji Sup Hwang** 136

Immediate Functional Recovery Following Brachial Plexus Neurolysis and Electrical Stimulation in Chronic Post-Stroke Upper Limb Paralysis
[1]Orthop Surg. Hanyang Univ., [2]E-Da Hospital
Young Seok Lee[1], Chang-Hun Lee[1], Yu-Huan Hsueh[2], Yuan-Kun Tu[2] 137

Can vascular flow change during provocation maneuvers predict surgical failure in neurogenic thoracic outlet syndrome?
Orthop Surg. Seoul National Univ.
Juneseok Won, Changhyon Lee, Jisup Hwang, Jihyeung Kim 139

Is cubital tunnel obliteration a safe and effective procedure for cubital tunnel syndrome?
Orthop Surg. Seoul National Univ.
Juneseok Won, Yongwoo Kim, Jisup Hwang, Jihyeung Kim 140

Electrophysiological Assessment of Reinnervation Following End-to-Side Anterior Interosseous Nerve Transfer for Advanced Cubital Tunnel Syndrome
Orthop Surg. Seoul National Univ.
Sung Ha Chun, Wan Kee Hong, Ji Sup Hwang, Ju Seok Ryu, Hyun Sik Gong 141

Anatomical Variations of the Recurrent Branch of the Median Nerve Encountered During Carpal Tunnel Release: A 10-Year Observational Study
Wellson Hosp. **Hyun Sik Park** 144

PROGRAM

Room B
(3F Graduate School of Public Health, Room 337)

Rethinking Pediatric Anesthesia in Hand Surgery: Beyond General Anesthesia
W Institute for Hand and Reconstructive Microsurgery, W General Hosp.
Soo Jin Woo, Yeong Hee Lee, Hyun Jae Nam, Yeong Woo Kim, Sang Hyun Woo 146

15:10-15:30 Coffee break

15:30-16:45 **Travelling Fellows' Session**
Orthop Surg. Sungkyunkwan Univ. **Min Jong Park**
Plast Reconstr Surg. Gwangmyeong Sungae General Hosp. **Dong Chul Lee**

Coverage of Fingertip Traumatic Amputation in Lesser Digits with Modified Volar Advancement Flap
University of Hong Kong **Marvin Man Ting Chung** 148

My Journey of Hand Surgery Travelling Fellowship: Insights and Experiences
Taipei Veterans General Hospital **Cheng-Yu Yin** 149

Lateral Shotgun Approach for the Proximal Interphalangeal Joint Silicone Arthroplasty
Kurashiki Central Hospital **Takuya Tsumura** 150

Innovation in Hand Surgery: Our Works Using AI and VR
Nagoya University Hospital **Hidemasa Yoneda** 151

The Practice of Hand Surgery in Greece: Insights from a Tertiary University Department
Papanikolaou Hospital **Eleni Karagergou** 152

16:45-17:45 **Symposium 4. Flexor Tendon Surgery: Expert Techniques & Interactive Discussion**
Plast Reconstr Surg. Yonsei Univ. **Jong Won Hong**
Plast Reconstr Surg. W General Hosp. **Hyun-Jae Nam**

Panel: Plast Reconstr Surg. Yonsei Univ. **Jiye Kim**
Plast Reconstr Surg. The Catholic Univ. of Korea **Bommie Florence Seo**

Flexor Tendon Repair: Stick to the Basic Principles
Gangnam Jaejun Plastic Clinic **Jae-Won Yang** 154

Zone 2 Combined FDS and FDP Injury
Plast Reconstr Surg. The Catholic Univ. of Korea **Sung-No Jung** 157

Two-Stage Flexor Tendon Reconstruction in the Hand
Plast Reconstr Surg. Korea Univ. **Seong Ho Jeong** 165

17:50-18:20 General Assembly & Award Ceremony Room A

Room C
(3F Graduate School of Public Health, Room 331)

08:00-08:10 Registration

08:10-08:20 Opening remarks

Chairman, KSSH **Sae Hwi Ki**
President, KSSH **Bong Cheol Kwon**

08:20-09:20 **Free Paper 2 (Arthritis: Hand)**

Orthop Surg. Korea Univ. **In Cheul Choi**
Plast Reconstr Surg. Korea Univ. **Deok-Woo Kim**

Finger-Specific Distribution Patterns of Digital Mucous Cysts: A Four-Year Surgical Series Analysis — Orthop Surg. SNU Seoul Hosp. **Sang Ho Kwak** 168

A Retrospective Review of Ganglion Cysts; Surgical Technique
Plast Reconstr Surg. DongGuk Univ.
KyoBin Choo, KyungHyun Kim, SooA Lim, SangHun Cho, SuRak Eo 169

Motion-Preserving Denervation for Finger Osteoarthritis : A Consecutive Case Series
W Institute for Hand and Reconstructive Microsurgery, W General Hosp.
Kyung-Chul Kim, Sang-Hyun Woo 170

Comparison of Union Rates and Clinical Outcomes between T-Plate and K-Wire Fixation in Trapeziometacarpal Joint Arthrodesis of the Thumb
[1]Orthop Surg. Yeson Hosp., [2]Orthop Surg. Kyung Hee Univ.
Jae-Hoon Lee[1], Jong-Hun Back[2], Duke Whan Chung[2], Jin-Sung Park[1], Ki-Hyeok Ku[2], Gi-Young Jang[2], Gwan kyu Son[2] 171

Dorsal versus Radial Plating for Trapeziometacarpal Arthrodesis: A Comparative Clinical Investigation
Orthop Surg. Yonsei Univ.
Jae-Yong Cho, Hyun-Kyo Kim, Won-Taek Oh, Il-Hyun Koh, Yun-Rak Choi 174

Advanced Trapeziometacarpal Arthritis: A Comparative Study of Arthrodesis and Arthroplasty
Orthop Surg. Yonsei Univ.
Jae-Yong Cho, Hyun-Kyo Kim, Won-Taek Oh, Il-Hyun Koh, Yun-Rak Choi 176

Two-Year Clinical and Radiologic Outcomes of Dorsoradial Ligament Reconstruction Using the Abductor Pollicis Longus Tendon for Trapeziometacarpal Joint Instability
[1]Orthop Surg. Catholic Kwandong Univ., [2]Orthop Surg. Yonsei Univ.
Sang-Hee Kim[1], Jae-Yong Cho[2], Won-Taek Oh[2], Il-Hyun Koh[2], Yun-Rak Choi[2] 178

09:20-09:40 Coffee break

09:40-10:40 **Free Paper 4 (TFCC, UIS: Wrist)**

Orthop Surg. Ajou Univ. **Kyeong Jin Han**
Orthop Surg. Soo Hosp. **Byung Ho Lee**

Association of Ulnar Variance with Primary Distal Radio-Ulnar Joint Arthritis: A Matched Case-Control Study
Orthop Surg. Asan Medical Center
Yun Jae Kim, Won Sun Lee, Young Ho Shin, Jae Kwang Kim 181

Room C
(3F Graduate School of Public Health, Room 331)

Who Needs More Than a Plate? Predicting TFCC Repair After Distal Radius Fracture
[1]Orthop Surg. National Health Insurance Service Ilsan Hosp., [2]Orthop Surg. Armed Forces Daejeon Hosp., [3]Orthop Surg. Yonsei Univ., [4]Orthop Surg. CHA Univ.
Min Jung Park[1], Cheungsoo Ha[2], Hyun Tak Kang[1], Jun-Ku Lee[1,3], Soo-Hong Han[4] 182

Clinical Outcomes of Arthroscopic Transosseous TFCC Repair using anchorless technique
Orthop Surg. Seoul National Univ. **Juneseok Won[1], Yohan Lee[2]** 183

Effect of the ulnar positive variance on the clinical outcomes of arthroscopic transosseous repair in the patients with the triangular fibrocartilage complex foveal tear
Orthop Surg. Korea Univ. **Jun Hong Won, Joung Woo Shin, Jung Il Lee** 184

Clinical Outcomes of Ulnar Shortening Osteotomy With Versus Without TFCC Foveal Repair in Idiopathic Ulnar Impaction Syndrome: Stratified Arthroscopic Analysis of the Foveal Lesion
Orthop Surg. Yonsei Univ.
Jae-Yong Cho, Hyun-Kyo Kim, Il-Hyun Koh, Won-Taek Oh, Yun-Rak Choi 185

Clinical Features and Outcomes of Sequential Bilateral Ulnar Shortening Osteotomy with Triangular Fibrocartilage Complex Foveal Repair
Orthop Surg. Chungnam National Univ. **Soo Min Cha** 186

Hamatolunate impingement with ulnar impaction syndrome: a case report
Wonju Yonsei Hosp. **김용빈** 200

10:40-11:40 **Free Paper 6 (DRF, Carpal Bone Fracture: Wrist)** Orthop Surg. Eulji Univ. **Sang Ki Lee**, Orthop Surg. Kangdong Sacred Heart Hosp. **Sanglim Lee**

The efficacy of surgical management for distal radius fractures with or without the use of arthroscopic assistance: a systematic review and meta-analysis of randomized controlled trials and prospective study
Orthop Surg. Yeungnam Univ. **Sam Guk Park** 204

Arthroscopic-Assisted Reduction and K-wire Fixation of Dorsal Ulnar Corner Fragments in Distal Radius Fractures
[1]Gayang Samsung Orthopaedic Clin., [2]Orthop Surg. Inje Univ., [3]Gohyeon Seoul Samsung Orthopaedic Clin.
Sang Hoon Chae[1], Seung Joo Kim[2], Dong Suk Kim[3], Hyun Il Lee[2] 205

Efficacy of Ultrasonographic Examination for Predicting Symptomatic Flexor Tendon Irritation Following Volar Plating for Unstable Distal Radius Fractures
Orthop Surg. Yonsei Univ.
Jae-Yong Cho, Hyun-Kyo Kim, Won-Taek Oh, Il-Hyun Koh, Yun-Rak Choi 206

Morphologic characteristic and fixation strategy of the dorsal ulnar fragment in intra-articular distal radius fractures: A CT-based analysis of 241 cases
[1]Orthop Surg. Dong-A Univ., [2]Orthop Surg. Gyeongsang National Univ.
Sung Yoon Jung[1], Gu-Hee Jung[2] 208

Room C
(3F Graduate School of Public Health, Room 331)

Comparison of outcomes of distal radius graft versus iliac crest graft for arthroscopic scaphoid nonunion surgery
W Institute for HHand and Reconstructive Microsurgery, W General Hosp.
Byoung Jin Kim, Sang Hyun Woo 210

What is the optimal method of fixation method for scaphoid nonunion relative to the location of the lesion?
Orthop Surg. Eulji Univ. **Jongwon Lee, Sang Ki Lee** 211

Learning Curve of Arthroscopic Osteosynthesis for Scaphoid Nonunion: a review of consecutive 50 cases
Orthop Surg. Yonsei Univ.
Won-Taek Oh, Seung-Eon Moon, Jae-Yong Cho, Il-Hyun Koh, Yun-Rak Choi 212

월상골 주위 탈구 및 골절 탈구의 장기 추시 결과
Orthop Surg. Soonchunhyang Univ. **Byung Sung Kim, Kyung Jin Lee** 213

11:40-12:10 **Keynote Speech** Room A

12:10-13:10 Group Photo & Lunch

13:10-14:10 **Free Paper 7 (Hand)**
Orthop Surg. The Catholic Univ. of Korea **Yang Guk Chung**
Plast Reconstr Surg. Saeson Hosp. **Jae In Chung**

Management of PIP joint contracture resulting from the fracture subluxation : a case review
Plast Reconstr Surg. DongGuk Univ. **Su Rak Eo, Kyung Hyun Kim, Soo A Lim, Sang Hun Cho** 216

Hybrid Fixation Using K-wire and Minimally Invasive Plating Osteosynthesis for Unstable Proximal Phalangeal Fractures: A Propensity-Matched Comparative Study
W Institute for Hand and Reconstructive Microsurgery, W General Hosp.
Chun Chan-yang, Soo Jin Woo, Dong-Ho Kang, Kim Jae-hyub 217

Location of the A1 and A2 Pulleys in Relation to the Palmar Creases: Implications for Percutaneous Release
[1]Orthop Surg. Inje Univ.
[2]Department of Anatomy, Catholic Institute for Applied Anatomy, The Catholic University of Korea,
[3]Gohyeon Seoul Samsung Orthopaedic Clin.
Seung Joo Kim[1], Young-In So[2], Yi-Suk Kim[2], Wu-Chul Song[2], Dong Suk Kim[3], Hyun-Il Lee[1] 226

Concurrent Pyogenic Granuloma and Onychomadesis after Splint Application
Jeonbuk National Univ. **박정균** 229

Room C
(3F Graduate School of Public Health, Room 331)

Preliminary Report of a Prospective Alternating-treatment Study Comparing Autogenous and Allogeneic Bone Grafting in the Treatment of Solitary Enchondroma of the Short Tubular Bones of the Hand
[1]Orthop Surg. Uijeongbu St. Mary's Hosp. The Catholic Univ. of Korea, [2]Orthop Surg. Yeouido St. Mary's Hosp. The Catholic Univ. of Korea, [3]Orthop Surg. St. Vincent's Hosp. The Catholic Univ. of Korea
Ho Youn Park[1], Taegu Lim[1], Jin-Hyung Im[2], Min Wook Joo[3] 231

Cutaneous Squamous Cell Carcinoma on Hand under Long-Term Immunosuppression
Plast Reconstr Surg. Bucheon St. Mary's Hosp. The Catholic Univ. of Korea
Byeol Kim, Daiwon Jun, Jung Ho Lee 232

Correlation and Optimal Cutoff Value of the Japanese Society for Surgery of the Hand Score for Satisfactory Postoperative Outcomes in Radial Polydactyly: A Retrospective Cohort Study
Orthop Surg. Ulsan Univ. **Wonsun Lee** 234

14:10-15:10 **Free Paper 9 (Wrist)**
Plast Reconstr Surg. Chonnam National Univ. **Jae Ha Hwang**
Orthop Surg. Konyang Univ. **Youn Moo Heo**

Comparative Case Series of Surgical Fixation Methods for Traumatic Radiocarpal Dislocation: A Focus on Bridge Plating
Orthop Surg. Yonsei Wonju Univ. **Sang Jun Lee, Jisu Park, Jin-Rok Oh** 244

Open resection versus arthroscopic resection for wrist ganglion cysts: a systematic review and meta-analysis
Orthop Surg. Yeungnam Univ. **Sam Guk Park** 245

Arthroscopic debridement for pisotriquetral joint arthropathy through standard radiocarpal portals of wrist arthroscopy
Orthop Surg. Jeonbuk National Univ. **Young Keun Lee, Ji Woong Ho** 246

Simultaneous Flexor Tendon Reconstruction and Hamate Hook Excision Under Wide -Awake Local Anesthesia No Tourniquet (WALANT): A Four-Case Series
MS Reconstruction Hosp. **Jin Sik Park** 247

Post-Traumatic Chylous Wrist Effusion: A Case Report
Orthop Surg. Eulji Univ. **Je-Chan Lee, Sang Ki Lee** 249

Volar Wrist Ganglion associated with Radial artery Atherosclerosis: A case report
Orthop Surg. Jeonbuk National Univ. **Jinyoung Kim, Young-Keun Lee, Jong Hong Kim** 251

A Novel Scapholunate Step-Off Sign for Scapholunate Predynamic Instability: An Arthroscopic and Imaging Analysis : preliminary report
Orthop Surg. Korea Univ. **Ji Hoon Park, Chi-Hoon Oh, Jong Woo Kang** 252

Room C
(3F Graduate School of Public Health, Room 331)

Epidemiological Trends and Features of Pediatric Hand and Elbow Fractures in Emergency Department Visits: A Nationwide Population-Based Study
Orthop Surg. Yeson Hosp. **Sang Beom Ma** 256

15:10-15:30 Coffee break

15:30-16:45 **Symposium 3. AI Strategies for Clinical Research and Presentation**
Plast Reconstr Surg. Konkuk Univ. **Dong-Hyeok Shin**
Plast Reconstr Surg. Keimyung Univ. **Jae hun, Choi**

GPT 프롬프트 설계방법
(Is it a Finding or a Fantasy?: Prompting Strategies for Grounding LLMs in Medical Reality)
Departments of Media Software, Sungkyul Univ. **Ho-Woong Choi** 260

LLM의 연구적용 (Application of LLMs in Research) Orthop Surg. Eulji Univ. **Seong Ju Choi** 261

LLM의 발표활용 (Application of LLMs for Presentation)
Orthop Surg. Seoul National Univ. **Yohan Lee** 262

성형외과 관점에서 바라보는 AI연구
(AI Research from the Perspective of Plastic and Reconstructive Surgery)
Plast Reconstr Surg. Kyungpook Univ. **Jeong Yeop Ryu** 267

16:45-17:45 **Symposium 5. Mastering Scaphoid Nonunion Surgery: Expert Talks and Open Q&A**
W General Hosp. **Young Woo Kim**
Orthop Surg. Yeson Hosp. **Jin Sung Park**

Panel: Orthop Surg. Seoul National Univ. **Min Bom Kim**
Orthop Surg. The Catholic Univ. of Korea **Soo Hwan Kang**

Conventional Cancellous Bone Graft for Scaphoid Nonunion
Orthop Surg. DongGuk Univ. **Jin Young Kim** 269

Vascularized Bone Graft for Scaphoid Nonunion Orthop Surg. Naeun Pil Hosp. **Jong Pil Kim** 274

Arthroscopic Bone Graft for Scaphoid Nonunion
Orthop Surg. Jeonbuk National Univ. **Young-Keun Lee** 275

17:50-18:20 General Assembly & Award Ceremony Room A

Room D
(6F Main Building, Seminar Room 2)

Hands-on Workshop (Ethicon / UCT medical)

09:40-11:40 Tenorrhaphy (Ethicon)

Lecturer
- **Hyo-Kon Kim** Orthop Surg. MS Reconstruction Hosp.

Table Instructor
- **Bommie Florence Seo** Plast Reconstr Surg. The Catholic Univ. of Korea
- **Joonha Lee** Orthop Surg. Yeson Hosp.

조편성

정심호 분당차병원
김민부 충북대병원
허시영 국군의무사령부
최민성 국방부
이강희 군의관
채원석 경북대병원
강정민 군의관
김정근 군의관

13:10-15:10 Fracture (UCT Medical; Distal Radius, Metacarpal)

Lecturer
- **Jung Il Lee** Orthop Surg. Korea Univ.
- **Hyo Seok Jang** Orthop Surg. Inje Univ.

Table Instructor
- **Chi-Hoon Oh** Orthop Surg. Korea Univ.
- **Sung Yoon Jung** Orthop Surg. Dong-A Univ.
- **Jisu Park** Orthop Surg. Yonsei Wonju Univ.

조편성

차주영 군의관
김재현 순천향대 부천병원
백근호 대전을지대병원
최봉규 W병원
김민섭 공보의
조영권 경북대병원
김민부 충북대병원
정심호 분당차병원

E-Poster

PROGRAM

E-Poster

2025년 대한수부외과학회

추계학술대회

역경에도 손을 맞잡고
Against All Odds, Hand in Hand

Room A

6F Main Building,
Eun-myung Grand Auditorium

2025년 대한수부외과학회
추계학술대회

Room A

Symposium 1.

Toward Human-Robot Collaboration in Microsurgery

Orthop Surg. Korea Univ. **Jong Woong Park**
Plast Reconstr Surg. DongGuk Univ. **Su Rak Eo**

Why Microsurgeons Need Robots?

Plast Reconstr Surg. Korea Univ.
Jae-Ho Chung

Microsurgery has achieved remarkable progress over the past decades, yet it continues to face intrinsic limitations associated with human fatigue, hand tremor, and restricted visualization at micro- and supermicrosurgical scales. As surgical targets become smaller and the demand for precision and consistency increases, robotic systems are emerging as transformative tools in overcoming these challenges. This presentation explores the rationale and necessity of robotic integration in microsurgery—focusing on how robotics can enhance surgical precision, ergonomics, and reproducibility while expanding the boundaries of reconstructive and lymphatic surgery.

Through analysis of current robotic platforms, including dedicated microsurgical robots and adapted systems from other surgical fields, the talk reviews technical principles, clinical applications, and recent outcome data. Comparative studies evaluating robot-assisted versus conventional manual microsurgery are summarized to illustrate objective benefits and ongoing limitations.

Robotic systems demonstrate measurable advantages in tremor elimination, motion scaling, and surgeon ergonomics, particularly in supermicrosurgery such as lymphaticovenular anastomosis and perforator dissection. Early clinical reports show equivalent or improved patency rates and reduced surgeon fatigue, although high cost and workflow integration remain barriers to widespread adoption.

Microsurgeons need robots not merely as substitutes for manual skill but as enablers of a new microsurgical paradigm—one characterized by enhanced precision, consistency, and long-term sustainability. The evolution of robotic microsurgery represents a crucial step toward expanding what human hands alone cannot achieve.

사람–로봇 협업을 위한 초미세수술 로봇 시스템 (Supermicrosurgical Robotic System for Human -Robot Collaboration)

Center for Humanoid Research, KIST
Yong Suk Ihn

수술로봇을 위한 다축 힘센싱 기술 연구 (Multi-axis force sensing technology for surgical robots)

Ajou Univ.
Uikyum Kim

초미세수술 자동화를 위한 인공지능 기반 요소기술 소개 (Toward Autonomous Microsurgical Robotics : Calibration, Pose Estimation, and Visual Servoing)

DGIST
Minho Hwang

Advances in surgical robotics have enabled greater precision and stability in minimally invasive procedures, yet true autonomy—especially in microsurgery—remains a significant challenge.

We aim to build AI-enabled microsurgical robots that support surgeons by automating repetitive subtasks—such as suturing—to improve precision, reduce fatigue, and enable remote procedures. I will share our lab's recent progress in developing AI-driven three key foundational technologies:

(1) High-precision calibration methods to improve the accuracy of surgical tool manipulation
(2) Markerless pose estimation of surgical instruments
(3) Visual servoing control frameworks that operate adaptively in dynamic environments.

2025년 대한수부외과학회
추계학술대회

Room A

Special Invited Lecture 1

Orthop Surg. Yonsei Wonju Univ. **Jin Rok Oh**
Plast Reconstr Surg. Gwangmyeong Sungae General Hosp. **Jin Soo Kim**

Multidisciplinary Management of the Mangled Hand

University of Washington
Jeffrey B Friedrich

2025년 대한수부외과학회
추계학술대회

Room A

TSSH Invitation Lecture

Orthop Surg. SM Christianity Hosp. **In Hyeok Rhyou**
Orthop Surg. Seoul National Univ. **Hyun Sik Gong**

Medial Femoral Condyle Flap for Extremity Reconstruction

Chang Gung Memorial Hospital
Chung-Chen Hsu

2025년 대한수부외과학회
추계학술대회

Room A

Special Invited Lecture 2

Orthop Surg. Kosin Univ. **Young Ho Kwon**
Orthop Surg. Chung-Ang Univ. **Jae Sung Lee**

Treatment of Thumb CMC Arthritis: LRSA – From Concept to Clinical Excellence

Fukuoka University
Osamu Soejima

For the Development of Hand Surgery - From Europe to Asia-Pacific

Juntendo University
Satoshi Ichihara

2025년 대한수부외과학회
추계학술대회

Room A

Keynote Speech

Orthop Surg. Yeson Hosp. **Goo Hyun Baek**
Plast Reconstr Surg. Inha Univ. **Sae Hwi Ki**

10 Recurring Lessons in Hand Reconstruction

Stanford University
James Chang

2025년 대한수부외과학회
추계학술대회

Room A

KSSH ‘W Grand Lecture’

W General Hosp. **Sang Hyun Woo**
Orthop Surg. Soonchunhyang Univ. **Byung Sung Kim**

10 questions I always have about congenital hand differences

Singapore General Hospital
Lam Wee Leon

The Current Trends in the Treatment for Brachial Plexus Injury and Spinal Cord Reconstructions

E-Da Hospital
Yuan-Kun Tu

2025년 대한수부외과학회
추계학술대회

Room A

Symposium 2.
Special Humanities Lecture

Plast Reconstr Surg. Chonnam National Univ. **Kwang Seog Kim**
Orthop Surg. Hallym Univ. **Bong Cheol Kwon**

Cultural Codes of Hands in Ancient China
(손으로보는문명의몇가지코드들)

Chonnam National Univ.
Sung Won Lee

The hands symbolize the cognitive abilities and technological advancements

that unfolded during the course of human evolution.

Various cultural and artistic codes, such as those for language, sense, life, and creation, are embodied in our hands.

We will find the civilizational codes contained within the hand across various cultures, including China, since antiquity.

2025년 대한수부외과학회
추계학술대회

Room A

Free Paper 10

(English Session: Basic Study)

Orthop Surg. Inje Univ. **Hyun Il Lee**
Plast Reconstr Surg. Seoul National Univ. **Byung Jun Kim**

Biomechanical Analysis of Intramedullary Nailing and Cerclage Wiring for the Oblique Metacarpal Shaft Fractures

Orthop Surg. Yeson Hosp.
Joonha Lee, Chung Hoon Lee

Purpose: Since the incidence of metacarpal shaft fractures is high, various treatment techniques have been introduced. I compared the stability of intramedullary nailing and cerclage wiring, a novel minimally invasive treatment, with conventional lag screw fixation and plate fixation.

Materials and methods: After oblique fractures were created in 20 artificial metacarpal bones, fixation was performed using four techniques: (1) two K-wires and two roll wires, (2) one K-wire and two roll wires, (3) two lag screws, and (4) a locking plate. The load-to-failure was measured and compared by a cantilever bending test using specimens.

Results: The average failure force was 35.67 ± 20.42 N in the two K-wires and two roll wires group, 40.17 ± 17.83 N in the one K-wire and two roll wires group, and 67.61 ± 14.79 N in the two lag screws group, with no statistically significant differences among them. On the other hand, a locking plate group showed a statistically significantly higher value of 140.39 ± 39.12 N compared to the other three groups.

Conclusion: In oblique metacarpal shaft fractures, intramedullary nailing and cerclage wiring is an easy and less invasive treatment that provides stability comparable to that of lag screws.

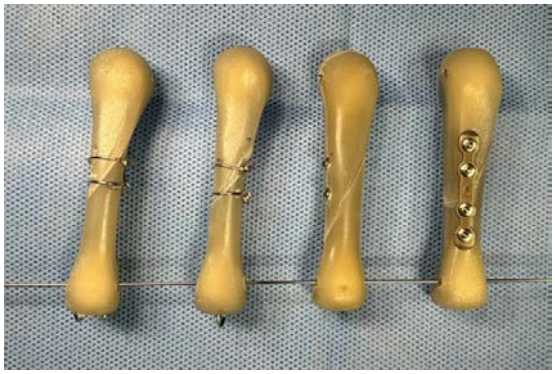

(Figure 1) Gross photo of specimens

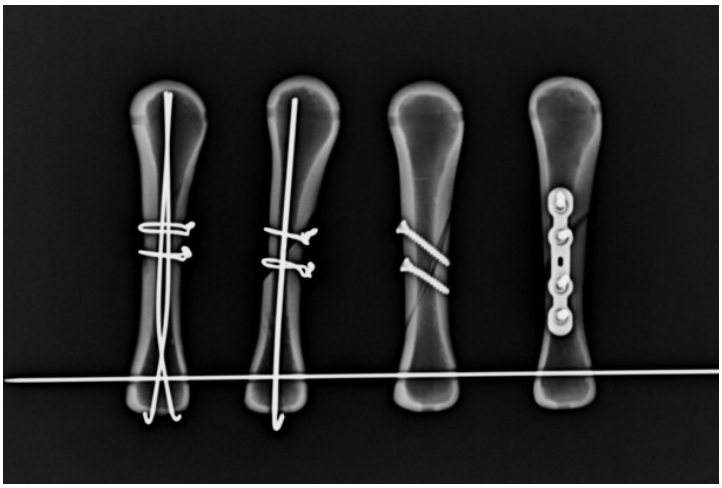

(Figure 2) Plain X-ray film of specimens

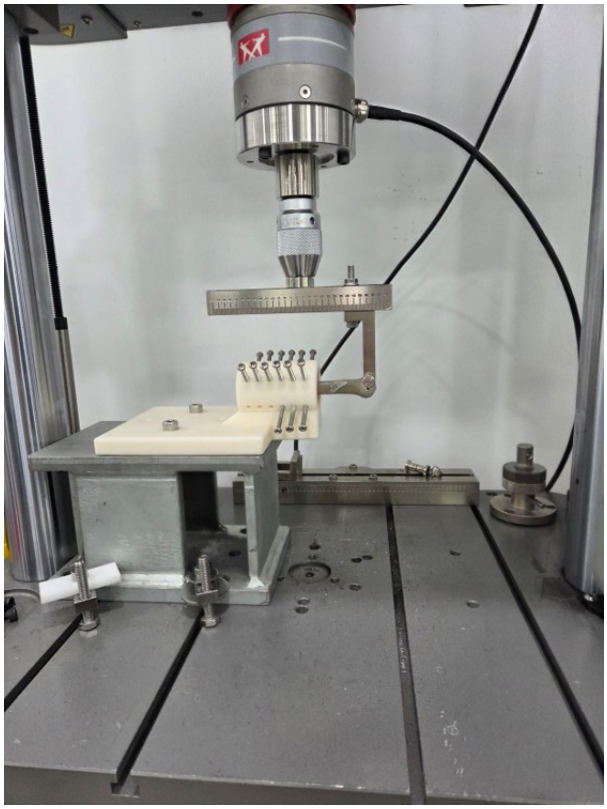

(Figure 3) Cantilever bending test setting

Clinical Impact of Radiographic Severity and Anatomical Location of Heterotopic Ossification on Elbow Flexion-Extension in Post-Traumatic Stiffness: A CT-Based Muscle-Guided Classification Study

Asan Medical Center
Jia Guo

Introduction: Up to 20% of surgically treated elbows after trauma develop post-traumatic heterotopic ossification (HO), which interferes with elbow motion. However, gaps remain in our understanding of the specific functional implications of HO. Radiological assessment, particularly with computed tomography (CT) scans, can clearly define ectopic ossification developed within the complex architecture of the elbow joint.

In the present study, we employed our previously proposed muscle-guided classification method to evaluate the location of HO. We aimed to investigate the clinical relevance of two key radiographic characteristics of post-traumatic HO, anatomical location and radiographic severity, on elbow flexion-extension in cases where HO is likely to be a major contributing factor.

Methods: A retrospective analysis was conducted on 56 patients with significant flexion-extension stiffness, defined as a flexion-extension (FE) arc of less than 100°. HO location was classified into seven categories based on a muscle-guided CT mapping system developed in a previous study. Radiographic severity was graded from 1 to 3 according to the extent and morphology of HO (Figure 1). Elbow motion including flexion contracture (FC), flexion, and the FE arc was evaluated. Statistical analyses were performed to assess the correlation between HO characteristics and motion loss.

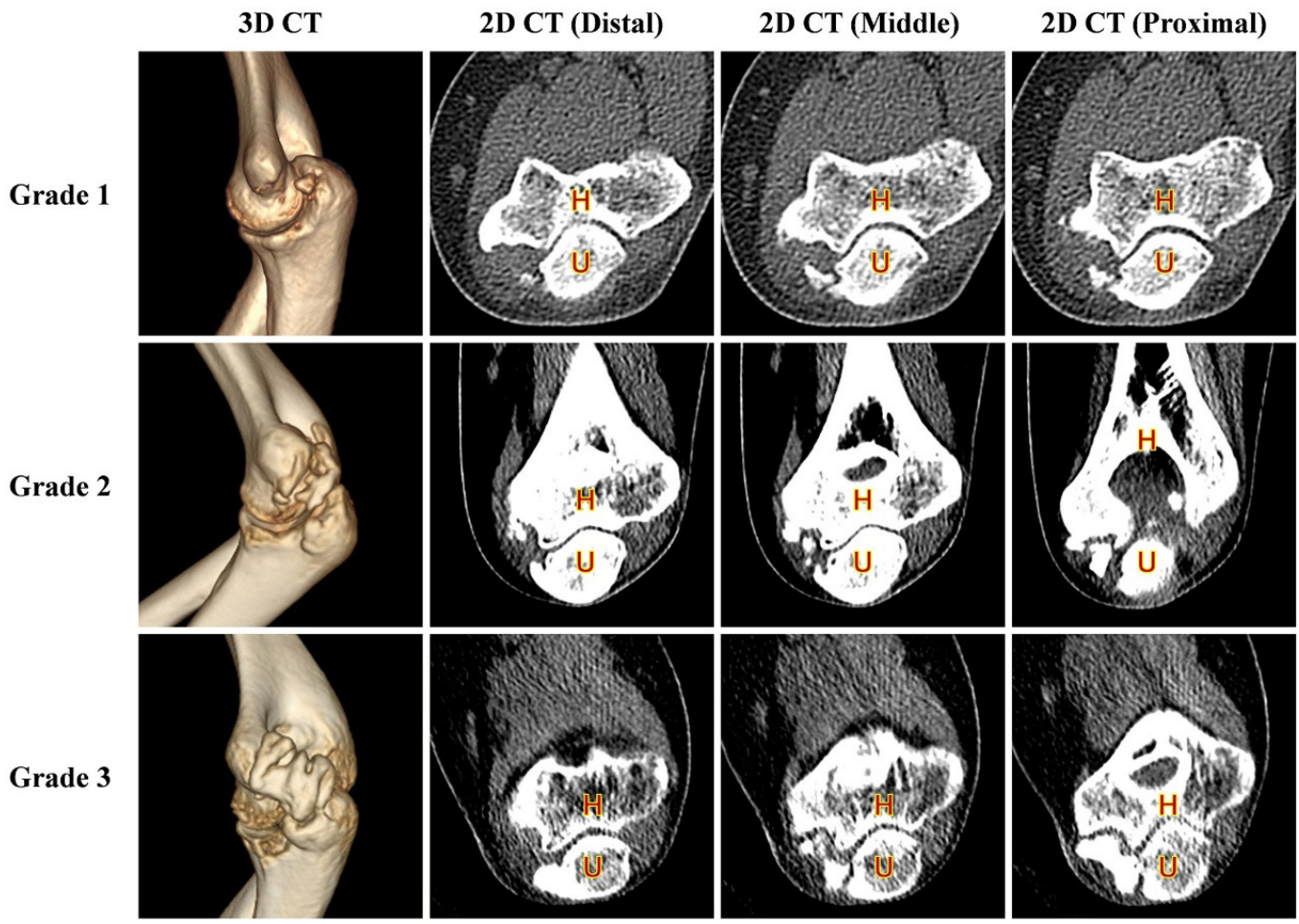

Figure 1. Three-dimensional (3D) and axial two-dimensional (2D) CT scans demonstrating the three grades of radiographic severity of heterotopic ossification (HO) located in the posteromedial region of the elbow. The HO is distributed within the medial gutter along the posteromedial aspect and follows the course of the flexor carpi ulnaris (FCU) muscle, as illustrated by CT sections from distal to proximal along the elbow joint. The location of HO in this case was classified as Posteromedial – Medial Gutter – Flexor Carpi Ulnaris (PM-MG-FCU) according to the muscle-guided classification system. H = humerus; U = ulna

Results: HO in the posterior compartment of the elbow joint, distributed along the triceps brachii, Flexor carpi ulnaris (FCU) and anconeus, showed a significant linear correlation between radiographic severity and both FC and the flexion-extension FE arc (Table 1).

Table 1. Spearman Correlation Analysis Between Radiographic Severity and Elbow Motion Across Seven HO Location Categories Based on the Muscle-Guided Classification

	FC		
	Categories	Correlation coefficient	p
1	P-O-T	**0.429****	**<0.001**
2	PM-MG-FCU	**0.499****	**<0.001**
3	PL-LG-AN	**0.268***	**<0.05**
4	M-ME-FLEX	0.061	0.654
5	L-LE-EXT	-0.182	0.181
6	A-HU-B	-0.085	0.533
7	A-HR-SP	0.256	0.057
	FF		
	Categories	Correlation coefficient	p
1	P-O-T	-0.091	0.505
2	PM-MG-FCU	**-0.299***	**<0.05**
3	PL-LG-AN	-0.014	0.920
4	M-ME-FLEX	-0.153	0.261
5	L-LE-EXT	**0.313***	**<0.05**
6	A-HU-B	0.012	0.928
7	A-HR-SP	-0.07	0.609
	FE arc		
	Categories	Correlation coefficient	p
1	P-O-T	-0.430**	**<0.001**
2	PM-MG-FCU	-0.593**	**<0.001**
3	PL-LG-AN	-0.299*	**<0.05**
4	M-ME-FLEX	-0.100	0.465
5	L-LE-EXT	0.287*	**<0.05**
6	A-HU-B	0.033	0.811
7	A-HR-SP	-0.224	0.097

FC = flexion contracture; FF = further flexion (equivalent to flexion); FE arc = flexion-extension arc.

Patients with Grade 3 HO demonstrated a significantly greater degree of FC (median: 60°) and a significantly lower FE arc (median: 35°) compared to those without Grade 3 HO (Figure 2). No significant differences in flexion were found among patients with varying radiographic severities of HO.

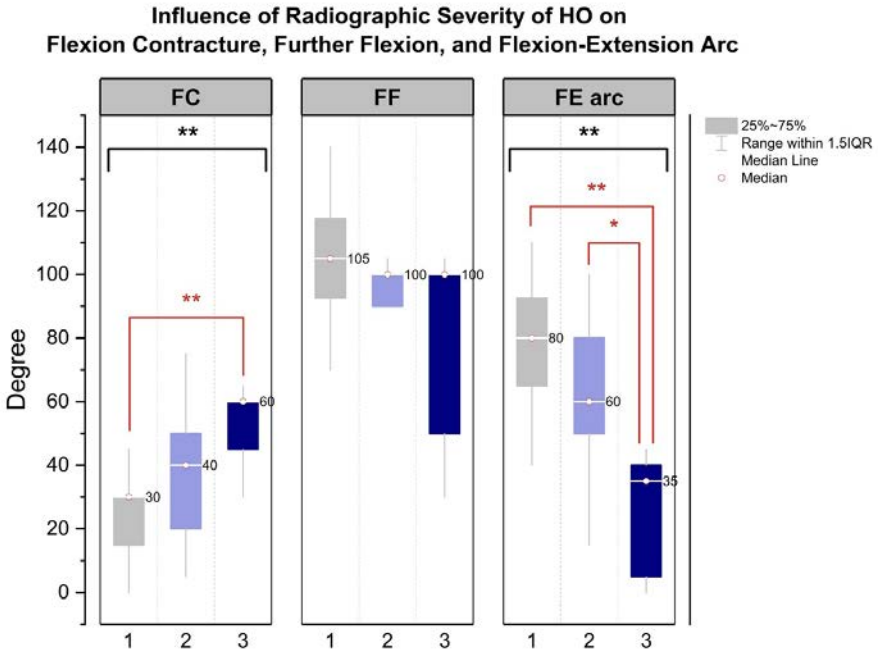

Figure 2. Graph showing the degree of elbow motion impairment—including flexion contracture (FC), flexion, and flexion-extension (FE) arc—according to the maximum grade of radiographic severity of HO.
The x-axis categories (1, 2, and 3) represent patient groups classified by the highest radiographic severity grade observed:
1 = Group 1, patients with only Grade 1 HO;
2 = Group 2, patients with Grade 2 HO but without Grade 3;
3 = Group 3, patients with Grade 3 HO, regardless of the presence of lower grades.
FC = flexion contracture; FF = further flexion (equivalent to flexion); FE arc = flexion-extension arc.
Double asterisks (**) indicate $p < 0.001$; single asterisks (*) indicate $p < 0.05$.

Discussion: In this study, we demonstrated the impact of HO location and radiographic severity on elbow motion.

Specifically, HO surrounding the FCU demonstrated the most pronounced impairment, with notable loss in flexion, extension, and the FE arc. HO along the triceps brachii and anconeus, corresponding to the P-O-T and PL-LG-AN categories, was specifically associated with extension loss and decreased flexion-extension arc, but not with significant flexion loss. Therefore, surgical resection of HO in these two regions may be more effective for improving extension than flexion。

In Contrast, HO formed in the anterior, medial, and lateral aspects of the elbow may have only a mild influence on the severity of stiffness.

Conclusion: HO located in the posterior compartment showed a significant correlation between radiographic severity and motion loss, particularly affecting extension. Among the posterior region categories defined by the

muscle-guided classification, HO surrounding the FCU demonstrated the most pronounced impairment, with notable loss in flexion, extension, and the FE arc.

In contrast, HO located in the anterior, medial, or lateral compartments showed limited clinical relevance with respect to radiographic severity.

Hyperflexion After Olecranon Osteotomy Enhances Visualization of the Distal Humerus in Coronal Shear Fractures: A 3D Simulation Study

W General Hosp.
신동주

Background : Coronal shear fractures of the distal humerus are technically challenging due to the anterior location of the capitellum and trochlea. Standard posterior approaches often provide limited exposure. Although olecranon osteotomy improves visualization, anterior access remains restricted, and surgical dislocation, while offering wider exposure, carries risks of soft tissue and neurovascular injury.

Purpose: To quantitatively evaluate the effect of elbow hyperflexion to 140° after olecranon osteotomy on distal humeral articular exposure compared with conventional 90° flexion using 3D CT-based simulation.

Methods : CT scans of 20 cadaveric elbows (10 male, 10 female) without prior pathology were reconstructed into 3D models. Virtual olecranon osteotomies were performed, and articular cartilage margins were manually annotated. Simulated elbow flexion was applied at 90° and 140°, and visible articular surface area was calculated as a percentage of the total distal humeral cartilage area. Analysis was conducted using Mimics 16.0 and Rapidform 2006.

Results : The mean total distal humeral cartilage surface area was 1,787.45 mm^2. At 90° flexion, the mean exposed area was 846.35 mm^2 (47.8% ± 7.0), whereas at 140° hyperflexion it increased to 1,245.00 mm^2 (70.3% ± 9.0). This represents a significant 22.5% improvement in exposure ($p < 0.001$).

Conclusion : Hyperflexion to 140° following olecranon osteotomy significantly enhances anterior articular visualization of the distal humerus compared with 90° flexion.

Figure 1. Three-dimensional simulation of distal humeral exposure following olecranon osteotomy at two flexion angles. 3D surface-rendered models demonstrate the exposed articular surface area of the distal humerus at (A) 90° and (B) 140° of elbow flexion. At 90° flexion (Figure 1A), the visible articular surface area was 1025.01 mm^2, while at 140° flexion (Figure 1B), the surface area increased to 1606.40 mm^2. The trochlear and capitellar regions (red) become significantly more exposed with hyperflexion, as the proximal ulna (yellow) shifts anteriorly, enabling enhanced visualization.

Figure1A

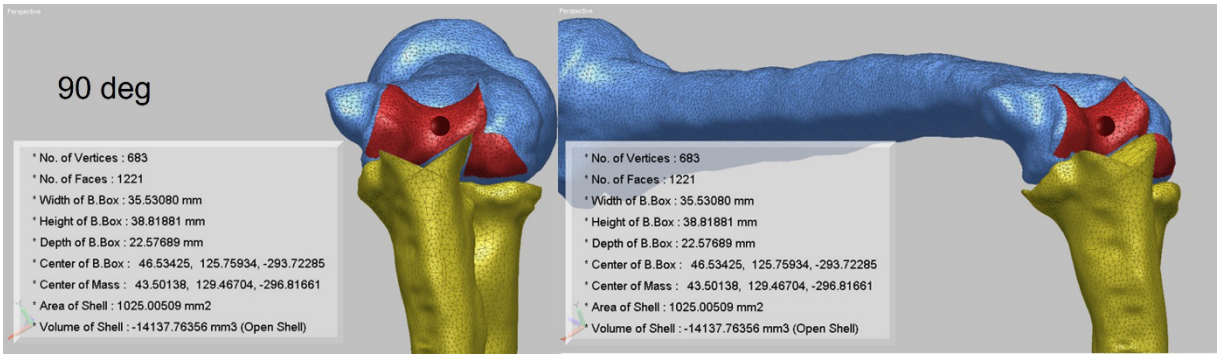

Figure 1B

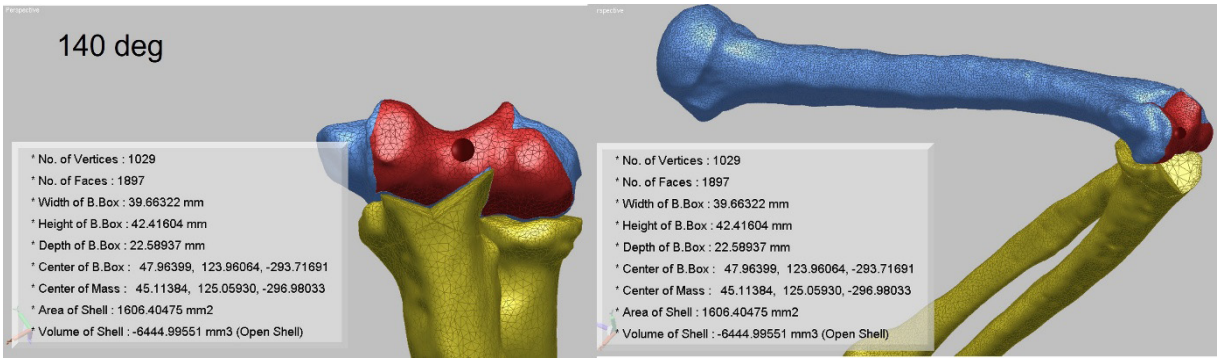

Table 1. Comparison of Articular Surface Exposure by Elbow Flexion Angle and Relative Increase According to Elbow Flexion Angle

Flexion Angle	Exposed Area (mm^2)	Exposure (%)
90°	846.35 ± 140.07	47.8 ± 7.0%
140°	1245.00 ± 188.92	70.3 ± 9.0%
Increase	+398.65	+22.5%

Biomechanical evaluation of the wrist after arthroscopic transosseous triangular fibrocartilage complex foveal repair using Biodex System 4 Isokinetic Dynamometer

[1]Orthop Surg. Korea Univ., [2]Sports Medical Center Korea Univ.,
[3]Christine M. Kleinert Institute for Hand and Microsurgery, University of Louisville, Louisville, Kentucky, USA
Yeongyoon Koh[1], Jinhyuk Lee[2], Kyubin Lee[2],Jae Jun Nam[1, 3,]
Jong Woong Park[1], In Cheul Choi[1, 2]

Objective: This study aimed to investigate the biomechanical basis of functional recovery following arthroscopic transosseous repair of triangular fibrocartilage complex (TFCC) foveal tears. Specifically, we sought to identify which isokinetic forearm motion parameter most closely reflects improvements in wrist function, thereby demonstrating the relationship between distal radioulnar joint (DRUJ) stability and clinical recovery.

Methods: A total of 52 patients (mean age, 33 years) who underwent TFCC repair for DRUJ instability were retrospectively analyzed. Forearm rotational strength was assessed pre- and postoperatively using the Biodex System 4 Isokinetic Dynamometer, measuring lower body-weight–normalized peak torque (PT), total work (TW), time to peak torque (TPT), and acceleration time (AT) for both pronation and supination. Additional assessments included grip strength, wrist ROM, and Q-DASH scores. Functional recovery was defined as a ≥10-point improvement in the Q-DASH score, based on previously reported minimal clinically important difference (MCID).

Results: Preoperatively, the involved side exhibited side-specific isokinetic deficits versus the contralateral side, with PT and TW in both supination and pronation ($p \leq 0.001$). Postoperatively, the average Visual Analog Scale (VAS) score decreased, and both the Mayo Wrist Score and Q-DASH score showed significant improvement. In biomechanical assessments, PT and TW for both supination and pronation significantly increased ($p<0.05$). AT also decreased significantly; however, TPT as well as grip and pinch strength did not show statistically significant changes. Among patients with a clinically significant improvement in Q-DASH (≥10 points), pronation peak torque ($r = 0.41$) and total work ($r = 0.34$) demonstrated the strongest correlations with patient-reported functional recovery, suggesting that objective measures of pronation strength and endurance are the most reliable indicators of meaningful clinical improvement after arthroscopic TFCC repair.

Conclusion: Preoperatively, TFCC-injured wrists exhibited significantly PT and TW than the contralateral side, confirming deficits in strength and endurance. Arthroscopic transosseous foveal repair was associated with meaningful gains in rotational strength and endurance at 1 year. Among isokinetic metrics, pronation PT and TW

showed the strongest correlations with clinically significant Q-DASH improvement, whereas TPT did not change and AT—despite decreasing—was less predictive of clinical recovery. PT and TW may serve as practical objective markers to complement patient-reported wrist function and guide rehabilitation and return-to-activity decisions.

Keywords: Triangular Fibrocartilage Complex (TFCC), Wrist joint, Distal radioulnar joint (DRUJ), Isokinetic test, Muscle strength

Rapidly dissolving microneedles incorporating lidocaine hydrochloride: a PVP/PVA-based approach for local anesthesia

[1]Orthop Surg. Chung-Ang Univ., [2]Spine Center, Bogang Hosp., [3]Neurosurg. Keimyung Univ.,
[4]College of Pharmacy and Research Institute of Pharmaceutical Sciences, Kyungpook National Univ
Hyoung-Seok Jung[1], Eugene Jae-Jin Park[2], Sae Min Kwon[3], Dong Wuk Kim[4]

Lidocaine is a widely used local anesthetic, typically administered via injections or topical creams. However, these conventional methods are associated with limitations such as pain upon administration, delayed onset of action, and patient anxiety or fear related to needle-based delivery. This study aimed to develop an optimized microneedle (MN) system containing lidocaine to enable rapid onset and improved patient compliance. Six lidocaine-loaded MN formulations were fabricated using polyvinylpyrrolidone (PVP) and polyvinyl alcohol (PVA), and evaluated for mechanical strength, skin insertion capability, physicochemical properties, drug release kinetics, and transdermal permeation. Well-defined, sharp pyramidal microneedles were successfully produced, with the PVP–PVA composite forming longer and mechanically superior needles compared to formulations comprising either polymer alone. Among them, the F5 formulation exhibited outstanding mechanical strength (>32 N) and effective skin penetration (penetrating four layers of Parafilm), releasing over 80% of the drug within 15 minutes. In the percutaneous absorption study, the F5 microneedles demonstrated a significantly faster onset of action than the commercial EMLA cream (5%), achieving a transdermal drug concentration exceeding 600 μg/mL—more than three times the minimum therapeutic threshold (200 ng/mg)—within 15 minutes. These findings highlight the potential of microneedle-based delivery as a rapid, painless, and patient-friendly alternative for local anesthesia, achieved by optimizing polymer composition and mechanical performance.

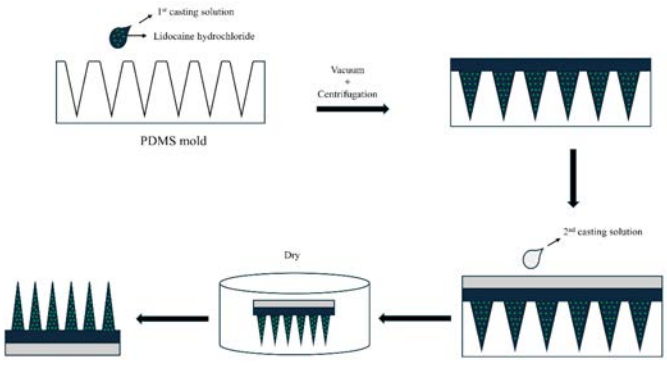

Preparation process of lidocaine-PVA/PVP microneedles.

Deep learning-based ankle angle and gait-phase estimation in a rat sciatic nerve injury model

[1]Biomedical Engineering, AMIST, Asan Medical Center, [2]Orthop Surg, Asan Medical Center,
[3]Convergence Medicine, Asan Medical Institute of Convergence Science and Technology, Asan Medical Center,
[4]Center for Cell Therapy, Asan Medical Center,
[5]Bigdata Research Center, Asan Institute for Life Science, Asan Medical Center
Youngjae Kim[1,3], Won Sun Lee[2], Min-Young Jo[2], Chae–Min Ryu[4], Hyunna Lee[5], Jae Kwang Kim[2]

Background: The ankle angle at toe-off is a sensitive marker of neuromuscular recovery after peripheral nerve injury. However, in rats, this angle has traditionally been measured using labor-intensive, observer-dependent manual methods.

Purpose: To develop and validate a deep learning pipeline that automatically estimates the ankle angle and classifies gait phases in a rat model of sciatic-nerve microsurgery.

Methods: Forty-six Lewis rats were filmed walking on a transparent walkway at 4, 8, and 16 weeks post-surgery. From 29 videos (3,495 frames), a two-stage model was trained: Faster R-CNN extracted regions of interest, and Keypoint R-CNN detected three hind-limb landmarks to compute ankle angles. Gait phase was classified using a ResNet-50 model. Performance was evaluated on 688 frames from 17 independent videos.

Results: The mean Euclidean keypoint error across all phases was 4.84 ± 2.17 pixels (0.25% of frame width). The ankle angle mean absolute error ranged from 4.80° ± 4.69° (mid-stance) to 10.17° ± 8.76° (mid-swing). Gait phase classification achieved 85.6% overall accuracy, with recall exceeding 97% for the initial contact and toe-off phases. All computations were fully automated and reproducible, without the need for manual frame selection.

Conclusion: This is the first automated system for ankle angle analysis in a rodent nerve injury model, enabling scalable, objective assessment of functional recovery.

1. Introduction

Rat models are the most commonly used experimental animals in peripheral nerve research due to their low cost, ease of handling, and adaptability to diverse experimental conditions [1,2]. Among the various nerve injury models, the sciatic nerve model is particularly valuable for investigating nerve regeneration, repair, and defect reconstruction [3,4].

Despite their widespread use, evaluating functional outcomes in these models remains challenging. The sciatic functional index (SFI), first introduced by Medinaceli et al. [5] and later refined by Bain et al. [6], has been a widely adopted metric. However, SFI has several well-documented limitations, including susceptibility to contractures [7], autotomy [8], smearing of paw prints [7], and poor correlation with actual reinnervation [9]. To overcome these limitations, video-based gait analysis methods have been proposed [10-12], allowing for the quantification of parameters such as stance duration [13], toe-out angle [14], and ankle angle [11,15]. Notably, ankle angles have been analyzed across different gait phases, including mid-stance [16], mid-swing, and terminal stance [15,17]. Among these, the ankle angle at the toe-off phase has been uniquely correlated with isometric tetanic force, a robust marker of functional muscle recovery [18].

However, traditional measurements of these gait parameters typically rely on manual or semi-manual frame-by-frame annotations of locomotion videos, which are labor-intensive, time-consuming, and susceptible to observer bias and human error [19]. To address these challenges, the present study proposes a deep learning-based approach for automated ankle angle measurement. This method aims to enable faster, more consistent, and unbiased assessments of functional recovery in sciatic nerve injury models.

1.1 Related work

Recent advances in computer vision and deep learning have led to growing interest in automated, video-based gait analysis in animal models. Sheppard et al. [20] used a high-resolution convolutional neural network (HRNet) to overcome the limitations of standard open-field assays, analyzing gait metrics and posture across 62 mouse strains. Their platform enabled quantitative assessment of gait and postural abnormalities in disease models such as Rett syndrome, ALS, and Down syndrome, facilitating genome-wide association studies. Similarly, Weber et al. [21] used DeepLabCut with a ResNet-50 architecture for 3D gait analyses in mice recovering from stroke. Their AI-based system detected locomotor deficits that were previously overlooked by conventional tests and automated the ladder rung walking test, significantly enhancing the speed and objectivity of the analysis. Umansky et al. [22] integrated Visual Gait Lab with DeepLabCut to analyze hind paw angles and stance widths in peripheral nerve injury (PNI) models. Their method yielded more sensitive and consistent gait recovery metrics than the traditional SFI, with improved reproducibility and faster analysis times. Aljovic et al. [19] developed Automated Limb Motion Analysis using markerless pose estimation with DeepLabCut. This system computed 44 gait parameters and detected paw contact events without the need for markers or specialized equipment, demonstrating versatility

across models, including spinal cord injury, traumatic brain injury, and multiple sclerosis. Together, these studies highlight the broad applicability of AI-based approaches in rodent gait analysis, enabling precise tracking of limb movement and automated classification of gait phases and abnormalities using keypoint detection algorithms.

2. Results

2.1. Keypoints and angle predictions

Keypoint prediction performance was evaluated using the Euclidean distance between predicted and ground truth keypoint locations (in pixels), as well as the mean absolute error (MAE) of the angle formed by the three predicted keypoints. Table 1 presents the keypoint and angle prediction errors for the test dataset, grouped by gait cycle phase. For the keypoint at the lower third of the tibia, the prediction errors were 3.6 ± 2.1 px, 3.2 ± 1.4 px, 3.4 ± 1.8 px, and 4.5 ± 6.1 px for initial contact, mid-stance, toe-off, and mid-swing, respectively. For the calcaneus, the errors were 2.8 ± 3.2 px, 2.6 ± 1.5 px, 3.6 ± 4.4 px, 4.6 ± 5.7 px, while for the fifth metatarsal head, the errors were 6.5 ± 2.9 px, 6.6 ± 3.4 px, 6.9 ± 4.3 px, and 9.8 ± 7.8 px, respectively. Overall, the Euclidean errors were small relative to the original input frame size (1920×1080 pixels), with a mean error of 4.8 ± 2.2 px across all gait phases. The ankle angle prediction errors were 7.1 ± 5.8 º , 4.8 ± 4.7 º , 6.5 ± 7.4 º , and 10.2 ± 8.8 º for the four gait phases, with the highest error occurring in mid-swing and the lowest in mid-stance (Figure 1).

2.2. Gait cycle classification

The model's gait cycle classification performance was assessed based on per-frame predictions. Out of 688 test frames, the model correctly predicted the gait cycle phase for 589 frames, yielding an overall accuracy of 0.86. The precision, recall, and F1-score for each phase were as follows: 0.88, 0.99, and 0.93 for the initial contact phase; 0.85, 0.76, and 0.81 for mid-stance; 0.78, 0.98, and 0.87 for toe-off, 0.97, 0.68, and 0.80 for mid-swing. Recall was nearly perfect for initial contact and toe-off (0.98–0.99), but relatively lower for mid-stance and mid-swing (0.68–0.76) (Table 2). Figure 2 shows the confusion matrix for classification results, while Figure 3 provides representative frames with overlaid keypoint and gait phase predictions.

3. Discussion

The present study introduced a novel deep learning-based pipeline for automated ankle angle estimation in a rat sciatic nerve injury model. By integrating Faster R-CNN for ROI extraction, Keypoint R-CNN for anatomical landmark detection, and a ResNet-50 classifier for gait phase recognition, our method demonstrated robust performance. In quantitative evaluations, keypoint predictions exhibited low Euclidean distance errors, while angle estimations showed acceptable accuracy, with mean absolute errors ranging from 4.8 º (mid-stance) to 10.2 º (mid-swing). Notably, the toe-off phase, a clinically meaningful phase for functional recovery, had a mean error of 6.5 º . Additionally, the gait cycle classification model achieved a high overall accuracy of

85.6%, with particularly strong recall values (>97%) in critical phases such as initial contact and toe-off.

To date, no study has applied deep learning-based techniques to automatically quantify the ankle angle in a rodent PNI model. Previous gait studies relied on manual or semi-automated tools. For example, Matias Júnior et al. [23] semi-automatically identified the ankle angle at toe-off phase as a key indicator of sciatic nerve injury recovery; however, their Kinovea-based workflow required laborious frame-by-frame labeling. Deep learning-based gait analysis has gained momentum in other fields—Weber et al. [8] performed a comprehensive 3D gait analysis in post-stroke mice using the DeepLabCut platform, and Aljovic et al. [19] introduced Automated Limb Motion analysis to quantify locomotor deficits in models of SCI and traumatic brain injury. Despite these advancements, deep learning-based approaches remain rare in PNI research, where traditional measures still dominate [23]. By enabling fully automated ankle angle estimation from video, our study fills this methodological gap and extends deep learning-based gait analysis into a new domain [24].

Automated deep learning-based gait analysis substantially increases throughput and sensitivity in preclinical studies. The rapid and complex nature of rodent locomotion poses challenges for observers attempting to detect subtle gait changes in real time—even experienced analysts often overlook details detectable through video-based analysis [24,25]. Our pipeline enables rapid and objective processing of large volumes of gait data, automating event detection that formerly required manual annotation [23].

Automation also adds rigor and objectivity to functional gait assessment. Traditional neurologic scoring scales depend on subjective visual interpretation, making them prone to human error [25]. In contrast, deep learning models apply uniform, algorithm-driven criteria to each frame [21]. Moreover, such models can reveal subtle gait alterations that may not be perceptible to the human eye [19,21].

Several limitations should be acknowledged. First, the current model uses 2D single-camera video, which precludes analysis of out-of-plane motion and may omit depth-related kinetic information. Second, performance is sensitive to video quality; lower resolution, motion blur, or complex backgrounds may reduce prediction accuracy. These challenges are common to all image-based gait analysis techniques, manual or automated. Third, our network was trained on data acquired in a single experimental setup, which may limit its generalizability to other settings, camera angles, or rodent strains.

We developed and validated a fully automated deep learning-based workflow that directly measures the hind-limb ankle angle and classifies gait phases in rats following sciatic-nerve microsurgery. The system achieved sub-pixel keypoint accuracy, single-digit-degree angle precision, and over 85% phase classification accuracy. By addressing a critical methodological gap in PNI research, this pipeline enables large-scale, unbiased functional screening of regenerative therapies.

4. Methods

4.1. Overview

A deep learning-based pipeline was proposed, operating on a per-frame basis and comprising two main components: (1) ankle angle estimation, using keypoints detected to identify critical anatomical landmarks on the rat's hind limb, and (2) gait cycle classification, which predicts the gait phase of each frame based on foot position. A schematic diagram of the pipeline is shown in Figure 4.

4.2. Animal care and ethics

All procedures involving animals were conducted in accordance with the relevant institutional and national guidelines and regulations. Ethical approval was obtained from the Institutional Animal Care and Use Committee (IACUC) of Asan Medical Center and Ulsan University College of Medicine (IACUC-2023-20-086). This study also adheres to the principles outlined in the ARRIVE (Animal Research: Reporting of In Vivo Experiments) guidelines. Euthanasia was performed using carbon dioxide inhalation after completion of all experimental procedures.

4.3. Preparation and implantation of sciatic nerve allograft

Sciatic nerve allografts were harvested from donor Lewis rats and decellularized according to the protocol described by Shin et al. [26]. After anesthetization by intraperitoneal injection of Zoletil (tiletamine-zolazepam, 20 mg/kg; Virbac Laboratories, Carros, France), the operative left hind limb was shaved and disinfected with 75% ethanol. A longitudinal skin incision was made along the femoral axis, and the underlying gluteal/femoral musculature was bluntly separated to expose the sciatic nerve at mid-thigh level, adjacent to the obturator muscle. The nerve was transected, and a 10 mm segment was excised. Both proximal and distal stumps were refreshed to obtain sharply cut ends. A size-matched, decellularized graft, trimmed immediately to exactly 10 mm before implantation, was interposed and coapted using two interrupted 9-0 nylon epineural sutures under an operating microscope (Ethicon, Somerville, NJ). The muscle layer was reapproximated, and the skin was closed using wound clips before recovery. A schematic diagram of the procedure is shown in Figure 5.

4.4. Video recording

Toe-off ankle angle recordings were performed in 46 rats at 4, 8, and 16 weeks post-surgery to quantify functional recovery. Each animal traversed a transparent acrylic walkway (1 m long, 10 cm wide, 10 cm high) while being filmed from the side using a digital camera (PowerShot SX-HS, Canon, Japan) positioned 1 m laterally (resolution: 1920 × 1080 px; frame rate: 30 Hz). Filming continued until at least three uninterrupted strides were recorded. Both the operated (left) and contralateral (right) hind limbs were recorded, with the right limb serving as the control.

4.5.1. Training and Test datasets

For the training dataset, 29 out of the 46 recorded toe-off ankle angle videos were selected to ensure a balanced distribution across post-operative weeks (4, 8, and 16) and inclusion of control subjects. The remaining 17 videos were used as the test dataset.

To generate frame-based datasets, the videos were first converted into individual PNG frames and manually selected based on clarity and relevance, resulting in a total of 3,495 frames for the training dataset and 688 frames for the test dataset. Note that fewer frames were selected for the test dataset, as only clinically relevant frames were retained for meaningful evaluation. Each of these frames was manually annotated with three keypoints: the lower third of the tibia, the calcaneus, and the 5th metatarsal head, as well as one of the gait cycle phases: initial contact, mid-stance, toe-off, or mid-swing [1]. The annotation process was conducted using the LabelMe tool by one of our authors (M.Y.Jo).

In each gait cycle, four events were distinguished [27]. Initial contact is the instant the paw first touches the walkway surface. Mid-stance, for the limb in stance, refers to the point when that weight-bearing paw is overtaken by the contralateral paw that is still in swing. Toe-off is the instant this same stance paw leaves the ground, marking maximal plantarflexion. Mid-swing describes, for the limb now in swing, the moment when its airborne paw passes in front of the contralateral paw that is on the ground. These definitions apply symmetrically to both the left and right hind limbs.

The training dataset comprised 1,008 frames for initial contact, 915 frames for mid-stance, 913 frames for toe-off, and 659 frames for mid-swing. The test dataset similarly included 173, 173, 178, and 164 frames for each respective class, ensuring a balanced distribution across gait cycle phases in both datasets.

4.5.2. ROI extraction for model training

To eliminate unnecessary background and standardize input data, the region of interest (ROI) was extracted from each frame by detecting the rat and cropping the image to a fixed size. Faster R-CNN [28], a two-stage object detection model known for its accuracy and speed, was trained using 100 randomly selected frames from the training dataset, each manually annotated with bounding boxes to localize the rat. The trained model was then applied to generate bounding boxes for the remaining frames in the training and test datasets.

The resulting bounding boxes from the Faster R-CNN varied in size, necessitating a standardized cropping approach. A fixed crop size of 1024×1024 pixels was applied to ensure uniform image dimensions. The bounding box with the highest confidence score was selected, and its center was used as the reference point for ROI cropping. The extracted ROIs were then used as inputs for keypoint detection and gait cycle classification, enhancing robustness to background variability and improving computational efficiency.

4.5.3. Ankle angle estimation

The ankle angle can be measured by computing the internal angle formed by two connected lines derived from three keypoints of a rat's hind limb: the lower third of the tibia, calcaneus, and the 5th metatarsal head. Given three keypoints , , and , where represents the midpoint (., the calcaneus), two vectors were defined based on the sorted y-coordinates:

$$V_1 = (x_1 - x_2,\ y_1 - y_2) \quad \text{and}$$
$$V_2 = (x_3 - x_2,\ y_3 - y_2) \qquad (1)$$

The θ_{angle} between these two vectors was calculated using the dot product formula:

$$\theta_{ankle} = \cos^{-1}\left(\frac{V_1 \cdot V_2}{\|V_1\|\|V_2\|}\right), \qquad (2)$$

where:

$$\|V_1\| = \sqrt{(x_1 - x_2)^2 + (y_1 - y_2)^2} \quad \text{and}$$
$$\|V_2\| = \sqrt{(x_3 - x_2)^2 + (y_3 - y_2)^2} \qquad (3)$$

The computed ankle angle always lies within the range of , as it represents the included angle between the two vectors.

To obtain the three keypoints required for calculation, we trained a keypoint detection model, Keypoint R-CNN [29], which automatically predicts the coordinates of the lower third of the tibia, the calcaneus, and the 5th metatarsal head. The model was trained using ROI-extracted frames and corresponding ground truth keypoint annotations. Once the trained model generated keypoint predictions for each frame, the previously described angle computation method was applied to derive the ankle angle.

4.5.4. Gait cycle classification

To classify the current frame into one of the gait cycle phases—initial contact, mid-stance, toe-off, or mid-swing—a ResNet-50[30] model was trained, selected for its deep architecture and residual learning framework, which enables efficient feature extraction. The input to the classification model was a refined ROI, obtained by further cropping the original ROI. This refined ROI was generated based on the keypoints detected in the previous step, ensuring that the cropped image minimally enclosed all detected keypoints while maintaining a fixed size of 256×256 pixels. If the cropped region extended beyond the original image boundaries, zero-padding was applied to preserve the intended dimensions.

Model training was conducted using Pytorch framework on a NVIDIA TITAN RTX 24GB GPU. The full implementation, including training and inference code, can be found on GitHub at https://github.com/provbs/DL_AA_prediction.

4.6. Statistical analysis

For evaluation, the Euclidean distance was calculated to compare the predicted keypoints with the ground truth annotations. Similarly, the ankle angle computed from the predicted keypoints was assessed against the ground truth using the MAE. Additionally, to evaluate the performance of gait cycle classification, key metrics such as precision, recall, and F1-score were calculated for each class, along with overall accuracy across all test cases. A confusion matrix was also generated to provide a visual representation of the classification results.

Funding

This work was supported by the Korean Fund for Regenerative Medicine funded by the Ministry of Science and ICT, and Ministry of Health and Welfare (RS-2023-00215003); by the Asan Institute for Life Sciences, Asan Medical Center (No. 2025IP0029); and by a grant of the Korea Health Technology R&D Project through the Korea Health Industry Development Institute (KHIDI), funded by the Ministry of Health & Welfare, Republic of Korea (grant number : HR20C0026).

Data availability

Data is provided within the manuscript. The datasets used during the current study are available from the corresponding author on reasonable request.

Authorship contribution statement

Youngjae Kim : Writing – original draft, data curation
Won Sun Lee – Writing – original draft, investigation
Min-Young Jo : Data curation
Chae-Min Ryu : Data curation, Resources
Hyunna Lee : Writing – review & editing, software, methodology
Jae Kwang Kim : Writing – review & editing, conceptualization

Declaration of competing interest

The authors declare that they have no known competing financial interests or personal relationships that could have appeared to influence the work reported in this paper.

References

1. Rui, J. et al. Gait Cycle Analysis: Parameters Sensitive for Functional Evaluation of Peripheral Nerve Recovery in Rat Hind Limbs. Annals of Plastic Surgery 73, 405–411. https://doi.org/10.1097/sap.0000000000000008 (2014).
2. Mackinnon, S. E., Dellon, A. L., Hudson, A. R. & Hunter, D. A. Chronic nerve compression–an experimental model in the rat. Ann Plast Surg 13, 112–120. https://doi.org/10.1097/00000637-198408000-00004 (1984).

3. Mackinnon, S. E., Hudson, A. R. & Hunter, D. A. Histologic assessment of nerve regeneration in the rat. Plast Reconstr Surg 75, 384–388. https://doi.org/10.1097/00006534-198503000-00014 (1985).
4. Madorsky, S. J., Swett, J. E. & Crumley, R. L. Motor versus sensory neuron regeneration through collagen tubules. Plastic and reconstructive surgery 102, 430–436. (1998).
5. de Medinaceli, L., Freed, W. J. & Wyatt, R. J. An index of the functional condition of rat sciatic nerve based on measurements made from walking tracks. Exp Neurol 77, 634–643. https://doi.org/10.1016/0014-4886(82)90234-5 (1982).
6. Bain, J. R., Mackinnon, S. E. & Hunter, D. A. Functional evaluation of complete sciatic, peroneal, and posterior tibial nerve lesions in the rat. Plast Reconstr Surg 83, 129–138. https://doi.org/10.1097/00006534-198901000-00024 (1989).
7. Dellon, A. L. & Mackinnon, S. E. Sciatic nerve regeneration in the rat. Validity of walking track assessment in the presence of chronic contractures. Microsurgery 10, 220–225. https://doi.org/10.1002/micr.1920100316 (1989).
8. Weber, R. A., Proctor, W. H., Warner, M. R. & Verheyden, C. N. Autotomy and the sciatic functional index. Microsurgery 14, 323–327. https://doi.org/10.1002/micr.1920140507 (1993).
9. Shenaq, J. M., Shenaq, S. M. & Spira, M. Reliability of sciatic function index in assessing nerve regeneration across a 1 cm gap. Microsurgery 10, 214–219. https://doi.org/10.1002/micr.1920100315 (1989).
10. Dijkstra, J. R., Meek, M. F., Robinson, P. H. & Gramsbergen, A. Methods to evaluate functional nerve recovery in adult rats: walking track analysis, video analysis and the withdrawal reflex. J Neurosci Methods 96, 89–96. https://doi.org/10.1016/s0165-0270(99)00174-0 (2000).
11. de Ruiter, G. C. et al. Two-dimensional digital video ankle motion analysis for assessment of function in the rat sciatic nerve model. J Peripher Nerv Syst 12, 216–222. https://doi.org/10.1111/j.1529-8027.2007.00142.x (2007).
12. Santos, P. M., Williams, S. L. & Thomas, S. S. Neuromuscular evaluation using rat gait analysis. J Neurosci Methods 61, 79–84. https://doi.org/10.1016/0165-0270(95)00026-q (1995).
13. Meek, M. F., Den Dunnen, W. F., Schakenraad, J. M. & Robinson, P. H. Long-term evaluation of functional nerve recovery after reconstruction with a thin-walled biodegradable poly (DL-lactide-epsilon-caprolactone) nerve guide, using walking track analysis and electrostimulation tests. Microsurgery 19, 247–253. https://doi.org/10.1002/(sici)1098-2752(1999)19:5<247::aid-micr7>3.0.co;2-e (1999).
14. Varejão, A. S. et al. Toe out angle: a functional index for the evaluation of sciatic nerve recovery in the rat model. Exp Neurol 183, 695–699. https://doi.org/10.1016/s0014-4886(03)00208-5 (2003).
15. Yu, P., Matloub, H. S., Sanger, J. R. & Narini, P. Gait analysis in rats with peripheral nerve injury. Muscle Nerve 24, 231–239. https://doi.org/10.1002/1097-4598(200102)24:2<231::aid-mus80>3.0.co;2-5 (2001).
16. Lin, F. M., Pan, Y. C., Hom, C., Sabbahi, M. & Shenaq, S. Ankle stance angle: a functional index for the evaluation of sciatic nerve recovery after complete transection. J Reconstr Microsurg 12, 173–177. https://doi.org/10.1055/s-2007-1006472 (1996).
17. Patel, M. et al. Video-gait analysis of functional recovery of nerve repaired with chitosan nerve guides.

Tissue Eng 12, 3189–3199. https://doi.org/10.1089/ten.2006.12.3189 (2006).
18. Lee, J.-Y. et al. Functional Evaluation in the Rat Sciatic Nerve Defect Model: A Comparison of the Sciatic Functional Index, Ankle Angles, and Isometric Tetanic Force. Plastic and Reconstructive Surgery 132, 1173–1180. https://doi.org/10.1097/PRS.0b013e3182a3bfeb (2013).
19. Aljovic, A. et al. A deep learning-based toolbox for Automated Limb Motion Analysis (ALMA) in murine models of neurological disorders. Communications Biology 5, 131. https://doi.org/10.1038/s42003-022-03077-6 (2022).
20. Sheppard, K. et al. Stride-level analysis of mouse open field behavior using deep-learning-based pose estimation. Cell Rep 38, 110231. https://doi.org/10.1016/j.celrep.2021.110231 (2022).
21. Weber, R. Z., Mulders, G., Kaiser, J., Tackenberg, C. & Rust, R. Deep learning-based behavioral profiling of rodent stroke recovery. BMC Biology 20, 232. https://doi.org/10.1186/s12915-022-01434-9 (2022).
22. Umansky, D. et al. Functional Gait Assessment Using Manual, Semi-Automated and Deep Learning Approaches Following Standardized Models of Peripheral Nerve Injury in Mice. Biomolecules 12. https://doi.org/10.3390/biom12101355 (2022).
23. Matias Júnior, I. et al. Effective Parameters for Gait Analysis in Experimental Models for Evaluating Peripheral Nerve Injuries in Rats. Neurospine 16, 305–316. https://doi.org/10.14245/ns.1836080.040 (2019).
24. Basso, D. M., Beattie, M. S. & Bresnahan, J. C. A sensitive and reliable locomotor rating scale for open field testing in rats. J Neurotrauma 12, 1–21. https://doi.org/10.1089/neu.1995.12.1 (1995).
25. Isvoranu, G., Manole, E. & Neagu, M. Gait Analysis Using Animal Models of Peripheral Nerve and Spinal Cord Injuries. Biomedicines 9. https://doi.org/10.3390/biomedicines9081050 (2021).
26. Shin, Y. H., Park, S. Y. & Kim, J. K. Comparison of systematically combined detergent and nuclease-based decellularization methods for acellular nerve graft: An ex vivo characterization and in vivo evaluation. Journal of Tissue Engineering and Regenerative Medicine 13, 1241–1252. https://doi.org/https://doi.org/10.1002/term.2874 (2019).
27. De Ruiter, G. C. et al. Two-dimensional digital video ankle motion analysis for assessment of function in the rat sciatic nerve model. Journal of the Peripheral Nervous System 12, 216–222. https://doi.org/https://doi.org/10.1111/j.1529-8027.2007.00142.x (2007).
28. Ren, S., He, K., Girshick, R. & Sun, J. Faster r-cnn: Towards real-time object detection with region proposal networks. Advances in neural information processing systems 28. (2015).
29. He, K., Gkioxari, G., Dollár, P. & Girshick, R. Mask r-cnn. In Proceedings of the IEEE international conference on computer vision. 2961–2969.
30. He, K., Zhang, X., Ren, S. & Sun, J. Deep residual learning for image recognition. In Proceedings of the IEEE conference on computer vision and pattern recognition. 770–778.

Figure legends

Figure 1. Box plots of (a) keypoint errors (in pixels) and (b) angle errors (in degrees).
Figure 2. Confusion matrix for gait cycle classification results. The matrix compares the ground truth and predicted gait phases for each frame of the test set. Higher values along the diagonal indicate greater classification accuracy, reflecting correct phase identification.
Figure 3. Example frames with overlaid predictions. Each frame displays predicted keypoints (light green), keypoint vectors (blue), the computed ankle angle (red), and a bar graph indicating the predicted gait phase. In both (a) and (b), the predicted gait phase matches the ground truth.
Figure 4. Schematic diagram illustrating the workflow of our proposed method.
Figure 5. Schematic diagram of sciatic nerve allograft implantation in a rat.

Tables

Table 1. Gait cycle class-wise errors for keypoints and ankle angle

Gait cycle class	Keypoint errors (Euclidean distance)[a]			Angle error (MAE)[b]
	Lower third of the tibia	Calcaneus	5th metatarsal head	
Initial contact	3.56 ± 2.05	2.84 ± 3.21	6.50 ± 2.91	7.10 ± 5.78
Mid-stance	3.17 ± 1.42	2.63 ± 1.45	6.60 ± 3.37	4.80 ± 4.69
Toe-off	3.37 ± 1.80	3.63 ± 4.41	6.93 ± 4.32	6.48 ± 7.43
Mid-swing	4.52 ± 6.12	4.60 ± 5.68	9.78 ± 7.77	10.17 ± 8.76

All data are mean ± standard deviation.
[a]Data are in pixels (px).
[b]Data are in degrees (ㅇ).

Table 2. Evaluation metrics assessed on the test set frames

Gait cycle class	Precision	Recall	F1-score
Initial contact	0.88 (171/195)	0.99 (171/172)	0.93
Mid-stance	0.85 (132/155)	0.76 (132/173)	0.81
Toe-off	0.78 (174/222)	0.98 (174/178)	0.87
Mid-swing	0.97 (112/115)	0.68 (112/164)	0.80

Data in the parentheses represent the number of cases used to compute each value.

Effect of Decellularized Amniotic Membrane Hydrogels on Enhanced Wound Healing in a UVB-Induced Burn Model in Rats

[1]Center for Biomaterials, Biomedical Research Institute, Korea Institute of Science and Technology (KIST), [2]Orthop Surg. Korea Univ. [3]Applied Bioengineering, Graduate School of Convergence Science and Technology, Seoul National Univ.

Seongryeol Ye[1,3], Yu-Jin Kim[1], Jin Yoo[1], Kangwon Lee[3], Jae Jun Nam[2], Yeungyoon Ko[2], In Cheul Choi[2], Youngmee Jung[1], Jong Woong Park[2]

Background and purpose: Ultraviolet (UV) radiation exposure induces various skin damages, including sunburns, skin cancer, and erythema. UVB, in particular, significantly contributes to inflammatory skin conditions. However, current treatment methods using hydrogel wound dressings aim to maintain a moist environment. Recently, researchers have attempted to develop hydrogels containing therapeutically effective substances. In this study, we developed an inflammation-relieving hydrogel containing bioactive substances using an decellularized porcine amniotic membrane (AM).

Methods: The AM, serving as the innermost membrane protecting the fetus, possesses bioactive properties such as abundant cytokines and growth factors related to anti-inflammatory and pro-angiogenic processes. We utilized decellularization of porcine AM (dPAM) using supercritical fluid carbon dioxide ($scCO_2$) to fabricate the ECM hydrogels. Then, we evaluated the levels of Decorin, Interleukin-28B, and Vascular Endothelial Growth Factor as critical factors regulating inflammation and tissue regeneration during the wound healing process. The dPAM fabricated by the $scCO_2$ process was assessed for DNA content, the quantities of collagen and glycosaminoglycan (GAG), and growth factor retention. In vitro tests involved assessing tubule formations using human umbilical vein endothelial cells (HUVEC) cultured with dPAM hydrogels. Also, the effects of pro-angiogenesis and inflammation regulation were examined in a UVB-induced inflammation skin animal model.

Results: The dPAM fabricated using the scCO2 process showed reduced DNA content, yet maintained levels of collagen, GAG, and growth factors comparable to native PAM. In vitro experiments validated improved tubule formation with dPAM hydrogels. Additionally, the therapeutic efficacy of dPAM was confirmed in inflammation wound healing by modulating macrophage phenotypes. In vivo evaluations demonstrated pro-angiogenic and inflammation-regulating effects conducive to wound healing in a UVB-induced inflammation skin animal model.

Conclusion: The fabricated dPAM hydrogel demonstrates high potential in alleviating inflammation and

promoting pro-angiogenesis for wound healing. This highlights the promising utility of dPAM as an advanced therapeutic approach for addressing inflammatory skin conditions.

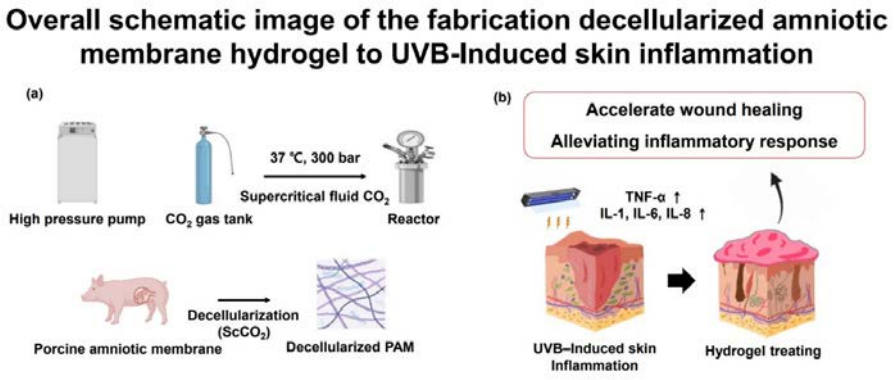

a, Supercritical carbon dioxide ($scCO_2$) decellularization method to porcine amniotic membrane. **b,** An overview of the therapeutic effect of decellularized amniotic membrane hydrogels to UVB-Induced skin inflammation.

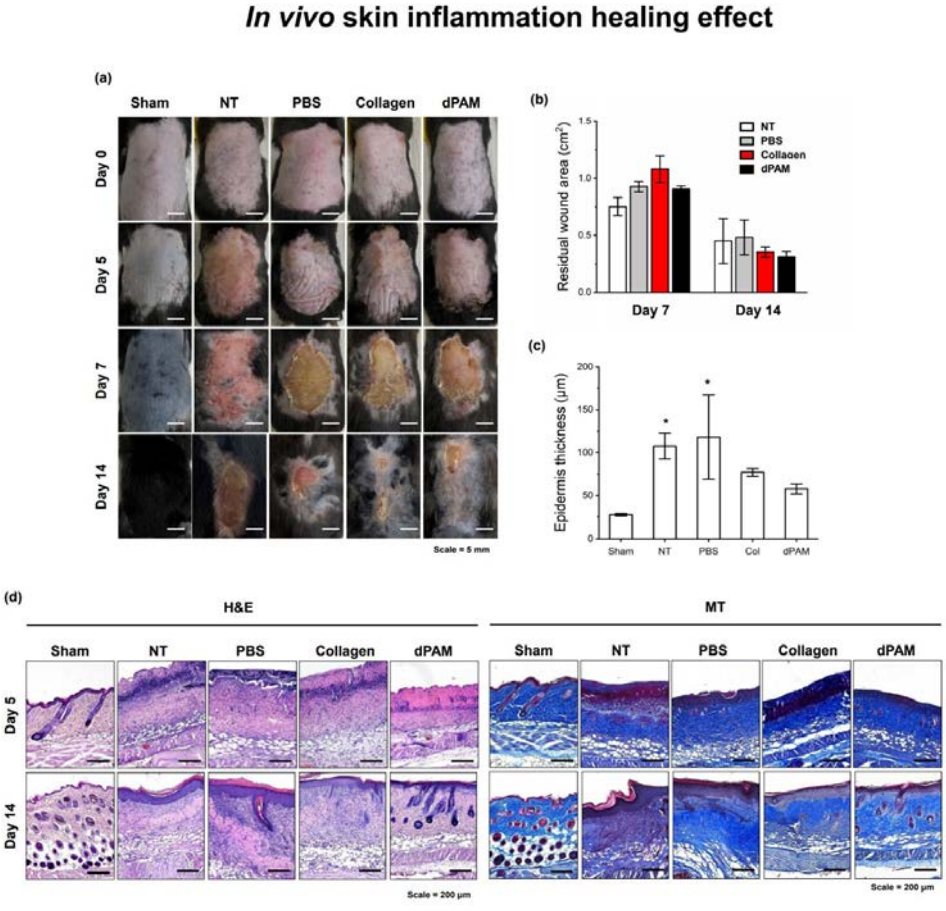

Fig 4. In vivo skin inflammation healing studies. **a,** Representative images of the wound on days 0, 5, 7, and 14 following the various treatments. **b,** Quantification of the residual wound area on day 14 (n = 3). **c,** Estimation of epidermis thicknesses of day 14 H&E stained images (n = 3).**d,** Representative H&E stained images of various treated wounds on day 5 and day 14. **e,** Representative MT stained images of various treated wounds on day 5 and day 14. All error bars are presented as mean ± SD. P-values were analyzed by one-way ANOVA with Tukey's post-hoc test. *p < 0.05, compared with that in the control group; #p < 0.05, compared with each group.

Strategy for Donor Nerve Selection in Nerve Transfers with an Emphasis on Functional Preservation

E-Da Hospital / I-Shou University
Yu-Huan Hsueh (Oscar)

2025년 대한수부외과학회
추계학술대회

Room A

NOVOSIS Trauma (rh BMP-2), JNJ MedTech

[Industrial Session]

W General Hosp. **Kyung-Chul Kim**
Orthop Surg. Konkuk Univ. **Seoung Joon Lee**

Bone Graft Option in Orthopedic Trauma, Challenging the Orthopedic Dogma

Orthop Surg. Korea Univ.
Jong-Keon Oh

2025년 대한수부외과학회
추계학술대회

Room A

Travelling Fellowship Report

Plast Reconstr Surg. Wonkwang Univ. **Young Cheon Na**
Plast Reconstr Surg. Ewha Womans Univ. **Bo Young Park**

Remarkable Moments in HKSSH 2025

Orthop Surg. Eulji Univ.
Seong Ju Choi

Remarkable Moments in TSSH 2025

Orthop Surg. Chung-Ang Univ.
Hyoung-Seok Jung

Remarkable Moments in JSSH 2025

Orthop Surg. Yonsei Univ.
Yun Rak Choi

Remarkable Moments in ASSH 2025

Orthop Surg. Ulsan Univ.
Young Ho Shin

2025년 대한수부외과학회

추계학술대회

역경에도 손을 맞잡고
Against All Odds, Hand in Hand

Room B

3F, Graduate School
of Public Health, Room 337

2025년 대한수부외과학회
추계학술대회

Room B

Free Paper 1

(Nationwide Study)

Orthop Surg. CHA Univ. **Soo-Hong Han**
Plast Reconstr Surg. Yonsei Univ. **Hii-Sun Jeong**

Trends in mean hand grip strength, cutoff value, and prevalence of low hand grip strength : An analysis of 2014–2019 Korea National Health and Nutrition Examination Survey (KNHANES) data

Orthop Surg. Chungnam National Univ.
Yun Ki Kim

The EWGSOP2 defines probable sarcopenia as low muscle strength detected by hand grip strength (HGS). According to this guideline, cutofff or low HGS is determined using a T-score of –2.5 based on age group showing the highest HGS (aged30– 39years). Our hypothesis is that temporal changes in mean HGS of Koreans may lead to changes in the cutoff values for low HGS and the prevalence of probable sarcopenia as defined by the EWGSOP2 guidelines.

We analyzed trends of HGS using 6 years of Korea National Health and Nutrition Examination Survey data. We used the EWGSOP2 guidelines to set yearly cutoff values for low HGS and calculated the prevalence of low HGS. The cutoff value for low HGS and the prevalence rate of low HGS in individuals aged 70 years or older were analyzed using linear regression and trend analysis.

We observed a significant decreasing trend from 2014 to 2019 in annual cutoff values for low HGS, ranging from 24.5 to 30.9 kg in men and 13.1–17.3 kg in women. Correspondingly, the prevalence of low HGS (probable sarcopenia) varied significantly from 10.4 to 34.2% in men and 9.1–20.8% in women, indicating notable year-to-year fluctuations ($p < 0.001$). While pooling multiyear data reduces some variability, it does not fully address fluctuations in prevalence of probable sarcopenia.

To enhance the reliability and clinical relevance of low HGS cutoff values, future guidelines should integrate outcome-based criteria with normative data, ensuring adaptability to temporal trends and population-specific characteristics.

What was different before and in COVID-19 pandemic in management of distal radius fracture aged over fifty: South Korea Nationwide Analysis Using Korea Health Insurance Dataset

Orthop Surg. Eulji Univ.
Seong Ju Choi

Background: The outbreak of COVID-19 is likely to have affected bone health in the elderly population in Korea. This study aims to analyze changes in the epidemiology and management of distal radius fractures in old age before and after COVID-19.

Methods: Patients with distal radius fractures, aged over 50 years in 2017, 2018, 2020, and 2021 were included in this study. Patients were classified into a group with distal radius fractures occurring between 2017 and 2018 (before COVID-19) and a group with distal radius fractures occurring between 2020 and 2021 (after COVID-19). We calculated the incidence rates of distal radius fracture and compared them between two groups. Also, we analyzed and compared the demographic data (age, sex, income, residence) and the operation rate of distal radius fracture between the two groups. Patient selection and treatment were based on ICD-10.

Results: A total of 140,763 patients with distal radius fracture (before COVID-19 = 69,906, after COVID-19 = 70,857) were included in this study. The incidence of distal radius fracture before COVID-19 (184.4/100,000 person-years) was higher than after COVID-19 (169.8/100,000 person-years). The operation rate was higher after COVID-19 (86.9%) than before COVID-19 (83.2%). Other demographics did not show significant differences between the two groups.

Conclusions: After the COVID-19 pandemic the incidence of distal radius fractures has decreased in South Korea. However, the rate of surgical treatment has increased, which is higher than the global surgical rate.

Level of Evidence: Prognostic – III Retrospective cohort study

Diagnostic Coding and Conservative Treatment Duration for Traumatic Triangular Fibrocartilage Complex Tears: A Survey of Korean Society for Surgery of the Hand

Orthop Surg. Yonsei Univ.
Yong Hyun Yoon

Background: Triangular fibrocartilage complex (TFCC) injuries are clinically significant, yet standardized diagnostic coding and treatment guidelines remain lacking—particularly regarding the optimal duration of conservative management before surgery. This study assessed current practices among Korean hand surgeons concerning diagnostic coding and conservative treatment for traumatic TFCC tears.

Methods: An online survey was distributed to 88 selected members of the Korean Society for Surgery of the Hand (KSSH). The questionnaire addressed diagnostic code selection for acute and chronic traumatic TFCC tears, and the recommended duration of conservative treatment. Multiple responses were permitted. Subgroup analyses considered clinical experience, hospital type, subspecialty certification, and board membership.

Results: Sixty-two hand surgeons responded (70.4% response rate). For acute TFCC tears, 76.8% selected code S63.3 (Traumatic rupture of ligament of wrist and carpus), and 53.8% recommended 3 months of conservative treatment. Chronic TFCC tears showed more variable coding, with increased use of M24.23 and unspecified codes. Subspecialists more consistently selected S63.3 for acute tears ($p = 0.040$), but no significant subgroup differences were observed regarding treatment duration or chronic tear coding.

Conclusion: Most Korean hand surgeons favor S63.3 for acute TFCC injuries and recommend a 3-month conservative treatment period. However, the variability in chronic coding and treatment practices underscores the need for TFCC-specific codes and unified clinical guidelines to support standardized care and administrative accuracy.

Wrist Arthroscopy in South Korea: Utilization, Disparities, and Complications from an 11-Year Nationwide Cohort

[1]Orthop Surg. National Health Insurance Service Ilsan Hosp., [2]Orthop Surg. Korea Univ., [3]Orthop Surg. Eulji Univ.
Hyun Tak Kang[1], Chi-Hoon Oh[2], SeongJu Choi[3], Jun-Ku Lee[1]

Purpose: To investigate nationwide trends, demographic and regional disparities, and postoperative complication rates associated with wrist arthroscopy in South Korea using a large-scale national claims database.

Material and methods: We conducted a retrospective nationwide analysis using Korean National Health Insurance claims data from 2013 to 2023. Procedures were categorized into diagnostic arthroscopy (P1), partial joint debridement or synovectomy (P2), and ligament or tendon reconstruction (P3). Trends were assessed by year, age, sex, region, and income level, with incidence rates calculated per 100,000 persons. Postoperative complications were also evaluated, including nerve injury, tendon injury, infection, and complex regional pain syndrome (CRPS).

Results: A total of 227,693 wrist arthroscopic procedures were identified. While overall volume remained stable, a temporary decline occurred during the COVID-19 pandemic. Over time, the proportion of P3 procedures increased, indicating broader adoption of advanced techniques. The 50–59 age group had the highest total volume, but the highest incidence of P3 procedures in 2023 was seen in the 20–29 group. Men increasingly underwent P3 procedures over time. No consistent income-related disparity was observed, but regional variation was present. The overall incidence of complications was low: 2.12% for infection, 1.14% for tendon injury, 2.00% for CRPS, and 0.11% for nerve injury.

Conclusion: This nationwide study demonstrates evolving trends in wrist arthroscopy in South Korea, with increasing use of complex procedures and low complication rates. These findings support the safety, accessibility, and expanding role of wrist arthroscopy in modern orthopedic practice.

Keywords: Wrist arthroscopy; National health insurance; Epidemiology; Postoperative complications; Surgical trends; Socioeconomic disparities

An 11-Year Nationwide Analysis of Infection related Complications After Wrist Arthroscopy : A Nationwide Population-Based Study in South Korea (2013–2023)

[1]Orthop Surg. Yonsei Wonju Univ., [2]Orthop Surg. Eulji Univ.,
[3]Orthop Surg. National Health Insurance Service Ilsan Hosp., [4]Orthop Surg. Yonsei Univ.
Jisu Park[1], Jun-Ku Lee[3,4], SeongJu Choi[2], Jin Rok Oh[1]

Background: Wrist arthroscopy has become an established surgical modality for diagnosis and treatment of various wrist disorders. Postoperative infection has been considered uncommon, with previous reports indicating an incidence of approximately 1%. However, these estimates are largely derived from single-center studies with limited sample sizes. A nationwide population-based analysis is warranted to determine the true incidence and to specify risk factors. We hypothesized that the reported low infection rate may not be fully reproducible in nationwide practice and that specific patient-, procedure-, and institution-related variables may be associated with increased risk.

Methods: We performed a retrospective cohort analysis using the South Korean National Health Insurance Service database. All patients who underwent wrist arthroscopy between 2013 and 2023 were identified, excluding those with concomitant ulnar shortening osteotomy. Postoperative infection within 30 days was determined using ICD-10 diagnostic codes including surgical site infection, infective tenosynovitis, abscess formation, septic arthritis, and osteomyelitis. Infections were categorized as superficial (antibiotic treatment ≥7 days) or deep (reoperation within 3 months in addition to antibiotics). Demographics, comorbidities, surgical details, and hospital characteristics were evaluated. Multivariable logistic regression was used to identify independent variables, with results presented as adjusted odds ratios (aOR) and 95% confidence intervals.

Results: The overall 10-year incidence of infection after wrist arthroscopy will be reported. Comparisons between infection and non-infection groups will clarify demographic and clinical differences. Multivariable models will determine independent predictors such as comorbidities, surgical complexity, and institutional factors. Temporal trends in infection rates between 2013 and 2023 will also be analyzed.

Conclusion: This nationwide population-based study will provide evidence on the incidence, risk factors, and temporal patterns of infection following wrist arthroscopy. The results will help clinicians recognize high-risk patients, inform perioperative decision-making, and improve safety in arthroscopic wrist surgery.

Key words: Wrist arthroscopy, Postoperative infection, Nationwide cohort, Risk factors, National Health Insurance Service (NHIS), Epidemiology, South Korea

Wrist Arthroscopic Management of Triangular Fibrous Cartilage Complex and Ligament Injury – South Korea Nationwide Study

[1]Orthop Surg. Korea Univ., [2]Orthop Surg. Eulji Univ.,
[3]Orthop Surg. National Health Insurance Service Ilsan Hosp., [4]Orthop Surg. Yonsei Univ.
Chi-Hoon Oh[1], SeongJu Choi[2], Hyun Tak Kang[3], Jun-Ku Lee[3,4]

Background: Traumatic tears of the triangular fibrocartilage complex (TFCC) are a common cause of ulnar-sided wrist pain and distal radioulnar joint instability. Arthroscopic TFCC repair has advanced, yet the optimal duration of preoperative conservative management remains unclear at a population level.

Methods: Using the National Health Insurance Service/Health Insurance Review & Assessment (NHIS/HIRA) database in South Korea, we identified adults (≥19 years) with a first diagnosis code S63.3 (traumatic rupture of ligament of wrist) between 2013 and 2021. Patients with distal radius fracture were excluded by ICD-10 diagnosis and procedure codes. We observed a 2-year window from diagnosis to ascertain arthroscopic surgery—N0703/N0708 (arthroscopic joint excision ± synovectomy) and N0931/N0932 (arthroscopic tendon/ligament repair)—and followed for 1 year after surgery to identify USO (N0304) as reoperation. Preoperative conservative duration was categorized as ≤30, 31–60, 61–90, 91–180, 181–365, and 366–730 days.

Results: A total of 8,814 patients underwent arthroscopic surgery after S63.3 diagnosis. Annual surgical volume increased toward 2021 with a proportional shift from N0703/N0708 toward N0931/N0932. Most patients proceeded to arthroscopy within 30 days of diagnosis (66.5%). Reoperation with USO within 1 year after arthroscopy occurred in 230 patients (2.6%).

Conclusions: Arthroscopic management of traumatic TFCC injury is increasingly utilized nationwide, with a contemporary preference for repair/reconstruction over debridement. Most patients underwent arthroscopy within 30 days of diagnosis and 1-year revisional ulnar shortening was uncommon, supporting effectiveness and safety. However, the optimal duration of preoperative conservative treatment remains uncertain and needs further trials to define optimal timing

Keywords: triangular fibrocartilage complex; wrist arthroscopy; conservative management; claims database; Korea.

2025년 대한수부외과학회
추계학술대회

Room B

Free Paper 3 (Elbow)

Orthop Surg. Yeungnam Univ. **Sam Guk Park**
Orthop Surg. Hanyang Univ. **Joo Hak Kim**

Clinical outcomes and risk factors for platelet-rich plasma injections in lateral epicondylitis

[1]Orthop Surg. Chung-Ang Univ., [2]Radiology. Chung-Ang Univ.
Min Su Chu[1], Jae-Sung Lee[1], Guen Young Lee[2], Hyoung-Seok Jung[1]

Background: Lateral epicondylitis is the one of the most common disorder affecting the elbow, and platelet-rich plasma (PRP) injections have been increasingly reported to offer favorable outcomes. However, not all patients experience satisfactory improvement, and studies investigating the risk factors associated with suboptimal response to PRP therapy remain limited. This study aimed to evaluate the clinical efficacy of platelet-rich plasma (PRP) in the treatment of lateral epicondylitis and to identify risk factors associated with suboptimal outcomes.

Methods: This retrospective study included 70 patients with lateral epicondylitis who underwent PRP injection after failing at least four weeks of conservative treatment. PRP was prepared using a standardized commercial kit and administered according to a consistent protocol. Clinical status before and after treatment was assessed using the Patient-Rated Tennis Elbow Evaluation (PRTEE) score, with a six-month follow-up serving as the primary endpoint. Ultrasound was used to evaluate tendon thickness, Doppler activity, and calcification. Simple radiographs were reviewed for the presence of soft tissue or enthesophytic calcification. Clinical and radiographic factors were analyzed using univariate and multivariate analyses.

Results: Among the 70 patients, PRP injection led to a significant improvement in PRTEE scores at six months (from 55.25 to 26.23, $p < 0.001$). Overall, 50 and 20 patients demonstrated good and poor functional outcomes, respectively, assessed according to the minimal clinically important difference of the PRTEE. On univariate analysis, patients with poor functional outcomes had a significantly higher prevalence of calcification (55% vs. 12%, $p = 0.013$) and tended to have a longer symptom duration (14.3 months vs. 8.7 months, $p = 0.006$). However, multivariate analysis identified the presence of calcification as the only independent risk factor for a suboptimal response (odds ratio: 3.87, $p = 0.015$).

Conclusion: PRP injection yields favorable outcomes in most patients with refractory lateral epicondylitis. However, radiologically detected calcification is a significant risk factor for a poor clinical response and should be considered when counseling patients or planning treatment.

Long term outcomes of Kudo type total elbow arthroplasty in rheumatoid arthritis

[1]Orthop Surg. Hanyang Univ., [2]Orthop Surg. Ajou Univ., [3]MS Reconstruction Hosp.
이창훈[1], 이영석[1], 최완선[2], Jin Sik Park[3], Joo Hak Kim[1]

Introduction : Total elbow arthroplasty(TEA) has been used for various conditions including rheumatoid arthritis (RA). While the Kudo TEA has been associated with favorable short-term outcomes, there is limited evidence on the long-term outcome of this device. The aim of this study is to investigate the long term outcomes of Kudo type TEA in patients with RA.

Methods: For this retrospective cohort study, we reviewed 32 patients with RA who underwent Kudo type TEA between 1996 and 2007. The patients were followed up for a mean of 10 (5-20)years. We investigated the survival with setting revision/removal as the end points.

Results: There was a significant improvement in elbow flexion after Kudo TEA. Preoperative and postoperative Mayo Elbow Performance Score improved significantly from 55 to 83. Aseptic loosening was observed in 5 patients (15.6%; ulna, n=2, both, n=3) Two patients underwent revision TEA due to periprosthetic fracture and metallosis, respectively. The survival rate was 94% at 10 years after surgery with stetting revision / removal as the endpoints.

Conclusions: The Kudo type TEA showed good results for up to long-term follow-up in the patients with RA.

Comparison of outcomes between primary total elbow arthroplasty and plate osteosynthesis in distal humerus fractures with concomitant osteoporosis

Orthop Surg. Chonnam National Univ.
Jun-Hyuk Lim, Myung-Sun Kim

Introduction: The aim of this study is to compare the functional and radiographic outcomes of total elbow arthroplasty and open reduction and internal fixation (ORIF) in patients with distal humerus fractures (DHF) accompanied by osteoporosis, with a follow-up period of at least three years.

Materials and methods: We conducted a retrospective analysis of 150 patients diagnosed with DHF who underwent surgical intervention between January 2005 and December 2019. We included 46 patients with a DEXA score of -2.5 or lower, followed for more than three years, and excluded those with nonunion or requiring revision surgery. The study consisted of 33 patients in the ORIF group and 13 patients in the TEA group. Functional outcomes included elbow motion assessments and scores from the Mayo Elbow Performance Score (MEPS), Disabilities of the Arm, Shoulder, and Hand (DASH), and pain measured by the visual analog scale (VAS). Radiographic outcomes assessed periprosthetic fractures, implant loosening, and infections.

Results: After more than three years of follow-up, the ORIF group reported significantly lower pain VAS scores compared to the TEA group. Functional outcomes as measured by MEPS and DASH scores showed no significant differences between the groups, although the TEA group scored higher in the motion subgroup of the MEPS. In terms of radiographic outcomes, aseptic loosening was observed in 30.8% of the TEA group, with none in the ORIF group. Ulnar nerve symptoms were similar in both groups.

Conclusion: No significant differences were found in functional outcomes between TEA and ORIF in patients with DHFs and osteoporosis. However, the TEA group exhibited poor radiographic outcomes, primarily due to high rates of aseptic loosening. Therefore, caution is advised when considering primary TEA as the first treatment option for osteoporotic DHFs.

Clinical comparison of single posterolateral plate with medial cannulated screw fixation and double plate fixation for extra-articular distal humerus fractures

Orthop Surg. Chung-Ang Univ.
Hyoung-Seok Jung[1], Min Su Chu[2], Jae-Sung Lee[2]

ground: Double plate fixation is the gold standard for extra-articular distal humerus fractures but is associated with significant ulnar neuropathy risk. Single posterolateral plate with medial cannulated screw fixation may reduce nerve complications while maintaining fracture stability. This study aimed to compare the clinical effectiveness of single plate with medial screw fixation versus double plate fixation for extra-articular distal humerus fractures.

Methods: Fifty-six patients who underwent surgery for extra-articular distal humerus fractures (AO/OTA classification A2 and A3) between January 2018 and August 2024 were divided into double plate and single plate with medial screw groups. The double plate approach was used in 30 patients, and the single plate with medial screw approach was used in 26 patients. All surgeries were performed using a posterior paratricipital approach. Bony union, radiographic healing, and loss of reduction were evaluated. Postoperative pain score (visual analog scale at 2 days after the operation), surgical time (minutes), range of motion of the elbow, elbow function (Mayo Elbow Performance Score [MEPS]), and the presence of postoperative ulnar neuropathy were compared between the two groups.

Results: The double plate and single plate with medial screw approaches were performed in 30 and 26 patients, respectively. The mean age was 54.8 ± 19 years (range, 17–85 years), and the mean follow-up duration was 18.2 ± 6.5 months (range, 12–38 months). All fractures achieved solid osseous union during follow-up. There were no significant differences between the groups in terms of postoperative pain score, range of motion, and MEPS (all $p > 0.05$). However, the surgical time was shorter for the single plate with medial screw approach than that for the double plate approach (112.5 ± 25.7 versus 172.2 ± 35.2 minutes, $p < 0.05$), and the surgical time was significantly associated with the fixation method ($p < 0.05$). In addition, postoperative ulnar neuropathy occurred less with the single plate approach than with the double plate approach (8% versus 37%, $p = 0.013$).

Conclusion: Both double platting and single plating with medial screw fixation showed comparable union rates and functional outcomes in extra-articular distal humerus fractures. However, single plating with medial screw fixation take shorter operation time and has lower incidence of postoperative ulnar neuropathy.

The outcomes of rhBMP-2 induced hydroxyapatite in treating distal humerus fracture with bone defects : a retrospective case series

Orthop Surg. Eulji Univ.
Seong Ju Choi

Hypothesis: Delayed union and nonunion of the distal humerus present significant challenges due to compromised biological healing potential and the complex anatomy of the elbow joint. Bone morphogenetic protein-2 (BMP-2) combined with hydroxyapatite has emerged as a potential osteoinductive agent for managing such cases, but clinical data in upper extremity applications remain limited. This study evaluates the clinical and radiographic outcomes of BMP-2–induced hydroxyapatite combined with cancellous allobone graft in elderly patients with distal humerus fracture nonunion or delayed union.

Methods: We retrospectively reviewed six patients (4 females, 2 males; mean age, 74.3 years [range, 53–87]) who underwent osteosynthesis with BMP-2 induced hydroxyapatite bone grafts for distal humerus fractures with bone defects. between January 2023 and June 2024. There were 2 patients with nonunion (>6 months with radiographic or clinical evidence of pseudarthrosis), 2 patients with delayed union (3~6 months post-injury without signs of healing), and 2 patients with subacute fracture (2~3 months). Each patient exhibited bone defect in the operative room and received 0.5 - 1 g of BMP-2–induced hydroxyapatite combined with 3–10 cc of cancellous allogeneic bone chips with nternal fixation using a parallel locking plate system (Synthes). Patients were followed for a mean duration of 11.5 months (range, 9–15).

Results: Radiographic union was achieved in all cases, with a mean time to union of 3.8 months (range, 3–5). The mean arc of elbow motion at final follow-up was 118° (range, 90–140°), and the mean VAS pain score was 2.1. Postoperative ulnar neuritis symptoms were observed in five patients (83.3%), with symptom duration ranging from 0 to 12 months (mean, 4 months). No cases of surgical site infection or ectopic ossification were reported. One patient sustained a periprosthetic fracture two weeks postoperatively, requiring revision surgery. Another patient underwent elective screw removal for hardware irritation under local anesthesia.

Summary: The use of BMP-2–induced hydroxyapatite in combination with cancellous allobone graft provided reliable union in elderly patients with distal humerus with bone defects. However, a high incidence of transient postoperative ulnar nerve neuritis was observed, warranting further investigation into potential inflammatory

responses associated with BMP-2 in the upper extremity.

Key Terms: Distal humerus fracture, nonunion, delayed union, Bone morphogenetic protein-2

Minimum four-year clinical outcomes after on-table reconstruction technique for Dubberley type III in coronal shear fractures of the capitellum and trochlea: a report of 10 patients

[1]Orthop Surg. Ewha Womans Univ., [2]Orthop Surg. Yonsei Univ.
Shin Woo Lee[1], Il-Hyun Koh[2], Ho-Jung Kang[2], Yun-Rak Choi[2], Ji-Sup Kim[1]

Background: Coronal shear fractures of the distal humerus, especially Dubberley type III with separate capitellar and trochlear fragments, are rare but technically demanding injuries. Conventional strategies such as open reduction and internal fixation (ORIF), fragment excision, or total elbow arthroplasty (TEA) are associated with high risks of nonunion, avascular necrosis (AVN), or poor durability. Although extra-corporeal "on-table" reconstruction has been described for radial head fractures, its role in Dubberley type III fractures remains unknown.

Methods: We retrospectively reviewed 32 patients treated surgically for distal humeral shear fractures between 2009 and 2019. Ten patients (mean age 52.7 years) with type IIIA fractures managed by on-table reconstruction and internal fixation with headless screws met inclusion criteria. All procedures were performed through a lateral approach, with extracorporeal anatomical reconstruction, screw fixation, and ligament repair as indicated. Minimum follow-up was four years (mean 54.7 months). Outcomes included union, range of motion, visual analogue scale (VAS), Disabilities of the Arm, Shoulder, and Hand (DASH), American Shoulder and Elbow Surgeons (ASES), and Mayo Elbow Performance Index (MEPI).

Results: All fractures united radiographically at a mean of 10.8 weeks, with no loss of reduction. Final mean scores were ASES 88.6, DASH 21.2, and MEPI 87 (excellent in 5, good in 4, fair in 1). Mean flexion–extension arc was 120°, with preserved forearm rotation. Complications included one case of partial asymptomatic capitellar AVN (10%) and one case of heterotopic ossification, without additional injury.

Conclusions: On-table reconstruction for Dubberley type IIIA capitellum and trochlea fractures achieved consistent union, satisfactory function, and a lower AVN rate than historically reported. The technique preserves the native joint and avoids prosthetic complications, representing a valuable alternative to excision or TEA, particularly in younger or active patients. Further studies with larger cohorts, inclusion of IIIB patterns, and longer-term follow-up are warranted.

Clinical Outcomes of Arthroscopic Release for Severe and Non-Severe Post-Traumatic Elbow Stiffness: A Comparative Study

Asan Medical Center
Jia Guo

Background and purpose: Post-traumatic elbow stiffness, defined as flexion <120° and/or loss of extension >30°, occurs in up to 56% of patients following elbow trauma. Based on the classification proposed by Mansat and Morrey, the severity of stiffness can be graded according to the flexion–extension arc: mild (>90°), moderate (60–90°), severe (30–60°), and extremely severe (<30°).

Surgical intervention is generally indicated when functional limitations fail to improve with non-operative management. Historically, open release has been regarded as the gold standard for treating a rigid elbow. However, this approach carries a notable complication rate of approximately 23% (ranging from 0% to 59%), and nearly 36% of patients fail to achieve a functional arc of motion ≥120° following open arthrolysis. Severe elbow stiffness has been identified as a risk factor for poor outcomes after open release. In recent years, arthroscopic contracture release has emerged as an alternative approach and, despite limited reports, has demonstrated outcomes that may be superior to those of traditional open procedures. Potential advantages of arthroscopic release include improved intra-articular visualization, the ability to perform inside-out debridement of adhesions and capsulectomy while preserving critical ligament structures, and the use of small portals that minimize soft tissue damage, thereby facilitating early postoperative rehabilitation. Furthermore, the absence of a large incision reduces the risk of skin scar contracture. Nevertheless, arthroscopic release is technically demanding, with potential risks of neurovascular injury, and severe contractures associated with extensive extra-articular soft-tissue adhesion remain relative contraindications.

To our knowledge, no previous study has directly compared clinical outcomes of arthroscopic release between patients with severe (<60° flexion–extension arc) and non-severe (≥60° flexion–extension arc) post-traumatic elbow stiffness. Therefore, the primary aim of this study was to compare clinical outcomes of arthroscopic release between these two groups. Specifically, we analyzed serial changes in range of motion (ROM), including flexion, extension, and the flexion–extension arc, as well as patient-reported outcomes over time. In addition, complication rates and the incidence of revision surgery were compared.

We hypothesized that arthroscopic release would yield comparable clinical outcomes in patients with severe and non-severe post-traumatic elbow stiffness at the final follow-up, although recovery of range of motion in the severe group would require a longer period.

Methods: Patients who underwent arthroscopic release for post-traumatic elbow stiffness between 2018 and 2024 were retrospectively reviewed. Surgery was generally offered to patients whose elbow stiffness significantly interfered with daily activities after failed conservative management. Patients with contraindications, including prior submuscular ulnar nerve transposition, extensive posterior heterotopic ossification, immature heterotopic ossification, malunion causing mechanical motion block, or complete destruction of the articular cartilage, were excluded.

Patients were divided into two groups based on the flexion–extension arc of motion, following the classification of Mansat and Morrey: those with an arc <60° were categorized as the severe group, and those with an arc ≥60° as the non-severe group. Clinical evaluations included range of motion (ROM), pain visual analog scale (VAS), Mayo Elbow Performance Score (MEPS), Single Assessment Numeric Evaluation (SANE), and QuickDASH score. Clinical outcomes, complication rates, and revision surgery rates were compared between the severe and non-severe groups.

Results: Data from 46 patients were analyzed (severe group, n = 18; non-severe group, n = 28). The mean ± SD age was 39.5 ± 8.9 and 42 ± 11.1 years in the severe group and non-severe group, respectively.

Both groups showed significant improvement at final follow-up (mean[range], 22.5 [12-61] months). Table 1 details preoperative and postoperative Flexion/Extension arc, flexion, extension, VAS pain score, MEPS, Quick-Dash score and SANE score

Table 1. Clinical Outcomes of Patients with Severe and Non-Severe Stiffness

	Severe Stiffness			Non-Severe Stiffness		
	Pre-op	Post-op	P	Pre-op	Post-op	P
Flex/Ext arc	41 ± 10	130 ± 15	<0.001	82 ± 18	124 ± 18	<0.001
Extension	41 ± 10	4 ± 7	<0.001	23 ± 11	7 ± 9	<0.001
Flexion	81 ± 12	134 ± 11	<0.001	105 ± 12	131 ± 12	<0.001
VAS	4 ± 2	0 ± 1	<0.001	5 ± 3	1 ± 2	<0.001
MEPS	59 ± 12	96 ± 7	<0.001	72 ± 13	93 ± 9	<0.001
Quick-Dash	38 ± 4	3 ± 5	<0.001	43 ± 7	7 ± 8	<0.001
SANE	31 ± 11	86 ± 11	<0.001	46 ± 17	80 ± 15	<0.001

At the last follow-up, the median [interquartile range, IQR] flexion–extension arc was 130° (125–140°) in the severe group and 125° (111.25–140°) in the non-severe group (p = 0.16). The median extension contracture was 0° (0–6.25°) in the severe group and 5° (0–10°) in the non-severe group (p = 0.23). Median flexion was 135°

(130–140°) in the severe group and 130° (120–140°) in the non-severe group (p = 0.305).

At the last follow-up, the median [interquartile range, IQR] visual analog scale (VAS) pain score was 0 (0–0.25) in the severe group and 0 (0–2) in the non-severe group (p = 0.06). The median MEPS was 100 (85–100) in both groups (p = 0.359). The median Quick-DASH score was 2 (0–5) in the severe group and 2 (2–11) in the non-severe group (p = 0.052). The median SANE score was 90 (80–91.25) in the severe group and 85 (70–90) in the non-severe group (p = 0.135).

Both groups showed comparable clinical outcomes in the serial assessments of ROM, VAS, MEPS, QuickDASH, and SANE at 3, 6, and 12 months postoperatively following arthroscopic release. (Figure 1-4)

Figure 1
Mean changes in Flexion-extension arc in severe group and non-severe group

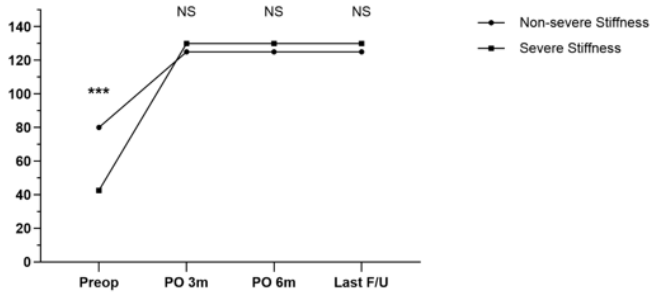

Figure 2
Mean changes in Extension contracture in severe group and non-severe group

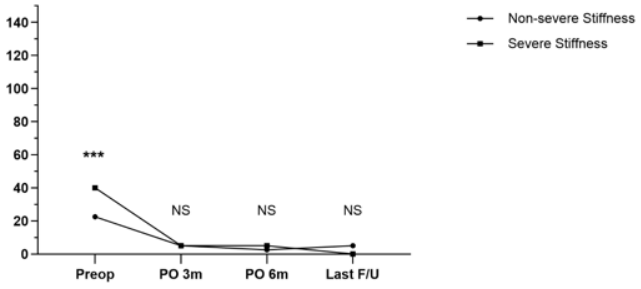

Figure 3
Mean changes in Flexion in severe group and non-severe group

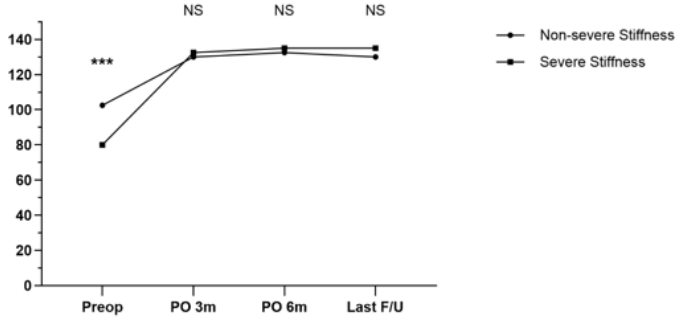

Figure 4

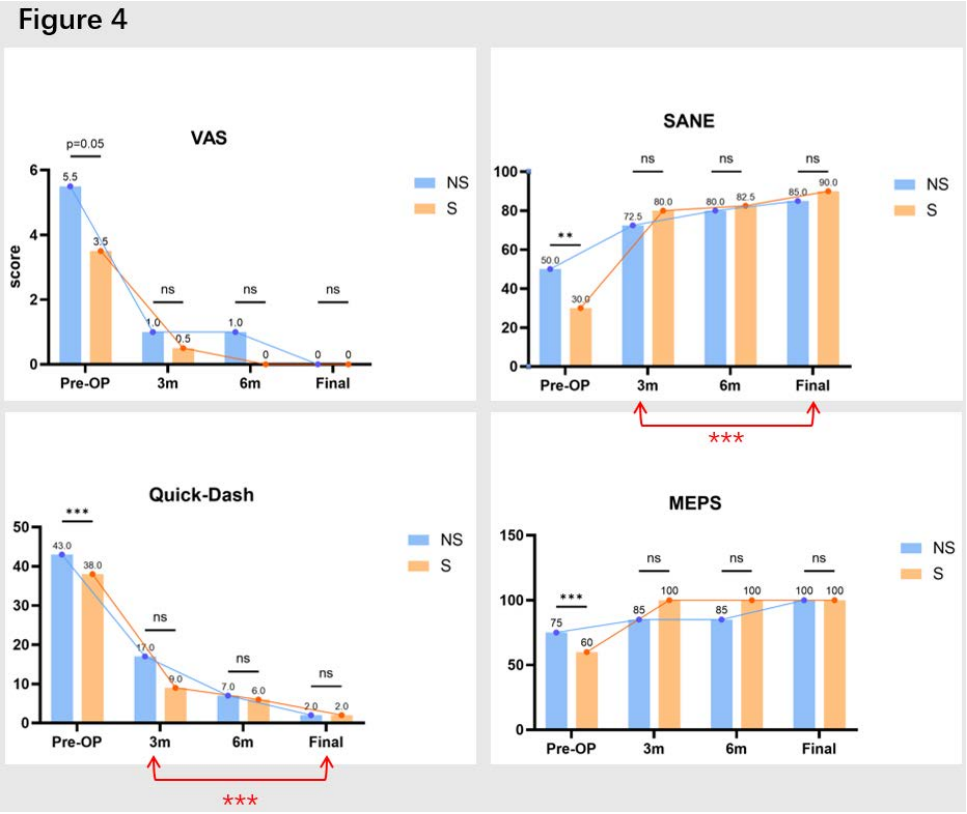

No neurovascular injuries occurred in either group after surgery. In the severe group, one patient developed recurrent heterotopic ossification (HO), which did not interfere with elbow motion. In the non-severe group, one patient underwent revision surgery 1 year after the primary procedure due to unsatisfactory elbow motion.

Conclusion: Arthroscopic release achieved comparable clinical outcomes in patients with both severe and non-severe post-traumatic elbow stiffness at a minimum of one year follow-up. Serial assessments at 3, 6, and 12 months also demonstrated similar clinical outcomes between the two groups.

Clinical Outcomes of Arthroscopic Release for post-traumatic and degenerative Elbow Stiffness: A Comparative Study

Asan Medical Center
Jia Guo

Background and purpose : Limitation in elbow range of motion (ROM) leads to impaired arm function and substantially interferes with daily activities. Loss of motion may arise from various etiologies, most commonly trauma and degenerative osteoarthritis. Post-traumatic stiffness is typically associated with capsular contracture, heterotopic ossification, and intra-articular adhesions, whereas degenerative stiffness primarily results from progressive osteophyte formation and capsular fibrosis. Previous studies have identified atraumatic causes as independent risk factors for not achieving the minimal clinically important difference (MCID) in ROM after open elbow arthrolysis.

With advances in surgical techniques and instrumentation, arthroscopic arthrolysis has become an established and effective treatment for elbow stiffness, offering the advantages of minimally invasive surgery with reliable functional recovery. However, although numerous reports have demonstrated the efficacy of arthroscopic release, most have assessed heterogeneous populations without distinguishing between post-traumatic and degenerative etiologies. Consequently, it remains unclear whether surgical outcomes differ depending on the underlying cause of stiffness, and whether etiology-specific factors should guide prognosis and clinical decision-making.

The present study was designed to address this gap by directly comparing the clinical outcomes of arthroscopic release in patients with post-traumatic versus degenerative elbow stiffness. By analyzing improvements in ROM, pain, and functional scores, we aimed to determine whether etiology influences surgical outcomes. Clarifying these differences has important clinical relevance, as it may improve patient counseling, help set realistic expectations, and refine surgical strategies for managing elbow stiffness.

Methods: We reviewed 100 consecutive patients who underwent arthroscopic release for elbow stiffness between January 2010 and December 2024 at a single tertiary referral center. Patients were classified into two groups according to etiology: post-traumatic stiffness (n = 46) and degenerative stiffness (n = 54). Exclusion criteria included prior open release, active infection, inflammatory arthritis, and incomplete follow-up data.

All procedures were performed by experienced elbow surgeons using a standardized arthroscopic release technique. Preoperative evaluation included demographic data, duration of stiffness, range of motion (ROM), pain visual analog scale (VAS), and Mayo Elbow Performance Score (MEPS). Postoperative assessments were conducted at 3, 6, and 12 months, and at the final follow-up, including flexion, extension, flexion–extension arc, extension contracture, VAS, and MEPS.

Clinical outcomes were compared between groups. Continuous variables were expressed as mean ± standard deviation (SD) and compared using the independent-samples t test or Mann–Whitney U test, depending on distribution. Paired comparisons within groups were performed using the paired t test or Wilcoxon signed-rank test. A P value < 0.05 was considered statistically significant.

Results: Data from 100 patients were analyzed (post-traumatic group, n = 46; degenerative group, n = 54). The mean ± SD age was 42.5 ± 13.0 years in the post-traumatic group and 57.2 ± 8.4 years in the degenerative group (P < 0.001). The mean follow-up duration was 38.5 months (range, 12–122 months).

Both groups showed significant improvement in the final follow-up (Table 1).

Table 1. preoperative and postoperative flexion, extension, and flexion/extension arc

	Post-traumatic Stiffness			Degenerative Stiffness		
	Pre-op	Post-op	P	Pre-op	Post-op	P
Flex/Ext arc	66 ± 25	127 ± 27	<0.001	90 ± 20	109 ± 21	<0.001
Extension	30 ± 14	6 ± 8	<0.001	19 ± 10	13 ± 11	<0.001
Flexion	96 ± 17	132 ± 12	<0.001	108 ± 14	121 ± 12	<0.001
VAS	4 ± 2	1 ± 1	<0.001	5 ± 2	2 ± 2	<0.001
MEPS	67 ± 14	94 ± 8	<0.001	62 ± 10	88 ± 12	<0.001

Preoperatively, the degenerative group had a significantly greater flexion–extension arc than the post-traumatic group (90° ± 20° vs 66° ± 25°, P < 0.001). At the last follow-up, the mean ± SD flexion–extension arc was 127° ± 17° in the post-traumatic group and 109° ± 21° in the degenerative group (P < 0.001). The mean ± SD extension contracture was 6° ± 8° in the post-traumatic group compared with 13° ± 11° in the degenerative group (P < 0.001). The mean ± SD flexion was 132° ± 12° in the post-traumatic group and 121° ± 12° in the degenerative group, with no significant difference (P = 0.305).

The degree of improvement in flexion–extension arc, extension contracture, and flexion were significantly greater in the post-traumatic group than in the degenerative group (all P < 0.001). Serial changes in flexion, extension, and flexion–extension arc at 3, 6, and 12 months after arthroscopic release are summarized in Table 2.

Table 2. Comparison of Pre- and Postoperative Range of Motion between the Post-traumatic and Degenerative Stiffness Groups at the preoperative, postoperative 3 months, 6 months and Final Follow-up Times

Variable	Post-traumatic	Degenerative	P
Flex/Ext arc			
preoperative	66 ± 25	90 ± 20	<0.001
PO 3 months	123 ± 16	108 ± 19	<0.001
PO 6 months	125 ± 15	110 ± 18	<0.001
Last F/U	127 ± 17	109 ± 21	<0.001
improvement	61 ± 32	20 ± 16	
Extension			
preoperative	30 ± 14	19 ± 10	<0.001
PO 3 months	6 ± 9	13 ± 9	<0.001
PO 6 months	5 ± 8	14 ± 18	<0.001
Last F/U	6 ± 8	13 ± 11	<0.001
improvement	24 ± 16	6 ± 10	<0.001
Flexion			
preoperative	96 ± 17	108 ± 14	<0.001
PO 3 months	129 ± 11	120 ± 12	<0.001
PO 6 months	131 ± 11	120 ± 19	<0.001
Last F/U	132 ± 12	121 ± 12	<0.001
improvement	37 ± 21	13 ± 11	<0.001

Preoperatively, the post-traumatic group had significantly higher MEPS values compared with the degenerative group (67 ± 14 vs 62 ± 10, P = 0.036). No significant differences were observed in VAS pain scores (P = 0.359). At the last follow-up, the post-traumatic group demonstrated significantly lower VAS pain scores (1 ± 1 vs 2 ± 2, P = 0.018) and higher MEPS values (94 ± 8 vs 88 ± 12, P = 0.007). However, the magnitude of improvement in both VAS and MEPS was comparable between the groups (P = 0.617 and P = 0.851, respectively). Serial changes of VAS and MEPS at 3, 6, and 12 months after arthroscopic release are summarized in Table 3.

Table 3. Comparison of Pre- and Postoperative VAS pain score and MEPS between the Post-traumatic and Degenerative Stiffness Groups at the preoperative, postoperative 3 months, 6 months and Final Follow-up Times

Variable	Post-traumatic	degenerative	P
VAS			
preoperative	4 ± 2	5 ± 2	0.359
PO 3 months	1 ± 1	2 ± 1	0.066
PO 6 months	1 ± 1	1 ± 1	0.036
Last F/U	1 ± 1	2 ± 2	0.018
improvement	4 ±3	3 ± 3	0.617
MEPS			
preoperative	67 ± 14	62 ± 10	0.036

PO 3 months	91 ± 8	84 ± 9	<0.001
PO 6 months	92 ± 8	85 ± 11	<0.001
Last F/U	94 ± 8	88 ± 12	0.007
improvement	28 ± 17	26 ± 14	0.851

Conclusions: Arthroscopic release provided significant functional improvement in both post-traumatic and degenerative elbow stiffness. Although patients with post-traumatic stiffness presented with more restricted preoperative motion, they achieved greater gains in flexion–extension arc, extension, and flexion compared with those with degenerative stiffness. At the last follow-up, the post-traumatic group also demonstrated superior pain relief and functional scores.

These findings suggest that arthroscopic release is an effective treatment for both etiologies, with particularly favorable outcomes in post-traumatic elbow stiffness.

2025년 대한수부외과학회
추계학술대회

Room B

Free Paper 5 (Microsurgery)

Plast Reconstr Surg. Kyung Hee Univ. **Sang Yoon Kang**
Orthop Surg. Pusan National Univ. **Sang Hyun Lee**

Semiocclusive Dressing for Fingertip Amputations: How Far Can We Go?

MS Reconstruction Hosp.
Jin Sik Park

Background: Fingertip amputations are often managed surgically with flaps or grafts, which may result in donor-site morbidity. Semiocclusive dressings provide a moist wound environment that promotes granulation and tissue regeneration, offering a nonsurgical alternative.

Methods: Eleven patients with fingertip amputations or soft-tissue defects were treated nonoperatively using semiocclusive dressings. The mean patient age was 56.2 years (range, 2–91 years). The cohort included diverse clinical scenarios, such as a super-elderly patient over 90 years of age, a case requiring stump revision after severe crushing injury, and a patient who developed infection and necrosis following a cat bite necessitating surgical debridement. After initial debridement, wounds were covered with a semipermeable film dressing, changed weekly, allowing secondary intention healing. Outcomes assessed included time to complete healing, complications, and patient-reported cosmetic and functional satisfaction.

Results: The mean time to complete healing was 36 days (range, 17–46 days). No major complications or recurrent infections occurred, and no patient required additional surgical intervention. All patients reported satisfactory cosmetic and functional outcomes.

Conclusions: Semiocclusive dressings represent a safe and effective option for fingertip amputations, providing excellent healing and patient satisfaction while avoiding the morbidity of surgical reconstruction. Patients, however, should be counseled regarding the relatively longer healing period and the possibility of minor nail deformities.

Location of the A1 and A2 Pulleys in Relation to the Palmar Creases: Implications for Percutaneous Release

W General Hosp.
Bong Gyu Choi, Soo Jin Woo, Kwang Hyun Park, Hyun Jae Nam, Sang Hyun Woo

Background: Bite wounds carry a high risk of infection, and the role of antibiotics and timing of wound closure remain controversial. Limited evidence exists regarding bite-related finger amputations, particularly for replantation and immediate wound coverage.

Methods: We retrospectively reviewed 58 patients treated surgically for bite-related finger amputations at our institute (2009–2024). Demographics, injury mechanism, amputation level, and complications were analyzed. Major infection was defined as cases requiring operative irrigation and debridement. Our observed infection rate was evaluated in relation to the infection rates previously reported in the literature for primary closure of bite wounds.

Results: Among 58 patients, 27 (46.6%) underwent immediate wound coverage and 31 (53.4%) delayed coverage. No major infections occurred in either group. Replantation was attempted in 10 cases, with an 80% success rate; all failures were due to arterial insufficiency, not infection. Minor infections responsive to antibiotics were observed but required no further surgery.

Conclusion: Immediate wound coverage, including replantation when indicated, was not associated with increased risk of major infection in bite-related finger amputations. These findings support the safety of immediate coverage and replantation, providing useful evidence for surgical decision-making in hand trauma.

Table 1. Patient's characteristics

Characteristics	Total	Immediate group	Delayed group
No. of patients	58	27	31
Age (yr)	53.1 ± 18.1	55.3 ± 21.4	51.2 ± 14.6
Sex, male	42 (72.4%)	17 (63%)	25 (80.6%)
Vector			
Human	27	11	16
Dog	29	16	13

Cow	1	-	1
Pig	1	-	1
Zone			
Thumb	10	3	7
Index finger	14	8	6
Long finger	11	6	5
Ring finger	14	7	7
Small finger	9	3	6
Amputation type			
Complete	43	19	24
Bone involvement	32	15	17
Tendon involvement	25	11	14
Incomplete	15	8	7
Bone involvement	11	5	6
Tendon involvement	8	4	4

Table 2. Surgical procedures and complications

	Immediate group	Delayed group
Total	27	31
Replantation	10 (37.0%)	0 (0%)
Revision amputation	7 (26.0%)	14 (45.2%)
Flap or skin graft surgery		
Local flap	8 (29.6%)	9 (29.0%)
Regional flap	1 (3.7%)	0 (0%)
Distant flap	1 (3.7%)	7 (22.6%)
Skin graft	0 (0%)	1 (3.2%)
Complications		
Major Infection	0 (0%)	0 (0%)
Replantation failure	2 (20%)	-

Table 3. Aerobic and facultative anaerobic bacteria isolated from 45 patients with animal or human bite wounds

	Animal bite	Human bite
Total	27	18
No growth	17	11
Aerobic		
Burkholderia cenocepacia	1	-
Acinetobacter baumannii	-	1
Chryseobacterium gleum	1	-
Facultative anaerobic		
Serratia marcescens	2	-
MRSA	2	1

MRSE	4	1
Klebsiella aerogenes	-	2
Aeromonas sobria	-	2

MRSA : Methicillin-resistant *Staphylococcus aureus*

MRSE : Methicillin-resistant *Staphylococcus epidermidis*

Figure 1. (A) A 64-year-old man with a dog bite induced amputation injury of the right long finger. (B-D) Clinical photograph of dog bite induced finger amputation managed initially with open dressing, followed by revision amputation after 7 days.

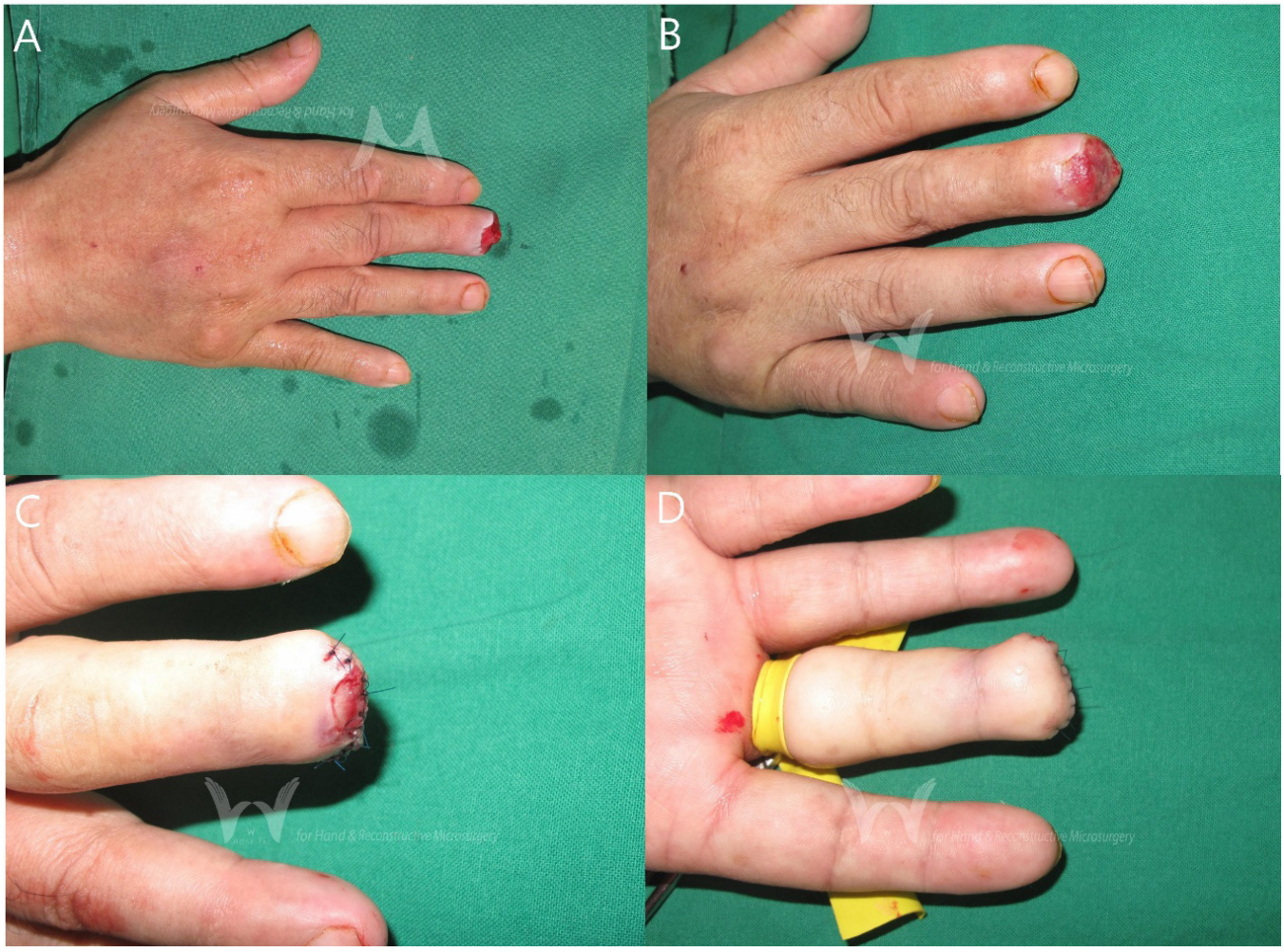

Figure 2. (A, B) A 58-year-old man sustained a dog bite induced amputation injury to his left long finger. (C-F) Immediate wound coverage of a dog bite induced finger amputation using a radial digital artery island flap and skin graft.

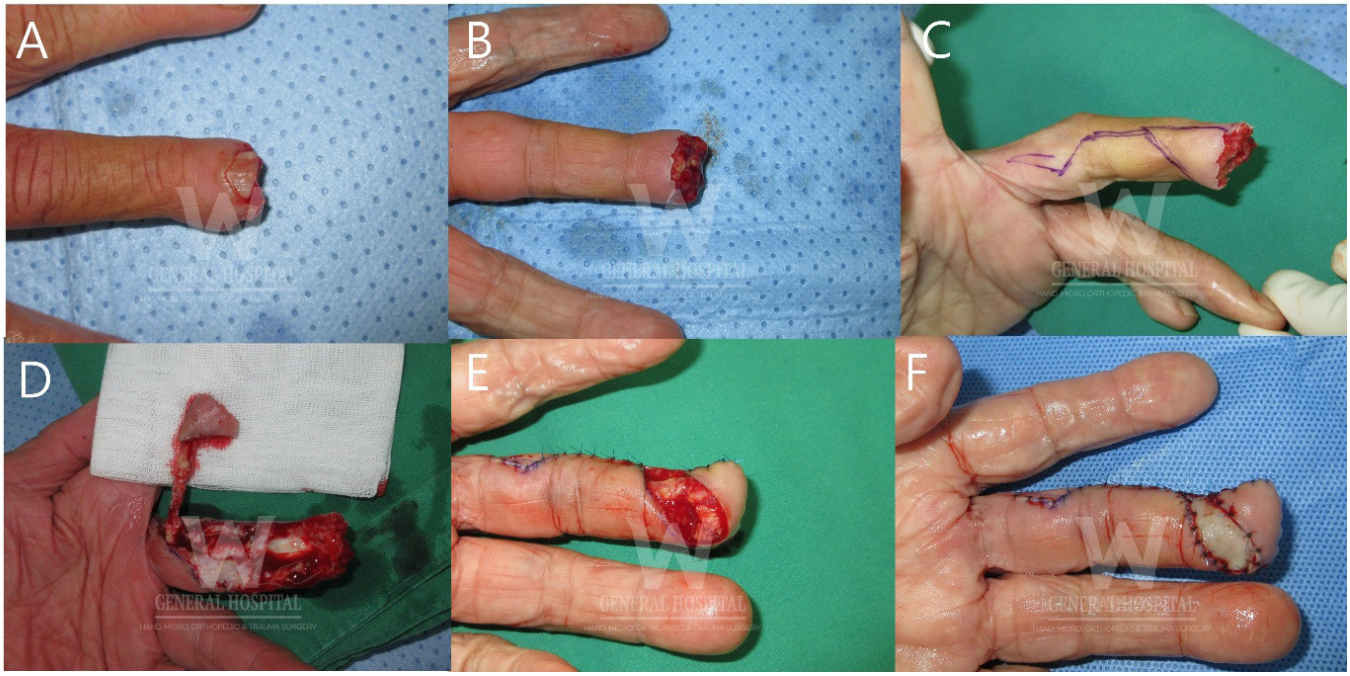

Figure 3. (A, B) A 49-year-old woman with a human bite induced amputation injury of the right thumb. (C, D) Postoperative images after immediate thumb replantation. (E, F) Clinical appearance at 3 months postoperatively.

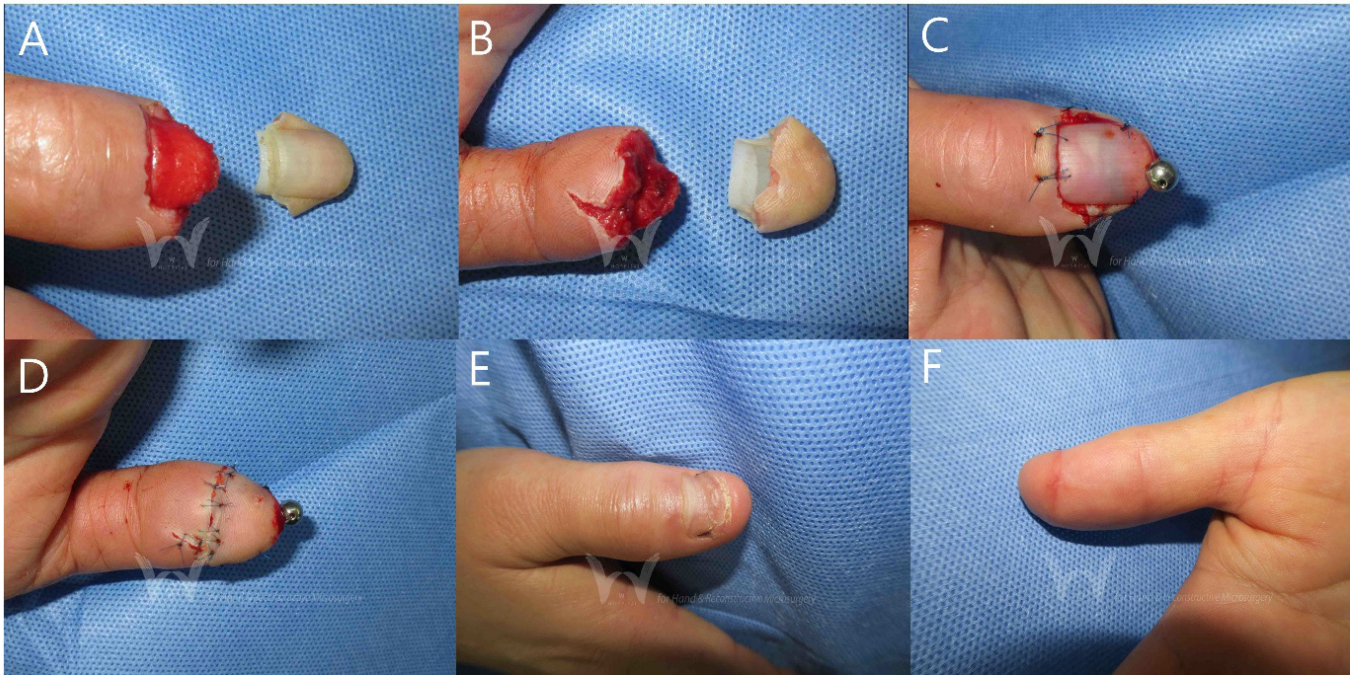

Revascularization of finger tip amputation through dorsal-approach: Result and clinical experience

West Busan Centum Hosp.
Hyung Seo Jang, Tae Yeong Yang

Introduction: In fingertip amputations, arterial anastomosis for revascularization is most commonly performed through a volar approach. However, the very small caliber of the vessels and the bulk and depth of the pulp tissue result in a narrow operative field. Excessive skin incision to improve exposure may further increase skin necrosis. In this study, we report the outcomes of fingertip replantations performed by a single orthopedic surgeon using a dorsal approach for arterial anastomosis.

Methods: Between November 2023 and December 2024, a retrospective review was performed on fingertip replantations by a single surgeon. Patients were grouped by approach: Volar (Group A, n = 22) or Dorsal (Group B, n = 17). Survival rate and degree of partial necrosis were assessed.

Results: In Group A (n = 22), two patients experienced complete necrosis (9.1%), and partial necrosis requiring flap surgery occurred in four patients (18.2%). In Group B (n = 17), two patients experienced complete necrosis (11.8%), while no cases of partial necrosis requiring flap surgery were observed.

Conclusion: The dorsal approach can`t replace the volar approach in all cases, and a sufficiently experienced microsurgeon can manage most fingertip amputations using the volar approach alone. However, in cases where arterial anastomosis through the volar approach is technically challenging, the dorsal approach may provide better operative field and make the procedure easier. By minimizing volar skin incisions, the dorsal approach may reduce the risk of pulp skin necrosis and concern about vessel exposure.

Figure 1. In severe volar oblique fingertip amputation, sometimes operative field for arterial anastomosis may noy be prepared via volar approach without additional skil incision

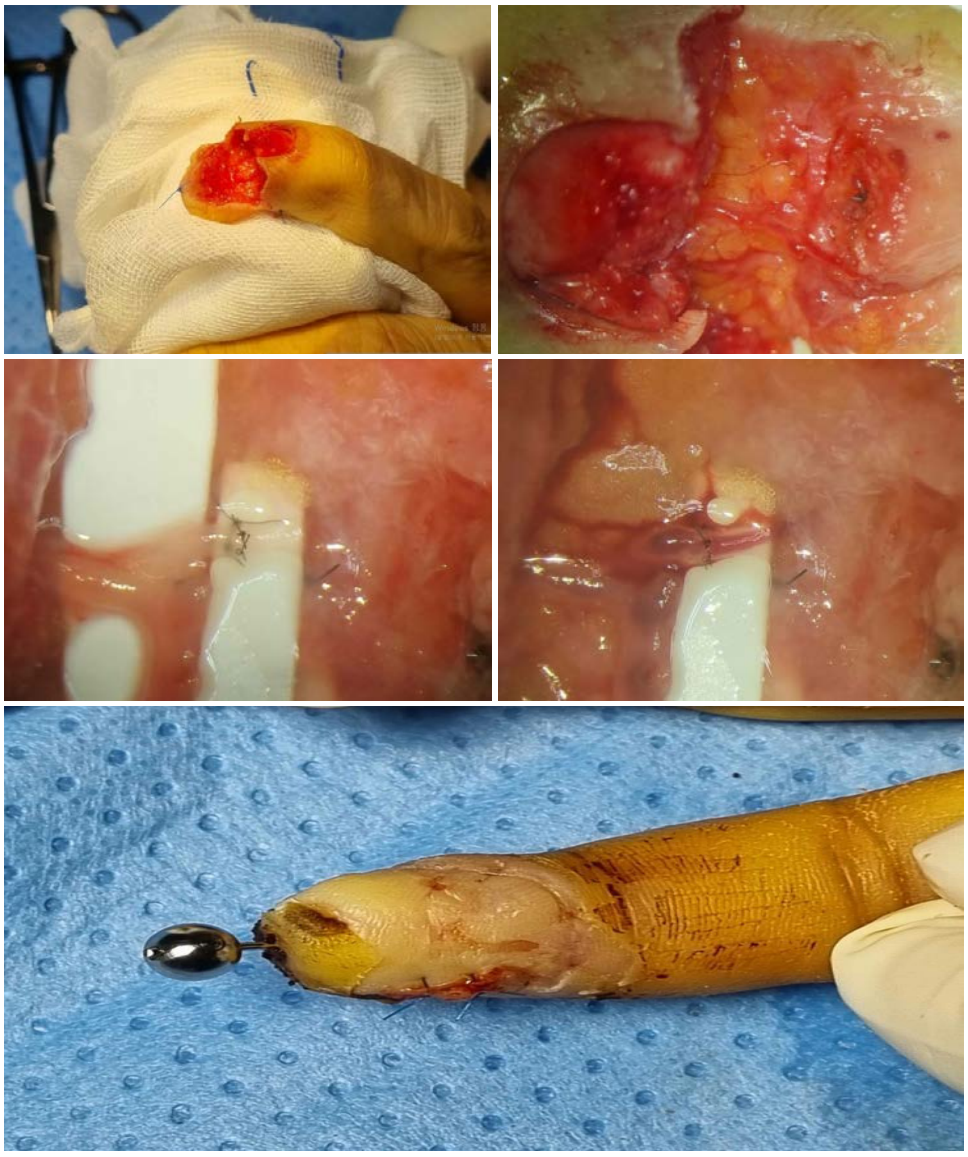

Figure 2. Sufficient operative field was obtained through the dorsal approach, and The amputated finger survived following external bleeding.

Early thenar flap division for finger soft tissue defect: Result and clinical experience

West Busan Centum Hosp.
Jae Yeon Kong, Tae Yeong Yang

Introduction: The thenar flap is a widely used option for reconstructing distal finger soft tissue defects, providing reliable vascularity and good functional outcomes. Conventionally, flap division has been done 2–3 weeks, but high survival rate after division within 7–10 days is documented in several case series. This study evaluates the outcomes of early thenar flap division by single surgeon.

Methods: We retrospectively reviewed 38 patients who underwent thenar flap surgery with early division (7–10 days after inset) by a single orthopedic surgeon between January 2023 and December 2024. In all cases, 1.2-mm K-wire fixation was applied to maintain metacarpophalangeal joint flexion. Patient demographics, comorbidities, smoking status, mechanism of injury, defect level, proximal tissue injury involvement, time to flap surgery, timing of division, need for additional closure and suvival rate were analyzed.

Results: No complete flap necrosis occurred. One patient developed marginal necrosis, which healed by secondary intention. According to the Strickland criteria, 31 of 38 patients (81.6%) achieved excellent results, 4 (10.5%) had good results, and 3 (7.9%) had fair results in final range of motion. Among the seven patients who did not reach excellent outcomes, Most were noted in cases with distal interphalangeal joint injuries or in patients undergoing delayed thenar flap after necrosis following replantation.

Conclusion: The thenar flap showed high survival even with division at 7–10 days. These findings suggest that early division can be performed safely under proper conditions without increasing flap necrosis rate while reducing patient discomfort and enabling early rehabilitation.

Figure 1. Rt. hand 2nd finger amputation with un-repairable amputated part. Thenar flap with stabilization K-wire was maintained 7-days. After flap division, exposed soft tissue healed by secondary intention after regular dressing.

Spindle Cell Hemangioma of the Wrist with Radial–Ulnar Artery Anomaly: A Rare Vascular Tumor with Anatomical Variation

Plast Reconstr Surg. Yonsei Univ.
Yohan Kim, Jong Won Hong

Introduction: Spindle cell hemangioma (SCH) is a rare benign vascular tumor that typically arises in the distal extremities. Its occurrence in the wrist is extremely uncommon, and the presence of arterial anomalies makes management more challenging. We describe a case of SCH of the wrist associated with radial–ulnar arterial variation and discuss its clinical significance.

Case Report: A 25-year-old right-handed male presented with a slowly enlarging volar wrist mass. MRI, ultrasonography with Doppler, angiography, and CT angiography confirmed a vascular lesion consistent with hemangioma. Doppler revealed a high-flow pattern, indicating that sclerotherapy would be ineffective; therefore, surgical excision was planned. Vascular studies revealed absence of a complete palmar arch, ulnar artery dominance supplying digits 3–5, and a proximally originating radial artery with delayed but preserved flow. The Allen test was normal, indicating adequate perfusion. Excision with microsurgical dissection was performed, and the mass was removed completely without vascular compromise. Histopathology confirmed spindle cell hemangioma. Postoperative recovery was uneventful.

Discussion: This case highlights two uncommon findings: the rare presentation of SCH in the wrist and the coexistence of arterial variation with an absent palmar arch. Such anomalies preclude the safe use of the radial forearm free flap (RFFF) as a donor site, emphasizing the need for detailed vascular evaluation in reconstructive surgery. In addition, identifying the lesion's high-flow nature helped avoid ineffective sclerotherapy and led to appropriate surgical management.

Conclusion: Spindle cell hemangioma of the wrist with arterial variation is exceptionally rare. Careful preoperative imaging is essential to define vascular anatomy, ensure safe resection, and anticipate reconstructive considerations in upper-extremity vascular tumors.

Figure 1. Preoperative evaluation.
(A) Clinical photograph showing a volar wrist mass.
(B) Upper extremity angiography demonstrating a hypervascular lesion with ulnar-dominant circulation.
(C)CT angiography (3D reconstruction) showing high origin of the radial and ulnar arteries and absence of a complete palmar arch.

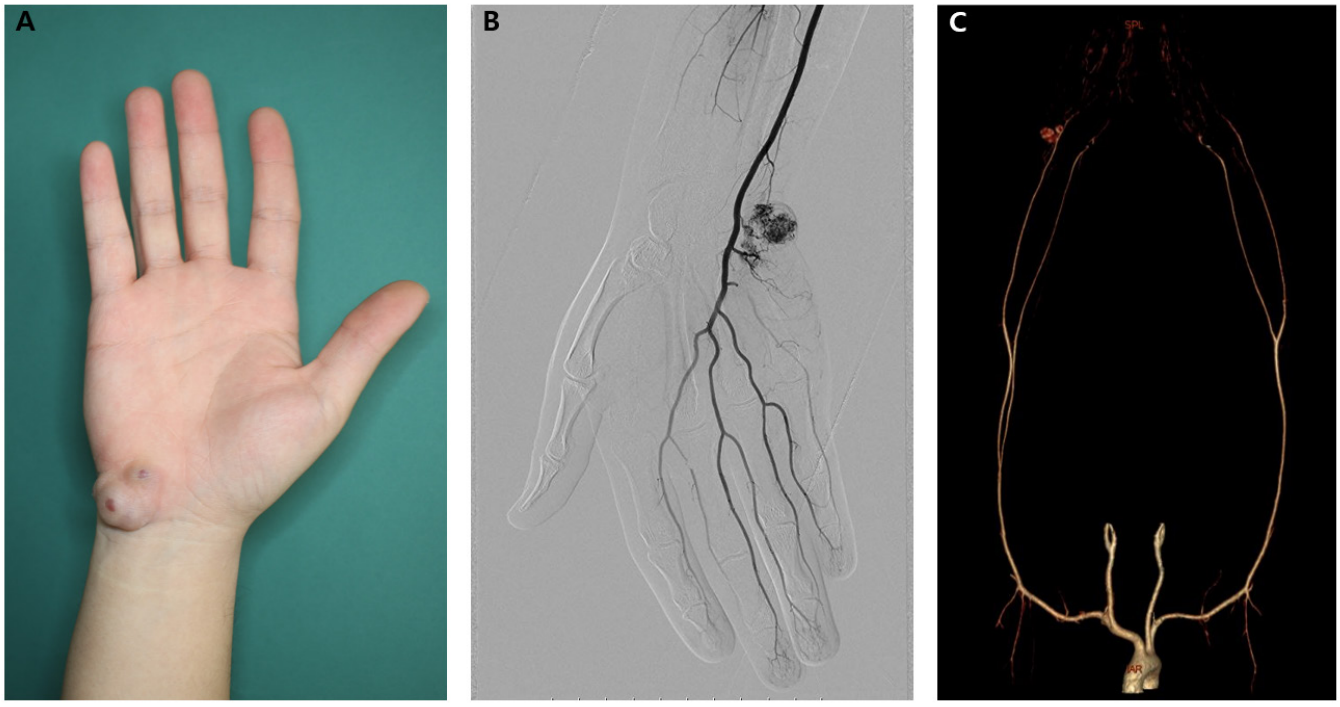

Figure 2. Intraoperative findings.
Intraoperative photograph demonstrating the hemangioma closely adjacent to the ulnar artery.

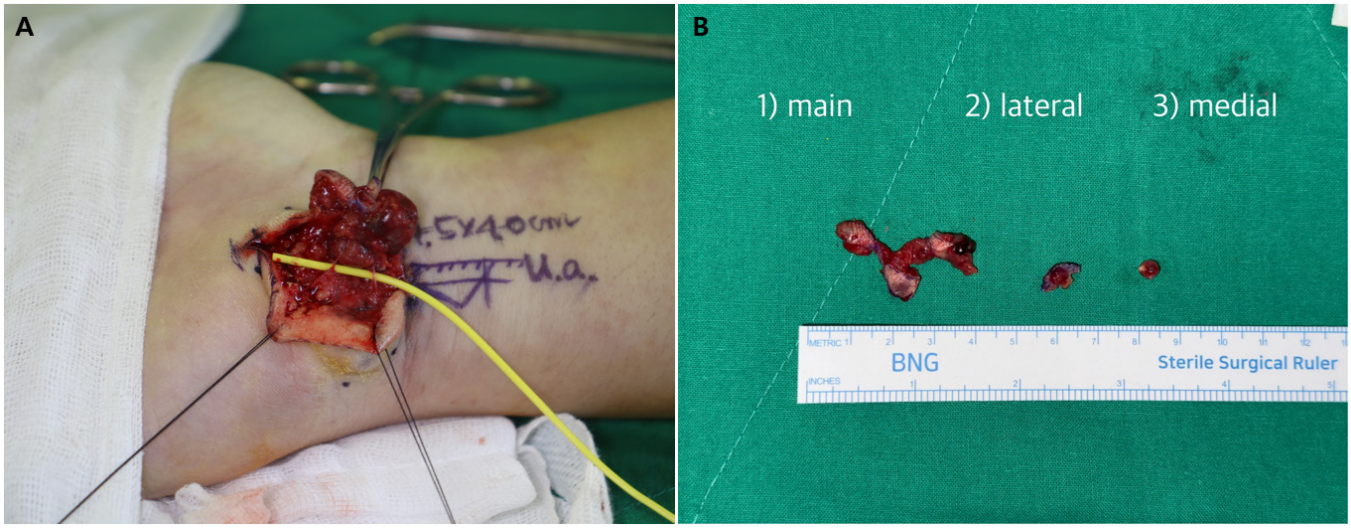

Figure 3. Postoperative outcome.
One-month follow-up photograph showing a well-healed scar without recurrence.

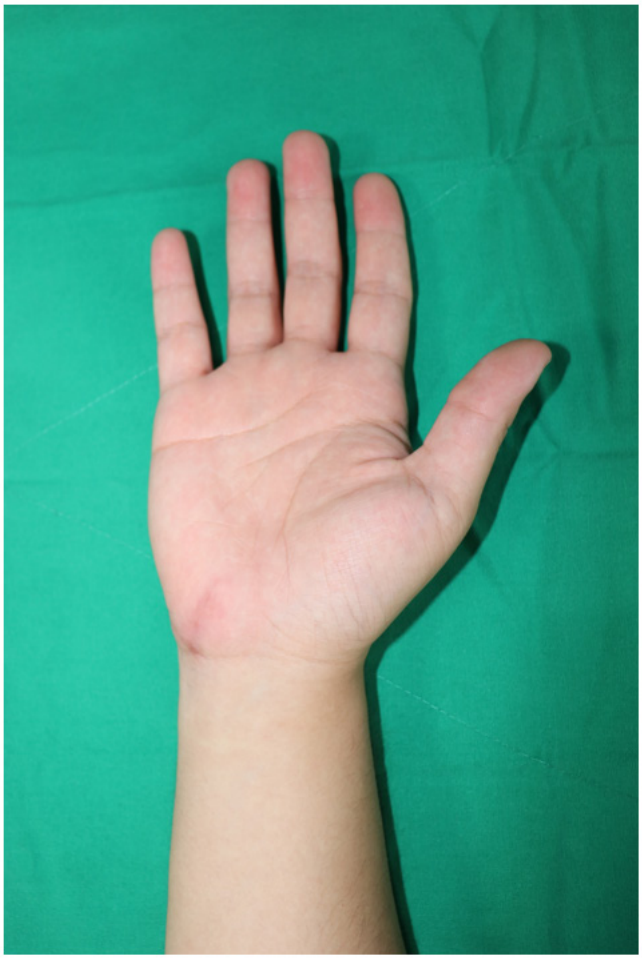

Evaluation of Suprafascial and Subfascial Radial Forearm Free Flap Techniques for Head and Neck Reconstruction

Plast Reconstr Surg. Inha Univ.
Sae Hwi Ki, Gun Hee Lee, Jee Hyun Moon

Purpose: The radial forearm free flap (RFFF) is a well-established method for head and neck reconstruction, though donor site morbidity is a limitation. This study compared outcomes between suprafascial and subfascial techniques in terms of flap survival and complications.

Methods: A retrospective review was performed on 32 patients who underwent RFFF by a single surgeon from 2006 to 2021. Patients were grouped by flap elevation method: subfascial (Group A, n=13) and suprafascial (Group B, n=19). Clinical data included demographics, flap size, complications, and acellular dermal matrix (ADM) use. Outcomes were analyzed and compared with reported literature.

Results: In Group A, mean age was 56.2 years (10 males, 3 females) and in Group B 59.1 years (16 males, 3 females). All patients had head and neck defects with a mean follow-up of 8 months. The average defect and flap sizes were 42.8 cm^2/51.0 cm^2 in Group A and 33.3 cm^2/44.5 cm^2 in Group B. ADM was used in 3 patients in Group A and 17 (90%) in Group B. Donor site complications were higher in Group A (62%) than Group B (26%). Tendon exposure requiring secondary surgery occurred only in Group A (23%). All flaps survived. Recipient site complications were observed in 2 patients (15%) in Group A and 3 (16%) in Group B.

Conclusion: Suprafascial RFFF reduced donor site morbidity while maintaining comparable flap survival and recipient outcomes. This technique also shortened treatment, supporting its value as an effective approach for head and neck reconstruction.

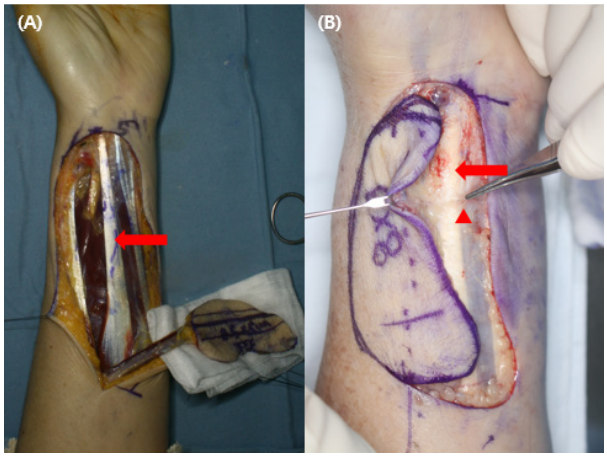

Fig 1. Subfascial and suprafascial dissection method of radial forearm free flap
(A) Subfascial dissection (Arrow: FCR tendon)
(B) Suprafascial dissection (Arrowhead: remaining fascia)

Fig. 2 Donor site complications of radial forearm free flaps
(A) Partial skin graft loss after subfascial dissection
(B) Partial skin graft loss after suprafascial dissection
(C and D) Tendon exposure after subfascial dissection

Table 1. Patient dermographic data

	Number (%)	
	Group A (subfascial)	Group B (suprafascial)
Age	41 – 79 years (56.15 years)	45 – 83 years (59.11 years)
Sex		
Male	10 (77%)	16 (84%)
Female	3 (23%)	3 (16%)
Medical comorbidity		
Smoking	6 (46%)	9 (47%)
Hypertension	2 (15%)	6 (32%)
DM	2 (15%)	3 (16%)
Infectious agents	0 (0%)	1 (5%)
Reconstruction site		
Tongue	6 (46%)	3 (16%)
Mouth floor	1 (8%)	3 (16%)
Retromolar trigone	0 (0%)	5 (26%)
Buccal mucosa	1 (8%)	6 (46%)
Hypopharynx	3 (23%)	0 (0%)
Pharynx	1 (8%)	1 (5%)
Nose	1 (8%)	0 (0%)
Cheek	0 (0%)	1 (5%)
Flap size	7.04 * 7.54 cm^2 (50.96 cm^2)	8.16 * 5.42 cm^2 (44.54 cm^2)
Whether to use ADM		
Used	3 (23%)	17 (90%)
Unused	10 (77%)	2 (10%)

Table 2. Donor site complications in the two groups

	Number (%)		p-value
	Group A(subfascial)	Group B(suprafascial)	
Treatment period	41 days	26 days	0.046
Delayed healing	8 (62%)	5 (26%)	0.046
Partial graft loss	2 (15%)	4 (21%)	0.686
Secondary skin graft	1 (8%)	0 (0%)	0.219
Tendon exposure	3 (23%)	0 (0%)	0.027

Table 3. Recipient site complication in the two groups

	Number (%)		p-value
	Group A(subfascial)	Group B(suprafascial)	
Total	2 (15%)	3 (16%)	0.975
Wound dehisence	1 (8%)	1 (5%)	0.780
Hematoma	0 (0%)	1 (5%)	0.400
Flap partial loss	1 (8%)	1 (5%)	0.780

Soft tissue reconstruction using arterialized venous free flap after resection of soft tissue tumor in the hand

Orthop Surg. Jeonbuk National Univ.
Ji Woong Ho, Young-Keun Lee

In patients with hand tumors, advances in medicine have led to a preference for limb-sparing surgery that offers functional and aesthetic advantages. However, limb-sparing surgery often results in soft tissue defects after tumor resection. We present our clinical results using arterialized venous free flaps to reconstruct defects after soft tissue tumor resection. Four patients who underwent arterialized venous free flap for hand reconstruction after soft tissue tumor resection between June 2016 and July 2020 were retrospectively reviewed. Pathological causes of soft tissue tumors were malignant melanoma, synovial sarcoma, malignant giant cell tumor, and recurrent epidermoid cyst. Tumor locations included the palm of the hand in two cases, the dorsum of the hand in one case, and the right long finger (RLF) in one case. Donor sites included the distal volar aspect of the ipsilateral forearm was the donor site in three cases and the contralateral forearm was the donor site in one case. Pure venous skin flaps were used in three cases. Only one case used a composite tendocutaneous flap. Flaps survived well in all the patients. The mean follow-up period of the flaps was 41.75 ± 9.09 months. Recurrence or metastasis was not found, except in one case. Kaplan-Meier survival analysis was performed. Restricted mean survival time of metastasis/recurrence was 57.00 ± 12.99 months. The color and texture of the flap were satisfactory in all the patients. Donor-site complications were not observed in any patient. Thus, an arterialized venous free flap is considered a valuable reconstruction option after soft tissue tumor resection.

Keywords: Tumors; Soft Tissue Neoplasms; Soft Tissue Injuries; Hand; Free Flap; Veins

Acknowledgements

The authors have no conflicts of interest relevant to this study to disclose.

Risk factors of flap reduction after free tissue transfer

Plast Reconstr Surg. Inha Univ.
Sae Hwi Ki, Do Hyuk Chung, Jee Hyun Moon, Min Ki Hong

Purpose: Secondary reduction of bulky flaps is often required for cosmetic and functional improvement. Safe reduction depends on appropriate timing and extent. This study aimed to define suitable intervals, reduction amounts, and risk factors for complications.

Methods: A retrospective review was performed of 30 patients who underwent flap reduction after free tissue transfer from March 2014 to April 2023. Variables included demographics, BMI, smoking history, surgical interval, extent of reduction, and complications.

Results: Thirty patients (21 men, 9 women; mean age 45.9 years; mean BMI 25.5) were included, with 10 smokers. Hypertension was the most common comorbidity (n=9). Reconstruction flaps were anterolateral thigh (n=17), thoracodorsal artery perforator (n=6), latissimus dorsi (n=5), gracilis musculocutaneous (n=1), and internal pudendal with obturator perforator (n=1). In total, 46 reductions were performed, mainly skin and subcutaneous excision. The mean reduction ratio was 46.9%, with an average interval of 6.1 months. Complications occurred in 10 cases, and smoking was a significant risk factor. In 9 patients reduced at only 2 months, the mean ratio was 48.9% with no major events.

Conclusion: Smoking increased complication risk. If the flap reduction is within the range of 50%, it is thought that reduction can be performed without major complications as early as 2 months.

Table 1. Patient demographic data

Characteristics	Number
Age	18 - 80 years (45.89 years)
Sex	
Male	21 (70.00 %)
Female	9 (30.00 %)

BMI	17.60 – 41.50 kg/m2 (25.47 kg/m2)
Smoking	10 (33.33%)
Underlying disease	
HTN	9 (30.00 %)
DM	4 (13.33%)
Dyslipidemia	4 (13.33%)
Cardiovascular	3 (10.00%)
PAOD	2 (6.67%)
Flap type	
ALT free flap	17 (56.67 %)
TDAP free flap	6 (20.00%)
LD free flap	5 (16.67 %)
Gracilis muscle free flap	1 (3.33 %)
Internal pudendal artery perforator with anterior obturator artery perforator flap	1 (3.33 %)
Reduction stage	
First reduction	30 cases (65.22 %)
Second reduction	16 cases (34.78 %)
Cause of reconstruction	
Trauma	23 (76.67 %)
Malignant tumor	3 (10.00%)
Diabetic mellitus foot	1 (3.33%)
Postoperative infection	1 (3.33%)
Vasoconstrictor use	1 (3.33%)
Chronic osteomyelitis	1 (3.33%)
Location	
Lower extremities	25 (83.33%)
Upper extremities	2 (6.67%)
Head and neck	2 (6.67%)
Genitals	1 (3.33%)

BMI, body mass index; HTN, hypertension; DM, diabetes mellitus; PAOD, peripheral arterial occlusive disease; ALT, anterolateral thigh; TDAP, thoracodorsal artery perforator; LD, latissimus dorsi

Table 2. Operative data Characteristics

	Reduction ratio (mean)	Reduction interval (mean)
Total	46.88 % (mean) (26.67 – 70.00%)	6.13 months (2 – 36 months)
Subgroups		
First reduction	48.39 % (26.67 – 70.00%)	6.00 months (2 – 22 months)
Second reduction	44.06 % (30.00 – 60.00%)	6.38 months (2 – 36 months)
	(Mean)	
Initial flap size	15.64 × 8.03 cm2	
Drain removal day	3.54 days	

Table 3. Complication

Complication	Number	Management
Hematoma	3 (6.52 %)	Surgical care (2)
		Conservative care (1)
Partial flap necrosis	2 (4.35 %)	Conservative care (1)
		Surgical care (1)
Flap color change	3 (6.52 %)	Conservative care
Wound dehiscence	1 (2.17 %)	Conservative care
Fluid collection	1 (2.17 %)	Conservative care

Table 4. Univariate comparisons of complications after flap reduction with direct excision

Characteristics	No complication (n=36)	Complication (n=10)	P-value	Odds ratio	Confidence interval
Age	45.97 years	45.60 years	0.96	1.00	0.97-1.03
Underlying disease			0.71	1.60	0.43-5.98
HTN	8 (22.22 %)	4 (40.00 %)			
DM	4 (11.11 %)	1 (10.00%)			
Dyslipidemia	1 (2.78 %)	1 (10.00 %)			
Cardiovascular	3 (8.33 %)	0 (0.00 %)			
PAOD	2 (5.56 %)	0 (0.00 %)			

BMI	25.03 kg/m2	27.03 kg/m2	0.12	1.07	0.93-1.23
Smoker	9 (25.00%)	5 (50.00 %)	0.047*	4.99	1.14-21.74
Initial flap size	14.93 × 7.74 cm2	18.15 × 9.05 cm2	0.067	1.08	0.24-6.96
Reduction ratio	46.16 %	49.5 %	0.32	1.04	0.97-1.11
Reduction interval	6.54 months	4.70 months	0.21	1.07	0.20-5.70

*Statistically significant
HTN, hypertension; DM, diabetes mellitus; PAOD, peripheral arterial occlusive disease; BMI, body mass index.

Table 5. Multivariate comparisons of complications after flap reduction with direct excision

Characteristics	Odds ratio	P-value	Confidence interval
Smoker	3.66	0.11	0.75-17.84
Initial flap size	1.01	0.17	1.00-1.02

2025년 대한수부외과학회
추계학술대회

Room B

ICL: Wrist Instability

Orthop Surg. Yeson Hosp. **Jae Hoon Lee**
Orthop Surg. Jeju National Univ. **Kyu Bum Seo**

원위 요척관절 불안정성 (Distal Radioulnar Joint Instability)

Orthop Surg. Korea Univ.
Jong Woo Kang

원위 요척 관절(Distal Radioulnar Joint, DRUJ) 불안정성은 전완의 회전 운동에 중요한 역할을 하는 원위 요척 관절에 불안정성이 존재하는 상태로 삼각 섬유 연골 복합체(TFCC)손상, 골성 변형 등 다양한 원인에 의해 발생한다. DRUJ 불안정성은 통증, 불안정감, 위약감 등을 유발하여 기능 저하를 야기하며 종국에는 관절염을 유발할 수 있으므로 조기 진단과 적절한 치료가 무엇보다 중요하다.

색인단어: 원위 요척 관절, 삼각 섬유 연골 복합체, 불안정성, 부정 유합, 관절염

서론

원위 요척관절(DRUJ)은 전완의 회전 운동을 담당하는 관절로, 손목과 전완의 기능적 움직임에 필수적이다. DRUJ 불안정성은 삼각 섬유 연골 복합체(TFCC) 손상, 선천성 기형, 부정유합 등으로 인한 골성 변형 등 다양한 원인에 의해 발생하며, 통증, 불안정감, 위약감으로 인한 기능 저하, 이차성 원위 요척 관절염 등으로 심각한 임상적 문제를 유발할 수 있다. 최근 손목 관절경을 통한 원위 요척관절 불안정성의 진단 및 치료 방법의 발전으로 좋은 임상 결과를 거두고 있다.

원위 요척 관절의 해부학 및 생역학

DRUJ는 원위 요골의 요골 절흔(sigmoid notch)과 척골두(ulnar head)로 구성되며, 전완 회전 운동의 축 역할을 하며 관절의 안정성은 골성 구조(요골, 척골)와 연부 조직, 특히 TFCC에 의해 유지된다. TFCC는 관절원판(articular disc), 요척간 인대(radioulnar ligaments), 척골수근 인대(ulnocarpal ligaments), 척수근 신건 (extensor carpi ulnaris, ECU) 등으로 구성하는 일종의 연골조직으로 TFCC의 심부 인대는 척골의 fovea에 부착되어 DRUJ의 전후방 안정성에 핵심적인 역할을 한다(Fig. 1).

골성 구조물은 DRUJ 안정성의 약 20%를 담당하며, 나머지는 대부분 삼각 섬유 연골이 담당한다. 동적 안정체로는 ECU 건막, 방형 회내근(pronator quadratus), 골간막(interosseous membrane) 등이 있다. 최근에는 원위 사선형 다발(distal oblique bundle, DOB)이 DRUJ의 동적 안정화에 그 중요성이 강조되고 있다.

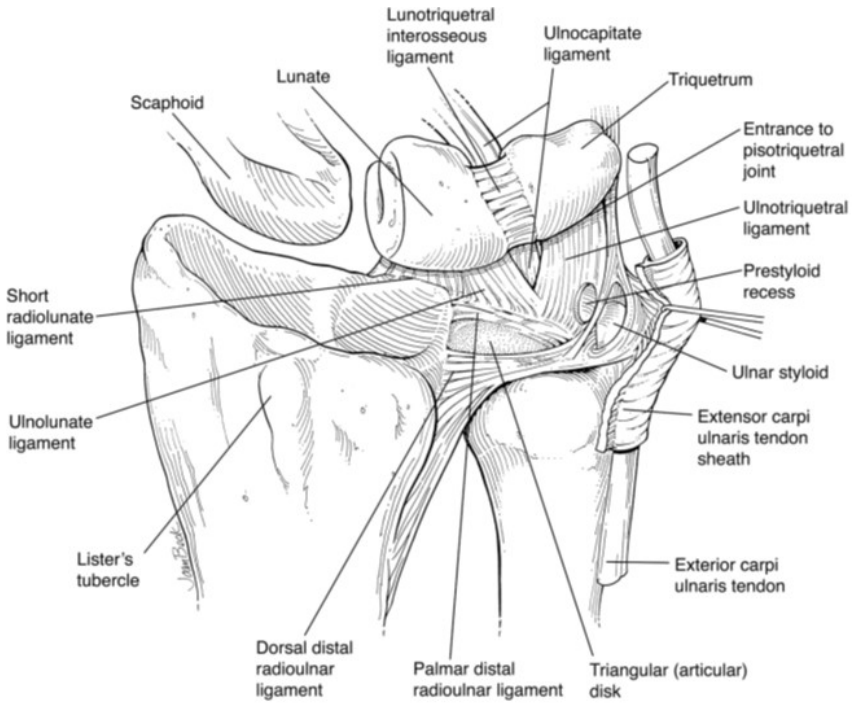

Fig. 1 Anatomy of ulnar wrist. Numerous and small anatomical structures overlap each other. Reprinted from Shin et al. with the permission of Wolters Kluwer.

병태생리

DRUJ 불안정성은 주로 외상(골절, 탈구 등)에 의해서 발생하는 경우가 많으나 선천적 기형, 척골 충돌 증후군, 염증성 관절염 등의 비외상성으로 발생한 수 있다. 외상성 손상에서는 원위 요골 골절 후 부정유합, TFCC 심부파열이 대표적이다. TFCC의 심부파열은 DRUJ의 전후방 및 횡 방향 안정성을 현저히 감소시켜 불안정성을 유발한다. 장기간 불안정성이 지속되면 DRUJ 내 충돌으로 인해 관절 연골 손상과 이차성 관절염으로 진행할 수 있다.

임상 증상 및 진단

환자는 전완의 회전 시 통증, 불안정감, 탄발음, 위약감 등의 증상 호소한다. Ballottement test, Piano key sign, Press test 등으로 DRUJ의 전후방 이동성과 통증 유발 정도를 평가할 수 있으며 가장 유용한 이학적 검사이다. 또한 원위 요척관절 배측에 압통이 있으며 삼각 섬유 연골 복합체 파열에 의해 불안정성이 유발되는 경우 척수근 관절의 척측 (foveal sign)의 압통이 관찰될 수 있다. 영상 진단은 불안정성의 원인을 감별하기 위한 목적으로 시행할 수 있다. 단순 방사선 검사에서는 요골과 척골의 정열, 변형의 유무를 건측과 비교하여 평가할 수 있으며 자기 공명 영상 검사 (Magnetic resonace image, MRI)을 통해 TFCC를 포함한 주변 연부 조직의 이상 여부를 평가할 수 있다. 동적 fluoroscopy 나 초음파는 실시간 DRUJ 관절 상태 평가에 유용하며 손목 관절경은 진단과 치료에 모두 유용하며 TFCC의 변연부 심부 파열 등 미세 병변까지 확인할 수 있다. Atzei 분류 등 TFCC 손상의 분류법 (Fig. 2)이 임상적 치료 방법 결정에 널리 활용되고 있다.

		DRUJ instability (ballotement test)	Quality of distal TFCC (appearance on RC arthroscopy)	Quality of proximal TFCC (appearance on DRUJ arthroscopy/ hook test)	Reparability of TFCC tear's margins (healing potential)	Quality of DRUJ cartilage (DRUJ arthroscopy)	Suggested treatment
	**Class 1 Repairable distal tear**	None/slight	Rupture	Intact	Good	Good	Repair: Ligament-to-capsule suture
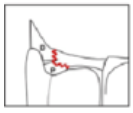	**Class 2 Repairable complete tear**	Mild/severe	Rupture	Rupture	Good	Good	Repair: Foveal refixation
	**Class 3 Repairable proximal tear**	Mild/severe	Intact	Rupture	Good	Good	Repair: Foveal refixation
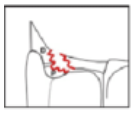	**Class 4 Non-repairable tear**	Severe	Rupture	Rupture	Poor	Good	Reconstruction: Tendon graft
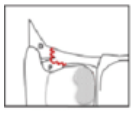	**Class 5 Arthritic DRUJ**	Mild/severe	Variable	Variable	Variable	Poor	Salvage: Arthroplasty or joint replacement

DRUJ: distal radio-ulnar joint; RC: radio-carpal; TFCC: triangular fibrocartilage complex.

Fig. 2 Classification of TFCC peripheral tears modified from Atzei (2009).

치료

보존적 치료

급성, 경증 불안정성은 4~6주간 장상지 석고 부목으로 고정하며, 이후 재활치료로 방형 회내근 및 척수근 신건의 강화운동을 시행하며 보존적 치료에 임상결과가 좋지 않거나 심한 불안정성은 수술적 치료를 시행한다. TFCC 심부의 완전 파열이 동반된 경우 관절경하 또는 개방적 접근으로 TFCC 심부 봉합술을 통해 fovea에 부착시켜준다. 원위 요골이나 원위 척골의 부정유합에 의해 불안정성이 유발되는 경우 교정 절골술(osteotomy)을 시행하여 DRUJ의 일치성을 회복 시켜야 한다. DRUJ의 만성 불안정성에서는 과거 Adams 술식을 통한 인대 재건술 시행하기도 하였으나 최근 관절경적 술기의 발전으로 현재 잘 시행하지는 않고 있다. DRUJ의 심한 관절염이 발생한 경우 Sauvé–Kapandji 술식, Darrach 수술 등의 구제적 수술(salvage procedure)을 통해 치료할 수 있다.

결론

DRUJ 불안정성은 통증, 불안정감, 위약감 등을 유발하여 기능 저하를 야기하며 종국에는 관절염을 유발할 수 있으므로 조기 진단과 적절한 치료가 무엇보다 중요하다. DRUJ 불안정성은 해부학적으로 복잡하고 다양한 유발 원인이 있어 그 진단과 치료가 어렵지만, 정확한 원인을 진단하여 적절한 치료를 시행하면 양호한 임상결과를 거둘 수 있다.

참고문헌

1. Dmour A, Tirnovanu S-D, Popescu D-C, Forna N, Pinteala T, Savin L, et al. Advancements in diagnosis and management of distal radioulnar joint instability: a comprehensive review including a new classification for DRUJ injuries. J Orthop Traumatol. 2024;24(3):e100.
2. Rodríguez-Merchán EC. Distal radioulnar joint instability: diagnosis and treatment. EFORT Open Rev. 2022;7(5):323-332.
3. Marès O, Dap F, Dap L, Dap T. Distal radioulnar joint instability: diagnosis and treatment. J Orthop. 2023;38:101-110.
4. Hohenberger G, Riggenbach M, Delbast F, et al. Distal oblique bundle influence on distal radioulnar joint stability: a biomechanical study. Sci Rep. 2023;13:48875.
5. Qazi S, Kim JK, Yi JW, Jeon SH. Distal radioulnar joint instability and associated injuries. J Hand Surg Asian Pac Vol. 2021;26(4):345-352.
6. Nishiwaki M, Welsh MF, Gammon B, Ferreira LM, Johnson JA, King GJW. Effect of volarly angulated distal radius fractures on forearm rotation and distal radioulnar joint kinematics. J Hand Surg Am. 2015;40(11):2236-2242.
7. Dy CJ, Jang E, Taylor SA, Meyers KN, Wolfe SW. The impact of coronal alignment on distal radioulnar joint stability following distal radius fracture. J Hand Surg Am. 2014;39(7):1264-1272.
8. Fujitani R, Omokawa S, Akahane M, Iida A, Ono H, Tanaka Y. Predictors of distal radioulnar joint instability in distal radius fractures. J Hand Surg Am. 2011;36(12):1919-1925.
9. Adams BD, Berger RA. An anatomic reconstruction of the distal radioulnar ligaments for posttraumatic distal radioulnar joint instability. J Hand Surg Am. 2002;27(2):243-251.
10. Adams BD. Anatomic reconstruction of the distal radioulnar ligaments for DRUJ instability. Tech Hand Up Extrem Surg. 2000;4(3):154-160.
11. Nilsson K, Hallberg P, Tesselaar E, Farnebo S. A novel technique to assess distal radioulnar joint stability using increasing torque. J Wrist Surg. 2019;8(4):327-334.
12. Nakamura R, Horii E, Imaeda T, Tsunoda K, Nakao E. Distal radioulnar joint subluxation and dislocation diagnosed by standard roentgenography. Skeletal Radiol. 1995;24(2):91-94.
13. Lindau T, Hagberg L, Adlercreutz C, Jonsson K, Aspenberg P. Distal radioulnar instability following distal radial fractures: an arthrographic and clinical study. J Hand Surg Br. 2000;25(5):437-443.
14. Wijffels MM, Keizer J, Buijze GA, et al. Clinical DRUJ instability does not influence the long-term functional outcome of conservatively treated distal radius fractures. Eur J Trauma Emerg Surg. 2017;43(2):237-243.
15. Kim JK, Yi JW, Jeon SH. The effect of acute distal radioulnar joint laxity on outcome after volar plate fixation of distal radius fractures. J Orthop Trauma. 2013;27(10):e228-e233.
16. Atzei A, Luchetti R. Foveal TFCC tear classification and treatment. Hand Clin. 2011;27(3):263-272.
17. Scheker LR. Distal radioulnar joint instability. J Hand Surg Am. 2008;33(6):1013-1025.
18. Nakamura T, Yabe Y, Horiuchi Y. Functional anatomy of the triangular fibrocartilage complex. J Hand Surg Br. 1996;21(5):581-586.

19. Garcia-Elias M, Lluch AL, Farreres A. The four-leaf clover: a new technique for DRUJ reconstruction. J Hand Surg Am. 1996;21(2):222-228.
20. Palmer AK, Werner FW. The triangular fibrocartilage complex of the wrist—anatomy and function. J Hand Surg Am. 1981;6(2):153-162.

Scapholunate Instability

Orthop Surg. The Catholic Univ. of Korea
Il-Jung Park

Primary stabilizer of the SL articulation

- **Scapholunate interosseous ligament (SLIL)**
  - *dorsal : strongest, most critical joint stabilizer*
  - palmar : thin, oblique
  - proximal membranous

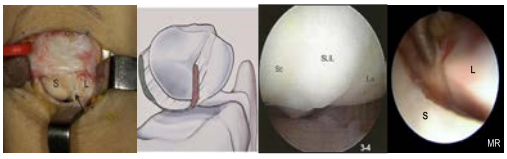

Natural history

Complete SLIL injury
+
Failure of secondary stabilizer
(DIC, STT, LRL)

↓

Abnormal carpal kinematics

↓

SLAC wrist

Isolated SLIL disruption is ***insufficient*** to produce **DISI deformity**

Complete tear of SLIL	Combined injury of 2nd stabilizers
Dynamic instability	Static instability

What is the most critical secondary stabilizer?

- Dorsal side
  - ✓ DIC
  - ✓ DRC
- Palmar side
  - ✓ STT
  - ✓ LRL

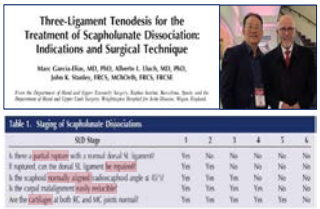

Stage 1: Partial scapholunate ligament injury
Stage 2: Complete disruption with repairable ligament
Stage 3: Complete disruption with irreparable ligament but normal alignment
Stage 4: Complete disruption with irreparable ligament and reducible rotary subluxation of the scaphoid
Stage 5: Complete disruption with irreducible malalignment and intact cartilage
Stage 6: Chronic SLIL disruption with cartilage loss (SLAC)

Scapholunate ligament reconstruction (stage 3, 4)

not only *restoration of SL widening* but also *addressing scaphoid flexion*

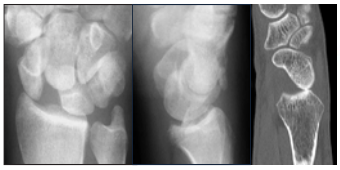

- Bone-ligament-bone
- RASL procedure
- SLAM procedure
- SwiveLock method
- Tendon reconstruction

Three-ligament tenodesis

Three-Ligament Tenodesis for the Treatment of Scapholunate Dissociation: Indications and Surgical Technique

Marc Garcia-Elias, MD, PhD, Alberto L. Lluch, MD, PhD, John K. Stanley, FRCS, MChOrth, FRCS, FRCSE

Garcia-Elias, 2006

The most widely performed procedure

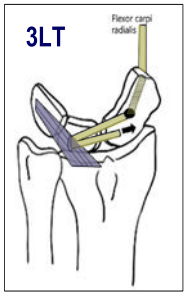

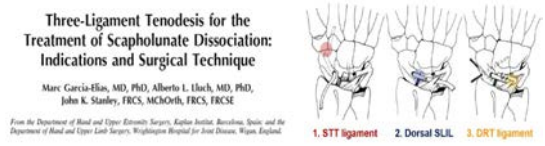

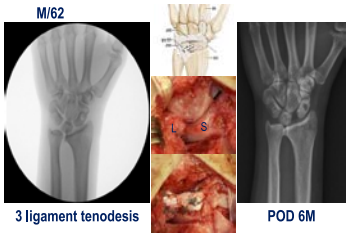

- Significantly relieved pain
- Increased grip strength
- Radiological recurrence of the deformity due to the *ligament loosening*

Tendon-to-ligament reconstructions

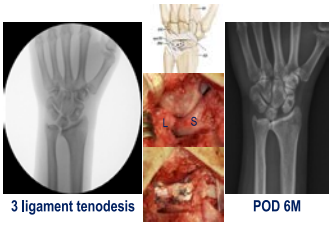

Ligament loosening resulted in recurrence of deformity

Because grafted tendon was stretched out and fixation was weak

Tendon-to-ligament reconstructions

Ligament loosening resulted in recurrence of deformity

Because grafted tendon was stretched out and fixation was weak

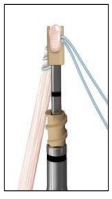

SwiveLock technique (SWT)

Autologous free tendon and synthetic tape (SutureTape)

Simple & reasonable surgical procedure

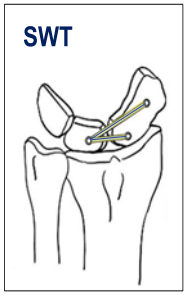

Original SWT (Reconstruction of only SLIL)

Reconstruction of only SLIL

Modified SWT (Simultaneous recon. of SLIL and DIC)

Reconstruction of only SLIL

Reconstruction of SLIL & DIC

Scapholunate ligament injury
Kienböck's disease

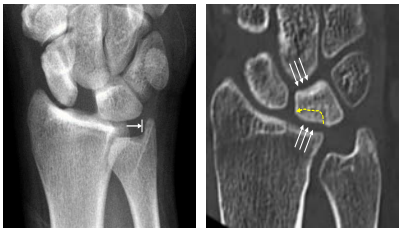

Kienböck's disease

"At-risk lunate"

It can be caused by
multiple factors

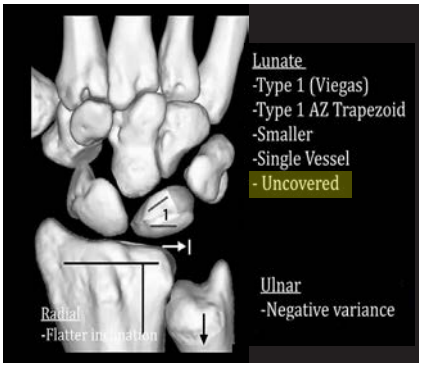

Bain GI et al. The etiology and pathogenesis of Kienböck disease. J Wrist Surg, 2016.

Uncovered lunate

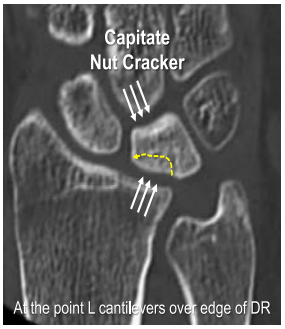

Repetitive loading
Stress fracture
Violates venous subarticular plexus
Localized venous hypertension
Edema of the fatty marrow
Increased osseous compartment Pr.
Producing avascular necrosis

Bain GI et al. The etiology and pathogenesis of Kienböck disease. J Wrist Surg, 2016.

Uncovered lunate

Etiology

✓Single major trauma
✓Repeated minor trauma

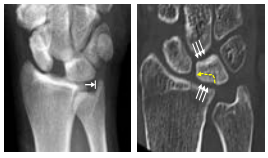

Vascular disruption of the lunate | Injury of the scapholunate ligament

↓

SL instability may have created abnormal forces on the lunate

It promotes vascular disruption of the lunate

Osteonecrosis of the lunate

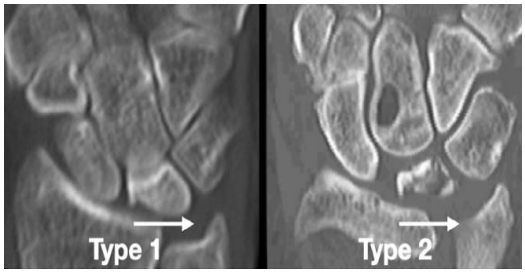

Failure of extrinsic stabilizers | Secondary to SL ligament rupture

Ulnar translocation in advanced KD

Hypothesis

- In SL dissociation, the pressure on the lunate will be greater than normal
- After SL dissociation is resolved, the pressure on the lunate will be greatly reduced

Unloading Procedures (Longitudinal Axis)

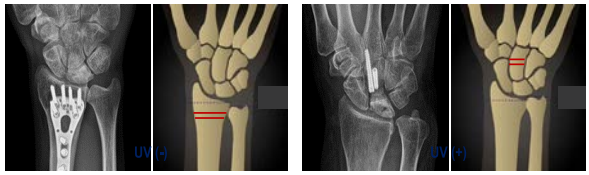

Radial shortening osteotomy | Capitate shortening osteotomy

Unloading Procedures (Transverse Axis)

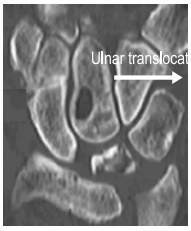

Ulnar carpal translocation

DST ligamentoplasty

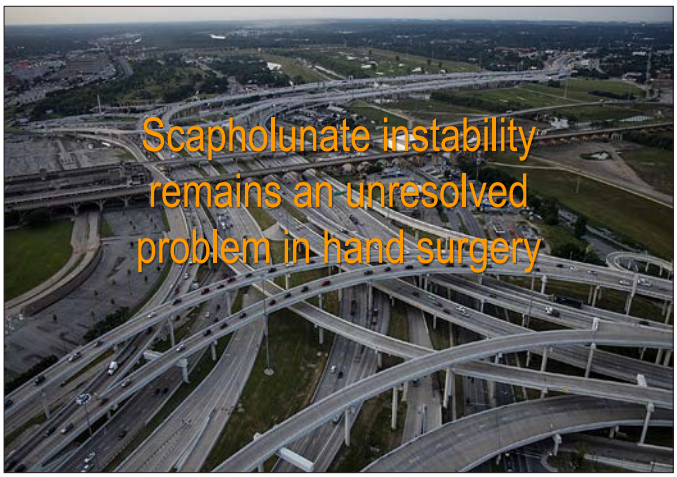

Midcarpal Instability

Orthop Surg. The Catholic Univ. of Korea
Joo Yup Lee

2025년 대한수부외과학회
추계학술대회

Room B

Free Paper 8 (Peripheral Nerve)

Plast Reconstr Surg. Hanyang Univ. **Seung Suk Choi**
Orthop Surg. Ulsan Univ. **Jae Kwang Kim**

Simultaneous transfer of spinal accessory and intercostal nerves to suprascapular, axillary, musculocutaneous, median, and ulnar nerves in preganglionic whole-arm type injuries of brachial plexus

Orthop Surg. Seoul National Univ.
Ji Sup Hwang

Introduction: For selected patients with preganglionic whole-arm type brachial plexus injury (BPI), we performed simultaneous transfer of spinal accessory and intercostal nerves to suprascapular, axillary, musculocutaneous, median, and ulnar nerves. We hypothesized that this surgery is a viable option in preganglionic whole-arm type BPI patients.

Methods: Two patients with the average age of 30 years were treated using simultaneous transfer of spinal accessory and intercostal nerves. The average interval between the BPI and the surgery was 4.9 months. Under prone position, one branch of spinal accessory nerve was transferred to suprascapular nerve, and remaining branch(es) to axillary nerve deltoid branch via sural nerve graft. Under supine position, 13 branches of intercostal nerve were harvested. Four motor branches were transferred to musculocutaneous nerve and two motor branches to median nerve. Remaining branches were transferred to median and ulnar nerves, with superficial radial nerve used as intervening nerve graft. Until one year post-surgical follow-up period, any complications were collected and the results of motor and sensory recovery were recorded using the modified British Medical Research Council grading system and the modified Highet's scale, respectively.

Results: No surgery-related complications were detected in the two patients. Shoulder abduction averaged 45 degrees, elbow flexor showed M2, and finger flexors M1. Sensibility in the median and ulnar nerve distribution of the hand was restored in all patients, with one S2 and one S3.

Conclusion: Simultaneous transfer of spinal accessory and intercostal nerves to suprascapular, axillary, musculocutaneous, median, and ulnar nerves seem to be a viable option in patients with preganglionic whole-arm type BPI.

Immediate Functional Recovery Following Brachial Plexus Neurolysis and Electrical Stimulation in Chronic Post-Stroke Upper Limb Paralysis: A Novel Peripheral Approach to Central Motor Deficits

[1]Orthop Surg. Hanyang Univ., [2]E-Da Hospital
Young Seok Lee[1], Chang-Hun Lee[1], Yu-Huan Hsueh[2], Yuan-Kun Tu[2]

Background: Post-stroke upper limb paralysis is traditionally attributed solely to central nervous system damage. However, secondary peripheral nerve entrapment and adhesions may contribute to functional deficits in chronic stroke patients.

Objective: To evaluate the immediate and sustained effects of brachial plexus external neurolysis combined with intraoperative electrical stimulation on upper limb function in chronic stroke patients with severe hemiparesis.

Methods: A patient with severe upper limb paralysis one-year post-ischemic stroke underwent brachial plexus external neurolysis. During surgery, electrical stimulation (2mA, Medtronic neurostimulator) was applied to the freed nerve structures. Grip strength, wrist/finger extension capability, and spasticity levels were assessed pre- and post-operatively.

Results: Immediately following neurolysis and electrical stimulation, the patient demonstrated remarkable improvement in grip strength and active wrist/finger extension. Flexor spasticity decreased substantially, allowing improved voluntary movement patterns. These initial gains were followed by progressive functional improvements during follow-up.

Discussion: The immediate functional recovery suggests that peripheral nerve adhesions and entrapment may significantly contribute to motor deficits in chronic stroke. Neurolysis likely restored nerve conduction in residual corticospinal pathways, while electrical stimulation may have reduced spinal hyperexcitability through reciprocal inhibition and enhanced proprioceptive feedback. The combination appeared to "unmask" latent motor capabilities previously blocked by peripheral factors.

Conclusion: Brachial plexus neurolysis with electrical stimulation represents a promising peripheral intervention for chronic post-stroke upper limb paralysis. This approach challenges the traditional central-only focus on stroke rehabilitation and suggests that addressing secondary peripheral nerve pathology can unlock residual

motor function. Further research is warranted to establish optimal patient selection criteria and stimulation parameters for this innovative treatment strategy.

Keywords: Stroke rehabilitation, Brachial plexus, Neurolysis, Electrical stimulation, Upper extremity paralysis, Peripheral nerve surgery

Can vascular flow change during provocation maneuvers predict surgical failure in neurogenic thoracic outlet syndrome?

Orthop Surg. Seoul National Univ.
Juneseok Won, Changhyon Lee, Jisup Hwang, Jihyeung Kim

Background: The need for simultaneous first rib resection during supraclavicular scalenectomy in patients with neurogenic thoracic outlet syndrome (NTOS) remains controversial. We have routinely evaluated vascular flow changes during provocation maneuvers through digital photoplethysmography. We asked whether the vascular flow change during provocation maneuvers can predict surgical failure after isolated supraclavicular scalenectomy for NTOS.

Methods: For 50 patients (mean age of 42.0 ± 16.5 years) who underwent supraclavicular scalenectomy for NTOS, we evaluated vascular flow change through digital photoplethysmography during several provocation maneuvers including Roos test, costoclavicular maneuver, and Adson maneuver before surgery. We calculated the adjusted odds ratio (OR) for surgical failure in association with the vascular flow change during each maneuvers with age, symptom duration, electrodiagnostic study findings, and number of visible vertebrae as covariates.

Results: Compared to the resting position, mean vascular flow during Roos test, costoclavicular maneuver, and Adson's maneuver was 46.0 ± 51.3 %, 42.9 ± 48.2 %, and 85.4 ± 64.1 %, respectively. Twelve patients (24%) were classified into surgical failure, and symptom duration (adjusted OR = 1.04, p = 0.04) and absent vascular flow during costoclavicular maneuver (adjusted OR = 23.30, p = 0.01) were significantly associated with failure.

Conclusions: A quantitative evaluation of the vascular flow changes that occur during provocation maneuvers can aid not only the diagnosis of NTOS but also help determine the optimal surgical treatment. In particular, if patients show absent blood flow during the costoclavicular maneuver, simultaneous scalenectomy and first rib resection should be considered.

Is cubital tunnel obliteration a safe and effective procedure for cubital tunnel syndrome?

Orthop Surg. Seoul National Univ.
Juneseok Won, Yongwoo Kim, Jisup Hwang, Jihyeung Kim

Background: Cubital tunnel obliteration aims to eliminate potential drawbacks of in situ decompression and anterior transposition of the ulnar nerve for treating cubital tunnel syndrome (CuTS). However, the safety of this technique has not been evaluated further, and no reports have focused specifically on its surgical outcomes. In this study, we evaluated patients who underwent cubital tunnel obliteration for established CuTS at a single institute. We questioned: (1) How are the electrophysiological and clinical outcomes of cubital tunnel obliteration? (2) What demographic and disease-related factors are associated with good electrophysiological outcomes?

Methods: Forty-three patients (mean age of 62 years) treated for CuTS between 2022 and 2023 were subjects of this study. We measured motor nerve conduction velocity (mNCV) and DASH scores four months and two years after surgery, respectively. We defined good electrophysiological outcome as normalization of the mNCV, for which we investigated the odds ratio (OR) with age, sex, body mass index, diabetes, etiology of cubital tunnel syndrome (idiopathic vs. secondary), and preoperative mNCV as covariates.

Results: The average mNCV improved from 28.9 ± 11.2 m/s to 38.1 ± 15.1 m/s and DASH score from 32.4 ± 18.7 to 11.7 ± 8.6. Good electrophysiological outcome was significantly associated with the absence of diabetes (adjusted OR = 0.04) and idiopathic CuTS (adjusted OR = 18.7), regardless of other factors.

Conclusions: Cubital tunnel obliteration seems to be a safe and reliable surgical option for treating CuTS and its short-term outcome was favorable for both idiopathic and secondary CuTS.

Electrophysiological Assessment of Reinnervation Following End-to-Side Anterior Interosseous Nerve Transfer for Advanced Cubital Tunnel Syndrome

Orthop Surg. Seoul National Univ.
Sung Ha Chun, Wan Kee Hong, Ji Sup Hwang, Ju Seok Ryu, Hyun Sik Gong

Background: Supercharge end-to-side (SETS) anterior interosseous nerve (AIN) transfer is a promising adjunct procedure to improve motor recovery in advanced cubital tunnel syndrome (CuTS). However, its effect is difficult to isolate, as conventional nerve conduction studies (NCS) cannot distinguish it from native ulnar regeneration. We introduce a modified NCS protocol to assess AIN-mediated reinnervation.

Methods: We developed a postoperative NCS protocol stimulating the median nerve at the wrist and recording compound muscle action potentials (CMAPs) from the first dorsal interosseous (FDI) and abductor digiti minimi (ADM) muscles. A response in either muscle upon median nerve stimulation was interpreted as evidence of reinnervation via the transferred AIN. FDI amplitudes over 4.0 mV were considered significant. Thirteen patients who underwent AIN SETS for CuTS were retrospectively reviewed and evaluated with this protocol at least six months postoperatively.

Results: Six showed clear evidence of AIN-mediated reinnervation, with FDI CMAPs over 4.0 mV. Four showed equivocal responses, suggestive of either ongoing reinnervation or volume conduction, and three showed none. FDI responses consistently exceeded ADM, indicating preferential reinnervation of the FDI. All reported sensory improvement.

Conclusion: The NCS protocol identified AIN-mediated reinnervation in about half of the patients, supporting its use in evaluating AIN SETS independent of native ulnar nerve recovery.

Table 1. Demographic and Surgical Characteristics of the Patients (n = 13)

Characteristic	Value
Sex	Male: 8 (61.5%), Female: 5 (38.5%)
Mean age ± SD, yr	62.8 ± 13.8 (range 28–79)
BMI ± SD, kg/m^2	26.0 ± 7.1
McGowan stage	IIB: 10 (76.9%), III: 3 (23.1%)
Surgical Side	Right: 9 (69.2%), Left: 4 (30.8%)
Electrodiagnostic Follow-up	6 months: 8 (61.5%), 12 months: 9 (69.2%), 18 months: 1 (7.7%)
Etiology	Compression with OA: 9 (69.2%) Trauma: 3 (23.1%) Pure compression: 1 (7.7%)
Additional Surgical Procedures	Epicondylectomy: 6 (46.2%) Transposition: 2 (15.4%) Debridement arthroplasty: 2 (15.4%)

BMI, body mass index; OA, osteoarthritis

Table 2. Electrophysiologic Findings in Case A

Timepoint	Muscle	Ulnar CMAP (mV)	Ulnar Latency (ms)	Median CMAP (mV)	Median Latency (ms)	Interpretation
Pre-op	FDI	0.5	13.06	–	–	Severe lesion
POD 6M	FDI	0.3	9.21	4.0	3.96	AIN signal present
POD 1Y	FDI	0.4	9.21	5.2	4.25	Sustained reinnervation
POD 1Y6M	FDI	0.9	7.23	6.3	4.0	Ongoing axonal growth
Pre-op	ADM	4.2	11.44	–	–	Severe lesion
POD 6M	ADM	3.3	8.23	0.5	3.73	Possible volume conduction
POD 1Y	ADM	3.6	8.21	NR	NR	No sustained signal
POD 1Y6M	ADM	3.6	8.23	NR	NR	No reinnervation

Table 3. Electrophysiologic Findings in Case B

Timepoint	Muscle	Ulnar CMAP (mV)	Ulnar Latency (ms)	Median CMAP (mV)	Median Latency (ms)	Interpretation
Pre-op	FDI	0.2	NR	–	–	Severe lesion
POD 1Y	FDI	0.5	NR	4.0	3.78	AIN signal present
Pre-op	ADM	3.4	8.99	–	–	Severe lesion
POD 1Y	ADM	3.1	9.13	0.4	3.67	Possible volume conduction

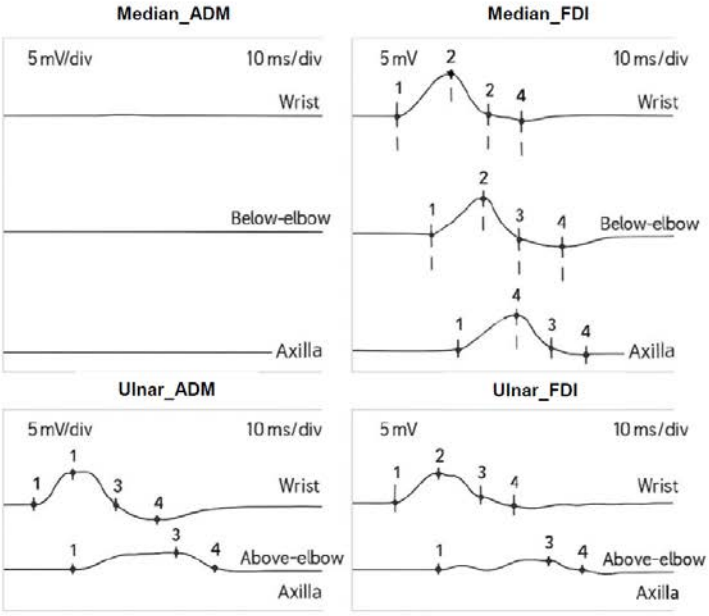

Figure 1. Compound muscle action potential (CMAP) waveforms of the abductor digiti minimi (ADM) and first dorsal interosseous (FDI) muscles at 18 months postoperatively. CMAPs were recorded following median and ulnar nerve stimulation. Stimulation of the median nerve elicited a clear response in the FDI but not in the ADM, indicating successful reinnervation via anterior interosseous nerve (AIN) supercharge end-to-side (SETS) transfer. In contrast, ulnar nerve stimulation evoked minimal response in the FDI and a preserved response in the ADM, suggesting selective reinnervation of the FDI by the transferred AIN, with limited native ulnar recovery.

Anatomical Variations of the Recurrent Branch of the Median Nerve Encountered During Carpal Tunnel Release: A 10-Year Observational Study

Wellson Hosp.
Hyun Sik Park

Background: In certain cases of carpal tunnel release, the motor branch of the median nerve (recurrent branch) traverses the transverse carpal ligament (TCL). If the distal TCL is divided sharply without careful inspection, there is a substantial risk of iatrogenic injury. Identifying such variations is critical for avoiding postoperative functional loss, especially in the thenar muscles.

Methods: A total of 292 patients (364 hands, including 72 bilateral cases) with carpal tunnel syndrome underwent open carpal tunnel release by a single surgeon over a 10-year period. The incision was made 5 mm ulnar to the main thenar crease, with maximal exposure. The midportion of the TCL was first incised with a scalpel, followed by proximal release under nerve protection up to the wrist crease. For distal release, meticulous blunt dissection was carried out until the superficial palmar arch was exposed. If fatty or nerve-like tissue was encountered, careful dissection traced the structure proximally and distally; suspected recurrent motor branches were confirmed via electrical stimulation-induced thenar muscle contraction. Anatomical variations were documented.

Results: In 8 of 364 cases (2.2%), a recurrent motor branch arose proximal to the distal edge of the TCL. Variations included:

- Radial origin directly to the thenar muscles (2 cases)
- Central origin coursing radially (2 cases)
- Ulnar origin traversing the TCL and running radially within it toward the thenar muscles (4 cases)

A persistent median artery was found in 1 case. One patient, in whom no recurrent branch was detected intraoperatively, presented postoperatively with persistent paresthesia and progressive thenar weakness.

Conclusion: A recurrent motor branch originating proximal to the distal edge of the TCL is not uncommon. Ulnar-origin branches crossing within the TCL present a higher risk during distal release. While proximal TCL

division poses minimal risk, distal release requires extreme caution. Stepwise blunt dissection, preferably with Metzenbaum scissors, is recommended over sharp, one-stroke division. In endoscopic procedures, the possibility of such anatomical variations should be anticipated to minimize the risk of nerve injury.

Keywords: Carpal tunnel release; median nerve; recurrent branch; transverse carpal ligament; anatomical variation; thenar muscle; nerve injury; surgical technique; endoscopic surgery

Clinical Relevance Statement: Surgeons performing carpal tunnel release should be cognizant of possible anatomical variations of the recurrent branch of the median nerve, particularly those arising ulnarly and traversing the transverse carpal ligament. Awareness and careful surgical technique can help prevent iatrogenic nerve injury, postoperative thenar weakness, and functional deficits. This study highlights the necessity of meticulous dissection during distal TCL release and recommends approaches to minimize risk in both open and endoscopic procedures.

Rethinking Pediatric Anesthesia in Hand Surgery: Beyond General Anesthesia

W Institute for Hand and Reconstructive Microsurgery, W General Hosp.
Soo Jin Woo, Yeong Hee Lee, Hyun Jae Nam, Yeong Woo Kim, Sang Hyun Woo

General anesthesia remains the standard approach in many institutions for pediatric hand surgery. While effective, it is not always necessary, and alternative methods may provide advantages in safety, efficiency, and recovery. At our center, we have adopted a broader, more flexible strategy that incorporates multiple anesthetic options tailored to patient age, cooperation level, and surgical complexity.

At a single high-volume hand surgery center, a range of anesthesia techniques has been selectively applied according to patient age, level of cooperation, and surgical complexity. This spectrum includes regional, local, and mask-based methods, often combined with non-pharmacologic adjuncts to improve tolerance. Such an approach has reduced dependence on intubated general anesthesia while maintaining surgical conditions and patient comfort.

Experience from this cohort indicates that pediatric hand surgery can be performed effectively across multiple anesthetic settings. The use of tailored strategies has the potential to lower perioperative risk, facilitate rapid recovery, and improve the overall surgical experience for children and their families. These findings suggest that expanding the armamentarium of pediatric anesthesia beyond conventional general anesthesia represents a practical and beneficial shift in clinical practice.

2025년 대한수부외과학회
추계학술대회

Room B

Travelling Fellows' Session

Orthop Surg. Sungkyunkwan Univ. **Min Jong Park**
Plast Reconstr Surg. Gwangmyeong Sungae General Hosp. **Dong Chul Lee**

Coverage of Fingertip Traumatic Amputation in Lesser Digits with Modified Volar Advancement Flap

University of Hong Kong
Marvin Man Ting Chung

My Journey of Hand Surgery Travelling Fellowship: Insights and Experiences

Taipei Veterans General Hospital
Cheng-Yu Yin

Lateral Shotgun Approach for the Proximal Interphalangeal Joint Silicone Arthroplasty

Kurashiki Central Hospital
Takuya Tsumura

Innovation in Hand Surgery: Our Works Using AI and VR

Nagoya University Hospital
Hidemasa Yoneda

The Practice of Hand Surgery in Greece: Insights from a Tertiary University Department

Papanikolaou Hospital
Eleni Karagergou

2025년 대한수부외과학회
추계학술대회

Room B

Symposium 4.

Flexor Tendon Surgery: Expert Techniques & Interactive Discussion

Plast Reconstr Surg. Yonsei Univ. **Jong Won Hong**
Plast Reconstr Surg. W General Hosp. **Hyun-Jae Nam**

Panel
Plast Reconstr Surg. Yonsei Univ. **Jiye Kim**
Plast Reconstr Surg. The Catholic Univ. of Korea **Bommie Florence Seo**

Flexor Tendon Tenorrhaphy: stick to the basic principles

Gangnam Jaejun Plastic Clinic
Jae-Won Yang

\굽힘힘줄손상의 치료에서 주요한 점은 힘줄봉합을 튼튼하게 하여 빠르고 효과적인 재활치료를 실시함으로써 손상 후 발생할 수 있는 운동제한을 최소화하여 최대한의 기능을 회복하는 것이라고 요약할 수 있을 것이다. 특히, 굽힘힘줄집(flexor tendon sheath; digital pulley system)이 있는 손가락(Zone II)부위는 굽힘힘줄이 협소한 굽힘힘줄집 안에서 활주해야 하는 제한적인 환경, 깊은굽힘힘줄과 얕은굽힘힘줄이 서로 교차하여 주행하는 것 그리고, 혈액공급이 다른 부위와 차이점을 보이는 해부학적 특징으로 인하여 힘줄유착에 따른 운동제한이 일어나기 쉬워서 굽힘힘줄 손상의 치료에서 도전적인 과제로 남아있다. 하지만, 굽힘힘줄들의 해부학적 특징, 치유과정, 효과적인 건봉합술 및 재건술, 재활치료, 발생 가능한 합병증 등에 대하여 이해하고 세심한 치료를 실시한다면 만족할 만한 결과를 얻을 수 있을 것이라 생각된다.

보통 일차힘줄봉합(primary tendon repair)은 수상 후 24시간 이내에 봉합하는 경우를 말하며, 지연일차힘줄봉합(delayed primary tendon repair)은 수상 후 24시간 - 2주 안에 개방된 창상을 통해 일차힘줄봉합이 된 경우를 말한다. 이차힘줄봉합(secondary tendon repair)은 2주가 지나서 창상절개 후 힘줄을 봉합하는 경우를 말한다.[1]

창상의 원인과 종류에 따라 접근방법이 다를 수 있으나, 창상이 깨끗해서 창상감염의 위험성이 적은 경우에는 가급적 일차힘줄봉합을 해주는 것이 좋다. 힘줄 끝이 심한 창상오염으로 감염이 우려되거나, 결손이 있는 것을 제외하고는 시기와는 상관없이 봉합해 줄 수만 있으면 언제든지 봉합해 주는 것이 좋다. 창상이 심하게 오염되어 있거나, 힘줄 결손이 있는 경우, 압궤손상이 심하여 연부조직의 일차적인 피복이 힘든 경우에는 창상이 치유된 후에 이차힘줄봉합 또는 힘줄이식술(tendon graft)을 고려할 수 있다.

손상된 힘줄의 치유과정 중 유착이 적게 일어나도록 하기 위해서는 다음과 같은 원칙을 지키는 것이 중요하다고 생각된다.

① 손상된 힘줄에 술자에 의한 추가 손상이 가해지지 않도록 노력한다. (atraumatic technique)
② 철저히 지혈하여 혈종 발생을 막는다. 혈종이 생기면 외인성 콜라젠이 많이 합성되며 콜라젠 재형성 기간이 오래 걸리게 되어 치유기간이 연장될 수 있다.
③ 조기에 봉합된 힘줄의 활주를 유도함으로써 튼튼한 힘줄치유를 유도한다. 근육의 수축력이 봉합해 준 힘줄에 알맞게 전달되면 콜라젠 배열이 조기에 양호해지며 장력이 증진된다. 수술 후에 조심스럽게 운동을 실시하는 이론적 근거가 여기에 있다. 그러나 외력이 너무 지나치게 가해지거나, 너무 일찍 가해지면 염증반응과 외인성 콜라젠 생성이 증가되어 유착을

초래하거나 힘줄봉합 부위가 벌어지게 된다 (gap formation). 이러한 현상은 힘줄봉합술 후 대개 4-5일부터 3-4주간에 일어날 수 있으므로 이 기간 동안에는 상당히 주의해야 한다.

손상기전과 정도, 생체 치유기전 이외에 힘줄봉합력(strength of tendon repair)에 영향을 주는 인자로는,

① 봉합면을 지나가는 봉합사의 수(numbers of suture strands)
② 봉합의 긴장도(tension of repair)
③ 힘줄속봉합(core suture)시 봉합면으로부터 봉합사가 힘줄을 물고 있는 길이(core suture purchase)
④ 봉합법간의 봉합력 차이; 묶음봉합법(locking: anchored)과 쥠봉합법(grasping: sliding)
⑤ 봉합사의 두께
⑥ 봉합사의 성상
⑦ 힘줄겉봉합(epitendinous suture)의 방법

등을 생각할 수 있으며, 이는 술자의 숙련도와 관련 있다고 하겠다.

힘줄의 봉합면을 가로지르는 봉합사의 수와 봉합력의 관계에 대한 연구들의 결과 봉합사 수가 4개 이상인 경우(여러가닥힘줄속봉합법; multiple strands core suture technique) 생체에서 측정된 정상수지 운동시 힘줄에 작용하는 힘보다 강한 봉합력을 가지므로 조기 운동치료에도 견딜 수 있는 힘을 가지는 것으로 알려져 있다. 봉합사를 너무 잡아당겨 봉합하면 힘줄이 접혀들어가게 되어 두께가 증가하게되므로(bunching) 굽힘힘줄집 안에서의 활주를 방해할 수 있으며, 너무 느슨하게 봉합하면 긴장도가 약하여 봉합면에 간극이 생겨 힘줄조직의 생성없이 섬유성 치유(fibrous healing)만 생기게 되어 지연힘줄파열(delayed tendon rupture)의 원인이 되기도 한다. 그러므로, 양쪽 힘줄끝이 맞닿을 정도로만 적절한 긴장도로 봉합해 주어야 한다. 이는 특히, 굽힘힘줄집이 있는 부위(Zone II)손상에서 특별히 신경 써야 할 기술적인 문제라고 생각된다. 봉합면으로부터 최소 0.7 – 1.0 cm 정도는 봉합사가 지나가 힘줄을 물고 있어야 힘줄을 견인할 수 있는 충분한 힘을 가진다고 한다. 힘줄을 지나가는 봉합사의 형태에 따라 분류하여 보면 묶음봉합법(locking suture method)와 쥠봉합법(grasping suture method)로 나누어 볼 수 있다. 보통 쥠봉합법이 묶음봉합법에 비하여 약한 것으로 알려져 있다. 힘줄의 두께에 따라 알맞은 두께의 봉합사를 사용하여야 하겠지만, 보통 FDP tendon의 힘줄속봉합을 위하여 3-0 또는 4-0 봉합사를 사용하는 것이 보통이다. 봉합사는 흡수성 또는 비흡수성 봉합사 모두 가능하지만, 힘줄 치유 기간동안 장력을 유지할 수 있는지를 고려하여 선택한다. 비흡수성, 다발성 봉합사인 FiberWire®는 강한 장력을 가지는 것으로 알려져 있다. 힘줄 봉합면을 매끄럽게 하여 활주를 방해하지 않도록 실시하는 힘줄겉봉합도 봉합력을 가지는 것으로 알려 있으며, 특히 깊은땀으로 봉합해주는 경우 봉합력이 크다고 한다.

힘줄봉합술이후 pulley와 tendon sheath를 봉합해 주어야 할 것인가 아닌 가에 대하여는 아직까지 논란의 여지가 있다. 하지만, 이는 유착에 대한 물리적인 장벽이 되며, 윤활액을 만들고, 힘줄에 영양을 공급하여 힘줄치유에 도움이 됩니다. 그러므로 봉합하는데 어려움이 있지만, 봉합해 주는 것이 힘줄 치유에 유리하다고 생각된다.

건봉합술의 방법

잘려진 힘줄의 몸쪽끝을 먼쪽끝이 있는 수준보다 5mm 더 당겨내어 23G 주사침으로 고정한다. 그렇게 힘줄봉합부위에 여유가 있도록 해 두어야 힘줄을 회전하여 뒷면도 쉽게 봉합할 수 있다. 봉합할 때는 수술용 확대경을 이용하는 것이 좋다.

저자는 몸쪽끝을 먼쪽끝에 닿도록 접근시킨 뒤 주사침을 피부 또는 굽힘힘줄집으로부터 힘줄에 찔러넣어 힘줄고정을 먼저 실시한다. 과도한 긴장도를 주어 당겨 봉합하여 봉합된 힘줄의 두께가 증가하거나, 부족한 긴장도로 간극이 생기는 것을 피하기 위하여 PDS 6-0로 힘줄겉봉합을 먼저 실시하여 절단면들이 알맞게 접근된 상태로 힘줄의 위치를 고정하면서 힘줄의 잘린면이 외부로 노출되지 않도록 매끈한 힘줄표면을 만들어 준다. 이후, ethibond 4-0 봉합사를 이용해서 힘줄속봉합을 보통 여덟에서 열가닥봉합법(8-10 strands core suture technique)해 준다. 이때 묶음봉합법(locking suture technique)를 사용하여 봉합사가 미끄러지면서 힘줄을 가르는 일이 없도록 한다. 힘줄의 혈액공급이 주로 힘줄의 손등쪽면을 따라 이루어지므로 힘줄속봉합시 봉합사가 힘줄의 손바닥쪽 1/2을 통과하도록 하는 것이 좋다. 굽힘힘줄집은 5-0 또는 6-0 봉합사로 봉합하며, 힘줄과 같이 봉합되지 않도록 주의한다. 손가락을 수동적으로 굽히거나 펴보아서 걸림 현상 없이 운동범위가 만족스러운지 검사한다.

수술 후 재활치료

굽힘힘줄의 봉합술 및 이식술 후 봉합 부위에 지나친 힘이 작용하여 생길 수 있는 재파열이 생기지 않도록 주의하면서 조기에 활주운동을 시켜 유착을 최소화하고 손가락뼈사이관절들의 강직을 막는 것이 수술 후 치료의 목적이라 할 수 있다.

1980년대에서 90년대에 이르러 여러가닥힘줄속봉합술(multiple strands core suture technique)을 이용한 튼튼한 힘줄봉합에 대한 연구가 진행됨에 따라 조기 능동운동이 제안되었다. 이러한 보고들 중 "Belfast Method"는 손목은 약간만 구부리고 손허리손가락관절은 90도 이하로 굽힌자세로 splint를 댄 후, 수술 후 약 48시간부터 능동운동을 시키며 수동운동도 함께 시킨다. 약 6주 후부터는 splint도 제거하고 운동시킨다고 한다.

저자도 굽힘힘줄을 여러가닥힘줄속봉합을 이용하여 봉합을 실시하면서부터, 손목은 약 20-30도, 손허리손가락관절은 약 60-70도 굽히고 손가락뼈사이관절들은 편상태로 손등쪽에 splint를 대어 고정하고, 창상의 출혈이 줄어들고 통증과 부종이 완화되는 수술 후 3-5일 사이에 능동운동을 시작하며 수동운동을 병행하고 있다. 보통 약 2주 후부터는 운동범위가 눈에 띄게 향상됨을 확인할 수 있다. 수술 후 약 6주부터는 splint를 떼고 능동적으로 손가락의 굽힘운동과 폄운동을 권유하는데 이때, 손목은 약 20-30도 구부린 자세로 운동하여 과도한 긴장도가 봉합부위에 작용하는 것을 막는다. 수술 후 7-8주부터는 수동폄운동도 추가하여 손가락의 운동범위가 정상범위에 이르도록 유도한다.

Zone 2 Combined FDS and FDP Injury

Plast Reconstr Surg. The Catholic Univ. of Korea
Sung-No Jung

Zone Ⅱ
Combined FDP and FDS injury

Department of Plastic and Reconstructive Surgery
College of Medicine, The Catholic University of Korea
Uijeongbu St. Mary's Hospital

THE CATHOLIC UNIVERSITY OF KOREA
CATHOLIC MEDICAL CENTER

Sung-No Jung

Anatomy of flexor tendon

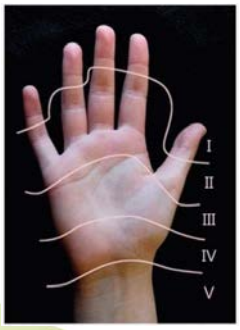

THE CATHOLIC UNIVERSITY OF KOREA
CATHOLIC MEDICAL CENTER

History of repair in zone Ⅱ

- **Sterling Bunnell – " no man's land"**
  - fibro-osseous digital canal: both the tendons interweave in a complex manner.
  - the increase its complexity because minimal swelling of the epitenon can impair free motion of the tendon
- **Three prominent surgeons of the era before 1960 named Bunnell, Mason, and Boyes preferred secondary tendon grafting as compared to primary repair in the " no man's land"**

THE CATHOLIC UNIVERSITY OF KOREA
CATHOLIC MEDICAL CENTER

- **Zone 2 repair after 1960**
  - Kleinert reported an 87% good to excellent results
  - Advance in technique – stronger repairs, meticulous surgical techniques, rehabilitation protocol and development of skills in surgeons

⇒ Primary tendon repair

THE CATHOLIC UNIVERSITY OF KOREA
CATHOLIC MEDICAL CENTER

Ideal primary flexor tendon repair (Strickland)

1. Easy suture placement
2. Secured knots
3. Smooth end to end tendon apposition
4. Minimal to no gapping ay the repair site
5. Avoiding injury to tendon vasculature
6. Having enough strength for early active postoperative motion

Achieving well functioning Intraoperative gliding for a flexor tendon in zone Ⅱ

⇩

balancing tendon strength and glide

THE CATHOLIC UNIVERSITY OF KOREA CATHOLIC MEDICAL CENTER

THE CATHOLIC UNIVERSITY OF KOREA CATHOLIC MEDICAL CENTER

Primary flexor tendon repair

- An increase in tendon diameter of approximately 10–20% is considered ideal after tenorrhaphy
  - <10% → May indicate insufficient core strands and inadequate tensile strength
  - >25% → Causes excessive friction, poor gliding, and higher adhesion risk.
- Perform a continuous epitendinous suture to smooth the surface

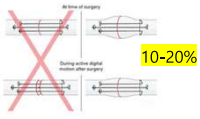

10-20%

THE CATHOLIC UNIVERSITY OF KOREA CATHOLIC MEDICAL CENTER

Epitendinous sutures

Reduce bulk
Increase strength (adds 20% to tensile strength)
Resist gap formation

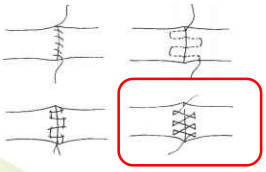

Locking looped epitenon suture (Silfverskiold)

THE CATHOLIC UNIVERSITY OF KOREA CATHOLIC MEDICAL CENTER

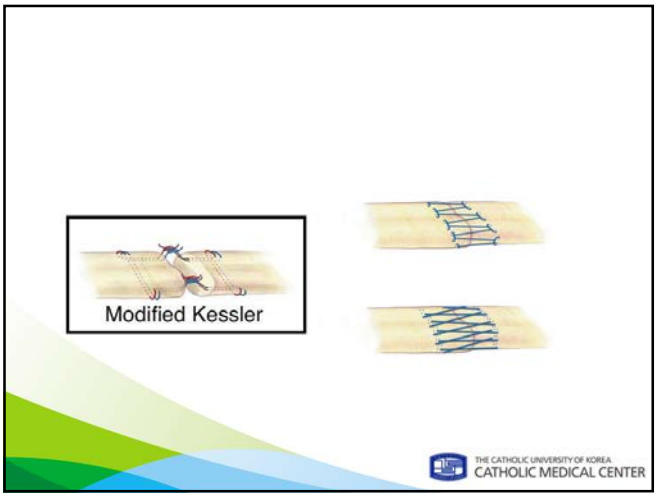

Both FDP and FDS injuries - Options

- **Repair of the FDP tendon only**
  - FDS tendon is severely damaged
  - Slips of FDS are to be repaired underneath A2 pulley
  - reduces adhesion formation
  - PIP joint flexion strength may be slightly reduced
- **Repair of both tendon**
  - both FDP and FDS tendons are cleanly lacerated
  - Provides stronger overall finger flexion
  - Prevent PIP joint hyperextension
  - increases the risk of tendon crowding, adhesions, and reduced glide
  - Combined volar plate injury/ radial collateral ligament injury
- **Repair of FDP with repair of one slip of FDS tendon**
  - Offers a balance between strength and gliding function

THE CATHOLIC UNIVERSITY OF KOREA
CATHOLIC MEDICAL CENTER

Effect of Repair Strategy on Gliding Resistance

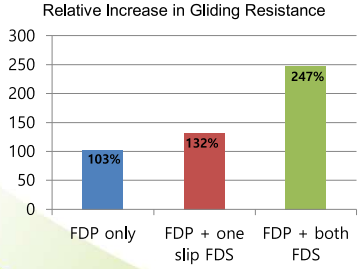

Clinical Implication
- Avoid excessive bulk in Zone 2
- Consider selective FDS repair (one slip) to optimize tendon gliding and functional recovery.

J. hand surg am. 2002: 27: 316-21

THE CATHOLIC UNIVERSITY OF KOREA
CATHOLIC MEDICAL CENTER

Pulleys

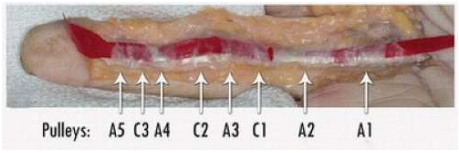

Bowstring : A2, A4,.....A1, A3 (A2 pulley injury)

THE CATHOLIC UNIVERSITY OF KOREA
CATHOLIC MEDICAL CENTER

A2 Pulleys

FDP excursion
23-27 mm

flexor tendons glide only 1.5 to 2 cm
with full digital extension and flexion

A2 Pulley
13-20mm

THE CATHOLIC UNIVERSITY OF KOREA
CATHOLIC MEDICAL CENTER

Pulley vent

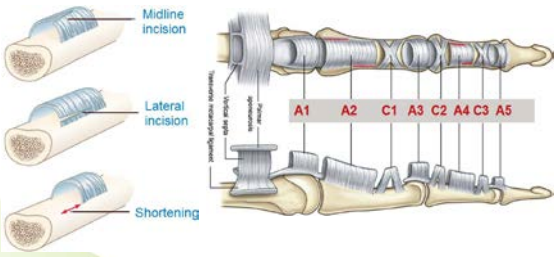

THE CATHOLIC UNIVERSITY OF KOREA
CATHOLIC MEDICAL CENTER

Incisions to vent the pulleys

- Injury at level of C1
  : vent the distal 1/3-1/2 of A2 pulley

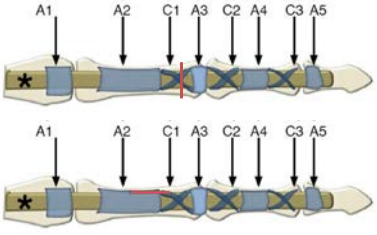

THE CATHOLIC UNIVERSITY OF KOREA
CATHOLIC MEDICAL CENTER

Incisions to vent the pulleys

- Injury at level of distal A2
  : vent the distal 2/3 of A2 pulley

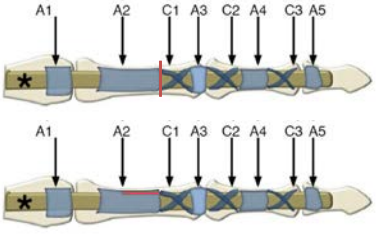

THE CATHOLIC UNIVERSITY OF KOREA
CATHOLIC MEDICAL CENTER

Incisions to vent the pulleys

- Injury at level of middle A2
  : vent the proximal 2/3 of A2 pulley

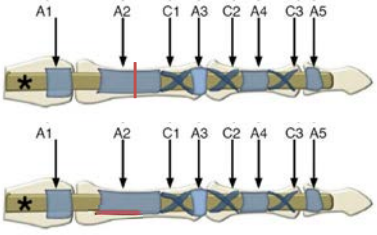

THE CATHOLIC UNIVERSITY OF KOREA CATHOLIC MEDICAL CENTER

Pulley enlargement

- Extensor Retinaculum Graft

- Triangular excision

- Omega plasty

THE CATHOLIC UNIVERSITY OF KOREA CATHOLIC MEDICAL CENTER

Pulley release safety without bowstringing

Pulley	Safe Release	Bowstring Threshold	Recommendation
A1	100%	None	Safe if A2 intact
A2	≤50–75%	≥75%	Maintain distal half
A3	100%	None	Minimal role
A4	≤50%	≥75%	Preserve proximal half

THE CATHOLIC UNIVERSITY OF KOREA CATHOLIC MEDICAL CENTER

A2 pulley release extent

Condition	A2 Pulley Release Extent	Supporting Study
Intact A1, A3, A4	Up to **100% (Full release)**	Tang (2014)
A1 + 50% A2 release	50%	Lu et al. (2016)
A2 + A4 25–75% release	≤75%	Mitonis et al. (2018)
Distal half of A2	50%	Cadaveric study (2019)
Multiple pulley release	≤50% (cumulative)	Recent studies (2020–2023)

Achieving well functioning Intraoperative gliding for a flexor tendon in zone 2 : Full A2 pulley release may be biomechanically safe with intact A1, but most surgeons limit to ≤75% for clinical safety.

THE CATHOLIC UNIVERSITY OF KOREA CATHOLIC MEDICAL CENTER

Pulleys and FDS management

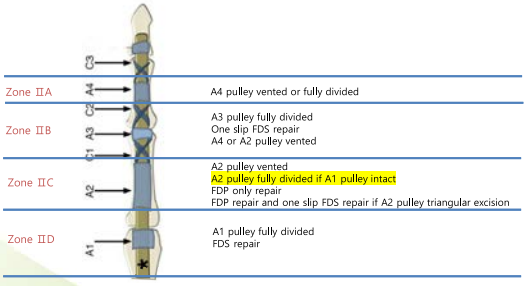

JHS(E) 2018:43: 474-479

THE CATHOLIC UNIVERSITY OF KOREA CATHOLIC MEDICAL CENTER

- **Before closure, tendon gliding through the pulleys should be assessed**
  - Wide awake surgery
  - Passive finger flexion and extension test
  - Passive tenodesis grasp and release test

THE CATHOLIC UNIVERSITY OF KOREA CATHOLIC MEDICAL CENTER

Order of repair: FDS VS FDP

- **FDP-first → gliding test & pulley management → (FDS or FDS one-slip)→ gliding test**

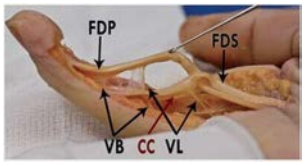

THE CATHOLIC UNIVERSITY OF KOREA CATHOLIC MEDICAL CENTER

Zone Ⅱ repair

- **Most hand surgeons prefer to repair the FDP and one slip of FDS, reasonably a good option** as the repair of both slips of FDS may produce overcrowding within the sheath and pulleys and compromise the result

THE CATHOLIC UNIVERSITY OF KOREA CATHOLIC MEDICAL CENTER

complications

- **Adhesion**
  - Between the FDP and FDS
  - Function in the finger can be improved by 50% by tenolysis
  - Three months is considered to be earliest time for flexor tenolysis

dorsal fascial flap

Hyaluronate hydrogel barrier ADM

- **Rupture**

THE CATHOLIC UNIVERSITY OF KOREA CATHOLIC MEDICAL CENTER

Flexor tendon rehabilitation

- **Edema control**
  - Edema in the repaired tendon and its surrounding soft tissues increases the resistance to finger flexion
- **Rehabilitation programs**
  - Kleinert:
    - Active extension
    - Passive flexion by rubber bands
  - Duran:
    - Controlled passive motion
  - Strickland:
    - Early active ROM

Goal: Full active ROM at 10-12 weeks

THE CATHOLIC UNIVERSITY OF KOREA CATHOLIC MEDICAL CENTER

- **Resistance to motion**
  - Days 0-4
    - Increase in resistance
  - Days 4-7
    - Resistance consistent
  - Days 7 beyond
    - Adhesion formation
- **Tendon weakest at 10-14 days**

THE CATHOLIC UNIVERSITY OF KOREA CATHOLIC MEDICAL CENTER

Active motion protocol

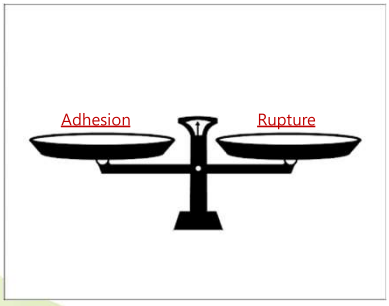

THE CATHOLIC UNIVERSITY OF KOREA CATHOLIC MEDICAL CENTER

Dorsal blocking splint

Start at 3-5 days if swelling allows

2wk

3wk

4wk

5 ~6wk

6wk : discontinue splint
7wk : passive extension

6 ~8 wk: Light strengthening begin

12 wk: normal activity

THE CATHOLIC UNIVERSITY OF KOREA CATHOLIC MEDICAL CENTER

Points

- Strong repair using at least a 4-strand core suture :
- Epitendinous suture :
  - 2-mm rim for repair
  - Deep
  - Locking looped epitendinous suture
- Bulky repairs should be avoided
- A2 pulleys may be vented up to 2/3
- Before closure, tendon gliding through the pulleys should be assessed
- Edema control

THE CATHOLIC UNIVERSITY OF KOREA CATHOLIC MEDICAL CENTER

Preferred method

- Wide awake surgery
- Repair FDP only / Repair FDP and one slip of FDS
- A2 pulley 2/3 vent

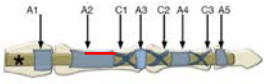

- Triangular excision

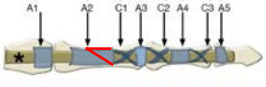

THE CATHOLIC UNIVERSITY OF KOREA CATHOLIC MEDICAL CENTER

Thank you for your attention

THE CATHOLIC UNIVERSITY OF KOREA CATHOLIC MEDICAL CENTER

Two-Stage Flexor Tendon Reconstruction in the Hand

Plast Reconstr Surg. Korea Univ.
Seong Ho Jeong

굴곡건 재건술은 일반적으로 1단계 힘줄 이식방법과 2단계 이식방법으로 나누어지고, 힘줄 재건이 필요한 부위의 연부조직 상태에 따라서 수술방법을 결정하는 것이 일반적이다. 힘줄을 싸고 있는 피막(Flexor tendon sheath)가 잘 보존되어 있으면서 주변 연부조직이 상대적으로 건강하고, 흉터조직 형성이 경미한 경우에는 힘줄을 채취하여 직접 이식하는 1단계 이식방법을 시행할 수 있다. 하지만 대부분의 환자에서 이러한 이상적 환경이 조성되기 어렵다는 점에서 1단계 재건을 통한 굴곡건 재건술은 매우 제한적인 경우에만 적용할 수 있다. 따라서, 대다수의 굴곡건 재건은 2단계 힘줄 재건술(Two stage tendon reconstruction)을 사용하여 시행되고 있다.

힘줄을 싸고 있는 피막이 파손되어 있고 그 주변의 연부조직도 흉터조직으로 변질되어 있는 경우에는 이식된 힘줄이 적절한 영향공급을 받지 못하여 생존자체가 위태로울 수 있으며, 이로 인해 적절한 생착이 이루어지지 않아 재활과정에서 힘줄이 파열되거나 이식한 힘줄 주변에 심한 유착이 발생할 확률이 높다. 이러한 경우에는 실리콘 힘줄 대체물(Hunter rod)을 우선 삽입하여 피막을 형성을 유도하는 1차 수술을 하고 일정 시간 경과 후에 자가 힘줄을 이식하는 2차 수술을 시행하게 되는데 이를 2단계 힘줄 재건술이라고 한다. 실리콘에 의해 유도된 피막은 이물 반응에 의해 생성된 것으로 이식한 힘줄의 피막(sheath)역할을 담당하게 되며, 확산(diffusion)에 의한 영향공급을 원활하게 함으로써 이식 힘줄의 생착에 큰 도움을 준다.

힘줄 재건술 시행 후에는 적절한 재활치료를 통해 점진적인 기능 회복을 유도해야한다. 재활치료의 기본원칙은 규칙적으로, 천천히 조기에 수동적으로 시작하는 것이며. 초기에 무리한 재활운동을 하는 것은 금물이다. 본 연제에서는 수부 굴곡건 재건을 위한 2단계 힘줄 재건술의 상세한 술기와 적응증, 재활방침에 대해 논하고자 한다.

2025년 대한수부외과학회

추계학술대회

역경에도 손을 맞잡고
Against All Odds, Hand in Hand

Room C

3F, Graduate School
of Public Health, Room 331

2025년 대한수부외과학회
추계학술대회

Room C

Free Paper 2 (Arthritis: Hand)

Orthop Surg. Korea Univ. **In Cheul Choi**
Plast Reconstr Surg. Korea Univ. **Deok-Woo Kim**

Finger-Specific Distribution Patterns of Digital Mucous Cysts: A Four-Year Surgical Series Analysis

Orthop Surg. SNU Seoul Hosp.
Sang Ho Kwak

Background: Digital mucous cysts (DMCs) are commonly associated with degenerative joint changes, yet their anatomical distribution across different digits remains poorly defined. Prior reports suggest a general radial-side predominance, but finger-specific variations have not been systematically investigated. This study aimed to analyze the anatomical distribution patterns of DMCs across all five digits in a consecutive surgical series.

Methods: We retrospectively reviewed 220 patients who underwent surgical treatment for DMCs between 2021 and 2024. Surgical indications included (1) nail deformity, (2) ≥2 episodes of spontaneous rupture, or (3) severe pain. Each DMC was classified as radial- or ulnar-sided relative to the central axis of the digit. Binomial tests were used to assess significant laterality preferences for each finger.

Results: A total of 220 DMCs were surgically excised. The middle finger was the most commonly affected (47.9%), followed by the index finger (12.9%) and thumb (11.7%). Thumb DMCs (n=28) showed a significant radial-side predominance (24 radial vs. 4 ulnar, $p<0.001$). Middle finger DMCs (n=115) demonstrated a significant ulnar-side predominance (40 radial vs. 75 ulnar, $p=0.001$). No significant laterality was observed in the index (20 vs. 11, $p=0.15$), ring (14 vs. 12, $p=0.845$), or little finger (14 vs. 6, $p=0.115$).

Conclusions: Digital mucous cysts exhibit distinct finger-specific distribution patterns, with the thumb favoring the radial side and the middle finger the ulnar side. These findings highlight the close relationship between DMCs and degenerative joint anatomy and may aid in diagnostic evaluation and surgical planning.

Keywords: Digital mucous cyst, anatomical distribution, finger-specific patterns, osteoarthritis, surgical treatment, biomechanics

A Retrospective Review of Ganglion Cysts; Surgical technique

Plast Reconstr Surg. DongGuk Univ.
KyoBin Choo, KyungHyun Kim, SooA Lim, SangHun Cho, SuRak Eo

Introduction: Ganglion cysts are the most frequent benign tumor of the wrist and hand, most commonly on the dorsal wrist, followed by the volar wrist, tendon sheath, and interphalangeal joint. They predominate in females, peaking early adulthood. Histologically, they are mucin-filled, non-synovial sacs with fibrous capsules. Conservative treatments are usually ineffective; even excision for symptomatic or enlarging lesions still shows recurrence near 50%.

Methods: We retrospectively reviewed 59 surgically treated patients (2008-2025). Data regarding cyst location, surgical technique, and recurrence were analyzed. All procedures were performed under tourniquet control until the cyst surface was fully delineated. Thereafter, the tourniquet was partially deflated, and meticulous dissection was performed under the surgical loupe or microscope when necessary, particularly when the radial artery was firmly adherent to the mass.

Results: Most cyst involved dorsal wrist (29%), volar wrist (27%), and finger joints (20%); others at foot (3%), palm (2%), and tendon sheath (2%). Only one recurrence requiring reoperation was observed. Microscope guidance enabled safe stalk identification and preservation of adjacent structures. One intraoperative radial artery injury was repaired by microsurgical end-to-end anastomosis without complication.

Conclusion: Surgical excision is effective for ganglion cysts when key technical principles are observed. Partial tourniquet release during cyst wall dissection helps avoid radial artery injury, while microscope assistance facilitates complete removal of deep stalks. Durable, low recurrence outcomes require (1) appropriate tourniquet control, (2) selective use of magnification, and (3) meticulous excision of the cyst wall with stalk excision and base repair.

Motion-Preserving Denervation for Finger Interphalangeal Joint Osteoarthritis : A Consecutive Case Series

W Institute for Hand and Reconstructive Microsurgery, W General Hosp.
Kyung-Chul Kim, Sang-Hyun Woo

Background: Osteoarthritis of the distal interphalangeal (DIP) and proximal interphalangeal (PIP) joints is a frequent cause of pain and functional limitation in the hand. Arthrodesis remains the standard surgical option but inevitably sacrifices motion. Denervation has emerged as a motion-preserving alternative for painful interphalangeal joint osteoarthritis.

Methods: We retrospectively reviewed 27 patients (30 joints: 12 DIP, 18 PIP) who underwent surgical denervation. Inclusion criteria were painful osteoarthritis refractory to conservative treatment and preserved range of motion. Pain was assessed using the Visual Analog Scale (VAS), and functional outcomes were measured by the Disabilities of the Arm, Shoulder, and Hand (DASH) questionnaire. Mean follow-up was 6.5 months for DIP joints and 13.1 months for PIP joints.

Results: In the DIP group, mean VAS decreased from 5.0 preoperatively to 1.2 postoperatively, with an average DASH improvement of 5.3 points. In the PIP group, mean VAS improved from 4.9 to 1.6, and DASH scores decreased by 25.1 points. No major complications, reoperations, or conversions to arthrodesis/arthroplasty were recorded during follow-up.

Conclusions: Denervation of the DIP and PIP joints provided significant pain relief and functional improvement while preserving mobility. The effect was more pronounced in the PIP group. These findings support denervation as a safe and valuable alternative to arthrodesis in selected patients with interphalangeal joint osteoarthritis.

Comparison of Union Rates and Clinical Outcomes between T-Plate and K-Wire Fixation in Trapeziometacarpal Joint Arthrodesis of the Thumb

[1]Orthop Surg. Yeson Hosp., [2]Orthop Surg. Kyung Hee Univ.
Jae-Hoon Lee[1], Jong-Hun Back[2], Duke Whan Chung[2], Jin-Sung Park[1], Ki-Hyeok Ku[2], Gi-Young Jang[2], Gwan kyu Son[2]

Purpose: In surgical treatment for thumb carpometacarpal joint arthritis, there are several treatment options including arthrodesis, ligament reconstruction and tendon interposition (LRTI), extension osteotomy, and distraction arthroplasty. Among them, arthrodesis and LRTI are the most widely used and are reported to yield excellent outcomes. However, the rate of nonunion following thumb CMC joint arthrodesis is considerable, and few studies have analyzed the nonunion rate and clinical outcomes based on the fixation method.

Materials and Methods: From July 2016 to June 2024, 22 thumbs underwent arthrodesis in our hospital. Twelve thumbs underwent arthrodesis using T-shaped locking plate. Ten thumbs underwent arthrodesis using K-wire cross pinning. In the K-wire fixation group, six patients underwent additional fixation with a single headless compression screw (HCS).

Results: In the T-plate group, there were 3 cases of nonunion (25%). One patient who was treated with a 2.0 plate (Aptus Hand) experienced separation of the screw and plate following a fall after discharge. Bone union was subsequently achieved after replacement with a larger screw. In T-plate group, four thumbs fixed with a 1.5-mm plate. In these four patients, two required revision surgery due to metal failure and nonunion.
In K-wire group, there were 4 cases of nonunion (40%). Five patients were fixed with 1.6 cross pin. Another 5 patients were fixed with two 1.4 K-wire cross pin and additional one HCS fixation. In 1.4 mm K-wire cross pin and one HCS group, there were 4 case of nonunion. In these four patients, two patients were revised by LRTI. Two patients with nonunion suffered from pain but refused additional surgery.

Discussion: To obtain reliable fixation to achieve bone union in thumb carpometacarpal joint arthrodesis, a plate of 2.0 mm or larger or a K-wire of 1.6mm or lager is recommended. Ligament reconstruction and tendon interposition(LRTI) are a good revision options when nonunion occurs after thumb CMCJ arthrodesis.

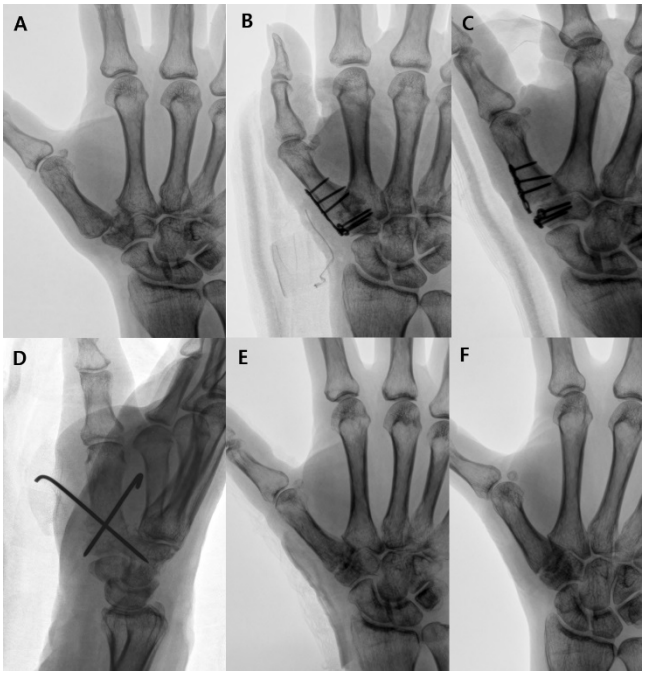

Fig. 1. A 55-year-old female patient with symptomatic thumb carpometacarpal (CMC) osteoarthritis of the right thumb. (A) Preoperative posteroanterior (PA) radiograph of the thumb demonstrates CMC osteoarthritis. (B) Immediate postoperative radiograph demonstrates arthrodesis with T-plate fixation using a 1.5-mm plate. © At 2 weeks postoperatively, radiograph demonstrates implant failure with plate breakage. (D) Radiograph after revision arthrodesis demonstrates removal of the plate and fixation with 1.6-mm K-wires. (E,F) At 6 months postoperatively, radiograph demonstrates complete bone union, and the patient reported improved pain and function.

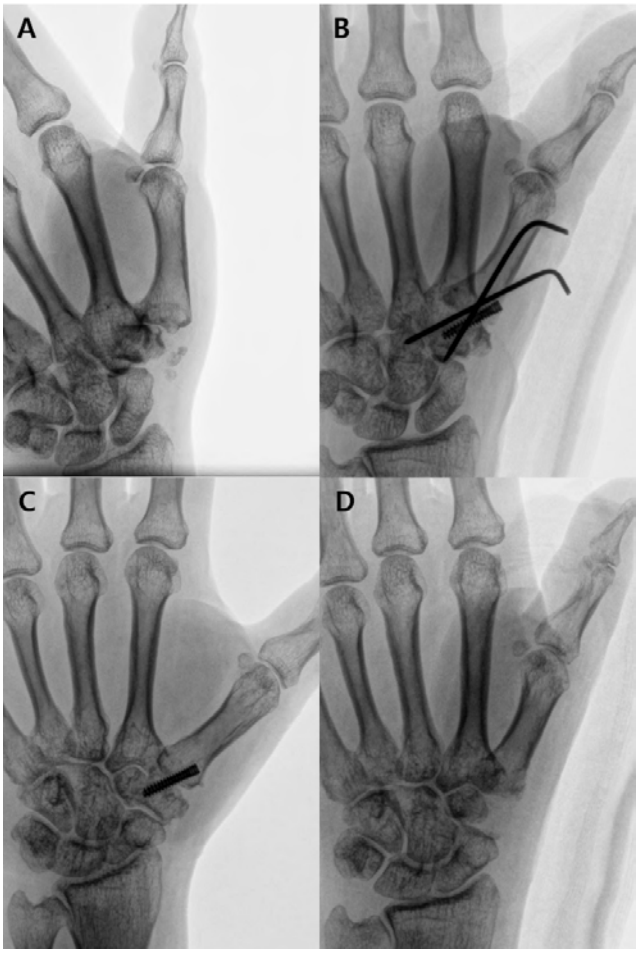

Fig. 2. A 61-year-old female patient with symptomatic thumb carpometacarpal (CMC) osteoarthritis of the left thumb. (A) Preoperative posteroanterior (PA) radiograph of the thumb demonstrates CMC osteoarthritis. (B) Postoperative radiograph demonstrates arthrodesis with two 1.4-mm K-wire cross-pins and a headless compression screw (HCS) fixation. © At 6 months postoperatively, radiograph demonstrates nonunion at the arthrodesis site. (D) Radiograph after revision surgery with ligament reconstruction and tendon interposition (LRTI).

Reference

1. Kim CH, Lee DH, Lee JS, Jung HS. Arthrodesis Versus Ligament Reconstruction and Tendon Interposition for Thumb Carpometacarpal Joint Arthritis: A Systematic Review and Meta-Analysis. J Hand Surg Am. 2025;50(3):282-291. doi: 10.1016/j.jhsa.2024.10.018
2. Sehjal R, Rusli W, Kedgley AE, Sagmeister ML, Williamson M, Smith A. Biomechanical Comparison of 5 Different Fixation Constructs in a Trapeziometacarpal Joint Arthrodesis Model. J Hand Surg Am. 2024;49(10):1036 e1031-1036 e1039. doi: 10.1016/j.jhsa.2022.12.010
3. London DA, Stern PJ. Carpometacarpal Arthrodesis: Indications and Techniques. Hand Clin. 2022;38(2):231-240. doi: 10.1016/j.hcl.2021.11.003
4. Eames M, Kruger N, Bain G. Extension arthrodesis of the thumb carpometacarpal joint for the 'Z' thumb. J Hand Surg Eur Vol. 2021;46(3):311-313. doi: 10.1177/1753193420950192
5. De la Red-Gallego MA, Barrera-Ochoa S, Sanchez Crespo MR. Total thumb carpometacarpal arthroplasty for failed trapeziometacarpal joint arthrodesis. Hand Surg Rehabil. 2021;40(3):347-349. doi: 10.1016/j.hansur.2020.12.014
6. van Laarhoven C, Schrier V, van Heijl M, Schuurman AH. Arthrodesis of the Carpometacarpal Thumb Joint for Osteoarthritis; Long-Term Results Using Patient-Reported Outcome Measurements. J Wrist Surg. 2019;8(6):489-496. doi: 10.1055/s-0039-1694062
7. Kenniston JA, Bozentka DJ. Treatment of advanced carpometacarpal joint disease: arthrodesis. Hand Clin. 2008;24(3):285-294, vi-vii. doi: 10.1016/j.hcl.2008.03.006
8. Proubasta I. Extra-articular arthrodesis of the carpometacarpal joint of the thumb. Tech Hand Up Extrem Surg. 2006;10(1):25-30. doi: 10.1097/00130911-200603000-00005

Dorsal versus Radial Plating for Trapeziometacarpal Arthrodesis: A Comparative Clinical Investigation

Orthop Surg. Yonsei Univ.
Jae-Yong Cho, Hyun-Kyo Kim, Won-Taek Oh, Il-Hyun Koh, Yun-Rak Choi

Background: Trapeziometacarpal joint (TMJ) arthrodesis is a well-established treatment option for advanced TMJ arthritis. Despite various efforts to improve its outcomes, complications such as nonunion and hardware-related problems remain a concern. This study aimed to investigate whether the position of locking plate fixation—dorsal versus radial—affects clinical and radiological outcomes.

Methods: We retrospectively reviewed patients with advanced TM arthritis who underwent TM joint arthrodesis with locking plates. Based on the position of the plate, patients were classified into group D (dorsal placement) and group R (radial placement). Baseline demographics were assessed. Clinical assessments included the VAS pain score, DASH score, Michigan Hand Questionnaire score, tip and key pinch strength, and Kapandji score. Radiological parameters included the 1-2 intermetacarpal angle and arthritic change in the first metacarpophalangeal and scaphotrapeziotrapezoid joints. Postoperative complications, including nonunion, hardware removal due to irritation, and major operation-related events (e.g., neurovascular injury or implant-related reoperations), were evaluated. Subgroup analysis was performed according to the presence of MCP hyperextension (>30°).

Results: A total of 52 patients were included (group D, n=22; group R, n=30), and the mean follow-up period was 29.5 ± 25.6 months. Baseline characteristics showed no significant differences between the two groups. All clinical outcome measures significantly improved postoperatively ($p<0.001$), with no statistically significant differences between the two groups at the final follow-up. The mean postoperative Kapandji score was 8.6. Although the observed difference in DASH scores was minimal (mean difference 0.6 points), the study had adequate power (≈83%) to detect the minimally clinically important difference (10.8 points), indicating the absence of a clinically meaningful difference. No major complications or revision surgeries occurred. Nonunion was observed more frequently in group D (18% vs 0%). Hardware removal due to irritation was significantly higher in group D (27% vs 0%, $p=0.004$, power=0.88). Radiologically, both groups demonstrated postoperative improvement in the 1–2 intermetacarpal angle without intergroup differences. In subgroup analysis, MCP

hyperextension was associated with a smaller postoperative 1–2 intermetacarpal angle (31.9° vs 36.1°), but clinical outcomes were comparable.

Conclusion: Radial plate fixation for TMJ arthrodesis achieved clinical outcomes comparable to dorsal plating and was associated with a significantly lower incidence of hardware-related complications, with a non-significant trend toward fewer nonunions.

Level of Evidence: III

Keywords: Osteoarthritis, Trapeziometacarpal joint, Arthrodesis, Locking plate

Advanced Trapeziometacarpal Arthritis: A Comparative Study of Arthrodesis and Arthroplasty

Orthop Surg. Yonsei Univ.
Jae-Yong Cho, Hyun-Kyo Kim, Won-Taek Oh, Il-Hyun Koh, Yun-Rak Choi

Introduction: Advanced trapeziometacarpal (TM) arthritis is the most frequently operated site of arthritis in the hand. Although many studies have been conducted, no procedure has been clearly shown to be superior, and the available evidence remains limited. Thumb metacarpophalangeal (MCP) hyperextension and zigzag deformity are well-recognized sequelae of advanced TM arthritis and are known to impair thumb function. The purpose of this study was to compare the clinical and radiological outcomes of arthrodesis and arthroplasty with a minimum follow-up of two years, and to perform a subgroup analysis in patients with MCP hyperextension.

Methods: We retrospectively reviewed patients who underwent either arthrodesis with a locking plate or PyroDisk interposition arthroplasty for advanced TM arthritis between 2013 and 2023, with a minimum follow-up of two years. Patients with neuromuscular disorders or prior fractures were excluded. Demographic data and the presence of passive first MCP hyperextension >30° were recorded. Clinical outcomes included VAS, DASH, and MHQ scores, tip and key pinch strength, and the Kapandji score at the final follow-up. Radiographic outcomes included the 1–2 intermetacarpal angle, the TM angle, and degenerative changes of the first MCP and STT joints. Major complications were defined as infection, neurovascular injury, or implant-related problems necessitating revision surgery, such as dislocation after arthroplasty and nonunion after arthrodesis. In statistical analysis, because age and preoperative pinch strength differed between groups, outcomes were compared using ANCOVA.

Results: A total of 96 patients were included: 52 in the arthrodesis group and 44 in the arthroplasty group. The mean follow-up period was 49.6 ± 35.7 months. Demographic characteristics were comparable between groups except for age. VAS, DASH, and MHQ scores improved significantly after surgery in both groups, with no significant differences between them. Tip and key pinch strength were significantly greater following arthrodesis, whereas the Kapandji score was significantly higher after arthroplasty. No major complications were observed in either group. In the subgroup analysis of patients with MCP hyperextension (29 in the arthrodesis group and 17 in the arthroplasty group), there were no significant differences in VAS, DASH, or MHQ scores at the final

follow-up. However, the arthroplasty group demonstrated a significantly lower 1–2 intermetacarpal angle, and TM angle, as well as more frequent arthritic changes at the first MCP joint.

Conclusion: In this study, both arthrodesis and arthroplasty resulted in significant clinical improvement in patients with advanced TM arthritis. Arthrodesis was associated with greater pinch strength, while arthroplasty achieved higher Kapandji scores. However, in patients with MCP hyperextension, radiological outcomes were more favorable in the arthrodesis group.

Two-Year Clinical and Radiologic Outcomes of Dorsoradial Ligament Reconstruction Using the Abductor Pollicis Longus Tendon for Trapeziometacarpal Joint Instability

[1]Orthop Surg. Catholic Kwandong Univ., [2]Orthop Surg. Yonsei Univ.
Sang-Hee Kim[1], Jae-Yong Cho[2], Won-Taek Oh[2], Il-Hyun Koh[2], Yun-Rak Choi[2]

Purpose: In thumb trapeziometacarpal (TM) instability, laxity of the surrounding ligaments leads to pain and weakness in grip and pinch strength, which predisposes patients to developing TM joint arthritis. Surgical reconstruction of the dorsoradial ligament (DRL), a primary stabilizer of the joint, has been proposed as a method to restore joint stability and prevent degenerative progression. This study aims to evaluate the clinical outcomes of a newly devised dorsoradial ligament (DRL) reconstruction technique using the abductor pollicis longus (APL) tendon in patients with symptomatic TM joint instability.

Methods: Between January 2012 and January 2023, 23 cases of DRL reconstruction using the APL tendon were performed in patients diagnosed with Eaton stage I trapeziometacarpal arthritis with instability. Pain and functional scores, including VAS, grip strength, tip/tripod/key pinch, and DASH score, were evaluated preoperatively and postoperatively.

Results: A total of 18 cases were included in the final analysis. Five cases were excluded due to follow-up loss (n=1), revision surgery before the 2-year follow-up (n=1), progression requiring arthrodesis before the 2-year follow-up (n=1), synovectomy for rheumatoid arthritis (n=1), and traumatic TM joint instability (n=1). At the 2-year follow-up, clinical outcomes showed statistically significant improvement compared to preoperative assessments: VAS pain score (6.3 ± 2.2 vs 1.2 ± 1.3, $p < 0.001$), grip strength (44.4 ± 23.5 lbs vs 53.8 ± 19.6 lbs, $p < 0.001$), tip pinch (3.9 ± 1.8 vs 6.2 ± 1.9, $p < 0.001$), tripod pinch (6.2 ± 2.6 vs 9.6 ± 3.3, $p < 0.001$), key pinch (8.3 ± 4.3 vs 11.9 ± 5.0, $p < 0.001$), and DASH score (44.9 ± 18.4 vs 19.2 ± 13.4, $p < 0.001$). Postoperative radiographs demonstrated improved TM joint alignment in all cases, and no arthritic changes were observed at the 2-year follow-up.

Conclusions: Dorsoradial ligament reconstruction using the APL tendon is a safe and effective surgical option for treating TM joint instability. The technique led to significant improvement in clinical outcomes, and no arthritic changes were observed at the 2-year follow-up.

Keywords: trapeziometacarpal joint, ligament reconstruction, dorsoradial ligament, abductor pollicis longus, clinical outcome, joint instability

2025년 대한수부외과학회
추계학술대회

Room C

Free Paper 4. (TFCC, UIS: Wrist)

Orthop Surg. Ajou Univ. **Kyeong Jin Han**
Orthop Surg. Soo Hosp. **Byung Ho Lee**

Association of Ulnar Variance with Primary Distal Radio-Ulnar Joint Arthritis: A Matched Case-Control Study

Orthop Surg. Asan Medical Center
Yun Jae Kim, Won Sun Lee, Young Ho Shin, Jae Kwang Kim

Purpose: Knowledge regarding risk factors for primary distal radioulnar joint (DRUJ) arthritis is limited. This study evaluated the association between ulnar variance (UV) and the development of primary DRUJ arthritis in a matched case-control cohort.

Methods: Patients with symptomatic DRUJ arthritis were identified from those attending an orthopaedic outpatient clinic between January 2017 and April 2023. The control group comprised individuals without radiographic evidence of DRUJ arthritis. Propensity score matching was performed, aiming for a 1:3 ratio with an age difference limit of 5 years or less. UV and grade of DRUJ arthritis were assessed using a previously described method. Differences in UV between the case and control groups, and the association between ulnocarpal joint (UCJ) and DRUJ arthritis, were analysed. Receiver operating characteristic (ROC) analysis was used to determine the UV cut-off value for predicting symptomatic DRUJ arthritis.

Results: The case group comprised 49 wrists from 44 patients, while the control group included 147 wrists from 132 individuals. The mean ages of the case and control groups were 69.6 and 67.5 years, respectively. UV was significantly higher in the case group (3.5 ± 2.9 vs. 1.6 ± 1.5 mm). The prevalence of UCJ arthritis increased with higher DRUJ arthritis grades. ROC curve analysis revealed a UV cut-off of 2.9 mm, with a sensitivity of 0.612 and specificity of 0.816.

Conclusions: A UV greater than 2.9 mm was associated with symptomatic primary DRUJ arthritis. Patients with more advanced DRUJ arthritis were also more likely to have concomitant UCJ arthritis.

Who Needs More Than a Plate? Predicting TFCC Repair After Distal Radius Fracture

[1]Orthop Surg. National Health Insurance Service Ilsan Hosp.,
[2]Orthop Surg. Armed Forces Daejeon Hosp., [3]Orthop Surg. Yonsei Univ., [4]Orthop Surg. CHA Univ.
Min Jung Park[1], Cheungsoo Ha[2], Hyun Tak Kang[1], Jun-Ku Lee1,3, Soo-Hong Han[4]

Background: Distal radius fractures (DRFs) are frequently accompanied by triangular fibrocartilage complex (TFCC) tears, which may lead to distal radioulnar joint (DRUJ) instability and ulnar-sided wrist pain. However, the necessity and timing of TFCC repair remain controversial, as many tears are asymptomatic and may not require surgical intervention. This study aimed to identify clinical characteristics of patients who required TFCC repair after DRF and evaluate their outcomes.

Methods: We retrospectively reviewed 354 patients (361 wrists) treated surgically for DRF between March 2021 and December 2024. Among them, 10 patients presented with persistent ulnar-sided pain and DRUJ instability after fracture union and were considered for TFCC repair (Group 1). The remaining patients, without TFCC-related symptoms, were designated as Group 2. We compared demographic and injury-related factors between the groups and evaluated clinical outcomes after TFCC repair using the Visual Analog Scale (VAS), Disabilities of the Arm, Shoulder, and Hand (DASH) score, and radiographic findings.

Results: Group 1 patients were significantly younger (median 39.0 vs. 65.0 years), taller, and more often male. High-energy or sports-related trauma mechanisms were common in Group 1. Of the 10 patients, 7 underwent delayed transosseous TFCC repair at a mean of 11.1 months postoperatively. Arthroscopic repair was performed in 6 patients, while 1 required an open procedure. After surgery, VAS improved from 5.7 to 2.5, and DASH from 46.9 to 17.5. Two patients developed arthritic changes, and one showed suspected TFCC retear.

Conclusion: TFCC repair is rarely required after DRF, typically in younger, active patients with persistent symptoms. Delayed repair yields favorable outcomes, but given the frequent asymptomatic nature of TFCC tears, careful patient selection is essential.

Keywords: Wrist, distal radius fracture, TFCC, transosseous repair, arthroscopy
Level of evidence: Therapeutic level III, retrospective comparison study

Clinical Outcomes of Arthroscopic Transosseous TFCC Repair using anchorless technique

Orthop Surg. Seoul National Univ.
Juneseok Won[1], Yohan Lee[2]

Background: Triangular fibrocartilage complex (TFCC) tears are a frequent source of ulnar wrist pain and distal radioulnar joint (DRUJ) instability. Anchor-based repair has drawbacks including tension imbalance, tissue tearing, and anchor pullout. We evaluated an arthroscopic one-tunnel transosseous anchorless repair to address these issues.

Methods: Between 2019 and 2024, 11 patients (mean age 41.6 years, 6 men) underwent anchorless TFCC repair. Exclusion criteria were prior wrist surgery, concomitant fracture, inflammatory disease, or <12 months follow-up. A 3.4-mm ulnar tunnel was created, and 2-0 PDS sutures were used. Knots were buried inside the tunnel. Outcomes were assessed preoperatively and at 12 months: wrist range of motion (ROM), QuickDASH, modified Mayo wrist score (MMWS), grip strength, and pain visual analog scale (VAS).

Results: At 12 months, all outcomes improved significantly ($p < 0.001$). ROM rose from 55.2% to 92.3%, QuickDASH decreased from 45.0 to 13.6, MMWS improved from 45.5 to 84.1, and grip strength from 51.0% to 91.2%. VAS dropped from 8.0 to 1.9. One patient showed mild residual DRUJ laxity without symptoms. No infection, nerve injury, or fracture occurred. All patients resumed daily activities with functional recovery.

Conclusions: Arthroscopic anchorless transosseous TFCC repair achieved reliable pain relief, functional restoration, and stability without anchor-related complications. Absorbable monofilament sutures enabled controlled tension and minimized irritation. This technique may be a useful alternative to anchor-based repair, meriting further comparative and long-term studies.

Effect of the ulnar positive variance on the clinical outcomes of arthroscopic transosseous repair in the patients with the triangular fibrocartilage complex foveal tear

Orthop Surg. Korea Univ.
Jun Hong Won, Joung Woo Shin, Jung Il Lee

Purpose: To investigate the effect of ulnar positive variance (UPV) and relative UPV (RUPV) on postoperative outcomes after arthroscopic transosseous triangular fibrocartilage complex (TFCC) repair.

Methods: This retrospective comparative study included 36 patients who underwent arthroscopic transosseous repair for traumatic TFCC foveal tears (Palmer 1B). Ulnar variance (UV) was measured on posteroanterior wrist radiographs, and RUPV was defined as the side-to-side positive difference of UV between the operated and contralateral wrists. Patients were divided into non-UPV (n = 18) and UPV (n = 18) groups, and into non-RUPV (n = 14) and RUPV (n = 22) groups. Patient-reported outcomes (QuickDASH and VAS pain scores) and objective outcomes (wrist range of motion and grip strength) were assessed preoperatively and at ≥12 months postoperatively (mean, 13.9 months).

Results: No significant intergroup differences were observed between non-UPV and UPV groups in QuickDASH, VAS scores, grip strength, or wrist motion (all $P > 0.05$). Similarly, no differences were found between non-RUPV and RUPV groups. Among the 22 patients in the RUPV group, UV decreased after surgery in 12 patients. These patients showed significantly lower VAS pain scores when lifting heavy objects compared with those whose UV did not decrease (1.8 ± 1.6 vs 4.6 ± 2.1, $P = 0.012$), although no other outcomes differed significantly.

Conclusions: UPV and RUPV did not adversely affect clinical outcomes after arthroscopic transosseous TFCC foveal repair. These results suggest that concomitant ulnar shortening procedure provides no additional clinical benefits when performing arthroscopic transosseous repair in ulnar positive patients with TFCC foveal tear.

Clinical Outcomes of Ulnar Shortening Osteotomy With Versus Without TFCC Foveal Repair in Idiopathic Ulnar Impaction Syndrome: Stratified Arthroscopic Analysis of the Foveal Lesion

Orthop Surg. Yonsei Univ.
Jae-Yong Cho, Hyun-Kyo Kim, Il-Hyun Koh, Won-Taek Oh, Yun-Rak Choi

Purpose: This study aimed to evaluate the clinical outcomes of ulnar shortening osteotomy (USO) with or without concurrent triangular fibrocartilage complex (TFCC) foveal repair in idiopathic ulnar impaction syndrome (UIS), with associated TFCC lesion on arthroscopy-based staging system to stratify foveal lesion severity.

Methods: We retrospectively reviewed 127 patients who underwent USO for idiopathic UIS associated with TFCC foveal lesion with a minimum follow-up of two years. Patients were divided into Group U (USO alone) and Group F (USO with concurrent foveal repair). Foveal lesions were arthroscopically classified as Stage 1 (intact with synovitis), Stage 2 (partial tear), or Stage 3 (complete tear). Clinical outcomes were assessed using VAS, DASH, Mayo Wrist Score (MWS), range of motion, and grip strength. Linear mixed models were used to analyze longitudinal clinical outcomes stratified by lesion stage. Secondary TFCC repair cases in Group U were evaluated separately.

Results: Stage 1 lesions were identified only in Group U (n = 31); Stage 2 in 38 patients in Group U and 23 in Group F; Stage 3 in 17 patients in Group U and 18 in Group F. In Stage 2, DASH showed a significant group-by-time interaction favoring Group F ($p = 0.039$). In Stage 3, DASH ($p = 0.003$), MWS ($p = 0.015$), and grip strength ($p = 0.023$) significantly favored Group F. Eight patients in Group U underwent secondary TFCC repair and showed significant improvement. No major complications occurred.

Conclusions: In patients with idiopathic UIS and arthroscopically confirmed TFCC foveal lesions, concurrent TFCC repair during USO may improve clinical outcomes when partial or complete tears are present.

Level of Evidence: II

Clinical Features and Outcomes of Sequential Bilateral Ulnar Shortening Osteotomy with Triangular Fibrocartilage Complex Foveal Repair

- Characterizing Sequential Bilateral Cases without Major Trauma-

Orthop Surg. Chungnam National Univ.
Soo Min Cha

Purpose: To retrospectively analyze the clinical features and surgical outcomes of a distinct subgroup of patients who underwent sequential bilateral ulnar shortening osteotomy (USO) with arthroscopic triangular fibrocartilage complex (TFCC) foveal repair for ulnar impaction syndrome (UIS) with distal radioulnar joint instability, despite having no clear history of major or minor trauma, and to contextualize these findings within the literature.

Methods: A retrospective review was conducted of 26 patients who underwent bilateral USO with TFCC foveal repair between 2015 and 2022, with at least 2 years of follow-up for each wrist. The inclusion criteria were radiologically positive ulnar variance (>3 mm), arthroscopic evidence of lunate chondromalacia, definitive foveal TFCC detachment, and distal radioulnar joint instability in both wrists.

Results: In 88% of the patients, the initial surgery was performed on the dominant side. The mean age was 34.08 ± 4.91 years, and the male to female ratio was 16:10. All preoperative statuses clearly improved at the final follow-up (mean of 30.0 months). Subsequent surgeries were conducted on the contralateral side with a mean interval of 15.7 months. Concurrently, statistically significant improvement compared with the preoperative status was seen at a mean of 29.3 months of follow-up. Compared with the condition at the initial surgery, the contralateral surgery group presented less preoperative deterioration in grip strength, VAS score, MMWS, and DASH score. However, both groups showed comparable improvements in all outcome measures at the final follow-up.

Conclusion: Sequential bilateral USO with TFCC foveal repair yielded consistently favorable outcomes, regardless of surgical side or baseline functional deficit. The short interval between surgeries and the absence of a history of trauma suggest that contralateral pathology may develop in the context of degenerative changes, potentially influenced by compensatory overuse during postoperative recovery.

Keywords: sequential; triangular fibrocartilage complex; fovea; transosseous; ulnar impaction; shortening osteotomy

Introduction

Ulnar impaction syndrome (UIS) is a common cause of ulnar-sided wrist pain, characterized by excessive loading between the ulna and the ulnar carpus, and is frequently associated with positive ulnar variance (UV) [1–2]. Similarly, traumatic tears of the triangular fibrocartilage complex (TFCC) are also a well-known source of ulnar-sided wrist pain. Biomechanical studies have shown that the deep fibers of the TFCC play a critical role in maintaining distal radioulnar joint (DRUJ) stability [3–6]. When the foveal attachment of the TFCC is disrupted, the ulnar head is prone to dorsal subluxation relative to the sigmoid notch of the radius, a condition that becomes more pronounced under pronation stress [7,8]. This alteration in the anatomical relationship between the radius and ulna can be observed on plain radiographs, often manifesting as changes in radiological parameters, such as an increase in UV [9].

However, positive UV does not always indicate UIS, especially in the absence of other hallmark features. Radiographic studies, involving techniques such as MRI, are essential for identifying additional indicators of UIS, such as chondromalacia of the lunate or ulnar head, TFCC perforation, and intercarpal ligament injuries [10]. In fact, foveal TFCC rupture alone has been shown to increase UV by 0.56 mm [11]. Similarly, recent systematic reviews and clinical studies have reported that isolated TFCC repair can yield favorable outcomes regardless of UV and that positive UV is not necessarily associated with a poor prognosis, even when DRUJ instability is present, if patients are treated with arthroscopic surgeries [12-15]. Conversely, some researchers argue that positive UV may impair healing potential after TFCC repair [8,12,16-18]. In these cases, a secondary ulnar shortening osteotomy (USO) may enhance the outcome, particularly for traumatic TFCC ruptures. Notably, Shim et al. reported that UV may progressively increase after TFCC tears, even following successful repair, potentially resulting in ulnocarpal impaction symptoms and DRUJ instability [8].

Over the past several decades, we have consistently performed both arthroscopic TFCC repair and USO in patients who met the critical indication of "UIS accompanied by DRUJ instability and definitive TFCC foveal tear". Interestingly, a subset of patients in our cohort had no history of major or minor trauma. Moreover, a few of these patients underwent the same surgical procedures on both wrists, separated by several months. Therefore, in this study, we aimed to analyze this unique subgroup and review previous reports.

Materials and Methods

Patient selection

The institutional review boards (IRBs) of the authors' affiliated institutions approved this research. We screened 308 patients with UIS accompanied by TFCC tears who were treated surgically by USO and arthroscopy from January 2015 to December 2022. Among them, 26 who met our inclusion/exclusion criteria were evaluated retrospectively. The following inclusion criteria were used: (1) age 20 years or older; (2) definitive clinical symptoms for UIS in both wrists [2,19]; (3) radiologically positive UV of more than 3 mm on a

neutrally positioned PA wrist view in both wrists; (4) radiological evidence for UIS, such as cystic lesions on simple radiographs or increased signal intensity on T2-weighted MRI of the lunate of both wrists; (5) lunate chondromalacia identified during the arthroscopic procedure in both wrists; (6) the presence of the fovea sign [20]; (7) definitive foveal detachment on MRI, followed by the classification of the TFCC lesion by arthroscopy in both wrists; (8) definitive DRUJ instability [21]; and (9) completion of a full course of postoperative rehabilitation with at least 2 years of follow-up. The exclusion criteria included (1) simultaneous bilateral USO with TFCC repair; (2) any associated fracture or fracture-dislocation of the wrist, including the distal radius and carpal bones; (3) any other presence of ligamentous injuries such as scapholunate or a lunotriquetral ligament identified by arthroscopy; (4) degenerative or inflammatory arthritis in the wrist, (5) concurrent flexor/extensor tenosynovitis the in wrist; (6) outstanding workers' compensation, (7) any history of ipsilateral trauma to the tendons, ligaments, bones or neurovascular structures below the midforearm; (8) a concurrent extensor carpi ulnaris (ECU) subsheath tear or acute/chronic subluxation/dislocation; and (9) any history of surgery in the same anatomical area and/or any congenital or acquired deformity of the forearm, wrist or hand. Trauma was defined as a condition restricting activities of daily living (at work and in leisure), even if the trauma required no treatment.

Demographic characteristics

We evaluated demographic factors, namely, age, sex, lesion dominance, medical comorbidities, occupation, symptom onset and duration before the initial surgery, and the interval between the initial surgery and the surgery on the contralateral side.

Clinical evaluation of instability

Clinical DRUJ instability was classified as static or dynamic. Static DRUJ instability was defined as pathological movement of the DRUJ when stressed without rotation of the forearm. This was determined using a stress test, in which the wrist was held in supinated and pronated positions while the physician attempted to manipulate the distal ulna in the dorsal and volar directions. The stress test was considered positive when there was greater laxity on the injured side than on the uninjured side [6,21]. Dynamic instability was defined as pathological movement of the ulna relative to the radius during pronosupination and was tested using the clunk test [22]. During the clunk test, the distal ulna was compressed between the physician's thumb and index finger with simultaneous passive pronosupination. The clunk test was considered positive if a 'clunk' was perceived by either the patient or the examiner.

Radiographic evaluation for instability, UV and TFCC status

We also measured the distance between the dorsal cortex of the distal radius and distal ulna in lateral projections on simple radiographs (the scaphopisocapitate [SPC] view) [23]. A distance greater than 6 mm was regarded as radiological instability [24]. The UV was measured using the method of perpendiculars; this value is the distance between a line drawn perpendicular to the longitudinal axis of the radius at its distal ulnar aspect and a line drawn at the end of the ulna. For accurate determination of UV, a posteroanterior radiograph

of the wrist was obtained with the shoulder in 90° of abduction, the elbow in 90° of flexion, the forearm in neutral rotation, and the wrist in neutral alignment. These parameters were evaluated preoperatively and at the final follow-up.

Evaluation of functional status

Grip strength was measured with a Jamar hydraulic hand dynamometer (Sammons Preston/Ability One, Germantown, WI, USA). We evaluated the preoperative and postoperative pain scores using the visual analog scale (VAS), active ROM, modified Mayo wrist score (MMWS) [25], and Disabilities of the Arm, Shoulder, and Hand (DASH) score. Clinical postoperative data were obtained once at the final follow-up.

Surgical indications

We performed USO and foveal repair on symptomatic wrists with more than 2 mm of UV and/or clinical or radiologic instability [26] in patients who did not respond to at least 6 months of conservative treatment (anti-inflammatory medication, orthotics, and immobilization) [27]. Surgery on the contralateral wrist was considered only after a minimum 6-month trial of conservative management and with at least a 6-month interval following the initial surgery. Notably, reevaluations and surgeries on the contralateral wrist were performed only at the patient's request, and the surgical indications were identical to those for the initial procedure.

Surgical procedure (USO)

All operations were performed by a single surgeon. In all cases, USO was performed before TFCC repair. The operations were performed with the patients under brachial plexus block or general anesthesia. The patient was placed in a supine position, and a tourniquet (280 mmHg) was applied. Only transverse osteotomy (free hand technique) was applied to shorten the ulna; a single ARIX 3.5-A large bone fragment compression locking 6-hole plate (Jeil Medical Corporation, Seoul, Korea) was used to fix the osteotomy portion [28,29]. The shortening amount was determined to be zero or −1 mm according to the target UV, and the procedure was performed with a single-blade mini-saw [26].

Surgical procedure (TFCC foveal repair)

The wrist was distracted using a finger and a traction device (TRIMANO FORTIS Support Arm and TRIMANO Wrist Positioner; Arthrex, Naples, FL) in the upright position, with the upper arm fixed on the operating table. The joint was inspected through a standard 3/4 portal to identify the TFCC foveal tear and any other intra-articular lesions. Trampoline and hook tests were conducted through the 6R portal to assess the tension in the TFCC and its insertion. One-tunnel arthroscopic transosseous repair was performed immediately after 6U portal preparation. The targeting device (C-Ring Aiming Guide; Arthrex, Naples, FL) was inserted through the 6U portal, and its tip was positioned arthroscopically at a point 2 mm radial to the ulnar apex of the TFCC. This position corresponds to the isometric point of the distal radioulnar joint, allowing for optimal tunnel orientation [30]. After a 1.1-mm K-wire was introduced to the center of the footprint of the TFCC foveal insertion through the targeting guide starting from 1 cm proximal to the tip of the ulnar styloid process, stepwise cannulated drilling was

performed sequentially with 2.4-, 2.7-, and 3.5-mm drills to create a transosseous tunnel. During the final step using a 3.5-mm drill, a gentle conical sweeping motion was applied to widen the outlet of the tunnel, allowing for a funnel-shaped configuration while preserving the cortical entry point. A 21-gauge needle loaded with a looped 3-0 monofilament suture was introduced through the tunnel and passed through the targeted portion of the TFCC for repair. The looped suture was retrieved using a grasper through the 6R portal, and a 2-0 FiberWire (Arthrex, Naples, FL) was shuttle-relayed, pulling one end of the FiberWire out through the transosseous tunnel. The same procedure was repeated; a second looped 3-0 monofilament suture was passed through the tunnel and another side within the TFCC footprint, and the remaining limb of the FiberWire was retrieved via the 6R portal using the shuttle relay technique. With both FiberWire limbs retrieved outside the tunnel, a 2.5-mm PushLock (Arthrex, Naples, FL) hole was created approximately 1 cm proximal to the transosseous tunnel. While maintaining appropriate tension on the TFCC, the FiberWire was secured to the proximal ulna using the PushLock anchor. Care was taken to avoid excessive tension, as this may result in FiberWire cut-through of the TFCC during anchor insertion. To reinforce the repair, a 21-gauge needle loaded with a looped 3-0 monofilament suture was again introduced through the transosseous tunnel and passed through the desired dorsal portion of the TFCC. A 2-0 PDS suture was shuttle-relayed through the loop, and this process was repeated in the desired volar portion to position a 2-0 PDS loop intra-articularly. The looped PDS suture was retrieved through the 6R portal and cut to yield two separate strands, allowing each limb to be present within the transosseous tunnel. Using a grasper through the 6U portal, the dorsal PDS strand on the TFCC was pulled outside the joint, resulting in the formation of a crossed suture configuration. Subcutaneous dissection was performed gently using curved mosquito forceps from the main ulnar incision toward the 6R and 6U portals to retrieve the suture limbs. After all the limbs were retrieved, they were securely tied over the bone periosteum, completing the capsulofoveal repair from the transosseous tunnel to the TFCC.

Postoperative immobilization

Postoperatively, a long-arm splint was applied with the elbow at 90° of flexion and the forearm in a neutral position. Two weeks after surgery, the splint was replaced with a wearable short-arm brace. Six weeks after surgery, the brace was removed, and passive and active flexion–extension exercises of the wrist were initiated. Forearm supination and pronation exercises were also started at this time, assisted by the contralateral hand. Gradual strengthening exercises, such as grip training, began approximately 10 weeks postoperatively. At approximately 12 weeks, resistance to forearm rotation and light return to sports activities were permitted.

Criteria for complications and treatment failure

Complications included postoperative infection, extensor tendon injury involving the extensor digiti minimi or ECU, sensory nerve damage to the ulnar nerve, and anchor breakage or loosening. In addition, nonunion, malunion, and implant-related issues such as plate or screw failure were thoroughly evaluated during the follow-up period. Treatment failure was defined as the presence of residual UV greater than 2.0 mm or recurrent DRUJ instability at the final evaluation. Furthermore, if any of the outcome measures, such as the VAS score for pain,

ROM, MMWS, or DASH score, deteriorated at the final follow-up compared with the preoperative assessment, the case was classified as a treatment failure [31].

Interobserver and intraobserver repeatability of the radiological assessments

The intraclass correlation coefficients (ICCs) of continuous variables served as indices of inter- and intraobserver repeatability [32]. Kappa values were calculated for the categorical variables [33]. According to Fleiss and Cohen, kappa values > 0.75 indicate excellent repeatability, whereas values of 0.40–0.75 correspond to good repeatability, and those < 0.40 correspond to poor repeatability.

Statistical analysis

Sample size estimation was performed using G*Power software (version 3.1.9.2) with the DASH score as the primary outcome, and a minimal clinically important difference of 8.3 was calculated as 50% of the standard deviation for changes between preoperative and postoperative scores using the distribution-based method [34]. A paired t test was used for sample size estimation, with a type I error rate of 0.05 and a statistical power of 0.80. The minimum expected effect size (Cohen's d) was set at 0.18, corresponding to the smallest detectable difference between pre- and postoperative status. The required sample size was calculated as 15 participants per group. After accounting for a 20% potential loss to follow-up, the minimum total sample size was estimated as 19 participants. To evaluate improvement after surgery, continuous variables were analyzed using paired t tests, and categorical variables were assessed using McNemar's test. For comparisons between the initial and contralateral surgery groups, continuous variables were analyzed using Student's t test, and categorical variables were assessed using Fisher's exact test. All statistical analyses were performed using SPSS Statistics software (version 26.0; IBM Corp., Armonk, NY, USA), and a P value < 0.05 was considered to indicate statistical significance.

Results

Among the total cohort in the corresponding period, 234 patients underwent arthroscopic TFCC repair + USO. Thus, 11.1% (26 patients) of the surgeries were performed bilaterally (Tables 1 and 2). In 88% (23/26) of the patients, the initial surgery was performed on the dominant side. The mean age was 34.08 ± 4.91 years, and the male to female ratio was 16:10. Chef was the most frequently reported occupation, followed by barista, yoga instructor, and military professional. At the time of the initial surgery, 3 and 23 patients presented Atzei class 2 and 3 lesions, respectively; lunate chondromalacia without TFCC wear (Palmer type 2B without type 2A) was identified in 21 patients, and the others presented type 2B. Type 1A and 1D coexisted with degenerative type 2 in 2 and 3 patients, respectively (Figs. 1 and 2). All preoperative statuses, such as physical findings, radiographic measurements, and clinical scores, clearly improved at the final follow-up (mean of 30.0 months, Table 3). Subsequent surgeries were conducted on the contralateral side with a mean interval of 15.7 months (Fig. 3). Atzei classes 2 and 3 were identified in 1 and 25 patients, respectively; lunate chondromalacia without

TFCC wear (Palmer type 2B without type 2A) was identified in 24 patients, and the others were classified as type 2B (Table 2). Concurrently, statistically significant improvement compared with the preoperative status was seen at a mean of 29.3 months of follow-up (Table 4). Compared with the condition at the initial surgery, the contralateral surgery group presented less preoperative deterioration in grip strength, VAS score, MMWS, and DASH score (Table 5). However, both groups showed comparable improvements in all outcome measures at the final follow-up (Table 6).

In terms of radiological measurements, both the inter- and intraobserver intraclass correlation coefficients indicated high reproducibility [32]. The kappa values of the categories for the shortening amount and the decision as to a final union were 0.92 and 0.95, respectively [33]. Serious complications or treatment failure affecting the final outcomes were absent in all patients after two surgeries.

Discussion

Although the Palmer and Atzei classification systems are widely utilized, emerging evidence suggests that certain TFCC lesions cannot be classified with precision under either framework. [35,36]. Among a large cohort of more than 110 individuals who were initially treated with arthroscopic debridement alone under the typical traumatic diagnosis of Palmer type 1A, Cho et al. highlighted 10 patients with positive UV who ultimately required secondary USO [37]. Notably, these patients had neither a clear history of trauma nor arthroscopic evidence of degenerative changes consistent with UIS. Similarly, Minhas et al. described 17 patients who met the diagnostic criteria for Palmer type 1A but were concurrently found to have foveal TFCC tears, a pattern not well accounted for by current classification systems. These patients exhibited varying degrees of DRUJ instability, and nearly half had a history of distal radius or ulnar styloid fractures. On the basis of these findings, the authors emphasized that when a central TFCC tear is identified (Palmer type 1), even subtle signs of DRUJ instability should raise suspicion for an associated foveal tear [36].

In our series, several patients presented deep-fiber TFCC rupture and arthroscopic findings consistent with those of Palmer type 1A or 1D lesions (Fig. 1), concurrently—typically classified as traumatic—despite having no definite history of trauma. Moreover, most patients were relatively young. If interpreted in line with Minhas et al. [36], these patients may represent unrecognized or occult traumatic foveal injuries. However, DRUJ instability and arthroscopic signs of UIS were clearly present in all the patients. Notably, all patients underwent contralateral wrist surgery several months after the initial procedure, and similar degenerative findings—such as lunate chondromalacia and TFCC wear—were observed in both wrists. These observations suggest that "TFCC degeneration" may have played a significant role in the lesion. Given that most patients relied heavily on the contralateral hand for daily activities during the postoperative immobilization period, these contralateral lesions could represent a form of short-term overuse syndrome rather than being purely traumatic in origin. Another specific point was that no classification of Palmer type 1 was found on the TFCC contralateral side, but all

subtypes were type 2.

Most importantly, our findings highlight that foveal detachment of the deep fibers of the TFCC in this series was strongly associated with "degeneration," rather than "major trauma" such as distal radius fracture, ulnar styloid fracture, or DRUJ dislocation. Furthermore, the rupture of deep fibers in the fovea might trigger elongation of the UV and associated lesions, such as central wear/perforation and lunate chondromalacia seen in Palmer type 2 lesions. Considering the broad spectrum of UIS, which progresses from initial foveal detachment to gradual central wear and eventually to complete TFCC perforation/ulnocarpal arthritis, our current series is notable in that all patients underwent surgical intervention during the early phase of the spectrum. In particular, there was no central perforation in any of the patients, and the superficial fibers remained substantially intact, corresponding to Atzei type 3, allowing for complete TFCC repair in the majority of patients. Another important finding in our series was that contralateral surgery was performed at a mean interval of 15.7 months after the initial procedure, and all the patients exhibited the same pathology, requiring both foveal TFCC repair and USO. Notably, all contralateral wrists showed degenerative changes consistent with Palmer class 2 lesions with no class 1 lesions (Fig. 2). In addition, patients reported no significant symptoms on the contralateral side at the time of the initial surgery, but during the postoperative stabilization period for the initial surgery, they relied heavily on the contralateral wrist for occupational and daily activities, which may have contributed to symptom progression with a relatively short duration of onset (Table). To date, no study has specifically reported on cases involving bilateral UIS concurrently treated with TFCC repair. In our series, a considerable number of patients were engaged in occupations that inherently require significant wrist use on both sides, such as baristas, cooks, delivery drivers, military professionals, and yoga instructors. It remains unclear whether the decision to proceed with surgery on the contralateral wrist was driven primarily by unavoidable activity during the immobilization period after the initial surgery or by the high level of satisfaction experienced with the initial outcome. However, considering that none of the patients reported noticeable symptoms on the contralateral side at the time of the initial procedure, it is plausible that once foveal TFCC rupture occurs, positive UV tends to develop relatively rapidly in patients in wrist-intensive occupations. Under such conditions, the progression of UIS may be influenced by multiple factors. This assumption is supported by our institutional experience, where many patients with positive UV do not present clinical/radiographic signs of UIS, and long-term follow-up of patients who undergo unilateral treatment often reveals that the contralateral wrist remains asymptomatic for extended periods [26,28,29,38].

The decision to evaluate and proceed with contralateral wrist surgery, following MRI and a full diagnostic workup, was made solely at the patient's discretion. This was likely influenced by the clear improvement in symptoms experienced after the initial procedure. Favorable outcomes for foveal TFCC repair have been reported using various techniques [1,5,30,34,39-41]. In our series, we employed a transosseous repair method using a combination of FiberWire and PDS sutures. This approach was intended to maximize the contact area for fixation by enlarging the tunnel diameter and optimizing suture placement, thereby enhancing reattachment

to the original footprint. On the basis of our surgical experience, we encountered several cases of poor-quality TFCC tissue in patients who were in their 40s or older. This raised concerns about the risk of cut-through by high-strength suture materials (FiberWire), as has been well documented in rotator cuff repair literature. In response to these concerns, surgeons have focused on exploring alternative suture techniques, materials (such as polyester versus polyblend), and configurations to increase the strength of the suture–tendon interface [42,43]. Accordingly, we adopted a hybrid approach by combining the classic transosseous repair technique using a FiberWire loop with the modified transosseous reconstruction method involving PDS augmentation, as previously introduced by Zhang et al. in chronic TFCC patients utilizing tendon grafts [44]. The first stitch made by the FiberWire was placed at an isometric point as suggested by Fujio [39]; then, to maximize the reinforced coverage around the point of the first stitch, the second stitch was applied in a cross-stitch configuration. While the second stitch unavoidably creates a subcutaneous knot, it tends to be absorbed within a few months and does not lead to any clinically significant complications, even when it is positioned adjacent to the ulnar sensory nerve branch.

As previously mentioned, all the patients expected to have a much better status, both objectively and subjectively, on the contralateral side because they were convinced by the favorable outcome of the procedure after the initial surgery. Additionally, strong eagerness to maintain their current occupational activities was an important motivation even for young patients. With the exception of 3 patients, the majority of initial surgeries were performed on the dominant wrist, indicating that this particular cohort is strongly associated with "occupational overuse". In clinical decision-making, performing TFCC repair alone versus combining it with USO reflects a fundamental difference in the surgical approach, specifically the addition of a bony procedure. Understandably, this distinction results in a considerable difference in the perceived surgical burden from the patient's perspective. Although the final outcomes after contralateral surgeries were comparable to those of the initial surgeries without significant differences, the relatively better preoperative grip strength, pain scores, and overall clinical status before the contralateral surgery seem to reflect the higher proportion of non-dominant wrist involvement.

There are several limitations to the current study. The most significant limitation is its retrospective design, which resulted in the absence of contralateral wrist radiographic data at the time of the initial surgery. Even basic assessment using simple radiographs to determine the presence of positive UV might have allowed for a clearer explanation of how inevitable compensatory use led to early TFCC foveal tears, subsequent UV progression, and ultimately, the development of early UIS. Second, although the authors adopted a specific technique for foveal TFCC repair, this study was not designed as a prospective comparative trial. Therefore, the clinical superiority of this technique over other established methods cannot be concluded, and comparisons of final outcomes with those of prior studies should be interpreted with caution. Last, it is difficult to statistically validate an occupational association with bilateral TFCC repair combined with USO in this study. However, compared with the previous literature, our series included younger patients in whom the indications for both procedures

developed bilaterally over time [12,17]. Therefore, occupational characteristics should be interpreted as potential contributing factors rather than definitive causative variables.

Conclusively, this study highlights a distinct subgroup of relatively young patients who underwent bilateral TFCC foveal repair combined with USO. The decision for contralateral surgery appeared to be influenced not only by the favorable outcome of the initial procedure, which was often performed on the dominant wrist, but also by the patients' desire to maintain a high level of occupational activity. Although this study suggests a potential association between specific wrist-intensive occupations and the indication for bilateral surgical intervention, further research is needed to confirm any definitive occupational association.

Ethical approval

This study was approved by our institutional review board. (IRB No. CNUH 2025-08-069).

Competing Interest

The authors declare that they have no conflict of interest.

Funding

This work was supported by research fund of
Chungnam National University Hospital, 2024 (2024-CF-012).

References

1. Atzei A, Luchetti R (2011) Foveal TFCC tear classification and treatment. Hand Clin 27:263–272. https://doi:10.1016/j.hcl.2011.05.014.
2. Tomaino MM, Elfar J (2005) Ulnar impaction syndrome. Hand Clin 21:567–575. https://doi:10.1016/j.hcl.2005.08.011.
3. Ahn AK, Chang D, Plate AM (2000) Triangular fibrocartilage complex tears: a review. Bull NYU Hosp Jt Dis 64:114–118.
4. Jawed A, Ansari MT, Gupta V (2020) TFCC injuries: how we treat? J Clin Orthop Trauma 11:570–579. https://doi:10.1016/j.jcot.2020.06.001.
5. Nakamura T, Sato K, Okazaki M, Toyama Y, Ikegami H (2011) Repair of foveal detachment of the triangular fibrocartilage complex: open and arthroscopic transosseous techniques. Hand Clin 27:281–290. https://doi:10.1016/j.hcl.2011.05.002.

6. Kleinman WB (2007) Stability of the distal radioulna joint: biomechanics, pathophysiology, physical diagnosis, and restoration of function what we have learned in 25 years. J Hand Surg Am 32:1086–1106. https://doi:10.1016/j.jhsa.2007.06.014.
7. Ehman EC, Hayes ML, Berger RA, Felmlee JP, Amrami KK (2011) Subluxation of the distal radioulnar joint as a predictor of foveal triangular fibrocartilage complex tears. J Hand Surg Am 36:1780–1784. https://doi:10.1016/j.jhsa.2011.08.032.
8. Shim JI, Im JH, Lee JY, Kang HV, Cho SH (2019) Changes in ulnar variance after a triangular fibrocartilage complex tear. J Wrist Surg 8:30–36. https://doi:10.1055/s-0038-1668153.
9. Shen J, Papadonikolakis A, Garrett JP, Davis SM, Ruch DS (2005) Ulnar-positive variance as a predictor of distal radioulnar joint ligament disruption. J Hand Surg Am 30:1172–1177. https://doi:10.1016/j.jhsa.2005.06.014.
10. Imaeda T, Nakamura R, Shionoya K, Makino N (1996) Ulnar impaction syndrome: MR imaging findings. Radiology 201:495–500. https://doi:10.1148/radiology.201.2.8888248.
11. Ryoo HJ, Kim YB, Kwak D, Choi IC, Park JW (2023) Ulnar positive variance associated with TFCC foveal tear. Skeletal Radiol 52:1485–1491. https://doi:10.1007/s00256-023-04280-0.
12. Papapetropoulos PA, Wartinbee DA, Richard MJ, Leversedge FJ, Ruch DS (2010) Management of peripheral triangular fibrocartilage complex tears in the ulnar positive patient: Arthroscopic repair versus ulnar shortening osteotomy. J Hand Surg Am 35:1607–1613. https://doi:10.1016/j.jhsa.2010.06.015.
13. Wolf MB, Haas A, Dragu A, Leclère FM, Dreyhaupt J, Hahn P, Unglaub F (2012) Arthroscopic repair of ulnar-sided triangular fibrocartilage complex (Palmer Type 1B) tears: a comparison between short- and midterm results. J Hand Surg Am 37(11):2325-30. https://doi:10.1016/j.jhsa.2012.08.027.
14. Jung KJ, Nho JH, Kim JH, Kim BS, Gong HS (2018) Triangular fibrocartilage complex repair and ulna variance: A systematic review. J Hand Surg Asian Pac 23:313–319. https://doi:10.1142/S2424835518300025.
15. Kim B, Yoon HK, Nho JH, Park KH, Park SY, Yoon JH, Song HS (2013) Arthroscopically assisted reconstruction of triangular fibrocartilage complex foveal avulsion in the ulnar variance-positive patient. Arthroscopy 29(11):1762-1768. https://doi:10.1016/j.arthro.2013.08.022.
16. Im JH, Lee JW, Lee JY (2023) Ulnar Impaction Syndrome and TFCC Injury: Their Relationship and Management. J Wrist Surg 14(1):14–26. https://doi.10.1055/s-0043-1776759.
17. Seo JB, Kim JP, Yi HS, Park KH (2016) The Outcomes of Arthroscopic Repair Versus Debridement for Chronic Unstable Triangular Fibrocartilage Complex Tears in Patients Undergoing Ulnar-Shortening Osteotomy. J Hand Surg Am 41:615–623. https://doi:10.1016/j.jhsa.2016.02.009.
18. Im JH, Lee JY, Kang HV (2021) The Combined Procedure of Ulnar Metaphyseal Shortening Osteotomy With Triangular Fibrocartilage Complex Foveal Knotless Repair. J Hand Surg Am 46:822.e1–822.e7. https://doi.10.1016/j.jhsa.2021.01.021.
19. Schmauss D, Pohlmann S, Lohmeyer JA, Germann G, Bickert B, Megerle K (2016) Clinical tests and magnetic resonance imaging have limited diagnostic value for triangular fibrocartilaginous complex lesions.

Arch Orthop Trauma Surg 136:873–880. https://doi.org/10.1007/s00402-016-2441-9.
20. Tay SC, Tomita K, Berger RA (2007) The "ulnar fovea sign" for defining ulnar wrist pain: an analysis of sensitivity and specificity. J Hand Surg Am 32:438–444. https://doi.org/10.1016/j.jhsa.2007.01.022.
21. Giddins G, Knapper T, Fine N, Pickering G (2025) The reliability of clinical assessment of distal radioulnar joint instability among non-United Kingdom European surgeons. J Hand Surg Eur Vol 50:389–392. https://doi.org/10.1177/17531934241275456.
22. Jupiter JB (2009) Commentary: the effect of ulnar styloid fractures on patient-rated outcomes after volar locking plating of distal radius fractures. J Hand Surg Am 34:1603–1604. https://doi.org/10.1016/j.jhsa.2009.06.022.
23. Yang Z, Mann FA, Gilula LA, Haerr C, Larsen CF (1997) Scaphopisocapitate alignment: criterion to establish a neutral lateral view of the wrist. Radiology 205:865–869. https://doi.org/10.1148/radiology.205.3.9393549.
24. Mirghasemi AR, Lee DJ, Rahimi N, Rashidinia S, Elfar JC (2015) Distal radioulnar joint instability. Geriatr Orthop Surg Rehabil 6:225–229. https://doi.org/10.1177/2151458515584050.
25. Cooney WP, Bussey R, Dobyns JH, Linscheid RL (1987) Difficult wrist fractures. Perilunate fracture-dislocations of the wrist. Clin Orthop Relat Res (214):136–147.
26. Cha SM, Shin HD, Kim KC (2012) Positive or negative ulnar variance after ulnar shortening for ulnar impaction syndrome: a retrospective study. Clin Orthop Surg 4:216–220. https://doi.org/10.4055/cios.2012.4.3.216.
27. Baek GH, Chung MS, Lee YH, Gong HS, Lee S, Kim HH (2005) Ulnar shortening osteotomy in idiopathic ulnar impaction syndrome. J Bone Joint Surg Am 87:2649–2654. https://doi.org/10.2106/JBJS.D.02983.
28. Cha SM, Shin HD, Kim YK, Lee KW (2022) Ulnar shortening osteotomy for posttraumatic ulnar impaction syndrome in adolescent (younger than 18 years) - Based on the Cha & Shin assessment. Injury 53:4038–4047. https://doi.org/10.1016/j.injury.2022.10.004.
29. Cha SM, Shin HD, Ahn KJ (2017) Prognostic Factors Affecting Union After Ulnar Shortening Osteotomy in Ulnar Impaction Syndrome: A Retrospective Case-Control Study. J Bone Joint Surg Am 99:638–647. https://doi.10.2106/JBJS.16.00366.
30. Matsumoto T, Tang P, Fujio K, Strauch RJ, Rosenwasser MP (2018) The optimal suture placement and bone tunnels for TFCC repair: a cadaveric study. J Wrist Surg 7:375–381. https://doi.org/10.1055/s-0038-1661361.
31. Mak MCK, Ho PC (2024) Complications after arthroscopic triangular fibrocartilage complex (TFCC) surgery. J Hand Surg Eur Vol 49:149–157. https://doi.org/10.1177/17531934231218608.
32. Shrout PE, Fleiss JL (1979) Intraclass correlations: uses in assessing rater reliability. Psychol Bull 86:420–428. https://doi.org/10.1037//0033-2909.86.2.420.
33. Fleiss JL, Cohen J (1973) The equivalence of weighted Kappa and the intraclass correlation coefficient as measures of reliability. Educ Psychol Meas 33:613–639. https://doi.org/10.1177/001316447303300309.
34. Kim JS, Kim KE, Lee SW, Jeon S, Yang H, Choi YR (2025) Generalized Joint Laxity Increases the Risk of Recurrence of Distal Radioulnar Joint Instability after Arthroscopic Foveal Repair of the Triangular Fibrocartilage Complex. Arthroscopy 41:2309–2316. https://doi.10.1016/j.arthro.2024.10.040.

35. Abe Y, Moriya A, Tominaga Y, Yoshida K (2016) Dorsal tear of triangular fibrocartilage complex: clinical features and treatment. J Wrist Surg 2016;5:42–46. https://doi.10.1055/s-0035-1570037.
36. Minhas S, Kakar S, Wall LB, Goldfarb CA (2023) Foveal Triangular Fibrocartilage Complex Tears: Recognition of a Combined Tear Pattern. J Hand Surg Am 2023;48:1063.e1–1063.e6. https://doi.10.1016/j.jhsa.2022.03.010.
37. Cho JY, Lee SW, Kim DH, Oh WT, Koh IH, Chun YM, Choi YR (2024) Prognostic factors for clinical outcomes after arthroscopic treatment of traumatic central tears of the triangular fibrocartilage complex. Bone Joint J 106-B(4):380-386. https://doi:10.1302/0301-620X.106B4.BJJ-2023-0642.R3.
38. Cha SM, Choi BS, Shin HD (2017) Radiological degenerative changes in the distal radioulnar joint after ulnar shortening osteotomy in patients with idiopathic ulnar impaction syndrome: Analysis of factors affecting degenerative lesions. J Orthop Sci 22:1042–1048. https://doi.10.1016/j.jos.2017.06.010.
39. Fujio K. Arthroscopic Management of Triangular Fibrocartilage Complex Foveal Injury (2017) Hand Clin 33:619–624. https://doi.10.1016/j.hcl.2017.07.009.
40. Waterman SM, Slade D, Masini BD, Owens BD (2010) Safety analysis of all-inside arthroscopic repair of peripheral triangular fibrocartilage complex. Arthroscopy 26:1474–1477. https://doi.10.1016/j.arthro.2010.02.027.
41. Desai MJ, Hutton WC, Jarrett CD (2013) Arthroscopic repair of triangular fibrocartilage tears: a biomechanical comparison of a knotless suture anchor and the traditional outside-in repairs. J Hand Surg Am 38:2193–2197. https://doi.10.1016/j.jhsa.2013.08.097.
42. Gerber C, Fuchs B, Hodler J (2000) The results of repair of massive tears of the rotator cuff. J Bone Joint Surg Am 82:505–515. https://doi.10.2106/00004623-200004000-00006.
43. Schneeberger AG, von Roll A, Kalberer F, Jacob HA, Gerber C (2002) Mechanical strength of arthroscopic rotator cuff repair techniques: An in vitro study. J Bone Joint Surg Am 84:2152-–2160. https://doi.10.2106/00004623-200212000-00005.
44. Zhang W, Hou P, Wang C, Wu T, Ho PC, Sun L (2022) Arthroscopic one-tunnel transosseous reconstruction of chronic triangular fibrocartilage complex foveal tears: outcomes in 12 patients. J Hand Surg Eur Vol 47:296–301. https://doi.10.1177/17531934211056854.

Figure legends

Figure 1. (A) T2-weighted MRI showing a foveal tear with minimal continuity of the superficial fibers in the dominant wrist. (B) Positive hook test. © Classified as Palmer type 1A and 2B lesion without type 2A involvement (lunate chondromalacia only, without TFCC wear). (D) Arthroscopic repair with one loop stitch using FiberWire and two separate stitches using PDS during the initial surgery.

Figure 2. (A) T2-weighted MRI showing a foveal tear with concomitant superficial fiber rupture in the dominant wrist. (B) Classified as Palmer type 1D and 2B lesion without type 2A involvement (lunate chondromalacia only, without TFCC wear). (C) Arthroscopic repair with one loop stitch using FiberWire and two separate stitches using PDS during the initial surgery.

Figure 3. (A) Symptomatic ulnar impaction syndrome with 3 mm positive ulnar variance. (B) T2-weighted MRI showing a foveal tear with concomitant superficial fiber rupture in the dominant wrist. (C) Arthroscopic repair of an Atzei type 2 TFCC tear using one loop stitch with FiberWire and one loop stitch with PDS. Classified as Palmer type 2B lesion without type 2A involvement (lunate chondromalacia only, without TFCC wear). (D) Final crossed-suture configuration. (E) Healed ulnar shortening osteotomy with restoration to neutral variance. (F) Contralateral wrist at 21 months after the initial surgery. (G) T2-weighted MRI showing a foveal tear with concomitant superficial fiber rupture in the non-dominant wrist. (H) Repaired in the same manner. (I) Healed ulnar shortening osteotomy with neutral ulnar variance.

Hamatolunate impingement with ulnar impaction syndrome: a case report

Wonju Yonsei Hosp.
김용빈

Hamatolunate impingement syndrome is an uncommon cause of ulnar-sided wrist pain, most frequently reported in individuals who repetitively perform ulnar deviation, such as waiters and golfers. Anatomical predisposition with a type II lunate has been described as a consistent feature. A 64-year-old retired miner presented with gradually worsening ulnar-sided wrist pain. Plain radiographs demonstrated a type II lunate. Preoperative magnetic resonance imaging revealed subchondral sclerosis, bone marrow edema, and cyst formation of the hamate articulating with the lunate. Additional findings included central perforation with foveal tear of the triangular fibrocartilage complex (TFCC) and bone marrow edema of the ulnar head. With a diagnosis of hamatolunate impingement combined with ulnar impaction syndrome, surgical treatment was conducted. Arthroscopy of the midcarpal joint was performed, including proximal pole resection of the hamate. At the ulnocarpal joint, TFCC central debridement, transosseous repair, and ulnar shortening osteotomy were performed. Postoperatively, the patient achieved pain relief, and bone union was confirmed at 6 months on plain radiographs. In patients with ulnar-sided wrist pain and type II lunate, hamatolunate impingement should be suspected.

Keywords: Hamatelunate impingement, ulnar impaction syndrome

Figure 1. Preoperative plain radiograph

Figure 2. Preoperative MRI

Figure 3. Midcarpal joint arthroscopic images

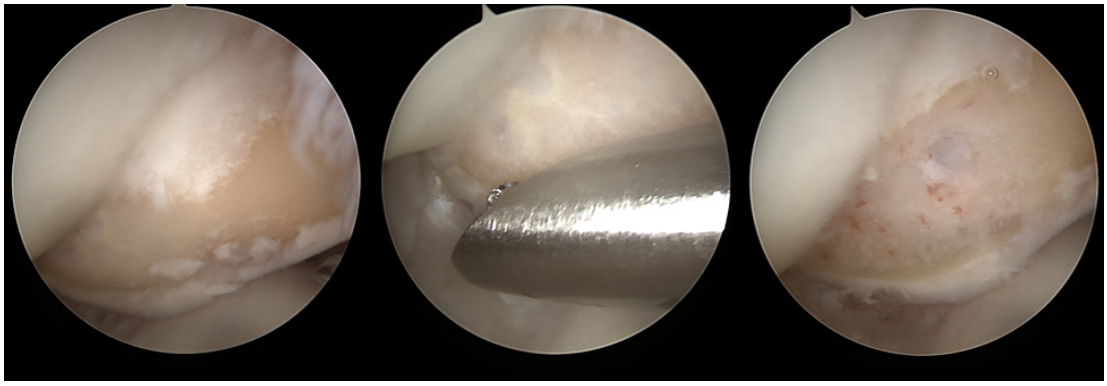

Figure 4. Ulnocarpal joint arthroscopic images

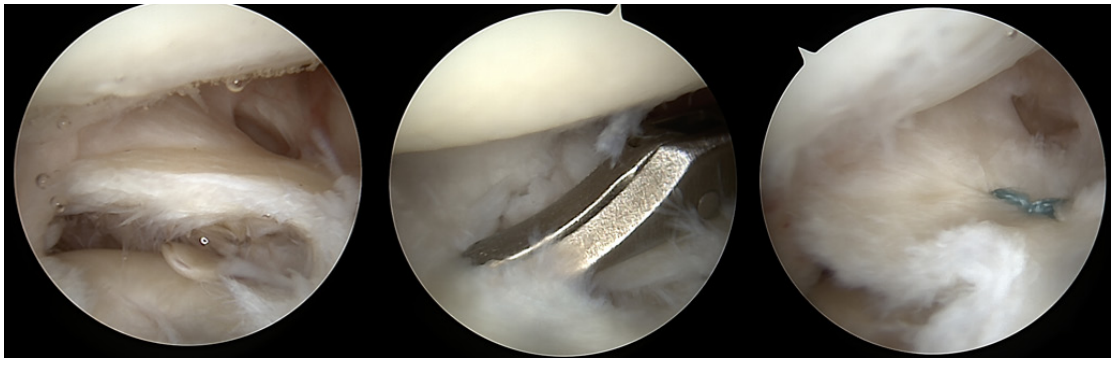

Figure 5. Postoperative plain radiograph

2025년 대한수부외과학회
추계학술대회

Room C

Free Paper 6.
(DRF, Carpal Bone Fracture: Wrist)

Orthop Surg. Eulji Univ. **Sang Ki Lee**
Orthop Surg. Kangdong Sacred Heart Hosp. **Sanglim Lee**

The efficacy of surgical management for distal radius fractures with or without the use of arthroscopic assistance: a systematic review and meta-analysis of randomized controlled trials and prospective study

Orthop Surg. Yeungnam Univ.
Sam Guk Park

Purpose: The objective of this study is to evaluate the efficacy of assistant arthroscopy in the surgical treatment of distal radius fractures by comparing the postoperative outcomes between the arthroscopic group and the control group.

Methods: We searched PubMed, Embase, Web of Science, and Cochrane Library databases for studies that compared the clinical outcomes of patients who underwent surgery with or without adjuvant arthroscopy. After screening of the studies, we obtained six randomized controlled trials and one prospective study. We analysis the radiological outcomes, range of motion, functional scores, pain scores, grip strength, operation time, and complication rates. The standardized mean difference (SMD) was used to analyze the differences in outcomes between the two groups. Statistical significance was set at $P < 0.05$.

Results: A total of 7 studies with 504 patients were included. Arthroscopic group showed superior radiologic parameters such as step-off (SMD = -1.18; 95% CI = -2.34, -0.02; I^2 = 93%) and gap (SMD = -0.71; 95% CI = -1.22, -0.2; I^2 = 64%). In addition, the arthroscopic group exhibited improved ranges of motion (extension, radial deviation, and ulnar deviation) and lower visual analog scale (SMD = -0.93; 95% CI = -1.85, -0.02; I^2 = 62%) than the control group. There were no significant differences in functional scores, grip strength, and complication rate between the two groups.

Conclusion: The results of this analysis showed that the arthroscopic assistant surgery for DRF produced significantly superior outcomes than the control group in radiologic outcomes (post-operative step-off and gap), range of motion (extension, radial deviation, and ulnar deviation), and VAS, despite the longer operation time.

Level of Evidence: Level II

Keywords: Distal radius fracture, wrist arthroscopy, meta-analysis.

Arthroscopic-Assisted Reduction and K-wire Fixation of Dorsal Ulnar Corner Fragments in Distal Radius Fractures

[1]Gayang Samsung Orthopaedic Clin., [2]Orthop Surg. Inje Univ., [3]Gohyeon Seoul Samsung Orthopaedic Clin.
Sang Hoon Chae[1], Seung Joo Kim[2], Dong Suk Kim[3], Hyun Il Lee[2]

Backgrounds: Distal radius fractures involving dorsal ulnar corner (DUC) fragments present a significant surgical challenge. Traditional approaches often face limitations in direct visualization, leading to inadequate reduction and an increased risk of hardware prominence. Achieving precise anatomical reduction and stable fixation of DUC fragments is crucial for optimal outcomes. This study evaluates an arthroscopic-assisted approach for the fixation of DUC fragments in distal radius fractures. Our technique utilizes simple dorsal-to-volar K-wire fixation to supplement standard volar locking plate fixation after arthroscopic reduction of the DUC fragment.

Materials and Methods: We applied this technique to 13 patients (14 wrists) with unstable intra-articular distal radius fractures and associated DUC fragments. Initial closed reduction was attempted, followed by arthroscopic-assisted reduction and internal fixation using the K-wire. The size of the DUC fragment and articular gap was measured on pre-operative CT scans, with post-operative gap or step-off re-measured on immediate post-operative CT scans. Clinical and radiographic outcomes were assessed at the final follow-up.

Results: The average initial DUC step-off was 3.5 mm (0.9~6.8 mm). Immediately post-operatively, the average DUC step-off was significantly reduced to 1.2 mm (0.5 ~ 2.5 mm) on CT. At an average follow-up of 9-months, radiographic outcomes showed an average ulnar variation of 0.4 mm and a volar tilt of 5.3°. Clinically, patients achieved an average wrist extension of 53.8° and flexion of 46.6°. Average grip strength was 81.2% of the contralateral wrist. Patient-reported outcomes were favorable, with an average P-VAS of 1.8, PRWE of 20, and DASH score of 23.8. Importantly, no patients experienced distal radioulnar joint instability.

Conclusions: Our findings demonstrate that arthroscopic-assisted K-wire fixation offers reliable solution** for accurately reducing DUC fragments in distal radius fractures. This approach provides an additional, simple method to stabilize DUCs, complementing standard volar locking plate fixation without increasing complications.

Efficacy of Ultrasonographic Examination for Predicting Symptomatic Flexor Tendon Irritation Following Volar Plating for Unstable Distal Radius Fractures

Orthop Surg. Yonsei Univ.
Jae-Yong Cho, Hyun-Kyo Kim, Won-Taek Oh, Il-Hyun Koh, Yun-Rak Choi

Background: Volar locking plate (VLP) fixation is a widely accepted surgical treatment for unstable distal radius fractures. However, it carries the risk of flexor tendon complications, particularly symptomatic tenosynovitis or rupture of the flexor pollicis longus and second flexor digitorum profundus tendons. Due to the high incidence of these fractures, a criterion for determining the need for subsequent implant removal is necessary. This study aimed to evaluate predictive factors of symptomatic flexor tendon irritation as potential prodromes of tendon rupture.

Methods: A prospective cohort of patients treated with VLP fixation for unstable distal radius fractures between July 2019 and February 2024 was analyzed. Demographic factors were assessed, and fracture configurations were evaluated based on AO/OTA classification using preoperative computed tomography. Clinical evaluations were conducted at 6 months postoperatively, including VAS pain score, DASH score, Mayo wrist score, grip strength, and range of motion. The primary outcome was symptomatic tendon irritation, defined as pain, edema, crackling sensation over the plates at 6 months postoperatively. Volar locking plates were categorized into two types based on the presence of a volar rim. Ultrasonographic assessments measured tendon-to-plate distances and evaluated the contact configuration between tendons and the plate (no contact, smooth contact, tenting sign). Tenting was classified when the edge of the plate appeared to indent or pierce the tendon, causing it to bend. Radiographic variables included ulnar variance, radial inclination, palmar tilt, and Soong classification.

Results: A total of 104 patients were included in the study, with 83 patients in the asymptomatic group and 21 in the symptomatic group. There were no significant differences in demographic factors between the two groups. In clinical outcomes, both the VAS pain score and the DASH score were significantly higher in the symptomatic group. Additionally, the proportion of patients who underwent hardware removal due to pain was significantly higher in this group ($p<0.001$). There were no significant differences in radiographic measurements between the two groups. However, sonographic findings revealed notable differences in both the distance to the plate ($p=0.006$) and the contact configuration ($p=0.028$). The symptomatic group showed a higher proportion of

cases with smooth contact or tenting signs on ultrasound. Multivariable analysis revealed that C-type fractures and the presence of a tenting sign on ultrasound were significantly associated with symptomatic tenosynovitis. However, the use of volar rim-type VLPs and the tendon-to-plate distance were not significantly associated.

Conclusion: In this study, symptomatic flexor tenosynovitis was significantly associated with the presence of a tenting sign on ultrasonography. In patients presenting with both clinical symptoms and a tenting sign, early hardware removal may be advisable. If only one of these findings is present, shared decision-making based on the patient's level of discomfort and functional demands is warranted, with either hardware removal or regular follow-up for close observation as reasonable options.

Level of Evidence: III

Morphologic Characteristics and Fixation Strategy of the Dorsal Ulnar Fragment in Intra-Articular Distal Radius Fractures: A CT-Based Analysis of 241 Cases

[1]Orthop Surg. Dong-A Univ., [2]Orthop Surg. Gyeongsang National Univ.
Sung Yoon Jung[1], Gu-Hee Jung[2]

Introduction: In fixation of distal radius fractures, volar locking plate can provide excellent subchondral support to the lunate facet, with locking screws extending from the palm to the dorsum. However, reducing and fixing the dorsal ulnar fragment emains technically challenging due to the inability to directly inspect it without posterior exposure. Several previous authors stressed that fixation of the dorsal ulnar fragment played a critical role in maintaining appropriate sagittal radiocarpal alignment and preventing dorsal collapse because the dorsal ulnar fragment occupies a part of both the radiolunate and the radioulnar articular surface. Therefore we aimed to assess the comminution patterns and morphologic features to evaluate the clinical relevance of DUF in the distal radius fracture after reformatting the CT scanning plane to eliminate the projection error.

Materials and methods: A total of 241 intra-articular distal radius fractures operated on at Changwon Gyeongsang National University Hospital and Dong-A University Hospital between 2016 and 2024 were analyzed. Using axial CT scan images, Articular fragments were classified into volar ulnar, central, radial styloid, and dorsal ulnar fragments. Each fragment was subsequently mapped with the Mimics program, and the length of the dorsal ulnar fragment was measured. The degree of distal radioulnar joint (DRUJ) involvement by the dorsal ulnar fragment was categorized as follows: < one-third of the anteroposterior diameter (Group 1), one-third to two-thirds (Group 2), and ≥ two-thirds (Group 3). Also, the length and trajectory of the most distal-ulnar locking screw in volar locking plate were analyzed.

Results: The extent of distal radioulnar joint (DRUJ) involvement by the dorsal ulnar fragment was observed as follows: Group 1, 77 cases (32%); Group 2, 112 cases (46%); and Group 3, 52 cases (22%). The mean length of the dorsal ulnar fragment was 10.2 ± 4.2 mm, and the ratio to the DRUJ anteroposterior diameter was 0.45 ± 0.18. The mean length of the locking screw on the volar plate was 20.4 ± 4.1 mm.

Conclusions: The dorsal ulnar fragment most commonly involves approximately one-half of the distal radioulnar joint (DRUJ). When fixation is performed using a volar locking plate, securing the fragment with a screw of at least one-half the DRUJ anteroposterior diameter in length appears necessary to maintain the reduction of the

dorsal ulnar fragment.

Keywords: Radius fractures, dorsal ulnar fragment, volar locking plate, computed tomography

Comparison of outcomes of distal radius graft versus iliac crest graft for arthroscopic scaphoid nonunion surgery

W Institute for HHand and Reconstructive Microsurgery, W General Hosp.
Byoung Jin Kim, Sang Hyun Woo

Background: The purpose of this study is to compare the outcomes of arthroscopic treatment of scaphoid nonunion with the use of distal radius and iliac crest bone grafts.

Methods: Between August 2020 and March 2025, 39 patients (40 wrists) with scaphoid nonunion received arthroscopic surgery. We evaluated the results with clinical outcomes based on Modified Mayo Wrist score (MMWS), range of motions and grip strength, and radiologic measurements

Results: 28 patients (29 wrists) were treated with iliac bone graft, and 11 patients (11 wrists) were treated with distal radius bone graft. There was no statistical difference in union rate between two groups (93.1% vs 90.9%, $P > 0.05$). And there was no significant difference in clinical and radiologic outcomes.

Conclusion: In arthroscopic scaphoid nonunion surgery, there is no significant difference in union rates between iliac crest and distal radius graft.

What is the optimal method of fixation method for scaphoid nonunion relative to the location of the lesion?

Orthop Surg. Eulji Univ.
Jongwon Lee, Sang Ki Lee

Introduction: Scaphoid nonunion is a typical complication of scaphoid fractures, with the nonunion rate varying by the location of the scaphoid. The current widely used method for treating scaphoid nonunion, which is challenging for surgeons, is the headless compression screw (HCS). Various surgical approaches, such as the scaphoid plate, have been proposed to address the problem of screw fixation; however, no consensus exists regarding the optimal treatment method. This study focused on analyzing appropriate treatment methods based on the anatomical location of the scaphoid nonunion.

Methods: 97 patients with scaphoid nonunion were treated between 2008 and 2023. All patients underwent treatment using one HCS or scaphoid volar locking plate with non-vascularized bone graft from the distal radius depending on the scaphoid's location. The scaphoid angle and bone union were confirmed using radiological examinations. The clinical evaluations included range of motion, pain, grip strength, and functional wrist scores.

Results: 57 patients were included in the final analysis. In the screw group, 26 patients [26/42 (62%)] obtained a bone union, and all 15 patients [15/15 (100%)] in the plate group obtained a union (p=0.005). In the waist group, 16 patients with screw [16/25 (64%)], and eight using a plate [8/8 (100%)] showed bony healing. In the proximal group, three patients with HCS [3/9 (33%)], and four using plate [4/4 (100%)] showed bone union. In the distal group, seven patients with a screw [7/8 (87%)] and three with the plate [3/3 (100%)] showed bone union. Significant differences were found in the waist (p=0.047) and proximal groups (p=0.026), but not in the distal group (p=0.521). All groups showed improved radiological angles associated with the scaphoid and better clinical outcomes postoperatively.

Conclusions: Plate fixation was overall superior to screw fixation for scaphoid nonunion, especially in the waist and proximal poles, providing better union rates and stability. For the distal group, both methods are effective, with the choice depending on the surgeon's expertise and patient factors. The results highlight the importance of the lesion's anatomical location in selecting the appropriate fixation method.

Keywords: Scaphoid nonunion, Location, Headless compression screw, Scaphoid volar locking plate

Learning Curve of Arthroscopic Osteosynthesis for Scaphoid Nonunion: a review of consecutive 50 cases

Orthop Surg. Yonsei Univ.
Won-Taek Oh, Seung-Eon Moon, Jae-Yong Cho, Il-Hyun Koh, Yun-Rak Choi

Background: Arthroscopic osteosynthesis, as an alternative to a conventional open technique in the treatment of scaphoid nonunion patients, has been recognized as one of the technically challenging procedures. Here we report 50 consecutive patients to determine the learning curve of this procedure using CUSUM (cumulative sum) analysis.

Methods: From Jan 2009 to March 2020, we reviewed the collected database of consecutive 50 patients diagnosed as scaphoid nonunion who underwent arthroscopic osteosynthesis. All the operations were held by a single surgeon. Patients were stratified in three groups (n = 17; Group1 and Group2, n = 16; Group 3), and their union rate, clinical and radiologic outcomes, and complication rate were compared. The CUSUM analysis based on operation time ($CUSUM_{OT}$) was also assayed. Then treatment failure, defined as persistent nonunion and secondary operation due to operation-related complication, was evaluated using learning curve-CUSUM (LC-CUSUM) and standard CUSUM. The acceptable failure rate was set at 0.1 and unacceptable at 0.2 referenced from previous literature (α = 0.05, β = 0.2).

Results: Among group comparisons, only the operation time showed significant differences ($p < 0.001$), which was shorter in Group 2 and 3 than Group 1 ($p = 0.001$ and 0.001). In $CUSUM_{OT}$ analysis, there were two peak phases in the 17^{th} and 42^{nd} case. In CUSUM analysis with the failure rate, it had reached an acceptable level at 25 cases, and none of the inadequate procedures was detected after that.

Conclusions: Surgical experience is crucial in arthroscopy of the wrist, especially when it needs advanced skill. Our analysis of arthroscopic osteosynthesis for the scaphoid nonunion revealed that approximately 25 cases are required to achieve the acceptable failure rate, although operation time was progressively decreased after the 17^{th} case.

월상골 주위 탈구 및 골절 탈구의 장기 추시 결과

Orthop Surg. Soonchunhyang Univ.
Byung Sung Kim, Kyung Jin Lee

Introduction: Perilunate dislocations and fracture-dislocations are severe injuries that often have serious functional sequelae. Our goal was to evaluate the long-term clinical and radiological results of these perilunate injuries, and to look for prognostic factors of a poor clinical outcome.

Materials and methods: We did a single-center, retrospective study of 17 patients who had either an isolated perilunate dislocation (n = 4) or fracture-dislocation (n = 13) in their wrist. Pain, range of motion, strength and functional scores (MWS, DASH) were evaluated. Radiographs were analyzed to look for amount of lunate displacement(stage), signs of osteoarthritis or carpal instability including scapholunate (SL) and radiolunate angle (RL), and carpal height ratio.
Sixteen were male and mean age was 32.3(17 ~ 50). Injuries occurred due to slip down(n = 5), fall from height (n = 4), sports activity (n = 4), motor vehicle accident (n = 3) and work related accident (n = 1). Average time period until surgery was 3.8 days (0~9). Scaphoid fractures were treated with reduction and internal fixation by using either a screw(14cases), a K-wires(1 case) or combined(2 cases). Temporary lunotriquetral fixation were performed in 17 cases, scapholunate fixation in 5 case and radiolunate fixation in 5 cases using Kirschner wires after reduction of the dislocations.

Results: Some injuries were accompanied with avulsion fractures such as radial styloid (n = 1), ulnar styloid (n = 2) and triquetrum (n = 5) and lunate (n = 1). Operation was performed through a dorsal approach in 13 wrists, volar approach in 2 wrists and combined(1 case). Arthroscopic assisted reduction and internal fixation was in 2 wrists. Median nerve injuries were associated in 2 cases.
The mean follow-up time was 9.5 years (4–20). The wrist joint had a mean flexion-extension of 81◦(0–140), radioulnar deviation of 33◦(0–65) and pronosupination of 150◦(120–180). The mean grip strength was 72% of contralateral side. The mean MWS and DASH scores were 75 and 29 respectively. At the last follow-up, average SL and RL angle were 52 and 1.1 degrees, respectively. The carpal height ratio was 0.55 at the last follow-up. At the final assessment, 4 patients (23.6%) had radiographic signs of osteoarthritis while one patient had residual

carpal instability. One patient had scaphoid nonunion. Older age at the time of injury seems to be predictor for the development of osteoarthritis. The magnitude of the lunate's displacement has no significant association with long-term functional outcome.

Conlusion: Despite optimal treatment, perilunate dislocations and fracture-dislocations at the wrist cause functional sequelae such as pain, stiffness, strength deficit and posttraumatic arthritis. The functional outcomes are determined by the patient's age.

Level of evidence: IV; retrospective observational study.

KeyWords: perilunate fracture–dislocation, scaphoid fracture.

2025년 대한수부외과학회
추계학술대회

Room C

Free Paper 7 (Hand)

Orthop Surg. The Catholic Univ. of Korea **Yang Guk Chung**
Plast Reconstr Surg. Saeson Hosp. **Jae In Chung**

Management of PIP joint contracture resulting from the fracture subluxation : a case review

Plast Reconstr Surg. DongGuk Univ.
Su Rak Eo, Kyung Hyun Kim, Soo A Lim, Sang Hun Cho

Proximal interphalangeal (PIP) injuries are often neglected or dismissed as nothing more than a "jammed" or sprained fingers, causing them commonly written off and left untreated. Although the goals of the management are well known as (1) maintaining a reduced joint, (2) reestablishing normal joint motion, and (3) allowing early range of motion, the treatments are still challenging due to its high risk of joint stiffness or flexion contracture.

We experienced the 62-year-old man with flexion contracture of left index finger PIP joint. He had got injury 18 months ago while hammering the nails on the wall. He recounted that he had been operated immediately in the local clinic resulting in his left index finger 90 degrees contracted volarly. The physical examination showed normal blood circulation and sensation. The X-rays revealed the healed fracture of the PIP joint. We planned to apply the dynamic external fixation for his PIP joint fracture dislocation.

Although the dynamic external fixation is well known for the useful technique for the PIP joint fracture dislocation, I'd like to share the clinical experience of the management of sequelae of the PIP joint fracture dislocation through a case presentation. This includes (1) neurovascular problems (2) proper dynamic external fixation (3) PIP joint arthroplasty.

Hybrid Fixation Using K-wire and Minimally Invasive Plating Osteosynthesis for Unstable Proximal Phalangeal Fractures: A Propensity-Matched Comparative Study

W Institute for Hand and Reconstructive Microsurgery, W General Hosp.
Chun Chan-yang, Soo Jin Woo, Dong-Ho Kang, Kim Jae-hyub

Purpose : we propose a novel hybrid fixation technique that combines Kirschner wire (K-wire) fixation with minimally invasive plate osteosynthesis (MIPO), aiming to overcome the biomechanical limitations of conventional K-wire fixation and improve fracture stability while facilitating early mobilization and functional recovery.

Mothord : This retrospective study included patients treated between January 2020 and May 2025. 114 patients (117 digits) were included in the final analysis. Of these, 101 patients (104 digits) underwent K-wire fixation, and 13 patients (13 digits) received hybrid fixation using both K-wire and minimally invasive plate osteosynthesis (MIPO). Total active motion (TAM) was the primary measure of functional outcome and was assessed at the final follow-up visit, at a minimum of 12 weeks postoperatively.

Results : When stratified by the American Society for Surgery of the Hand (ASSH) criteria, 69.3% of hybrid digits were classified as Excellent or Good, compared to 46.1% in the K-wire group (p = 0.307). Poor outcomes were observed in 38.5% of the K-wire group, with none observed in the hybrid group (p = 0.003). The overall complication rate was higher in the K-wire group (23.1%) compared to the hybrid group (7.7%). Complications comprised nonunion or malunion, superficial infection, reduction loss, and tenolysis. However, the difference in complication rates between the groups was not statistically significant

Conclusions: This hybrid fixation technique combining K-wire stabilization with minimally invasive plate osteosynthesis (MIPO) provides sufficient mechanical stability to support early ROM while preserving the biological environment. Given these advantages, it may represent an effective treatment option for unstable extra-articular proximal phalangeal fractures.

Introduction

Phalangeal and metacarpal fractures are among the most common injuries of the upper extremity, with fractures of the proximal phalanges occurring more frequently than those of the middle and distal phalanges [1,2]. The stability of proximal phalangeal fractures is primarily determined by factors such as fracture geometry (e.g., obliquity, comminution), displacement (e.g., angulation >10–15°, shortening >2 mm, rotational malalignment), and the inability to maintain reduction under passive motion or functional loading [3–5]. Unstable extra-articular proximal phalangeal fractures are relatively common in clinical practice and often require surgical stabilization to restore hand function and alignment [6–8].

Although numerous surgical techniques have been described for the treatment of these fractures, the optimal fixation strategy remains controversial [9]. Nevertheless, closed reduction followed by percutaneous pinning using K-wires remains a widely utilized and biomechanically effective option across different techniques and fracture types [9]. Despite being a minimally invasive technique, K-wire fixation has notable limitations, including insufficient rotational control, difficulty maintaining reduction, risk of secondary displacement, and potential for prolonged immobilization and pin tract infection, which may lead to limited functional outcomes in many cases.

In this study, we propose a novel hybrid fixation technique that combines Kirschner wire (K-wire) fixation with minimally invasive plate osteosynthesis (MIPO), aiming to overcome the biomechanical limitations of conventional K-wire fixation and improve fracture stability while facilitating early mobilization and functional recovery.

Method

This study was conducted at Institution OO in the Hand and Microsurgery Department and was approved by the institutional review board.

Demographics

This retrospective study included patients treated between January 2020 and May 2025. A total of 191 patients (204 digits) who underwent surgical treatment for unstable proximal phalangeal fractures were initially screened. Patients with intra-articular fractures (5 patients, 5 digits), those treated with plate fixation or intramedullary nailing (8 patients, 8 digits), and those lost to follow-up (64 patients, 74 digits) were excluded. Following these exclusions, 114 patients (117 digits) were included in the final analysis. Of these, 101 patients (104 digits) underwent K-wire fixation, and 13 patients (13 digits) received hybrid fixation using both K-wire and minimally invasive plate osteosynthesis (MIPO).

[Figure 1]

Surgical Technique and Postoperative Protocol

After sterile preparation and exsanguination of the upper extremity, a pneumatic tourniquet was inflated to 250 mmHg. Manual closed reduction was performed under fluoroscopic guidance, and alignment was confirmed in both anteroposterior and lateral views. Two or three 1.0-mm Kirschner wires were inserted percutaneously for provisional stabilization of the fracture. After confirming rotational alignment, a 2.0-mm low-profile miniplate was positioned under fluoroscopy. Two separate 1.0-cm longitudinal incisions were made at the dorsal midline of the proximal phalanx. The extensor tendon was carefully elevated, and the plate was inserted subperiosteally using a minimally invasive plate osteosynthesis (MIPO) technique. Cortical screws were inserted into the most proximal and distal holes of the plate. Final fluoroscopic images were obtained during passive range of motion (ROM) testing to confirm stable reduction. All surgeries were performed by three board-certified hand surgeons with substantial experience in hand trauma and microsurgical reconstruction. [Figure 2]

Rehabilitation was initiated approximately 1 week postoperatively, once pain and swelling were adequately controlled. ROM exercises were started with buddy taping and use of a dorsal protective splint. Kirschner wires were removed in the outpatient clinic between 2 and 3 weeks after surgery, and splinting was continued until postoperative week 4 if tenderness at the fracture site persisted. At 6 weeks, radiographic evidence of callus formation permitted return to unrestricted daily activities. Return to heavy labor and sports was allowed at 3 months postoperatively.

Outcome measures

Total active motion (TAM) was the primary measure of functional outcome and was assessed at the final follow-up visit, at a minimum of 12 weeks postoperatively. According to the American Society for Surgery of the Hand (ASSH), TAM is calculated as the sum of active flexion at the metacarpophalangeal, proximal interphalangeal, and distal interphalangeal joints, with extension deficits subtracted. Measurements were obtained using a finger goniometer placed dorsally over each joint. TAM values were expressed as a percentage of either the contralateral normal digit or a standard reference of 260°, and were categorized based on ASSH criteria as excellent (≥85%), good (70–84%), fair (50–69%), or poor (<50%) [10].

Additional clinical assessments included postoperative complications and the timing of K-wire removal. Complications were defined as any of the following: reduction loss, malunion (angular deformity >15° or rotational malalignment), delayed union (no radiographic bridging at 8 weeks), nonunion (no evidence of healing at 12 weeks), or superficial infection requiring treatment. Complications also included secondary surgical procedures, such as tenolysis for persistent ROM limitations. K-wires were removed once sufficient stability was achieved to initiate active motion exercises. In the K-wire group, removal was typically performed no earlier than 4 weeks postoperatively, while in the hybrid group, K-wires were removed at approximately 2 to 3 weeks.

Radiographic union was confirmed in all cases except those classified as complications. Return to unrestricted

daily activity was assessed clinically and through patient self-report but was not included in the comparative analysis.

Stastical Analysis: Propensity Score Matching (PSM)

To reduce potential selection bias and confounding between treatment groups, we performed 1:2 propensity score matching (hybrid group to K-wire group) using a logistic regression model. The matching model included the following covariates: patient age, diabetes status, smoking history, and fracture type (open and/or comminuted), selected based on their known or suspected influence on clinical outcomes following phalangeal fracture fixation. Nearest-neighbor matching without replacement was employed without a caliper to maximize case retention. Covariate balance between the matched groups was assessed using standardized mean differences (SMDs), with an SMD of less than 0.1 considered indicative of adequate balance. The matched cohort was subsequently used for outcome comparisons.

Result

Patient Matching and Baseline Comparison

A total of 117 digits from patients with unstable extra-articular proximal phalangeal fractures were initially screened. After applying exclusion criteria and ensuring adequate follow-up, 13 digits treated with hybrid fixation and 104 digits treated with conventional K-wire fixation were included in the matching pool. Of these, 13 digits in the hybrid group were matched to 26 digits in the K-wire group using 1:2 propensity score matching. Baseline characteristics of the matched cohorts are shown in Table 2. Standardized mean differences (SMDs) were < 0.2, indicating acceptable balance. Pre-matching characteristics are summarized in Table 1.

Functional Outcomes: Total Active Motion

All outcome comparisons were performed in the propensity score–matched cohort. Total active motion (TAM) at final follow-up was the primary outcome. The hybrid group demonstrated a significantly higher mean TAM at final follow-up compared to the K-wire group ($p = 0.0081$). The mean TAM in the hybrid group was 81.0% ± 13.5% (95% CI: 73.5–88.5), whereas the K-wire group showed 54.3% ± 21.3% (95% CI: 45.0–63.6). The mean follow-up duration was 265 days (~38 weeks) in the hybrid group and 171 days (~24 weeks) in the K-wire group. Both groups exceeded the minimum 12-week requirement for TAM assessment, as shown in Table 3 and Figure 3.

When stratified by the American Society for Surgery of the Hand (ASSH) criteria, 69.3% of hybrid digits were classified as Excellent or Good, compared to 46.1% in the K-wire group ($p = 0.307$). Poor outcomes were observed in 38.5% of the K-wire group, with none observed in the hybrid group ($p = 0.003$), as shown in Figure 4.

Postoperative Outcomes: Complications and K-wire Removal

The overall complication rate was higher in the K-wire group (23.1%) compared to the hybrid group (7.7%). Complications comprised nonunion or malunion, superficial infection, reduction loss, and tenolysis. However, the difference in complication rates between the groups was not statistically significant ($p = 0.388$).

The timing of K-wire removal also differed significantly between groups ($p < 0.001$).
In the hybrid group, K-wires were removed at a mean of 2.23 ± 0.60 weeks postoperatively (95% CI: 1.88–2.59, n = 13), whereas in the K-wire group, removal occurred at 5.23 ± 0.99 weeks (95% CI: 4.82–5.63, n = 26).

Discussion

The management of unstable extra-articular proximal phalangeal fractures remains challenging, and no single fixation method has been universally accepted as optimal [11, 12]. Common surgical options include percutaneous K-wire pinning, plating, and intramedullary nailing. K-wire fixation is minimally invasive and preserves soft tissue, but it often lacks sufficient mechanical stability, particularly against rotational and angular displacement [13, 14]. Plating techniques provide rigid fixation that enables early mobilization, but they require extensive soft-tissue dissection, which may lead to tendon adhesion and postoperative stiffness [15, 16]. Intramedullary nailing offers a less invasive approach and allows early ROM, but its limited rotational control may result in deformity or loss of reduction [17, 18].

To our knowledge, this is the first clinical report to introduce a hybrid fixation technique that combines percutaneous K-wire stabilization with minimally invasive plate osteosynthesis (MIPO) for the treatment of proximal phalangeal fractures. Hybrid fixation techniques are designed to combine the mechanical benefits of existing methods while mitigating their respective complications, such as tendon irritation, instability, or loss of motion. This technique provides relative stability while preserving the biological environment through limited surgical exposure. By minimizing soft-tissue disruption and preserving periosteal blood supply, MIPO facilitates optimal conditions for bone healing [19]. Although it does not aim for absolute stability, the hybrid fixation offers sufficient rigidity to permit early micromotion, which supports secondary bone healing through callus formation, in accordance with the AO principles of relative stability [20, 21].

Furthermore, multiple studies have demonstrated that initiating early ROM is significantly associated with improved total active motion (TAM) recovery following hand injuries [22-24]. Consistent with these findings, the hybrid fixation group allowed for earlier removal of K-wires—typically at 2 to 3 weeks postoperatively—compared to 5 or more weeks in the K-wire group. This earlier K-wire removal allowed for early ROM initiation, likely contributing to superior TAM outcomes in the hybrid group. These findings highlight the potential clinical value of this approach, though certain limitations must be considered.

This study has several limitations. First, this study compared hybrid fixation exclusively to percutaneous pinning and did not include other fixation methods such as plating or intramedullary nailing. Further comparative studies

will be needed to assess how the hybrid technique performs relative to these alternatives. Second, the hybrid fixation group included only 13 digits, which limits the statistical power and generalizability of our findings. Larger, prospective studies are warranted to confirm the reproducibility of these results. Third, the mean follow-up duration differed between groups, with the hybrid group having a longer average follow-up period. Although both groups exceeded the minimum required for TAM assessment, this discrepancy may have influenced the degree of functional recovery and outcome interpretation.

Despite these limitations, our findings suggest that hybrid fixation provides a favorable balance between preservation of the biological environment and mechanical stability, enabling early mobilization and potentially improving functional outcomes in the treatment of unstable proximal phalangeal fractures. Further prospective research is recommended to validate its advantages in broader patient populations and across diverse clinical settings.

Conclusion

This hybrid fixation technique combining K-wire stabilization with minimally invasive plate osteosynthesis (MIPO) provides sufficient mechanical stability to support early ROM while preserving the biological environment. Given these advantages, it may represent an effective treatment option for unstable extra-articular proximal phalangeal fractures.

Reference

1. Van Onselen EB, Karim RB, Hage JJ, Ritt MJ. Prevalence and distribution of hand fractures. J Hand Surg Br. 2003;28(5):491–5.
2. Hove LM. Fractures of the hand: distribution and relative incidence. Scand J Plast Reconstr Surg Hand Surg. 1993;27:317–9.
3. Wolfe SW, Hotchkiss RN, Pederson WC, Kozin SH, Cohen MS. Green's Operative Hand Surgery. 8th ed. Philadelphia: Elsevier; 2021.
4. American Society for Surgery of the Hand. ASSH Manual of Hand Surgery. 2nd ed. Rosemont, IL: ASSH; 2016.
5. AO Foundation. AO Surgery Reference: Phalanges – Proximal Fracture Management.
6. Robinson LP, Gaspar MP, Strohl AB, et al. Dorsal versus lateral plate fixation of finger proximal phalangeal fractures: a retrospective study. Arch Orthop Trauma Surg. 2017;137(10):1389–95. doi:10.1007/s00402-017-2650-x
7. Pfanner S, Del Chiaro A, Suardi C, et al. Choosing the proper implant for extra-articular fractures of proximal

phalanges: A study on 75 cases. Injury. 2024. doi:10.1016/j.injury.2024.01.045
8. Vervloesem N, Glassey N, Kerr A. Rehabilitation following extra-articular proximal phalangeal fractures of the fingers in adults: a scoping review. Hand Ther. 2023. doi:10.1177/17589983231155270
9. Nikci V, Effiong L, Freibott CE, Gardner TR, Strauch RJ. Percutaneous fixation of unstable proximal phalanx fractures: a biomechanical study. Hand (N Y). 2021;16(5):696–702. doi:10.1177/15589447211017224
10. Adams L, L. G, E. T. Range of Motion. In: TherapistsASoH, editor. Clinical Assessment Recommendations1992.
11. Henry MH. Fractures of the proximal phalanx and metacarpals in the hand: preferred methods of stabilization. J Am Acad Orthop Surg. 2008;16(10):586-595.
12. Wong HK, Lam CY, Wong KY, Ip WY, Fung KK. Treatment of phalangeal and metacarpal fractures: a review. J Orthop. 2008;5(1):1-10.
13. Lögters TT, Lee HH, Gehrmann S, Windolf J, Wild M. Proximal phalanx fracture management. Hand (N Y). 2018;13(4):415-421.
14. Khan J, Ahmed R, Ahmad T, Sheraz M. K-wires fixation versus plating in metacarpal and phalangeal fractures: a randomized control trial. Isra Med J. 2018;10(2):130–133
15. Gaspar MP, Robinson LP, Strohl AB, et al.Dorsal versus lateral plate fixation of finger proximal phalangeal fractures: a retrospective study.Arch Orthop Trauma Surg. 2018;138(9):1265–1272.
16. Tam CY, Koo JJSC, Li PMC, et al.Clinical outcome of dorsal versus lateral plating in proximal phalangeal fracture: a retrospective study.J Hand Surg Asian Pac Vol. 2024.
17. Chao J, Patel A, Shah A. Intramedullary screw fixation: comprehensive technique guide for metacarpal and phalanx fractures—pearls and pitfalls. Plast Reconstr Surg Glob Open. 2021;9(10):e3893.
18. Schmidt GJ, Dent C, Nguyen A, Nydick J. Early postoperative outcomes of surgical fixation of proximal phalanx fractures with intramedullary nails versus Kirschner wires. Hand (N Y). 2025;Published online.
19. Farouk O, Krettek C, Miclau T, et al. Minimally invasive plate osteosynthesis: does percutaneous plating disrupt femoral blood supply less than the traditional technique? J Orthop Trauma. 1999;13(6):401–406.
20. Xue Z, Xu H, Ding H, Qin H, An Z. Comparison of the effect on bone healing process of different implants used in minimally invasive plate osteosynthesis. Sci Rep. 2016;6:37902.
21. Lujan TJ, Henderson CE, Madey SM, Fitzpatrick DC, Bottlang M. Locked plating of distal femur fractures leads to inconsistent and asymmetric callus formation. J Orthop Trauma. 2010;24(3):156–162
22. Ataker Y, Uludag S, Ece SC. Early active motion after rigid internal fixation of unstable extra-articular fractures of the proximal phalanx. J Hand Surg Eur Vol. 2017;42(7):703–709
23. Renberg M, Svingen J, Arner M, Farnebo S. Range of motion following flexor tendon repair: comparing active and passive protocols. J Hand Surg Am. 2024

Aims: Unstable extra-articular proximal phalangeal fractures are difficult to treat due to the limitations of conventional fixation methods. This study aimed to evaluate the clinical outcomes of a novel hybrid fixation

technique combining percutaneous Kirschner wire (K-wire) stabilization with minimally invasive plate osteosynthesis (MIPO), compared with traditional K-wire fixation alone.

Methods: A retrospective cohort of 114 patients (117 digits) who underwent surgical treatment for unstable proximal phalangeal fractures between 2020 and 2025 was reviewed. After applying inclusion criteria, 13 digits treated with hybrid fixation were compared to 26 digits treated with K-wire fixation using 1:2 propensity score matching based on age, diabetes status, smoking, and fracture characteristics. The primary outcome was total active motion (TAM) at a minimum of 12 weeks postoperatively. Secondary outcomes included complication rate and K-wire removal time.

Results: The hybrid fixation group showed significantly greater TAM (mean 81.0% ± 13.5%) compared to the K-wire group (54.3% ± 21.3%, $p = 0.0081$). K-wires were removed significantly earlier in the hybrid group (2.23 ± 0.60 weeks vs 5.23 ± 0.99 weeks, $p < 0.001$), facilitating earlier mobilization. The complication rate was lower in the hybrid group (7.7%) than in the K-wire group (23.1%), although this was not statistically significant ($p = 0.388$).

Conclusions: The hybrid fixation technique offers improved functional outcomes and enables earlier rehabilitation by combining mechanical stability with soft tissue preservation. It may be a valuable alternative to conventional K-wire fixation in managing unstable proximal phalangeal fractures.

Level of evidence: Level III, retrospective comparative study.

Aims: Unstable extra-articular proximal phalangeal fractures remain challenging to manage, and the optimal fixation strategy has yet to be established. This study aimed to evaluate the clinical outcomes of a novel hybrid fixation technique—combining percutaneous Kirschner wire (K-wire) stabilization with minimally invasive plate osteosynthesis (MIPO)—as compared with conventional K-wire fixation.

Methods: A retrospective cohort of 114 patients (117 digits) treated surgically between 2020 and 2025 was reviewed. After applying inclusion criteria, 13 digits treated with hybrid fixation were matched to 26 digits treated with K-wire fixation using 1:2 propensity score matching based on age, diabetes status, smoking history, and fracture characteristics. Outcomes assessed were total active motion (TAM), K-wire removal time, and postoperative complications, with a minimum follow-up of 12 weeks.

Results: The hybrid fixation group demonstrated significantly greater TAM at final follow-up (81.0% ± 13.5%) compared with the K-wire group (54.3% ± 21.3%; $p = 0.0081$). K-wires were removed significantly earlier in the hybrid group (2.23 ± 0.60 weeks vs 5.23 ± 0.99 weeks; $p < 0.001$), facilitating earlier mobilization. Although the complication rate was lower in the hybrid group (7.7%) than in the K-wire group (23.1%), this difference was not

statistically significant (p = 0.388).

Abstract

Unstable extra-articular proximal phalangeal fractures often require surgical intervention to restore alignment and function. While percutaneous K-wire fixation is widely used, it frequently lacks sufficient mechanical stability to permit early mobilization, resulting in suboptimal range of motion. This study introduces a hybrid fixation technique that combines K-wire stabilization with minimally invasive plate osteosynthesis (MIPO) and evaluates its clinical outcomes compared with conventional K-wire fixation. A retrospective review was conducted of 114 patients (117 digits) treated between 2020 and 2025. After applying inclusion criteria and performing 1:2 propensity score matching based on age, diabetes status, smoking, and fracture characteristics, 13 digits in the hybrid group were matched to 26 digits in the K-wire group. The primary outcome was total active motion (TAM), measured at a minimum of 12 weeks postoperatively. The hybrid group demonstrated significantly higher TAM (81.0% ± 13.5%) compared with the K-wire group (54.3% ± 21.3%; p = .0081). K-wires were removed significantly earlier in the hybrid group (2.23 ± 0.60 weeks vs 5.23 ± 0.99 weeks; p < .001), allowing for earlier initiation of range-of-motion exercises. The complication rate was lower in the hybrid group (7.7%) than in the K-wire group (23.1%), although this difference was not statistically significant (p = .388). These findings suggest that hybrid fixation offers improved functional outcomes and facilitates earlier rehabilitation by combining mechanical stability with minimal soft tissue disruption.

Location of the A1 and A2 Pulleys in Relation to the Palmar Creases: Implications for Percutaneous Release

[1]Orthop Surg. Inje Univ.
[2]Department of Anatomy, Catholic Institute for Applied Anatomy, The Catholic University of Korea,
[3]Gohyeon Seoul Samsung Orthopaedic Clin.
Seung Joo Kim[1], Young-In So[2], Yi-Suk Kim[2], Wu-Chul Song[2], Dong Suk Kim[3], Hyun-Il Lee[1]

Trigger finger occurs when a tendon becomes inflamed or thickened and becomes trapped in the A1 pulley at the metacarpophalangeal joint. This study aimed to provide an anatomical basis for the successful outcome of percutaneous A1 pulley release. Specifically, we used the easily identifiable skin crease as a reference point to locate the A1 and A2 pulleys during surgery. A total of 156 fingers from 39 Korean adult cadavers were examined. Before dissection, surface landmarks such as the palmar crease and palmar digital crease were identified, and the distances between nearby creases were measured. Following meticulous dissection, nine distances, including the lengths of the A1 and A2 pulleys and the distance between the pulley edge and nearby crease, were recorded. The results varied according to the fingers, with the A1 pulley averaging about 7.2 mm (ranging from 6.9 to 7.4 mm) and the A2 pulley averaging about 17.1 mm (ranging from 15.5 to 18.6 mm) in fingers 2 to 4. This study revealed that the A1 pulley is distal to the palmar crease and that the gap between the A1 and A2 pulleys is relatively narrow (3.4 mm). We confirmed the locations of the A1 and A2 pulleys relative to the skin surface creases, and based on this information, we provided basic data for pre-operative mapping of the locations of A1 and A2 on the skin of palm. These findings can provide valuable information for performing percutaneous A1 pulley release effectively as a minimally invasive procedure.

Table 1. Measurement values

Items	2nd finger	3rd finger	4th finger	5th finger
#1 PIPC~PDC	21.8 ± 2.1	23.7 ± 2.6	21.8 ± 2.3	18.0 ± 2.4
#2 PDC~DPC or PPC	23.1 ± 2.5	24.3 ± 2.9	27.4 ± 2.9	21.4 ± 2.5
#3 Length of A1 pulley	7.4 ± 2.0	7.2 ± 2.1	6.9 ± 1.7	5.9 ± 1.6
#4 Length of A2 pulley	15.5 ± 3.0	18.6 ± 2.8	17.3 ± 2.4	12.1 ± 2.4
#5 A2 pulley(proximal)~A1 pulley(distal)	3.5 ± 1.7	3.6 ± 1.7	3.1 ± 1.0	3.4 ± 1.7

#6 A1 pulley(proximal)~DPC or PPC	4.7 ± 2.7	3.1 ± 2.2	4.9 ± 2.8	4.0 ± 2.3
#7 PDC~A1 pulley(proximal)	18.4 ± 2.3	21.2 ± 2.2	22.5 ± 3.4	17.4 ± 2.6
#8 PDC~A1 pulley(distal)	11.0 ± 2.9	14.0 ± 3.0	15.6 ± 3.5	11.5 ± 2.9
#9 PDC~A2 pulley(proximal)	7.5 ± 3.3	10.4 ± 3.1	12.4 ± 3.9	8.0 ± 3.4

mean±S.D., Unit: mm

Figure legends

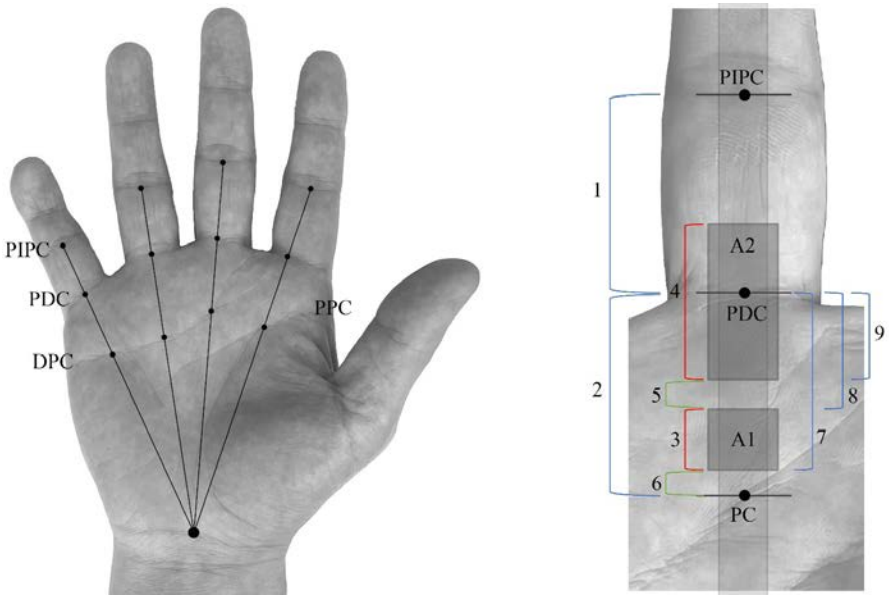

Fig. 1. Surface landmarks and distances. DPC, distal palmar crease. PDC, proximal digital crease. PC, palmar crease. PIPC, proximal interphalangeal crease. PPC proximal palmar crease. The distances (#1~#9) are explained in text and Table 1.

Fig. 2. Anatomical finding of the pulleys of four fingers. Arrows, gap between A1 and A2 pulleys.

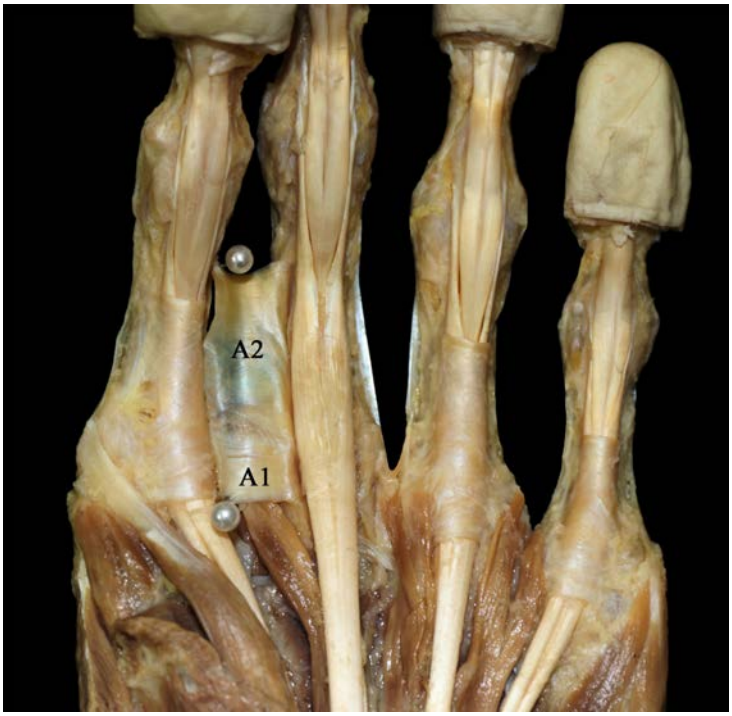

Fig. 3. Internal surface of A1 and A2 pulleys. The gap between A1 and A2 pulleys was well identified on the internal surface.

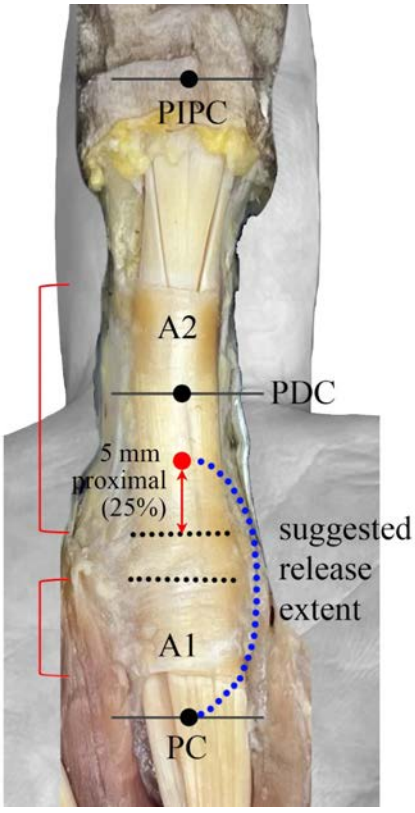

Fig. 4. Suggestion for percutaneous release. PC, palmar crease. PDC, proximal digital crease. PIPC, proximal interphalangeal crease.

Concurrent Pyogenic Granuloma and Onychomadesis after Splint Application

Jeonbuk National Univ.
박정균

Introduction: Splint immobilization is a common postoperative measure after hand trauma, but it may rarely lead to periungual complications, such as pyogenic granuloma (PG) and onychomadesis. These changes can result from mechanical pressure, microtrauma, and altered local circulation, highlighting splint application as a potential precipitating factor.

Case: A 16-year-old patient presented with a finger injury caused by glass. He underwent flexor tenorrhaphy of the middle finger and wound closure of the ring finger, followed by splint immobilization. Months later, periungual masses developed on the injured fingers (Figure 1). The lesions were friable, erythematous nodules from the proximal nail folds. On follow-up, the middle-finger mass regressed, while the ring-finger lesion enlarged (Figure 2). Excisional biopsy was performed (Figure 3), and histopathology confirmed PG (Figure 4).

Discussion: Splint application may precipitate periungual PG and onychomadesis. Mechanical pressure, repetitive microtrauma, and impaired local circulation during immobilization likely contribute. In this case, the simultaneous occurrence of PG and onychomadesis confined to immobilized fingers, and the clear relationship, strongly suggest a causal role of immobilization. Although definitive causality cannot be established from a single case, a few previous reports support this association. Awareness of these benign and self-limiting complications can prevent misdiagnosis overtreatment, with most cases managed by simple excision or conservative treatment.

Conclusion: This case highlights splint application as a potential trigger for periungual PG and onychomadesis. Mechanical and vascular changes induced by immobilization may explain their concurrent development. Periodic follow-up after immobilization allows timely reassurance, with most cases resolving simple excision or conservative treatment.

Figure 1

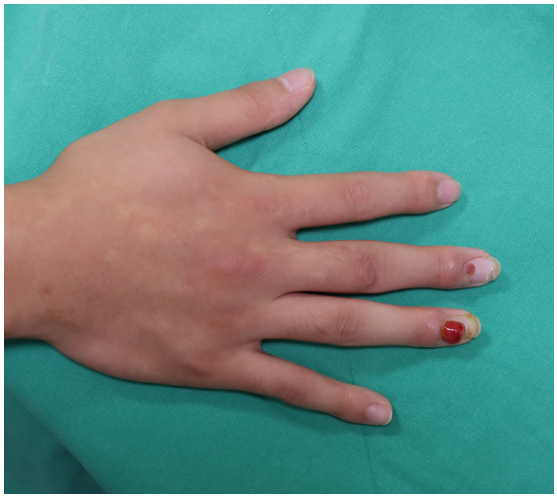

Figure 2

Figure 3

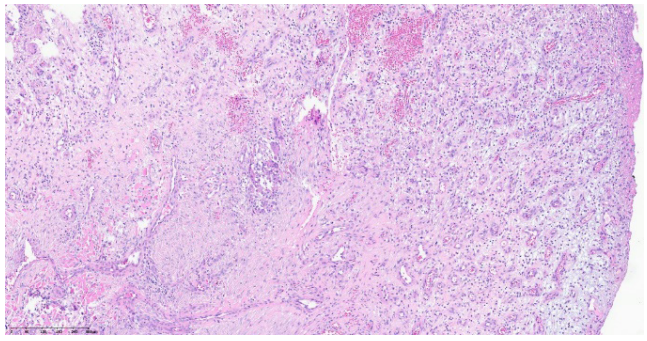

Figure 4

Preliminary Report of a Prospective Alternating-treatment Study Comparing Autogenous and Allogeneic Bone Grafting in the Treatment of Solitary Enchondroma of the Short Tubular Bones of the Hand

[1]Orthop Surg. Uijeongbu St. Mary's Hosp. The Catholic Univ. of Korea,
[2]Orthop Surg. Yeouido St. Mary's Hosp. The Catholic Univ. of Korea,
[3]Orthop Surg. St. Vincent's Hosp. The Catholic Univ. of Korea
Ho Youn Park[1], Taegu Lim[1], Jin-Hyung Im[2], Min Wook Joo[3]

Background: Enchondroma is a frequently occurring benign bone tumor affecting the hand. While both autologous and allogeneic bone grafts are widely implemented following curettage, there is a notable absence of high-level studies directly comparing their surgical outcomes. The objective of this study was to directly compare the radiographic and functional results of autologous versus allogeneic cancellous bone grafting in treating solitary enchondroma of the hand.

Methods: Patients with symptomatic solitary enchondroma of the hand were prospectively enrolled from October 2018 to October 2023, with each patient followed for a minimum of 12 months through December 2024. Patients were allocated to receive either autologous iliac bone grafting or allogeneic cancellous bone chip impaction grafting following curettage using a prospective alternating treatment protocol. Clinical evaluation included the visual analog scale (VAS) score, range of motion (ROM), and Disabilities of the Arm, Shoulder, and Hand (DASH) score. Radiographic healing was evaluated using the Tordai classification. Postoperative assessments were performed at two, four, eight, and 12 weeks, and subsequently at six months and one year.

Results: A total of 34 patients were evenly distributed between autograft and allograft groups. Radiographic consolidation was observed in all cases, with the median time to healing being 4.0 weeks for both groups ($p = 0.358$). There were no statistically significant differences between group in VAS scores, ROM, or DASH scores at any follow-up visit. Both groups demonstrated improvement in DASH scores, with values approaching normal by one year. No postoperative complications, including donor site pain or infection, were recorded.

Conclusion: Allogeneic bone grafts yielded radiographic and functional outcomes comparable to those of autologous grafts for the treatment of solitary hand enchondromas. In light of the lack of donor site morbidity, allografts present a viable and effective alternative. Additional randomized controlled trials are needed to validate these results.

Keywords: hand, enchondroma, curettage, autograft, allograft

Cutaneous Squamous Cell Carcinoma under Long-Term Immunosuppression

Plast Reconstr Surg. Bucheon St. Mary's Hosp. The Catholic Univ. of Korea
Byeol Kim, Daiwon Jun, Jung Ho Lee

Purpose: Cutaneous squamous cell carcinoma (SCC) most frequently arises in the head and neck, but the hand is also a common site due to chronic ultraviolet exposure and repeated trauma. Because of the thin dermis, tumors in this region are prone to early invasion of tendons, muscles, and bone with risk of functional loss. This vulnerability is amplified in immunocompromised patients, in whom SCC occurs more often and behaves more aggressively. We report a case of dorsal hand SCC in a kidney transplant recipient.

Methods: A 67-year-old male presented with a fungating mass on the dorsum of the left hand persisting for one year despite multiple cryotherapy sessions at a local clinic. He had undergone kidney transplantation 15 years earlier and was maintained on long-term immunosuppression with azathioprine, cyclosporine, and deflazacort. Wide local excision was performed to achieve R0 resection, and the defect was reconstructed with a full-thickness skin graft.

Results:

Histopathology confirmed a moderately differentiated SCC, 2.0 cm in diameter and 7.0 mm in thickness, invading the reticular dermis. Margins were tumor-free. The wound healed uneventfully, hand function was preserved, and no recurrence was observed during three years of follow-up.

Conclusion: SCC of the hand in immunocompromised patients is a high-risk condition due to anatomical vulnerability and biologic aggressiveness. Compared with immunocompetent individuals, transplant recipients show higher incidence, deeper invasion, more frequent recurrence, and increased metastatic risk. Early recognition and timely surgical excision are crucial for minimizing resection extent and preserving function. In addition, many patients on chronic immunosuppression are unaware of their elevated risk, emphasizing the importance of education and regular dermatologic surveillance.

Figure 1. Preoperative view of a fungating squamous cell carcinoma on the dorsum of the left hand.

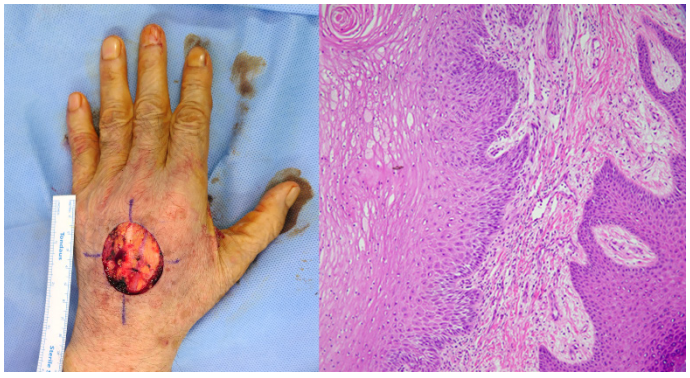

Figure 2. Intraoperative views showing the defect after wide local excision (left) and histopathology of the excised lesion showing moderately differentiated squamous cell carcinoma with invasion into the reticular dermis (H&E, ×20, right).

Figure 3. postoperative appearance after 3 years follow-up with no sign of recurrance.

Correlation and Optimal Cutoff Value of the Japanese Society for Surgery of the Hand Score for Satisfactory Postoperative Outcomes in Radial Polydactyly: A Retrospective Cohort Study

Orthop Surg. Ulsan Univ.
Wonsun Lee

Purpose: To assess the correlation between the Japanese Society for Surgery of the Hand (JSSH) score and parental satisfaction in patients with radial polydactyly and to identify the optimal JSSH score that correlates with parental satisfaction.

Methods: A retrospective study was conducted on 144 patients (144 thumbs) who underwent surgery for radial polydactyly between October 2017 and September 2023. Patients were classified according to the modified Wassel-Flatt classification, excluding hypoplastic types. Postoperative outcomes were evaluated using the JSSH scoring system, totaling 20 points distributed across functional, appearance, and subjective parameters. Parental satisfaction regarding function and appearance was assessed each using a 5-point Likert scale. Spearman's rank correlation assessed the relationship between the JSSH score and parental satisfaction, and receiver operating characteristic (ROC) curve analysis was used to determine the optimal cutoff value of the JSSH score corresponding to parental satisfaction.

Results: The JSSH score demonstrated a significant correlation with overall parental satisfaction. The optimal cutoff value for predicting parental satisfaction was determined to be 18.5, with an area under the ROC curve (AUC) of 0.82. The effect size between satisfied and unsatisfied parents was 1.26. Parents reported significantly lower satisfaction with appearance outcomes compared with functional outcomes. Notably, the appearance parameter of the JSSH score showed a weak correlation with appearance satisfaction, along with limited discriminative ability and a small effect size.

Conclusions: We noted a significant correlation between JSSH score and parental satisfaction in patients with radial polydactyly and established an optimal cutoff value of 18.5 points.

Clinical relevance: Future development of a scoring system that better integrates both functional and aesthetic consideration (social function) could enhance the evaluation and management of patients with polydactyly.

Introduction

Radial polydactyly is among the most common congenital hand anomalies [1], and various methods have been introduced to measure postoperative outcomes [2,3]. The Tada score, one of the earliest and most widely adopted instruments, relies exclusively on clinician-measured variables—range of motion, joint instability, and malalignment [1,4,5]. Building on this clinician-centered approach, Ogino and Larsen each proposed modified assessment schemes [4,6]. To address appearance-related concerns, Cheng introduced a composite evaluation system that incorporated both clinician-measured functional parameters and a aesthetic (social function) parameters [7]. More recently, scoring systems such as the Japanese Society for Surgery of the Hand (JSSH) scoring system have incorporated patient-reported parameters, including pain and satisfaction [8,9]. Among these, the Tada and the JSSH scores have been most widely used.

Comparative analyses are essential for identifying the most appropriate scoring system. Dijkman et al. reported that the JSSH scoring system exhibits superior interobserver reliability and the best correlation with functional and aesthetic visual analog scale scores [10]. Many studies have therefore adopted the JSSH scoring system to evaluate postoperative outcomes [11-14].

In the JSSH scoring system, outcomes are categorized into four grades based on total points achieved: 0–13 points are considered as poor outcome, 14–16 as fair, 17–19 as good, and 20 as excellent. Chen et al. reported an average JSSH score of 18.3 across all types of radial polydactyly [11], while Shen et al. observed a median JSSH score of 18 in patients with Wassel type IV-D, known for its poor outcomes [14].

Because of the highly skewed distribution of JSSH scores, applying the original grading system yielded outcomes predominantly classified as "good" or "excellent," with very few cases in lower categories. Consequently, our study aimed to determine the optimal cutoff value of the JSSH score that corresponds to parental satisfaction. We also aimed to investigate the correlation between parental satisfaction and the JSSH score to better understand its clinical relevance.

Materials and Method

Participant selection

This single-center retrospective cohort study was approved by our institutional review board. We reviewed the medical records of patients who underwent surgery performed by a single surgeon at our hospital between October 2017 and September 2023. Patients were classified according to the modified Wassel-Flatt classification [15]. Hypoplastic type, characterized by an extra digit composed of a small, underdeveloped bone with no bony or articular connection to the main digit, were excluded due to their generally favorable prognosis [16,17]. For bilateral cases, only the right thumb was retained to ensure independence of observations. Initially,

168 thumbs from 159 patients were considered for inclusion. After excluding patients with incomplete medical records, those with less than one year of follow-up and those with bilateral cases, 144 thumbs from 144 patients were included in the final analysis.

Assessment

Demographic data–including sex, race, and ethnicity, and clinical data such as age at surgery, follow-up period after surgery, and operation side were obtained from electronic medical records. Postoperative outcomes were assessed by one author (**Blinded by JHS**), who evaluated all patients annually starting from one year after surgery using the JSSH scoring system and assessing parental satisfaction.[8] The JSSH scoring system comprises functional, aesthetic, and subjective parameters. The functional parameter comprises seven items, each scored up to 2 points (maximum 14); the aesthetic parameter comprises four items, each scored up to 1 point (maximum 4); and the subjective parameter comprises two items, each scored up to 1 point (maximum 2) (Supplementary Table 1). The total score ranges from 0 to 20 points, categorized as either poor (0–13 points), fair (14–16 points), good (17–19 points), or excellent (20 points). Additionally, parental satisfaction was evaluated by two single item anchor questions: parental satisfaction score regarding function (PSF) and parental satisfaction score regarding appearance (PSA). Both were rated on a 5 point-Likert scale from 1 (very unsatisfied) to 5 (very satisfied). The total parental satisfaction score (TCS) was then calculated by summing the PSF and PSA. All outcomes were assessed based on the most recent data available.

Statistical analysis

The normality of the JSSH score, as well as the functional and aesthetic parameters of the JSSH score, PSF, and PSA, was assessed using the Shapiro-Wilk test. As the data were found to be non-normally distributed, Spearman's rank correlation test was employed to evaluate the strength of the relationships between the JSSH score and TCS, between the functional parameter of the JSSH score and PSF, and between the aesthetic parameter of the JSSH score and PSA. Correlation coefficients (ρ) were interpreted as either weak (0.2–0.39), moderate (0.4–0.59), or strong (0.6–0.79) [18,19].

Receiver-operating-characteristic (ROC) analysis was conducted with parental satisfaction (reference standard) dichotomised as satisfied (scores 4 or 5 on both PSF and PSA) versus unsatisfied (all other combinations). The index test was the postoperative JSSH score considered across its full range. For every possible JSSH cut-off, we plotted sensitivity (true-positive rate for satisfied parents) on the Y-axis against 1 – specificity (false-positive rate) on the X-axis. Sensitivity was the proportion of satisfied cases correctly identified, whereas specificity was the proportion of unsatisfied cases correctly identified.

The optimal cutoff value was determined using Youden's index, which identifies the point closest to the top left-hand corner of the ROC curve, where sensitivity and specificity are balanced. The area under the ROC curve (AUC) was calculated to evaluate the model's discriminative ability. An AUC of 0.5 indicates a model performing at the

level of random chance, while an AUC closer to 1.0 indicates superior discriminatory performance. An AUC of 0.8 or higher is generally considered acceptable [20].

Hedges's g was calculated to assess the effect size of the difference in JSSH scores between satisfied and unsatisfied cases. Effect sizes were interpreted as either small (0.2–0.49), medium (0.5–0.79), or large (≥ 0.8) [21].

We also performed the same analyses separately for the functional and appearance parameter of the JSSH score to determine their optimal cutoff values for discriminating between satisfied and unsatisfied cases based on PSF and PSA, respectively. For parameter-specific analyses, parental satisfaction was defined as a PSF score of 4 or 5 for the functional parameter, and as a PSA score of 4 or 5 for the appearance parameter. The same ROC–curve analysis and Hedges's g effect–size calculation were performed separately for the functional and appearance parameters. To compare parental functional and appearance satisfaction scores, we performed a paired (dependentsamples) ttest between PSF and PSA. An a priori power analysis (G*Power 3.1) showed that the available paired sample (n = 144) provides > 99 % power to detect a medium withinpair effect size (Cohen's d = 0.50) at α = 0.05. Group differences in JSSH scores between the satisfied (n = 120) and unsatisfied (n = 24) groups were examined with Welch's ttest; this contrast had 86 % power to detect d = 0.60.

Results

Outcome measures

A total of 144 thumbs from 144 patients were included in the final analysis. The median age at surgery was 10 months (range: 8–48 months), and the median follow-up duration was 24 months (range: 12–72 months). Altogether, 82 were male, and 62 were female. All cases included in this study were of Asian ethnicity.

The distribution of cases according to the modified Wassel-Flatt classification is shown in Table 1. Type IV was the most prevalent, with 87 cases (60%). JSSH scores ranged from 11 to 20, with the highest frequency (58 cases) observed at 20 points. A higher number of cases corresponded to higher JSSH scores (Figure 1). The overall mean JSSH score was 18.6 (95% confidence interval [CI] 18.3–18.9).

The distribution of cases based on parental satisfaction is summarized in Table 2. Parents reported significantly lower PSA (mean: 4.3 [95% CI: 4.1–4.5]) than PSF (mean: 4.6 [95% CI: 4.5–4.7]) (P<0.05). In total, 120 cases (83.3%) were classed as satisfied, while 24 cases (16.7%) were classed as unsatisfied. The demographic data of satisfied and unsatisfied groups, based on parental satisfaction with both function and appearance, are presented in Table 3.

However, a significant correlation was found between the JSSH score and TCS (ρ = 0.60, P < 0.05). The mean

JSSH scores for satisfied and unsatisfied cases are shown in Table 3, with a significant difference observed between the two groups.

The ROC curve for the JSSH score is shown in Figure 2 with the optimal cutoff value determined to be 18.5. The AUC for the JSSH score was 0.82 (95% CI, 0.73–0.90), and the effect size was 1.26.

The demographic data based on the PSF and PSA are presented in Supplementary Tables 2 and 3, respectively.

A significant correlation was observed between the functional parameter of the JSSH score and PSF (ρ = 0.48, P < 0.05). The ROC curve for the functional parameter (Figure 2) identified an optimal cutoff value of 11.5. The AUC for the functional parameter was 0.70 (95% CI, 0.52–0.87), and the effect size was 0.88.

The appearance parameter of the JSSH score showed a significant but weak correlation with PSA (ρ = 0.35, P < 0.05). The ROC curve for the appearance parameter (Figure 2) identified an optimal cutoff value of 3.5. The AUC for the appearance parameter was 0.64 (95% CI, 0.54–0.75) with an effect size of 0.74.

Discussion

Incorporating patients' (or their surrogate's) perspectives when interpreting treatment outcomes is crucial for improving the quality of care [22-25]. Consequently, efforts have been made to integrate patient outcomes into scoring systems. One commonly used method for incorporating subjective patient outcomes is the minimally clinically important difference (MCID), which assess the minimum improvement that a patient considers worthwhile by comparing preoperative and postoperative scores [26]. However, the JSSH score was designed specifically to evaluate postoperative outcomes of radial polydactyly. Several components—such as alignment of the reconstructed thumb, active range of motion, postoperative appearance, and satisfaction for surgery—cannot be scored meaningfully before surgery because the extra digit distorts these domains. For that reason, pretreatment JSSH scores are not obtainable, and our analysis therefore relies on postoperative scores and their cutoff values.

In this study, we identified a correlation between the JSSH score and parental satisfaction and determined an optimal cutoff value. The JSSH score demonstrated a significant correlation with the TCS, with a correlation coefficient (ρ) of 0.60. Dijkman et al. utilized a visual analog scale (VAS) for function and appearance to compare assessment systems and found correlations between patient-rated satisfaction and the JSSH scoring system, with ρ ranging from 0.45 to 0.63 [10]. Our findings align with their results as we also confirmed a significant correlation between the functional parameter of the JSSH score and the PSF (ρ = 0.48). A significant difference of 2.1 points in the JSSH score was observed between the satisfied and unsatisfied groups. As previously mentioned, the JSSH score is a postoperative scoring system specific to polydactyly

and cannot be assessed preoperatively; thus, an MCID for this scale has not been established. Therefore, interpreting this difference in terms of clinical relevance remains limited. However, considering the large effect size of 1.26 between the satisfied and unsatisfied groups, it is likely that this magnitude reflects a clinically meaningful difference in perceived outcome, although this cannot be concluded definitively without a formally established MCID. This finding may provide a useful reference point for establishing clinically meaningful thresholds and for informing power or samplesize calculations, given the observed large effect size.

The ROC analysis identified 18.5 points as the optimal JSSH cutoff (AUC = 0.82; Hedges's g = 1.26), confirming satisfactory discriminative performance. In contrast, the original grading thresholds—0–13 (poor), 14–16 (fair), 17–19 (good), and 20 (excellent)—were introduced without empirical validation. Applying these historical categories to our cohort produced a markedly rightskewed distribution: 58 patients (40.3 %) were rated "excellent," 69 (47.9 %) "good," while only 14 (9.7 %) and 3 (2.1 %) fell into the "fair" and "poor" groups, respectively. Comparable clustering has also been reported in the literature. For example, Chen et al. reported an average JSSH score of 18.3 across 47 cases of radial polydactyly [11], and Shen et al. reported a median score of 18 across 91 cases, even among Wassel type IV-D thumbs—traditionally associated with poorer outcomes [14]. Taken together, these data highlight the limitations of the current grading system and support the need for an evidencebased recalibration.

Parents reported significantly lower PSA scores compared to PSF. However, PSA showed a significant but weak correlation with the appearance parameter of the JSSH score, which also had the lowest AUC and effect size among all parameters evaluated. Although both functional and aesthetic outcomes influence parental satisfaction [27-29], aesthetic assessments are intrinsically subjective, prone to ceiling effects, and susceptible to wide individual variability [30]; several items further blur the boundary by affecting both domains [31,32]. Measurement theory warns that these limitations can erode the reliability and validity of composite scores and may even compromise the integrity of the score system [33,34]. In line with previous reports [27], our data therefore indicate that—despite the JSSH's overall good correlation and high interobserver reliability [10]—the aesthetic subscale should be refined to reduce ceiling effects, improve sensitivity, and strengthen clinical validity.

This study has several limitations. First, JSSH scores were only measured by a single evaluator. Although the scoring system has high interobserver reliability [10], employing multiple evaluators in future studies could further minimize potential scorer bias. Second, because the median followup was only about two years, the children were still too young to articulate their own perceptions of the outcome; therefore, the cutoff value was determined using parental rather than patient satisfaction. Thus, patients' own perspectives and satisfaction levels could differ significantly from those of their parents as they mature. Children begin to develop self-awareness around the age of 2 years [35]. By 4 to 5 years old, they not only become aware of themselves but also start to understand how they are perceived by others and how they present themselves socially [35]. Moreover, since the mean time to reoperation after surgery for preaxial polydactyly is 29.4 months [36], our team conducts routine follow-up only up to 2 years postoperatively, performing additional annual follow-ups only for patients

with special issues or complications. Consequently, the mean follow-up duration in this study was 27.1 months. Third, the number of unsatisfied patients was smaller compared than the satisfied group. However, when considering the AUC and effect size, there was a significant difference between the satisfied and unsatisfied groups. Fourth, aesthetic standards may vary according to region or culture. For example, Asians rated a six-finger hand more positively than a four-finger hand, whereas Europeans showed the opposite tendency [37]. Therefore, the cutoff value determined in this study reflects the aesthetic perspective of a single population, which may not be directly applicable to other regions or cultures. Fifth, the 5point Likert satisfaction scores were heavily clustered at the upper end, indicating a potential ceiling effect. Finally, this retrospective cohort study was conducted using a convenience sample of patients who underwent surgery at a single institution. As a result, the sample may not fully represent the entire population of patients with radial polydactyly.

In conclusion, our study demonstrates a significant correlation between the JSSH score and parental satisfaction, which we used to establish an optimal cutoff value of 18.5 points. Developing a scoring system that more comprehensively reflects both functional and aesthetic aspects could improve the evaluation and management of patients with polydactyly.

Reference

1. Chung MS, Baek GH, Gong HS, Lee HJ, Kim J, Rhee SH. Radial polydactyly: proposal for a new classification system based on the 159 duplicated thumbs. J Pediatr Orthop. 2013;33:190–196. doi:10.1097/BPO.0b013e3182648ca8
2. Goldfarb CA, Patterson JM, Maender A, Manske PR. Thumb size and appearance following reconstruction of radial polydactyly. J Hand Surg Am. 2008;33:1348–1353. doi:10.1016/j.jhsa.2008.03.011
3. Tada K, Yonenobu K, Tsuyuguchi Y, Kawai H, Egawa T. Duplication of the thumb. A retrospective review of two hundred and thirty-seven cases. JBJS. 1983;65:584–598.
4. Ogino T, Ishii S, Takahata S, Kato H. Long-term results of surgical treatment of thumb polydactyly. J Hand Surg Am. 1996;21:478–486. doi:10.1016/s0363-5023(96)80366-2
5. Breidung D, Megas IF, Dittrich Y, Reichert B, Nöth U, Habild G. Experience with Management of Radial Polydactyly: The Multicenter Analysis of 28 Surgical Procedures with Follow-Up. Healthcare (Basel). 2023;11. doi:10.3390/healthcare11233045
6. Larsen M, Nicolai JP. Long-term follow-up of surgical treatment for thumb duplication. J Hand Surg Br. 2005;30:276–281. doi:10.1016/j.jhsb.2004.12.011
7. Cheng JC, Chan KM, Ma GF, Leung PC. Polydactyly of the thumb: a surgical plan based on ninety-five cases. J Hand Surg Am. 1984;9:155–164. doi:10.1016/s0363-5023(84)80133-1
8. Committee JCH. Evaluation sheet for polydactyly of the thumb [in Japanese]. J Japan Soc Surg Hand. 2007;24.
9. Brouwer N, Biezen J. After thumb duplication: A proposal for evaluation of the result: The ALURRA system. European Journal of Plastic Surgery - EUR J PLAST SURG. 2006;29:1–4. doi:10.1007/s00238-005-0019-9

10. Dijkman RR, van Nieuwenhoven CA, Selles RW, Hovius SE. Comparison of functional outcome scores in radial polydactyly. J Bone Joint Surg Am. 2014;96:463–470. doi:10.2106/jbjs.M.00067
11. Chen PA, Sun WC, Chen BPR, et al. Prediction of Surgical Outcomes of Radial Polydactyly From the Wassel-Flatt Type and Symmetry of Duplication. J Pediatr Orthop. 2023;43:e305–e309. doi:10.1097/bpo.0000000000002349
12. Horii E, Koh S, Otsuka J, Hamada Y, Saito T. Midterm Surgical Outcomes of Duplicated Thumbs According to New Classification. Plast Reconstr Surg. 2023;152:116e–125e. doi:10.1097/prs.0000000000010267
13. Yeung CM, Choi AKY, Tong JWS, Fok W, Chan YF, Chow YY. Long-Term Results of Surgically Treated Radial Polydactyly - An Outcome Correlation Study. J Hand Surg Asian Pac Vol. 2019;24:264–269. doi:10.1142/s2424835519500322
14. Shen XF, Yin F, Wang J, et al. Reconstruction of Wassel IV-D radial polydactyly with a boot-shaped neurovascular island flap: A Consecutive series of 91 thumbs. J Plast Reconstr Aesthet Surg. 2020;73:1801–1805. doi:10.1016/j.bjps.2020.05.071
15. Kim JK, Al-Dhafer BAA, Shin YH, Joo HS. Polydactyly of the thumb: a modification of the Wassel-Flatt classification. J Hand Surg Eur Vol. 2021;46:346–351. doi:10.1177/1753193420981541
16. Lee W, Shin YH, Kim JK. Surgical outcomes of radial polydactyly according to a modified Wassel-Flatt classification: A retrospective study of 211 patients with 223 thumbs. J Hand Surg Eur Vol. 2025:17531934241310718. doi:10.1177/17531934241310718
17. Lee W, Shin YH, Kim JK. Surgical outcomes of radial polydactyly according to a modified Wassel-Flatt classification: A retrospective study of 211 patients with 223 thumbs. J Hand Surg Eur Vol. 2025;50:922–929. doi:10.1177/17531934241310718
18. Altman DG. Practical statistics for medical research: Chapman and Hall/CRC; 1990.
19. Dawson J, Doll H, Coffey J, Jenkinson C. Responsiveness and minimally important change for the Manchester-Oxford foot questionnaire (MOXFQ) compared with AOFAS and SF-36 assessments following surgery for hallux valgus. Osteoarthritis and Cartilage. 2007;15:918–931. doi:https://doi.org/10.1016/j.joca.2007.02.003
20. Nahm FS. Receiver operating characteristic curve: overview and practical use for clinicians. Korean J Anesthesiol. 2022;75:25–36. doi:10.4097/kja.21209
21. Lakens D. Calculating and reporting effect sizes to facilitate cumulative science: a practical primer for t-tests and ANOVAs. Frontiers in Psychology. 2013;4:863. doi:10.3389/fpsyg.2013.00863
22. Smith MV, Calfee RP, Baumgarten KM, Brophy RH, Wright RW. Upper extremity-specific measures of disability and outcomes in orthopaedic surgery. J Bone Joint Surg Am. 2012;94:277–285. doi:10.2106/jbjs.J.01744
23. Hoang-Kim A, Pegreffi F, Moroni A, Ladd A. Measuring wrist and hand function: common scales and checklists. Injury. 2011;42:253–258. doi:10.1016/j.injury.2010.11.050
24. Alderman AK, Chung KC. Measuring outcomes in hand surgery. Clin Plast Surg. 2008;35:239–250. doi:10.1016/j.cps.2007.10.001

25. Chung KC, Burns PB, Davis Sears E. Outcomes Research in Hand Surgery: Where Have We Been and Where Should We Go? The Journal of Hand Surgery. 2006;31:1373–1379. doi:https://doi.org/10.1016/j.jhsa.2006.06.012
26. Hwang ST, Ardebol J, Ghayyad K, et al. Quantifying Threshold Scores for Patient Satisfaction After Massive Rotator Cuff Repair for the Interpretation of Mid-Term Patient-Reported Outcomes. Arthroscopy: The Journal of Arthroscopic & Related Surgery. 2024;40:204–213. doi:https://doi.org/10.1016/j.arthro.2023.06.031
27. Dijkman R, Selles R, van Rosmalen J, et al. A clinically weighted approach to outcome assessment in radial polydactyly. J Hand Surg Eur Vol. 2016;41:265–274. doi:10.1177/1753193415601336
28. Yen C, Chan W, Leung H, Mak K. Thumb Polydactyly: Clinical Outcome after Reconstruction. Journal of Orthopaedic Surgery. 2006;14:295–302. doi:10.1177/230949900601400312
29. Dobyns J, Lipscomb P, Cooney W. Management of thumb duplication. Clinical Orthopaedics and Related Research (1976-2007). 1985;195:26–44.
30. Roca H, Maughan-Egbert G, Garcia BN, Kazmers NH. Evaluation of Test–Retest Reliability for the Patient-Reported Outcomes Measurement Information System Upper Extremity and Pain Interference Computer Adaptive Tests in a Hand Surgery Population. Journal of Hand Surgery. 2025;50:648–655. doi:10.1016/j.jhsa.2025.03.006
31. Goldfarb CA, Patterson JM, Maender A, Manske PR. Thumb size and appearance following reconstruction of radial polydactyly. The Journal of hand surgery. 2008;33:1348–1353.
32. Tonkin MA. Thumb duplication: concepts and techniques. Clinics in Orthopedic Surgery. 2012;4:1–17.
33. U.S. Food and Drug Administration. Guidance for industry: patient-reported outcome measures: use in medical product development to support labeling claims. Silver Spring, MD: FDA; 2009.
34. Mokkink LB, Prinsen CAC, Patrick DL, et al. COSMIN study design checklist for patient-reported outcome measurement instruments. Amsterdam, The Netherlands: COSMIN; 2019.
35. Rochat P. Five levels of self-awareness as they unfold early in life. Consciousness and Cognition. 2003;12:717–731. doi:https://doi.org/10.1016/S1053-8100(03)00081-3
36. Shin YH, Yoon JO, Kim SS, Joo HS, Al-Dhafer BAA, Kim JK. Reoperation after primary operation for pre-axial polydactyly of the hand: A 12-year experience at a single institute. J Plast Reconstr Aesthet Surg. 2022;75:2658–2663. doi:10.1016/j.bjps.2022.04.015
37. Nietosvaara NN, Sommarhem AJ, Puhakka JM, Tan RES, Schalamon J, Nietosvaara AY. Appearance of congenital hand anomalies. Scandinavian Journal of Surgery. 2021;110:434–440. doi:10.1177/1457496920903987

Legends

Figure 1. Distribution of cases based on the JSSH score.
Figure 2. ROC curve of overall JSSH score, functional parameter, and appearance parameter.

2025년 대한수부외과학회
추계학술대회

Room C

Free Paper 9 (Wrist)

Plast Reconstr Surg. Chonnam National Univ. **Jae Ha Hwang**
Orthop Surg. Konyang Univ. **Youn Moo Heo**

Comparative Case Series of Surgical Fixation Methods for Traumatic Radiocarpal Dislocation: A Focus on Bridge Plating

Orthop Surg. Yonsei Wonju Univ.
Sang Jun Lee, Jisu Park, Jin-Rok Oh

Background: Radiocarpal dislocation (RCD) is a rare, high-energy injury often associated with poor outcomes. External fixation and K-wire fixation remain standard, yet are limited by pin site infection, malalignment, and patient discomfort. Dorsal spanning (bridge) plating has recently been introduced as a stable alternative with fewer complications and is increasingly reported in systematic reviews and case series.

Methods: We retrospectively reviewed 6 male RCD patients (mean age 47 years) treated at a Level 1 Trauma Center between July 2020 and October 2023, all operated on by a single surgeon, with an average follow-up of 10 months. Patients were managed with bridge plating (n=2), external fixation followed by internal fixation (n=3), or K-wire with plate fixation (n=1). Outcomes included ROM, VAS, Mayo score, QuickDASH, radiographic alignment, and complications.

Results: All patients achieved stable reduction and union. Bridge plating yielded mean (VAS 1.5, QuickDASH 19.4, and Mayo 75), comparable to external fixation (VAS 1.67, QuickDASH 18.2, Mayo 80) and K-wire fixation (VAS 2, QuickDASH 15.9, Mayo 70). Despite the limited number of cases, our bridge plating results were comparable with previously reported outcomes. Regarding range of motion, most patients recovered 50–74% of the contralateral side, while two cases treated with bridge plating achieved 75–99% of normal ROM. No major complications occurred, and bridge plating avoided the pin-site issues can occur in external fixation.

Conclusion: Bridge plating provided functional outcomes at least equivalent to external fixation and K-wire fixation, with added benefits of stable internal fixation, greater comfort, and reduced infection risk. Considering that Mayo scores above 70 are generally classified as good, our results compare favorably with published series and align with recent reviews suggesting bridge plating as a safe, effective, and increasingly accepted strategy for RCD. Larger prospective studies are warranted to validate these findings.

Open resection versus arthroscopic resection for wrist ganglion cysts: a systematic review and meta-analysis

Orthop Surg. Yeungnam Univ.
Sam Guk Park

This study aimed to review the postoperative outcomes of surgical treatment options for wrist ganglion cysts and perform a meta-analysis comparing the 2 most common techniques: open resection and arthroscopic resection.We searched PubMed, Embase, Web of Science, and Cochrane Library databases for articles that compared the clinical outcomes of patients who underwent arthroscopic or open resection of the ganglion of the wrist. After screening, we identified two randomized controlled trials and four retrospective comparative studies. We assessed the methodological quality of randomized controlled trials and cohort studies using the Cochrane Handbook for Systematic Reviews and the Newcastle-Ottawa scale, respectively. Recurrence rates, other complications, functional scores, pain scores, operative time, and postoperative satisfaction were analyzed. A total of 151 abstracts were identified and screened; 22 full-text articles were reviewed and 6 studies met inclusion criteria for data extraction and qualitative synthesis. The two groups had no significant differences in the recurrence rate, postoperative pain, patient satisfaction, and clinical scores. The arthroscopic group had better results than the open group in terms of time to return to work. However, the arthroscopic group had a longer operation time than the open group. The results of this analysis indicate that arthroscopic resection for wrist ganglion cysts does not yield significantly enhanced outcomes in terms of recurrence rate, postoperative pain, patient satisfaction, and clinical scores. Despite the disadvantage of long operation time, the time until return to work following surgery is shorter than that of the open group.

Keyword: Ganglion cyst, wrist arthroscopy, meta-analysis.

Arthroscopic debridement for pisotriquetral joint arthropathy through standard radiocarpal portals of wrist arthroscopy

Orthop Surg. Jeonbuk National Univ.
Young Keun Lee, Ji Woong Ho

This study aimed to report outcomes of arthroscopic synovectomy, debridement, and thermal shrinkage performed through a standard radiocarpal wrist arthroscopic portal in patients with piso-triquetral (PT) arthrosis. Medical records of 12 patients with PT joint arthrosis who were treated with diagnostic wrist arthroscopy and arthroscopic debridement between December 2019 and September 2022 were retrospectively reviewed. Functional outcome was evaluated by comparing Quick disabilities of the arm, shoulder, and hand (DASH) and visual analog scale (VAS) scores for pain (0 = no pain, 10 = worst pain) measured preoperatively and at the final follow-up visit. Average follow-up period was 25 months (range, 12 - 41 months). At the final follow-up, average VAS score (5.3→0.3) and average Quick DASH score (36.7→8.5) improved significantly. Arthroscopic debridement and thermal shrinkage using standard wrist arthroscopic portals are reliable treatment methods for patients with PT arthrosis who are unresponsive to conservative treatment before considering pisiformectomy.

Keywords: Pisotriquetral joint; Arthrosis; Surgical treatment; Wrist arthroscopy

Acknowledgements
The author declared no potential conflicts of interest with respect to the research, authorship, and/or publication of this article.

Simultaneous Flexor Tendon Reconstruction and Hamate Hook Excision Under Wide-Awake Local Anesthesia No Tourniquet (WALANT): A Four-Case Series

MS Reconstruction Hosp.
Jin Sik Park

Background: Attritional rupture of the flexor digitorum profundus (FDP) tendon of the little finger occurs most often in association with nonunion of the hamate hook, but it can also arise in the absence of overt bony pathology due to shear stress from the sharp angulation of the tendon over the hook [1,2]. Surgical strategies for this rare condition remain heterogeneous: some reports describe primary repair, others staged tendon reconstruction, and while several authors have advocated excision of the hamate hook, others have not specified its removal [3–6]. Functional outcomes after reconstruction are therefore uncertain, with only a few isolated case reports documenting restoration of full active flexion [4,7]. Although no clear gold standard exists, excision of the hamate hook is generally considered helpful to prevent recurrence [1,3]. In this context, Wide-Awake Local Anesthesia No Tourniquet (WALANT) may provide distinct advantages by permitting intraoperative adjustment of tendon tension and confirmation of gliding, but to date, combined tendon reconstruction and hamate hook excision under WALANT has not been reported.

Methods: Four patients (three hamate hook excisions and one hamate hook excision with concomitant distal radioulnar joint osteophyte removal) underwent surgery under WALANT between 2023 and May 2025. The anesthetic solution consisted of 1% lidocaine, 0.75% ropivacaine, and normal saline in a 9:6:5 ratio, with 1% epinephrine diluted to yield a final concentration of 1:200,000. Two patients underwent interposition grafting using the palmaris longus tendon, while the other two underwent flexor digitorum superficialis transfer of the ring finger to reconstruct the flexor digitorum profundus of the little finger. Intraoperative assessments included the number and severity of pain episodes during injection, intraoperative pain perception, and postoperative range of motion.

Results: All four patients tolerated the procedures without conversion to sedation or general anesthesia. Intraoperative VAS pain scores averaged 1.2, consistent with previous WALANT series. Functional testing during surgery allowed accurate adjustment of tendon tension. Hemostasis was satisfactory despite the absence of a tourniquet. No complications, including infection, rerupture, or hematoma, were observed. At a mean follow-up

of six months, all patients demonstrated improved active flexion of the little finger; however, none of the cases achieved full range of motion as observed intraoperatively.

Conclusions: This case series demonstrates that WALANT is a safe and effective technique for combined bone excision and tendon reconstruction, permitting dynamic intraoperative assessment even in procedures traditionally performed under general anesthesia. Given the scarcity of prior literature, these findings broaden the potential indications of WALANT and support its application in more complex hand reconstructions. Larger studies are warranted to confirm safety and long-term functional outcomes.

References

1. Yamazaki H, Kato H, Usui M, Murakami S, Minami A. Closed rupture of the flexor digitorum profundus tendon of the little finger due to nonunion of the hook of the hamate. J Hand Surg Br. 2006;31(3):337–341.
2. Lee MYT, et al. Attritional rupture of the little finger flexor digitorum profundus tendon in a patient with acromegaly. J Hand Surg Eur. 2016;41(7):787–789.
3. Hosokawa T, et al. Spontaneous flexor tendon rupture due to an insufficiency fracture of the hamate hook in a patient with systemic lupus erythematosus. J Orthop Sci. 2016;21(6):864–868.
4. Jeong SH, et al. Two-staged tendon reconstruction for flexor tendon rupture secondary to fracture of the hamate hook. Ann Plast Surg. 2012;69(2):157–160.
5. Pajares-López M, et al. Rupture of the flexor digitorum profundus tendon due to nonunion of the hamate hook: a case report. Orthopedics. 2011;34(2):142.
6. Lee GJ, et al. Spontaneous zone III rupture of flexor tendons of the ulnar three digits in elderly Korean farmers. J Hand Surg Eur. 2015;40(3):281–286.
7. Shirley R, Mousa M. Unusual twisting of a reconstructed FDP tendon of the little finger after spontaneous attrition rupture on the hamate bone: a case report. J Surg Case Rep. 2022;2022(10):rjac539.

Post-Traumatic Chylous Wrist Effusion: A Case Report

Orthop Surg. Eulji Univ.
Je-Chan Lee, Sang Ki Lee

Chylous joint effusion is a rare condition characterized by the presence of a milky, viscous synovial fluid with abnormal lipid concentrations. The thorax is the most common site of involvement. Only a handful of cases have been reported in the field of orthopedic surgery, and even fewer have been reported involving uncommon location such as the knee. Treatment of chylous joint effusion may require surgical intervention, along with the use of somatostatin or octreotide and a low-fat diet. We present herein a case of post-traumatic chylous effusion in the wrist treated with surgical incision and drainage, octreotide, and a low-fat diet. There have been few reports of chylous effusion in the knee; however, to our knowledge, this is the first report of post-traumatic chylous effusion in the wrist.

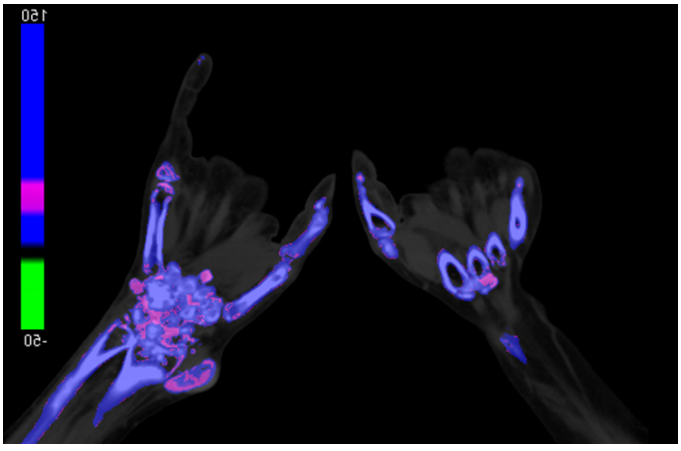

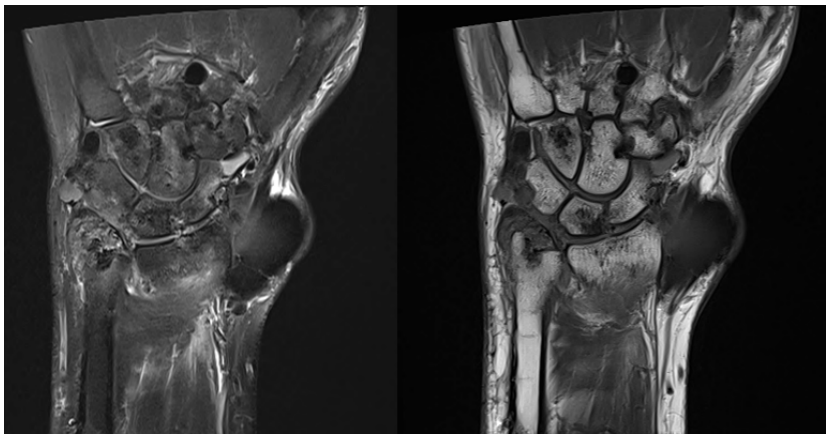

Key words: Chylous effusion, Post-traumatic, Wrist

Volar Wrist Ganglion associated with Radial artery Atherosclerosis: A case report

Orthop Surg. Jeonbuk National Univ.
Jinyoung Kim, Young-Keun Lee, Jong Hong Kim

Introduction: There have been no reports of volar wrist ganglions being associated with atherosclerosis of the radial artery. Good results were obtained with radial artery reconstruction through ganglion excision and autogenous vein grafting. Hence, we report a previously unreported case, along with a review of the literature.

Patients concerns and clinical findings: A 58-year-old female presented with the chief complaint of a mass on the volo-radial side of her right wrist. The patient complained of a tingling sensation in the thumb, index, and extensor zones that worsened when pressing the mass.

Diagnoses, Interventions, Outcomes: Sonography revealed a well-defined, anechoic cystic lesion adjacent to the radial artery. Exploration was performed using a zig-zag incision on the mass. The superficial radial nerve (SRN), which innervates the thumb, is distorted by the mass and the nerve is dissected from the mass. However, the artery and ganglion cysts were not separated completely in a part where hardening of the artery wall progressed as a result of degenerative changes, showing multiple small, hard, and yellowish masses. We resected the radial artery (approximately 1.5 cm) along with the ganglion and sent it for histological examination. The radial artery was then reconstructed using an autogenous venous graft. At the 34-months follow-up, the patient was asymptomatic. Radial artery patency was normal without recurrence of the ganglion cyst.

Conclusions: In patients with risk factors for radial artery atherosclerosis, a more careful diagnosis is required for the surgical treatment of the volar wrist ganglion. In addition, if the ganglion and radial artery are not completely dissected, excision of the radial artery and subsequent reconstruction of the radial artery using an autogenous vein may be a good surgical strategy.

The authors received no funding for this study.
The datasets generated and/or analyzed during the current study are available from the corresponding author upon reasonable request.

Key Words: Ganglion; Wrist; Radial artery; Atherosclerosis
Abbreviations: superficial radial nerve = SRN,

A Novel Scapholunate Step-Off Sign for Scapholunate Predynamic Instability: An Arthroscopic and Imaging Analysis : preliminary report

Orthop Surg. Korea Univ.
Ji Hoon Park, Chi-Hoon Oh, Jong Woo Kang

Introduction: Scapholunate (SL) instability is one of the most frequent and challenging causes of chronic wrist pain and functional limitation, especially in young and active individuals. It represents a spectrum of injuries, progressing from partial ligament tears to complete dissociation and, if left untreated, leading to scapholunate advanced collapse (SLAC). According to Mayfield's mechanism of carpal instability, SL injury often begins with volar SL ligament disruption, followed by progressive involvement of membranous and dorsal components, and eventually injury to extrinsic ligaments such as the radioscaphocapitate and radiotriquetral ligaments. This progression alters carpal kinematics, ultimately resulting in degenerative arthritis.

The European Wrist Arthroscopy Society (EWAS) classification is the most widely adopted arthroscopic system for SL ligament injuries, while the Dorsal Capsular Scapholunate Septum (DCSS) classification has been introduced for dorsal capsular lesions. However, both systems have limitations, particularly in detecting subtle predynamic instability where radiographs remain normal. During arthroscopic evaluation in our institution, we consistently observed a morphological irregularity at the SL interval, characterized by a vertical mismatch of the scaphoid and lunate articular surfaces, which we have termed the 'step-off sign.' This feature has not been Described in existing classifications.

The purpose of this study was to (1) define and characterize the SL step-off sign, (2) evaluate its correlation with established arthroscopic and imaging findings, and (3) assess its potential utility as an early marker of SL predynamic instability.

Materials and Methods: This retrospective study included patients who underwent both MRI and diagnostic wrist arthroscopy at Korea University Ansan Hospital between January 2014 and January 2025. Inclusion criteria were: (1) arthroscopically confirmed SL ligament evaluation, (2) available midcarpal portal documentation, and (3) complete plane x-ray and MRI dataset. Exclusion criteria included isolated TFCC repairs without SL evaluation, arthroscopy without midcarpal view, and cases lacking MRI imaging.

The SL step-off sign was defined as a measurable vertical offset between the articular surfaces of the scaphoid and lunate, visualized from the midcarpal radial portal. The measurement was performed using a arthroscopic probe calibration.

Collected data included patient demographics, injury mechanism, hand dominance, side, EWAS and DCSS grades, and presence of arthroscopic findings: dorsal, volar, and membranous SL ligament injuries; dorsal intercarpal (DIC) lesions; capsule hypertrophy; radiocarpal synovitis; and occult ganglion. Radiographic parameters (SL angle, lunocapitate angle, SL gap, SL gap difference) were measured from standardized PA and lateral radiographs.

Statistical analyses: Logistic regression was used to evaluate associations between step-off (continuous, mm) and binary arthroscopic findings. Linear regression assessed relationships with continuous radiologic parameters. Multinomial logistic regression evaluated EWAS and DCSS grades. Significance was set at $p < 0.05$.

Results

Radiographic Findings

Linear regression analysis revealed no statistically significant correlations between step-off distance and radiographic parameters.

For the SL angle, the regression coefficient was –0.6438 (standard error [SE] 2.3287, p = 0.7839), with an R^2 value of 0.0023, indicating negligible explanatory power. For the LC angle, the coefficient was –1.9723 (SE 2.6241, p = 0.4576, R^2 = 0.0168). Similarly, the SL gap demonstrated a coefficient of –0.0763 (SE 0.1939, p = 0.6965, R^2 = 0.0047), and the SL gap difference showed a coefficient of –0.0293 (SE 0.1603, p = 0.8562, R^2 = 0.0010). None of these parameters reached statistical significance. (Table 1)

MRI Findings

Logistic regression analysis indicated no significant associations between step-off distance and MRI findings. The presence of an occult ganglion was associated with an odds ratio (OR) of 1.621 (95% confidence interval [CI]: 0.456–5.767, p = 0.4555). Radiocarpal synovitis had an OR of 1.313 (95% CI: 0.305–5.649, p = 0.7148). Capsule hypertrophy demonstrated an OR of 0.607 (95% CI: 0.111–3.326, p = 0.5650). All MRI-derived variables failed to reach statistical significance. (Table 2)

Arthroscopic Findings

Several arthroscopic parameters demonstrated statistically significant associations with step-off distance. The presence of a dorsal intercarpal (DIC) lesion was strongly associated with step-off, yielding an OR of 139.54 (95% CI: 3.513–>999.999, p = 0.0086). Volar SL ligament injury showed an OR of 22.183 (95% CI: 1.396–352.472,

p = 0.0281), while membranous SL ligament injury had an OR of 7.309 (95% CI: 1.281–41.695, p = 0.0252). In multinomial logistic regression for EWAS grading, step-off distance was significantly higher in stage 3 compared to stage 0 (OR = 87.388, 95% CI: 3.125–2443.99, p = 0.0085). The comparison between stage 2 and stage 0 showed a trend toward significance (OR = 52.651, p = 0.0630). Other arthroscopic findings, including dorsal SL ligament injury (OR = 4.887, p = 0.1299) and DCSS stage (stage 1 vs 0: OR = 4.584, p = 0.0649), did not meet the threshold for statistical significance. (Table 3)

Discussion: Our results demonstrate that the SL step-off sign captures a distinct pathological feature of early SL instability. The marked association with DIC lesions may indicate a link between dorsal capsular injury and altered proximal carpal row congruency. Given that SL angle, LC angle, and SL gap failed to correlate, this underscores the limitation of plain radiographs in detecting early instability, reinforcing the importance of arthroscopic assessment.
From a biomechanical perspective, volar and membranous SL ligament injuries may cause localized subsidence or malalignment between the scaphoid and lunate articular surfaces, producing the measurable step-off. This offset may alter load transmission, predisposing to progressive instability. Early identification of step-off could thus influence surgical decision-making, favoring early ligament repair over conservative management in certain cases.

Study limitations include its retrospective nature, single-center design, and relatively small cohort. Long-term outcomes were not evaluated, and the prognostic significance of step-off magnitude remains to be determined. Nevertheless, the strong associations found in this study justify further prospective, multicenter investigations with standardized measurement protocols.

Future research directions include: evaluating its predictive value for progression to dynamic/static instability, and integrating the finding into revised arthroscopic classification systems for SL instability.

Conclusion: The SL step-off sign is a novel arthroscopic finding strongly associated with DIC lesions, volar and membranous SL ligament injuries, and higher EWAS grades. These relationships suggest that step-off reflects early biomechanical alterations within the SL joint that are not detected by radiographic parameters or existing arthroscopic classifications. Its incorporation into arthroscopic evaluation may allow earlier diagnosis and intervention in patients at risk for progression to dynamic or static instability.

Table 1, Radiographic finding (°, mm)

	Coefficient	p-value
SL angle	-0.6438	0.7839
LC angle	-1.9723	0.4576
SL gap	-0.0763	0.6965
SL gap diff	-0.0293	0.8562

SL : scapho-lunate, LC : luno-capitate

Table 2, MRI finding

	OR	95% CI	p-value
Occult ganglion	1.621	0.456 – 5.767	0.4555
Radiocarpal synovitis	1.313	0.305 – 5.649	0.7148
Capsule hypertrophy	0.607	0.111 – 3.326	0.5650

Table 3, Arthroscopic finding

	OR	95% CI	p-value
DIC lesion	139.54	3.513 – >999.999	0.0086
SL lig. injury - Dorsal	4.887	0.627 – 38.078	0.1299
SL lig. injury - Volar	22.183	1.396 – 352.472	0.0281
SL lig. injury - Membranous	7.309	1.281 – 41.695	0.0252
EWAS stage 3 vs 0	87.388	3.125 – 2443.99	0.0085
DCSS stage	4.584	0.910 – 23.080	0.0649

DIC : Dorsal Inter-Carpal, SL : Scapho-Lunate, lig. : ligament, EWAS : European Wrist Arthroscopy Society, DCSS : Dorsal Capsulo-Scapholunate Septum

Epidemiological Trends and Features of Pediatric Hand and Elbow Fractures in Emergency Department Visits: A Nationwide Population-Based Study

Orthop Surg. Yeson Hosp.
Sang Beom Ma

Purpose: Epidemiological studies on pediatric upper extremity fractures have been conducted in various countries. However, in Korea, there has been a lack of recent epidemiological studies on pediatric upper extremity fractures. We aimed to investigate the recent epidemiological characteristics of pediatric hand and elbow fractures that visit the emergency departments (ED) in Korea.

Methods: Pediatric patients under 19 years of age who visited ED nationwide for hand or elbow fractures in 2022 were included in this study using data from the National Emergency Department Information System (NEDIS). Demographic and clinical variables—including sex, age, cause of injury, fracture site, season, day of the week, and time of day—were analyzed. Incidence patterns were examined across these variables.

Results: Male patients accounted for 70.9% of cases, with a boy-to-girl ratio of 2.4, which increased with age but was nearly equal in children under 5. Distinct patterns were observed for each variable. The highest incidence of fractures occurred among males aged 11–14 years and females aged 5–10 years. Incidence peaked in early summer and autumn, with emergency visits most frequent on weekends and between 4:00 and 8:00 PM. Distal humerus and proximal forearm fractures were mostly caused by falls, forearm shaft fractures were commonly associated with bicycle accidents, and distal forearm fractures were most frequently related to slipping. Phalangeal fractures predominantly resulted from being struck by others.

Conclusion: Pediatric hand and elbow fractures exhibit distinct patterns, influenced by various factors. The differences seem to come from both biological and behavioral causes associated with age and gender. These findings may aid in developing targeted prevention strategies for pediatrics.

Keywords: Epidemiology, pediatrics, upper extremity, emergency service, fracture

	Distal humerus	Proximal forearm	Forearm shaft	Distal forearm	Carpal bone	Metacarpal	Phalanx
Sex							
Male	2,310 (17.0)	1,417 (10.2)	1,295 (9.3)	4,232 (30.4)	153 (1.1)	1,138 (8.2)	3,299 (23.7)
Female	1,424 (25.0)	707 (12.4)	398 (7.0)	1,366 (24.0)	17 (0.3)	142 (2.6)	1,644 (28.8)
Age							
0~4	1,224 (42.7)	444 (15.5)	233 (8.1)	319 (11.1)	0 (0.0)	32 (1.1)	612 (21.4)
5~9	2,015 (30.6)	928 (14.1)	615 (9.4)	1,725 (26.2)	5 (0.1)	113 (1.7)	1,176 (17.9)
10~14	473 (6.5)	506 (6.9)	721 (9.9)	2,772 (38.1)	58 (0.8)	552 (7.6)	2,201 (30.2)
15~18	82 (2.8)	246 (8.5)	124 (4.3)	782 (27.1)	107 (3.7)	587 (20.4)	954 (33.1)
Admitted month							
January	201 (20.3)	86 (8.7)	75 (7.6)	281 (28.3)	13 (1.3)	68 (6.9)	268 (27.0)
February	179 (23.5)	81 (10.6)	46 (6.0)	185 (24.2)	5 (0.7)	73 (9.6)	194 (25.4)
March	243 (22.6)	115 (10.7)	80 (7.5)	291 (27.1)	7 (0.7)	67 (6.2)	270 (25.2)
April	355 (19.0)	202 (10.8)	149 (8.0)	578 (31.0)	10 (0.5)	106 (5.7)	465 (24.9)
May	444 (16.9)	285 (10.9)	238 (9.1)	878 (33.5)	29 (1.1)	142 (5.4)	604 (23.1)
June	475 (19.4)	253 (10.3)	223 (9.1)	736 (30.1)	16 (0.7)	167 (6.8)	575 (23.5)
July	369 (20.3)	200 (11.0)	181 (10.0)	507 (27.9)	19 (1.0)	114 (6.3)	427 (23.5)
August	314 (22.4)	177 (12.6)	130 (9..3)	365 (26.1)	19 (1.4)	87 (6.2)	309 (22.1)
September	419 (21.2)	199 (10.1)	180 (9.1)	556 (28.1)	19 (1.0)	125 (6.3)	480 (24.3)
October	352 (18.2)	222 (11.5)	170 (8.8)	538 (27.8)	14 (0.7)	140 (7.2)	498 (25.7)
November	270 (16.6)	188 (11.6)	136 (8.4)	400 (24.7)	10 (0.6)	113 (7.0)	505 (31.1)
December	173 (15.8)	116 (10.6)	85 (7.8)	283 (25.8)	6 (0.8)	82 (7.5)	348 (31.8)
Cause of injury *							
Car accident	43 (10.2)	46 (10.9)	43 (10.2)	173 (40.9)	19 (4.5)	45 (10.6)	54 (12.8)
Bicycle accident	147 (14.3)	100 (9.7)	131 (12.8)	466 (45.4)	19 (1.9)	57 (5.6)	106 (10.3)
Fall down	1,277 (43.9)	515 (17.7)	299 (10.3)	731(25.1)	5 (0.2)	27 (0.9)	55 (1.9)
Slip down	1,031 (23.4)	578 (13.1)	521 (11.8)	1,657 (37.5)	28 (0.6)	260 (3.4)	450 (10.2)
Struck by others	370 (9.8)	198 (5.2)	157 (4.1)	559 (14.7)	33 (0.9)	436 (11.5)	2,038 (53.8)
Others	200 (16.9)	120 (10.2)	83 (7.0)	250 (21.2)	9 (0.8)	71 (6.0)	449 (38.0)
Result of treatment							
Discharge	2,682 (16.1)	1,816 (10.9)	1,350 (8.1)	4,920 (29.5)	154 (0.9)	1,166 (7.0)	4,594 (27.5)
Transfer	92 (39.3)	37 (10.7)	25 (10.7)	35 (15.0)	0 (0.0)	7 (3.0)	38 (16.2)
Admission	1,016 (38.1)	266 (10.0)	317 (11.9)	634 (23.8)	16 (0.6)	111 (4.2)	307 (11.5)
Expire	0 (0.0)	1 (33.3)	1 (33.3)	1 (33.3)	0 (0.0)	0 (0.0)	0 (0.0)
Disappear	4 (36.4)	4 (36.4)	0 (0.0)	2 (18.2)	0 (0.0)	0. (0.0)	1 (9.0)

Epidemiology of pediatric upper extremity fractures of emergency department visits according to fracture site

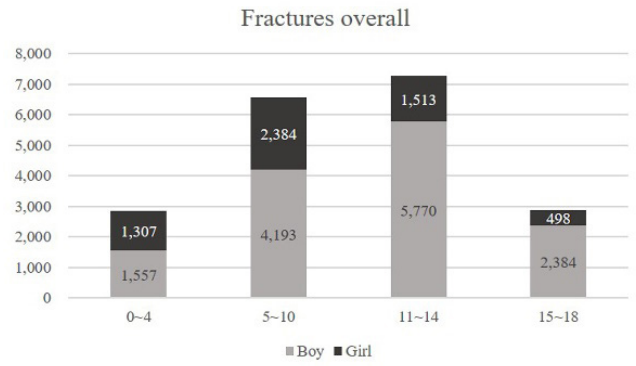

Figure 1. Pediatric upper extremity fractures emergency department visit according to age and sex, fractures overall

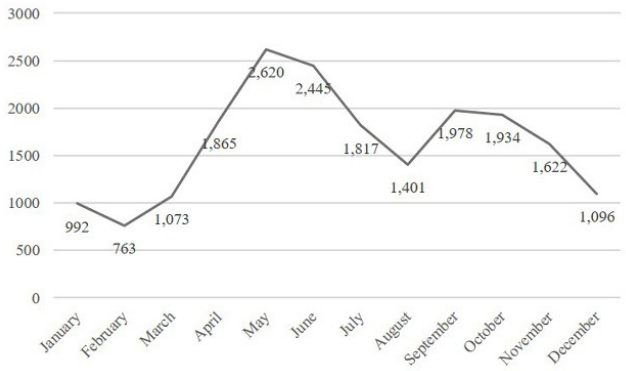

Figure 2. Pediatric upper extremity fractures emergency department visit according to month

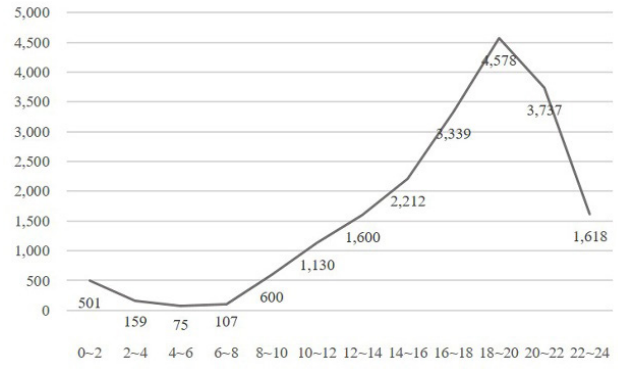

Figure 3. Pediatric upper extremity fractures emergency department visit according to day of the week

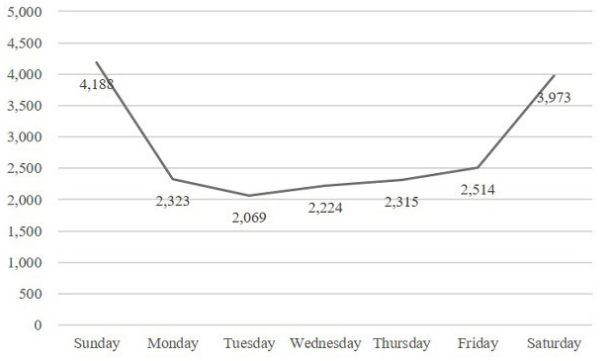

Figure 4. Pediatric upper extremity fractures emergency department visit according to the time

2025년 대한수부외과학회
추계학술대회

Room C

Symposium 3.

AI Strategies for Clinical Research and Presentation

Plast Reconstr Surg. Konkuk Univ. **Dong-Hyeok Shin**
Plast Reconstr Surg. Keimyung Univ. **Jae hun, Choi**

GPT 프롬프트 설계방법 (Is it a Finding or a Fantasy?: Prompting Strategies for Grounding LLMs in Medical Reality)

Departments of Media Software, Sungkyul Univ.
Ho-Woong Choi

LLM의 연구적용

Orthop Surg. Eulji Univ.
Seong Ju Choi

인공지능 중 대규모 언어 모델(LLM)의 등장은 의료 연구 분야에 새로운 가능성을 열고 있다. 연구의 과정을 시간에 따라 분류하면 1. 아이디어 구상, 2. 문헌고찰, 3. 연구 설계, 4. 연구 실행, 5. 데이터분석, 6. 논문 작성 순으로 나타낼 수 있다. 가장 널리 알려진 LLM 중 하나인 GPT-4는 다양한 분야 간 지식 통합, 창의적 표현, 멀티스텝 추론에서 인간과 유사한 수준의 능력을 보였으며, 이는 단순한 요약을 넘어 연구 설계와 결과 해석 등의 연구의 전 과정에서 co-worker로 활용될 수 있다.

이러한 LLM의 발전은 학술 연구 환경에 근본적 변화를 일으키고 있다. 최근 전 세계 연구자들을 대상으로 한 설문조사에 따르면, 과반수 이상이 향후 AI가 자신의 연구에 필수적인 역할을 하게 될 것이라 응답한 바 있다. 실제로 LLM은 문장 교정, 기존 문헌의 요약, 연구 초안의 작성 등에서 널리 활용되고 있으며, 비영어권 연구자들의 언어 장벽을 낮추는데도 유용한 도구이다.

연구의 핵심은 독창적인 관점과 창의성, 그리고 그를 뒷받침하는 데이터의 확립이라 할 수 있다. LLM은 연구의 다양한 과정에서 반복적이고 소모적인 작업을 대체함으로써, 연구자가 창의성과 사고가 요구되는 본질적인 작업에 집중할 수 있는 환경을 제공할 수 있다.

일부 학술지는 AI 의 활용을 제한하고 있으나, 많은 학술지에서 책임 있는 사용과 투명한 공개를 전제로 LLM의 활용을 용인하고 있으며, 최종 결과물에 대한 책임은 적적으로 인간 연구자에게 있다는 점을 강조하고 있다. 이는 AI를 단순 보조 도구가 아닌 연구 생산성과 효율성을 혁신할 수 있는 수단으로 보는 관점이다.

본 발표에서는 의료분야의 연구에 LLM이란 무엇인지, LLM이 어떤 방식으로 활용될 수 있는지 정리하고, 생산성을 높이기 위한 개인화 작업법, LLM의 한계점, 그리고 향후 방향성을 제시하고자 한다.

대형 언어모델(LLM)을 활용한 발표 준비 전략의 실제와 한계

Orthop Surg. Seoul National Univ.
Yohan Lee

1. 서론

학회 발표 준비는 주제 선정부터 문헌 검색, 자료 분석, 핵심 메시지 도출, 시각자료 제작, 발표 원고 작성, 반복 연습까지 이어지는 복합적 과정이다. 수부외과 영역에서는 원위요골 골절, 수지 재접합술, 피판 재건술, 가측상과염 등 다양한 술기와 임상 결과를 다루며, 수술 영상, 방사선 이미지, 통계 도표 등의 시각자료가 필수적으로 요구된다. 임상의들은 진료와 수술로 바쁜 일정 속에서도 이러한 발표를 완성해야 하는 부담을 안고 있다.

최근 급속히 발전한 대형 언어모델(Large Language Model, LLM)은 발표 준비 과정을 효과적으로 지원하는 도구로 주목받고 있다. LLM은 단순한 텍스트 생성을 넘어 발표의 전 과정을 체계적으로 보조할 수 있으며, 발표자는 이를 활용해 논리적 구조를 신속하게 구축하고 자료를 효율적으로 정리할 수 있다.

본 연구에서는 LLM을 활용한 발표 준비를 ① 문헌 검색 및 요약, ② 발표 구조 설계, ③ 세부 내용 작성, ④ 자료 검증 및 시각화, ⑤ 발표 원고 작성의 5단계로 체계화하여 제시한다. 또한 최신 LLM 모델들의 특성과 발표 지원 도구를 비교 분석하고, 환각(hallucination)과 망각(memory decay) 문제에 대한 대응 전략을 논의한다. 특히 Claude의 Model Context Protocol(MCP) 기능을 활용한 통합 작업 환경 구축 방안을 실제 사례와 함께 소개한다.

2. 본론

(1) 발표 준비의 5단계 전략

- 1단계. 문헌 검색 및 요약 (Literature Search & Synthesis)

LLM은 방대한 문헌 자료를 신속하게 분석하고 핵심 내용을 추출하는 능력을 보인다. 발표자가 "2022년 이후 발표된 원위요골 골절의 수술적 치료 결과를 요약하라"는 명령을 입력하면, 모델은 금속판 고정술의 종류별 임상 결과, 합병증 발생률, 기능적 예후 등을 체계적으로 정리한다. 마찬가지로 "수지 재접합술의 생착률과 위험 인자에 대한 최신 연구 동향"을 요청하면, 최근 문헌들의 생착률 통계, 실패 예측 인자, 재수술 빈도 등을 종합적으로 제시한다.

LLM은 효과적인 문헌 검색 전략 수립도 지원한다. 모델에게 PubMed 검색식 작성을 요청하면 다음과 같은 구조화된 쿼리를 생성한다:

("Distal Radius Fractures"[MeSH]) AND ("Bone Plates"[MeSH] OR "Fracture Fixation, Internal"[MeSH]) AND ("2022/01/01"[PDAT] : "2025/12/31"[PDAT])

이러한 체계적 검색식은 문헌 검색의 정확도와 효율성을 향상시킨다. 그러나 LLM이 제시하는 요약과 인용은 항상 원문과 대조 검증이 필요하다. 발표자는 제시된 논문의 실제 존재 여부와 인용 수치의 정확성을 PubMed, Google Scholar 등에서 직접 확인해야 한다. LLM은 효율적인 보조 도구이지만, 최종 검증 책임은 발표자에게 있다.

- 2단계. 발표 구조 설계 (Presentation Architecture)

LLM은 발표의 전체 구조를 체계적으로 설계하는 데 유용하다. "원위요골 골절의 수술적 치료에 대한 12분 발표의 슬라이드 구성을 제안하라"는 요청에 대해 모델은 다음과 같은 구조를 제시할 수 있다:

1. 서론: 원위요골 골절의 역학 및 중요성 (1분)
2. 분류체계 및 치료 결정 알고리즘 (2분)
3. 수술 기법별 비교 분석: 전방 접근법 vs 후방 접근법 (3분)
4. 임상 결과: 기능적 예후와 합병증 (3분)
5. 복잡 골절의 치료 전략 (2분)
6. 결론 및 임상 권고사항 (1분)

이러한 구조화된 접근은 제한된 발표 시간 내에서 핵심 내용을 효과적으로 전달하는 데 도움이 된다.

- 3단계. 세부 내용 작성 (Content Development)

발표 구조가 확정되면 LLM은 각 슬라이드의 세부 내용을 작성한다. "수술 기법별 비교표를 작성하라"는 요청에 대해 다음과 같은 체계적인 표를 생성할 수 있다:

수술 기법	적응증	장점	단점
전방 금속판 고정술	불안정 골절, 관절내 골절	해부학적 정복 용이, 조기 재활 가능	굴곡건 자극 가능성
후방 금속판 고정술	후방 전위 골절, 후방 피질 분쇄	직접적 골편 정복	신전건 합병증 위험

또한 모델은 청중의 수준과 발표 목적에 따라 내용의 깊이와 표현을 조절할 수 있다. 전문의 대상 발표와 전공의 교육용 발표에서 요구되는 설명 수준의 차이를 반영하여 내용을 구성한다.

- 4단계. 근거 기반 내용 보강 (Evidence-Based Enhancement)

Retrieval-Augmented Generation(RAG) 기법을 활용하면 LLM 생성 내용의 신뢰도를 크게 향상시킬 수 있다. 발표자가 특정 논문 파일을 업로드하고 "이 논문들을 참조하여 원위요골 골절의 수술 방법별 임상 결과를 정량적으로 비교하라"고 요청하면, 모델은 실제 논문의 표와 그림에서 추출한 데이터를 바탕으로 정확한 수치를 제시한다.

예를 들어, 업로드된 메타분석 논문에서 "전방 금속판 고정술의 평균 DASH 점수는 12.5±4.3점, 후방 접근법은

15.8±5.1점"과 같은 구체적 데이터를 추출하여 발표 자료에 반영한다. 이러한 RAG 접근법은 환각 현상을 최소화하고 근거 중심의 발표 내용을 구성하는 데 핵심적이다.

- 5단계. 시각화 및 검증 (Visualization & Validation)

LLM은 데이터 특성에 따른 최적의 시각화 방법을 제안한다: "골절을 동반한 연부조직 결손에서 복합피판 수술의 예후에 대하여 정리한 내용이 있다. 이에 대하여 적절한 그래프를 제안하라."라고 요청하면 모델은 다음과 같은 예시를 추천할 수 있따.

- 시간 경과에 따른 통증 변화: 선 그래프
- 수술 방법별 생착률 비교: 막대 그래프
- 합병증 발생 비율: 원 그래프 또는 적층 막대 그래프

검증 과정에서는 생성된 모든 내용에 대한 체계적인 사실 확인이 필수적이다. 발표자는 "제시된 통계 중 과장되거나 부정확한 부분이 있는지 검토하라"와 같은 메타인지적 질문을 통해 피드백 루프를 형성한다. 이 과정에서 발표자는 단순한 사용자가 아닌 비판적 검토자로서 기능해야 한다.

(2) 최신 LLM 모델 비교 분석

- 주요 모델 특성

2025년 현재 활용 가능한 주요 LLM 모델들의 특징은 다음과 같다:

모델	주요 특징	발표 준비 활용
Claude	다양한 작업 수행, 빠른 응답 속도, 플러그인 생태계	복잡한 발표 구조 설계, 대량 논문 분석, MCP 통합 작업
ChatGPT	고급 추론 능력, 긴 문맥 처리(200k 토큰), 멀티모달 지원	초안 작성, 번역, 문체 교정
Gemini	Google 서비스 연동, 100만 토큰 컨텍스트 윈도우	최신 문헌 검색, 대용량 문서 분석

- 발표 지원 도구 생태계

도구	핵심 기능	활용 시나리오
Gamma	AI 기반 자동 슬라이드 생성, 디자인 템플릿	텍스트를 즉시 프레젠테이션으로 변환
Microsoft Copilot	Office 통합, 문서-PPT 자동 변환	기존 문서 기반 발표 자료 생성
Beautiful.AI	디자인 규칙 기반 자동 레이아웃	시각적 일관성이 중요한 발표
Canva	템플릿 라이브러리, Magic Write 기능	포스터, 인포그래픽 제작

(3) Claude-MCP를 활용한 통합 워크플로우

Claude의 Model Context Protocol(MCP)은 발표 준비의 전 과정을 통합 관리할 수 있는 환경을 제공한다. MCP는 로컬 파일 시스템에 직접 접근하여 PowerPoint, Excel, Word 문서를 읽고 수정할 수 있으며, 다음과 같은 워크플로우를 지원한다:

1. 자동 자료 수집: 로컬 폴더에서 관련 논문과 이전 발표 자료를 자동으로 검색하고 분석
2. 데이터 통합: Excel의 임상 데이터를 직접 읽어 그래프와 표로 변환
3. 슬라이드 생성: 기존 템플릿을 활용하여 일관된 디자인의 슬라이드 자동 생성
4. 실시간 수정: 발표 연습 중 피드백을 즉시 반영하여 내용 수정

예를 들어, "작년 수부외과 학회에서 발표한 자료에서 원위요골 골절 결과 데이터를 찾아 이번 발표에 업데이트하여 삽입하라"는 명령을 수행할 수 있다. 이는 기존 LLM의 텍스트 생성 능력을 넘어 실제 작업 환경과 통합된 지능형 어시스턴트로 기능한다.

(4) LLM의 한계와 극복 전략

- 환각 현상 관리

LLM의 가장 큰 한계점인 환각 현상은 존재하지 않는 논문을 인용하거나 부정확한 통계를 생성하는 형태로 나타난다. 이를 효과적으로 관리하기 위한 핵심 전략은 RAG(Retrieval-Augmented Generation) 방식과 다중 모델 교차 검증이다.

RAG 접근법은 모델이 상상으로 내용을 생성하는 것을 방지하고 실제 문서에 기반한 답변을 유도한다. 발표자는 관련 논문 PDF 파일이나 데이터셋을 직접 업로드하고, "업로드한 문서만을 참조하여 답변하라"고 명시함으로써 환각 발생을 원천적으로 차단할 수 있다. 특히 수술 결과의 통계 수치나 합병증 발생률과 같은 정량적 데이터를 다룰 때는 RAG 방식이 필수적이다.

교차 검증 전략은 동일한 질문을 Claude, GPT-4, Gemini 등 여러 LLM에 제시하여 응답을 비교하는 방법이다. 모델들이 일치하는 내용은 신뢰도가 높은 반면, 불일치하는 부분은 추가 검증이 필요한 영역으로 판단할 수 있다. 예를 들어 "원위요골 골절의 전방 접근법 합병증"에 대해 세 모델이 모두 "굴곡건 자극"을 언급한다면 이는 확립된 사실로 볼 수 있지만, 발생률 수치가 서로 다르다면 원문 확인이 필요하다.

또한 발표자는 모델에게 "모르는 내용은 추측하지 말고 '확인이 필요하다'고 답하라"는 명확한 지침을 제공해야 한다. 이러한 다층적 접근을 통해 환각 현상을 효과적으로 관리하면서도 LLM의 장점을 최대한 활용할 수 있다.

- 망각 현상 극복 전략

LLM은 대화가 길어질수록 초기에 논의된 내용을 점진적으로 잊어버리는 망각 현상을 보인다. 이는 모델의 컨텍스트 윈도우 한계와 주의력 메커니즘의 특성 때문에 발생하며, 발표 준비처럼 연속성이 중요한 작업에서 심각한 문제가 될 수 있다.

망각을 극복하는 가장 효과적인 방법은 작업을 의도적으로 여러 세션으로 분할하는 것이다. 예를 들어, 서론 작성, 방법론 정리, 결과 분석, 결론 도출을 각각 독립된 대화 세션에서 진행하되, 각 세션 시작 시 이전 세션의 핵심 결과물을 명시적으로 제공한다. "이전에 작성한 서론은 다음과 같다: [서론 내용]. 이를 바탕으로 방법론 섹션을 작성하라"와 같은 방식으로

연속성을 유지한다.

핵심 정보의 반복적 재입력도 중요한 전략이다. 발표의 핵심 주제, 대상 청중, 시간 제한 등 기본 정보는 새로운 작업을 시작할 때마다 반복하여 입력한다. 이는 비효율적으로 보일 수 있지만, 일관성 있는 결과물을 얻는 데 필수적이다. 특히 "이 발표는 12분 분량의 원위요골 골절 수술 결과 발표이며, 대상은 수부외과 전문의다"와 같은 맥락 정보를 주기적으로 상기시켜야 한다.

외부 메모리 시스템을 활용하는 것도 효과적이다. Claude-MCP와 같은 도구를 사용하면 작업 과정을 로컬 문서로 저장하고 필요시 다시 불러올 수 있다. 발표 준비의 각 단계별 산출물을 파일로 저장하고, 다음 단계에서 이를 참조 문서로 제공하면 망각 없이 일관된 작업이 가능하다. 예를 들어, "outline.txt"에 발표 구조를 저장하고, "references.txt"에 핵심 문헌을 정리하여, 필요할 때마다 "outline.txt 파일을 참조하여 슬라이드 3의 내용을 작성하라"와 같이 활용한다.

프롬프트 체이닝 기법도 유용하다. 복잡한 작업을 작은 단위로 분해하고, 각 단계의 출력을 다음 단계의 입력으로 명시적으로 연결한다. "단계 1의 결과: [결과]. 이제 단계 2로 진행하여..."와 같은 방식으로 작업의 연속성을 보장한다. 이러한 체계적 접근은 망각으로 인한 일관성 손실을 최소화하면서도 복잡한 발표 준비 작업을 성공적으로 완수할 수 있게 한다.

- 문맥 유지 전략

긴 대화 과정에서 발생하는 문맥 손실 문제는 발표 준비의 일관성을 해치는 주요 요인이다. 이를 방지하기 위해 발표자는 주기적으로 "지금까지 논의된 핵심 사항을 요약하라"는 요청을 통해 모델의 작업 기억을 재정렬해야 한다. 또한 새로운 작업을 시작할 때 "앞서 논의한 원위요골 골절 분류 체계를 바탕으로"와 같이 명시적으로 이전 내용을 참조하도록 지시하는 것이 효과적이다.

복잡한 발표 구조를 다룰 때는 번호나 제목을 사용한 구조화된 프롬프트를 활용하여 명확한 계층 구조를 유지해야 하며, 중요한 결정 사항이나 합의 내용은 별도로 기록하여 체크포인트로 활용하는 것이 권장된다. 특히 Claude-MCP 환경에서는 작업 내용을 로컬 파일로 저장하고 필요시 다시 불러와 참조할 수 있어, 긴 작업 과정에서도 문맥의 일관성을 유지할 수 있다.

3. 결론

대형 언어모델과 Claude-MCP 같은 통합 도구는 의학 발표 준비 방식을 근본적으로 변화시키고 있다. 문헌 검색부터 슬라이드 제작, 발표 연습까지 전 과정을 효율적으로 지원하며, 특히 수부외과와 같이 복잡한 시각 자료와 데이터 분석이 요구되는 분야에서 그 효용성이 크다.

그러나 이러한 도구들은 어디까지나 보조적 역할을 수행하며, 의학적 판단과 학술적 엄밀성의 책임은 여전히 발표자에게 있다. AI 도구의 적절한 활용은 발표 준비의 효율성을 높일 뿐 아니라, 더 많은 시간을 핵심 메시지 전달과 청중과의 소통에 할애할 수 있게 한다.

향후 AI 기술의 지속적인 발전과 함께, 의학 교육과 학술 커뮤니케이션 방식의 패러다임 전환이 예상된다. 임상의들은 이러한 변화를 능동적으로 수용하되, 비판적 사고와 학술적 책임감을 유지하며 AI와 협업하는 새로운 역량을 개발해야 할 것이다.

성형외과 관점에서 바라보는 AI연구 (AI Research from the Perspective of Plastic and Reconstructive Surgery)

Plast Reconstr Surg. Kyungpook Univ.
Jeong Yeop Ryu

2025년 대한수부외과학회
추계학술대회

Room C

Symposium 5.

Mastering Scaphoid Nonunion Surgery: Expert Talks and Open Q&A

W General Hosp. **Young Woo Kim**
Orthop Surg. Yeson Hosp. **Jin Sung Park**

Panel
Orthop Surg. Seoul National Univ. **Min Bom Kim**
Orthop Surg. The Catholic Univ. of Korea **Soo Hwan Kang**

Conventional method to treat scaphoid nonunion (non-vascularized bone grafting with internal fixation)

Orthop Surg. DongGuk Univ.
Jin Young Kim

Scaphoid nonunion (1)

- Failure of union : 6 months' duration
- Treatment goal: a healed scaphoid with anatomic alignment

- Risk factors

1. Delay of treatment for more than 4 weeks
2. Proximal pole fractures
3. Fracture displacement greater than 1 mm
4. Osteonecrosis
5. Tobacco use
6. Associated carpal instability

Scaphoid nonunion (2)

- **Stable nonunion (Type D1)**
  - Firm fibrous nonunion
  - X-ray
    - indistinct fracture line
    - variable cystic change
  - Progress to unstable nonunion & osteoarthritic change

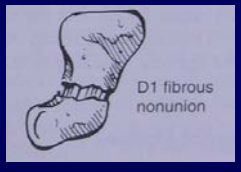

Scaphoid nonunion (3)

- **Unstable nonunion (Type D2)**
  - **Sclerotic bone surface**
  - **Bone fragment size discrepancy**
  - **Instability, collapse, deformity**

->secondary OA

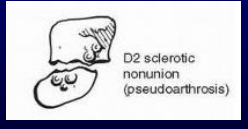

Management of scaphoid nonunion

Type of Fracture	Treatment
I. Delayed union	Mini-open rigid fixation with headless compression screw
II. Established waist nonunion, no deformity Fibrous nonunion, waist Sclerotic nonunion, waist	Open repair and autogenous bone grafting Dorsal or volar
Humpback nonunion	Volar approach Russe or Matti-Russe corticocancellous autograft Intercalated wedge autograft Hybrid Russe autograft
III. Proximal pole nonunion, viable	Dorsal approach Open bone grafting and fixation with headless screw Percutaneous bone grafting with headless screw Lock midcarpal joint with Kirschner wire(s) or miniscrew(s)
IV. Dysvascular nonunion, waist or proximal pole	Nonvascularized vs. vascularized bone graft: dorsal or palmar approach Osteoarticular graft

Conventional Tx?

- Open repair
- Autogenous bone grafting (iliac bone or distal radius)

Management of scaphoid nonunion

Type of Fracture	Treatment
I. Delayed union	Mini-open rigid fixation with headless compression screw
II. Established waist nonunion, no deformity Fibrous nonunion, waist Sclerotic nonunion, waist	Open repair and autogenous bone grafting Dorsal or volar
Humpback nonunion	Volar approach Russe or Matti-Russe corticocancellous autograft Intercalated wedge autograft Hybrid Russe autograft
III. Proximal pole nonunion, viable	Dorsal approach Open bone grafting and fixation with headless screw Percutaneous bone grafting with headless screw Lock midcarpal joint with Kirschner wire(s) or miniscrew(s)
IV. Dysvascular nonunion, waist or proximal pole	Nonvascularized vs. vascularized bone graft: dorsal or palmar approach Osteoarticular graft

"Bone grafting & internal fixation"

- Goal:

✓ Achieve bony union

✓ Correct carpal deformities

✓ Prevent progressive carpal instability and arthritis

OR + non-vascularized BG

- Bone graft (biologic environment)
  - Cancellous bone graft
  - Cortico-cancellous bone graf
- Internal fixation (mechanical stability)
  - K-wires
  - Headless screw
  - Number of implant

Volar vs dorsal approach

- Excellent visualization of whole volar scaphoid
- Less inj. to bld. Supply
- Easier reduction or bone grafting
- Potential LOM ,DF
- Volar carpal lig. Inj.
- STT arthrosis
- Improved fixation of prox. Pole fx.
- Better visualization of SL ligament
- Increased risk of blood supply disruption

Bone grafting (inlay vs interposition)

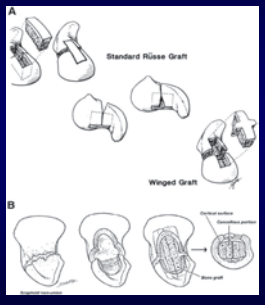

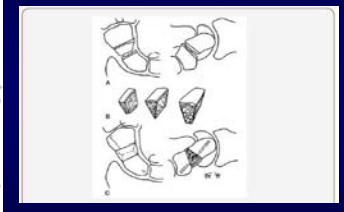

Correction of deformity

- Humpback def. : Volar approach
- Interposition > inlay
- Cortico-cancellous > cancellous only
- Headless screw > k-wire

Strut stability and Union rate

- Screw or k-wire ?
- number of implant ?
- Cortico-cancellous or cancellous bone only ?
- Which combination is the best?

Screw or k-wire?

- Increase the strength of fixation and stiffness when compared to K-wires
- Adequate strength
- Easy to use
- Smooth surface
- Configuration control
- Economic

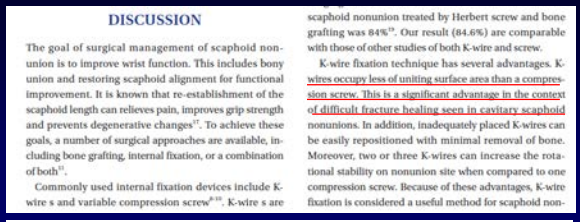

DISCUSSION

The goal of surgical management of scaphoid nonunion is to improve wrist function. This includes bony union and restoring scaphoid alignment for functional improvement. It is known that re-establishment of the scaphoid length can relieves pain, improves grip strength and prevents degenerative changes[17]. To achieve these goals, a number of surgical approaches are available, including bone grafting, internal fixation, or a combination of both[17].

Commonly used internal fixation devices include K-wire s and variable compression screw[8-10]. K-wire s are

scaphoid nonunion treated by Herbert screw and bone grafting was 84%[19]. Our result (84.6%) are comparable with those of other studies of both K-wire and screw.

K-wire fixation technique has several advantages. K-wires occupy less of uniting surface area than a compression screw. This is a significant advantage in the context of difficult fracture healing seen in cavitary scaphoid nonunions. In addition, inadequately placed K-wires can be easily repositioned with minimal removal of bone. Moreover, two or three K-wires can increase the rotational stability on nonunion site when compared to one compression screw. Because of these advantages, K-wire fixation is considered a useful method for scaphoid non-

We also believe the orientation of the K-wires is important, with the use of convergent K-wire placement being the most favorable. This allows the K-wires to pass through the most surface area of the scaphoid as well as allows for a more targeted placement into the proximal pole. It is recognized that parallel K-wires were less strong and less stable versus compression screws; however, the trade-off to using a screw is there is more scaphoid volume occupied by the screw which decreases the amount of bone graft that can be placed [32].

Number of implant

Two or three K-wires can increase the rotational stability on nonunion site when compared to one compression screw

DISCUSSION

- 2 headless screws: There is increased momentum for dual screw fixation constructs, intended to provide greater stability and reduce the risk of nonunion. *(2023, JHSE)*

Cortico-cancellous or cancellous bone only ?

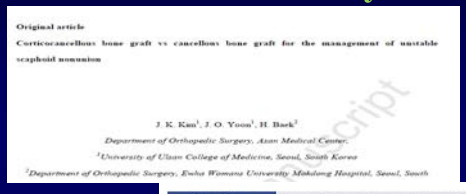

Original article

Corticocancellous bone graft vs cancellous bone graft for the management of unstable scaphoid nonunion

J. K. Kim[1], J. O. Yoon[1], H. Baek[2]

Department of Orthopaedic Surgery, Asan Medical Center, [1]University of Ulsan College of Medicine, Seoul, South Korea
[2]Department of Orthopaedic Surgery, Ewha Womans University Mokdong Hospital, Seoul, South

Original Article The Journal of Hand Surgery (Asian-Pacific Volume) 2021;26(4):697-704 • DOI: 10.1142/S2424835521500673

A Comparison of Non-vascularized Bone Grafting and Internal Fixation in the Treatment of Unstable Scaphoid Waist Nonunion

Jin Young Kim*, Sang Lim Lee†, Sung Yoon Park*, Kyung Hwi Kim*, Ji Hyun Yeo*

*Department of Orthopedic Surgery, Dongguk University Ilsan Hospital, Goyang, †Department of Orthopedic Surgery, Sanggye Baik Hospital, Seoul, Korea

Cancellous bone grafting (1)

The other type of bone graft used is cancellous bone grafting. It was originally used to treat stable scaphoid nonunion without deformity [14,15]. However, some surgeons prefer cancellous grafting even in cases of unstable scaphoid nonunion, because of the relative straightforward nature of the surgical preparation and its superior osteogenic potency [16,17]. In fact, it has been proposed that pressive force between the fragments. Most of surgeons don't think that cancellous bone grafting can maintain a correction of deformity and prevent re-collapse when treating the scaphoid nonunion with deformity. In fact, "tightly-packed abundant cancellous bone with several K-wires" provided adequate stability to maintain the corrected shape and length of scaphoid until bony union was achieved. This study also shows that there was no

Cancellous bone grafting (2)

Conclusions: Cancellous bone grafting was found to lead to earlier bone union than corticocancellous bone grafting and to similar restorations of scaphoid deformity and wrist function when scaphoid nonunion was treated by headless compression screw fixation and bone grafting.

Conclusions: When treating unstable nonunion of scaphoid waist with non-vascularized bone grafting with internal fixation, cancellous bone grafting with K-wire fixation seems to be advantageous in terms of mean time to union. It seems that both bone grafting and fixation method affected "mean time to union" but the type of bone grafting was more influential in achieving union. The failure to union might be frequent in case of Herbert type D2 nonunion combined with cortico-cancellous bone grafting.

Which combination is the best?

Original Article The Journal of Hand Surgery (Asian-Pacific Volume) 2021;26(4):697-704 • DOI: 10.1142/S2424835521500673

A Comparison of Non-vascularized Bone Grafting and Internal Fixation in the Treatment of Unstable Scaphoid Waist Nonunion

Jin Young Kim*, Sang Lim Lee†, Sung Yoon Park*, Kyung Hwi Kim*, Ji Hyun Yeo*
*Department of Orthopedic Surgery, Dongguk University Ilsan Hospital, Goyang,
†Department of Orthopedic Surgery, Sanggye Baek Hospital, Seoul, Korea

Table 1. Patients' Data of Each Group Are Summarized

	Group 1 (cortico-cancellous + K-wire)	Group 2 (cortico-cancellous + headless screw)	Group 3 (cancellous bone + K-wire)
Number	12	13	13
Mean age (year) (range)	31.2 (18–49)	32.2 (19–50)	26.5 (16–56)
Sex (male/female)	12/0	12/1	12/1
Rt/Lt	7/5	8/5	6/7
Smoking	5 (42%)	6 (46%)	6 (46%)
Nonunion type	D1: 4 (33.3%) D2: 8 (66.7%)	D1: 4 (30.8%) D2: 9 (69.2%)	D1: 5 (38.5%) D2: 8 (61.5%)
Mean time to surgery (month) (range)	59.8 (12–336)	56.3 (12–288)	54.2 (16–192)
DISI deformity	6 (50%)	8 (62%)	7 (54%)
Humpback deformity	9 (75%)	11 (85%)	9 (69%)
Marked shortening (> 5 mm)	6 (50%)	8 (62%)	6 (46%)

Table 2. Union Rate and Time to Union Were Compared between Groups with Statistical Analysis

	Group 1	Group 2	Group 3	Overall	*p*-value
Union	10/12 (88.3%)	10/13 (76.9%)	13/13 (100%)	33/38 (88.4%)	0.247
Mean time to union (range) (weeks)	22.4 (16–28)	24.8 (20–28)	18.2 (16–24)	21.8 (16–28)	0.0001

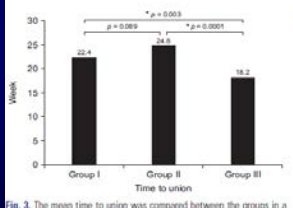

Fig. 3. The mean time to union was compared between the groups in a bar graph.

Table 3. Results of Multiple Regression Analysis Evaluating Factors Affecting Union Time

Variables	β coefficient	*p* value
Age (years)	−0.04	0.925
Sex (male/female)	−0.01	0.781
Involved hand (Rt/Lt)	0.002	0.988
Smoking status	−0.13	0.305
Nonunion type (D1/D2)	−2.33	0.007*
DISI deformity	0.08	0.116
Humpback deformity	0.153	0.284
Marked shortening (> 5 mm)	0.004	0.987
Fixation type (K-wire/headless screw)	0.23	0.106
Graft type (cancellous/cortico-cancellous bone graft)	−3.81	< 0.0001*

DISI: dorsal intercalated segment instability.

Failure to union
(type D2 : cortico-cancellous + 1 headless screw)

Fig. 4. A case of "Failure to union": a 38 year-old male was presented with left wrist pain persisting for several years after falling down on his left hand. (A) Pre-operative plain radiographs showed nonunion of distal scaphoid waist. Each fragment had a sclerotic end and dorsal rotation of lunate (DISI deformity) was observed. (B) The nonunion of scaphoid waist was treated with cortico-cancellous bone grafting with headless screw fixation, which is seen quite well on oblique view. (C) Seven months after the surgery, the plain radiographs were taken and they showed prominent radiolucent line between the grafted cortico-cancellous bone and the distal fragment.


•Case series

Vascularized Bone Graft for Scaphoid Nonunion

Orthop Surg. Naeun Pil Hosp.
Jong Pil Kim

Arthroscopic Bone Graft for Scaphoid Nonunion

Orthop Surg. Jeonbuk National Univ.
Young-Keun Lee

Anatomically, scaphoid is an almost entire intraarticular bone and 80% of the bone is covered by cartilage, which allows only few potential sites for the entrance of perforating vessels. The scaphoid has a tenuous blood supply. Moreover, the scaphoid is an important insertion site for ligaments forming carpal joints; it is the key link between the proximal carpal row and distal carpal row, and controls the carpal kinematics. Therefore, preservation of the scaphoid anatomy and vascularity is critical for normal hand and wrist functions. Another outstanding feature of the scaphoid is its shape in the mid-carpal joint, i.e., the gentle curvature of the waist and proximal portion of the scaphoid provides surgeons with a fairly stable and spacious platform and enables them to take down the nonunion site and carry out bone grafting. Therefore, if arthroscopy is applied to the scaphoid, ligament injury can be avoided, the scaphoid can be completely assessed through mid-carpal and radio-carpal joint, and the blood supply to the scaphoid can be preserved as much as possible.

Arthroscopy in scaphoid nonunion can have diagnostic and therapeutic roles. The diagnostic roles are: 1) confirmation of the healing status of the fracture site; 2) assessment of the possibility of healing potential, i.e., the presence of punctate bleeding; 3) assessment of the cartilage status; 4) assessment of associated injuries that account for the symptoms, especially the ulnar side wrist pain; and 5) more comprehensive assessment of combined injuries such as scapho-lunate (SL), luno-triquetral (LT), Triangular fibrocartilage complex (TFCC) injuries and chondral injuries. The therapeutic roles are styloidectomy, carpectomy, and bone grafting, of which arthroscopic assisted bone grafting is most important.

For bone grafting, an arthroscope is introduced in the MCU portal to continuously show the nonunion site, a 3.8 mm cannula is introduced to the nonunion site through the MCR portal, and cancellous chip bone is delivered to the entrance of the cannula. The bone graft is packed with a 3.2 mm trocar until a satisfactory volume of graft is achieved. After completely filling the defect, fibrin glue is routinely injected onto the surface of the graft substance. After arthroscopy, the wrist is taken out of traction to allow the natural compression from the capitate onto the graft. Definitive fixation with two 1.2 mm K-wires is performed under the C-arm image

intensifier. Additional SL K-wires fixation is performed to fix the unstable nonunion and kept in place for 8 weeks. If there is an RL K-wire, it is left for 2 weeks. K-wires are then placed outside the skin.

Recent report has shown that the bone union rate of arthroscopic bone grafting is approximately 93.5%, which is not better than the open method, but is at least equivalent to the results of pedicled vascularized bone graft. We think that the arthroscopic bone graft also has some limitations. We consider the salvage procedure as more effective for severe SNAC and severely destructed wrist joint combined with avascular nonunion; having non-reconstructable fragmented proximal pole than arthroscopic bone grafting. Significant arthrofibrosis of the wrist joint causes difficulty in arthroscopic bone grafting.

In conclusion, arthroscopic bone grafting seems to be an effective treatment method for patients with scaphoid nonunion. It can provide comprehensive assessment of the fracture status and combined injuries at the time of arthroscopic treatment. This technique can preserve the biology of scaphoid fragments which may promote the bone union.

2025년 대한수부외과학회

추계학술대회

역경에도 손을 맞잡고
Against All Odds, Hand in Hand

E-poster

Clinical Characteristics and Outcomes of Diabetic Hand Infections: A 10-Year Retrospective Study

Seoul Medical Center
Seong-Kee Shin, Seung-Yeon Cho, Kyu-Jin Kim

Background: Diabetic patients are vulnerable to hand infections due to immune dysfunction, angiopathy, and poor wound healing. However, diabetic hand infections remain under-recognized despite their potential for severe complications. This study aimed to evaluate the clinical features of diabetic hand infections and identify factors associated with adverse outcomes.

Methods: We retrospectively reviewed 23 diabetic patients hospitalized for hand infections at a single tertiary institution between January 2015 and December 2024. Infections were categorized as superficial hand infection (SHI) or deep hand infection (DHI). Clinical characteristics, microbiological findings, surgical interventions, and outcomes were analyzed. Predictors including BMI, HbA1c, diabetes duration, insulin dependence, infection depth, renal failure, and culture type were evaluated for association with outcomes such as amputation, multiple surgeries (≥2), and mortality using chi-square and logistic regression analysis.

Results: Of the 23 patients (mean age 63 years), 15 had DHI and 8 had SHI. All patients required surgical debridement; 47.8% underwent primary amputation, and 17.4% underwent secondary amputation. Deep infection was significantly associated with higher amputation risk ($p=0.045$), while dialysis was significantly associated with mortality ($p=0.033$). Neither HbA1c, insulin use, nor infection type were significantly associated with mortality. The overall mortality rate was 22.7%. Gram-negative organisms were more commonly isolated than expected, and fungal infections were observed in 3 patients.

Conclusion: Deep hand infection is a significant predictor of amputation, and renal failure is strongly linked to mortality in diabetic patients with hand infections. Prompt surgical intervention and recognition of high-risk features are critical to improving outcomes. Further prospective, multicenter studies are warranted to guide optimized treatment protocols.

Keywords: Diabetes, Hand infection, Amputation, Deep infection, Dialysis, Surgical outcomes

lexor Tendon Subluxation and Attritional Tear Following Open Carpal Tunnel Release: A Case Report and Literature Review

Yeson Hosp.
Sang Beom Ma

Introduction: Despite the high prevalence of carpal tunnel syndrome and a substantial amount clinical research, late-onset subluxation and attritional tearing of flexor tendons after carpal tunnel release (CTR) have been rarely reported.

Case: We present three cases of delayed-onset flexor tendon pathology involving four wrists, characterized by attritional tearing and subluxation, all of which necessitated revision surgery (Table 1). Favorable outcomes were achieved following revision surgery including excision of hamate hook, or reconstruction of ruptured flexor tendon.

Discussion: Based on our findings, contributing factors may include excessive ulnar-sided dissection, absence of early postoperative immobilization, and anatomical predisposition. Although rare, flexor tendon pathology can arise even after technically uncomplicated CTR and may lead to significant morbidity. Careful surgical technique and temporary wrist immobilization in a neutral position may help prevent such complications.

Keywords: Carpal tunnel syndrome, Hamate bone, Tendon, Postoperative complication, Tendon injuries, Reoperation

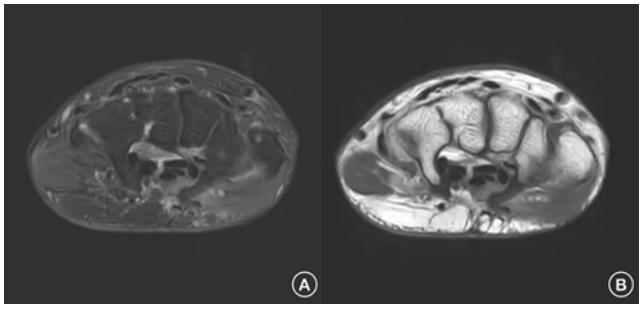

Figure 1. Axial MR images of the carpal tunnel (case 3). (A) T1-weighted image. (B) T2-weighted image. Images show volar subluxation of the flexor tendons, absence of the fifth FDS and FDP (flexor digitorum profundus) tendons, and diffuse tenosynovitis

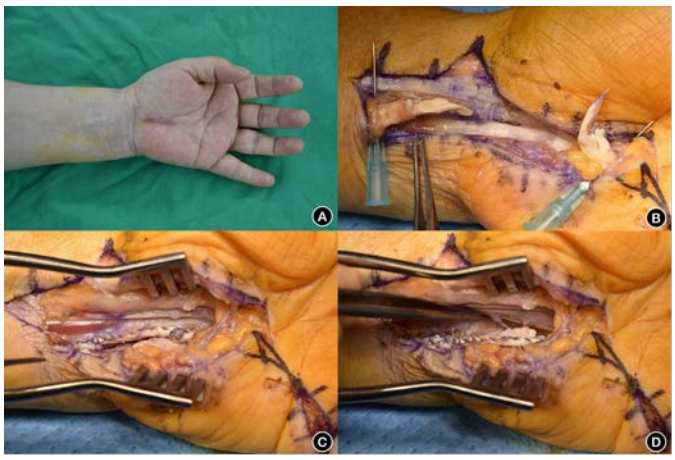

Figure 2. Intraoperative clinical photographs (case 3). (A) Surgical scar on the ulnar side of the thenar crease of the left wrist. (B) Complete rupture of the fifth FDP tendon with a significant gap and attritional degeneration. © Reconstruction of the fifth FDP tendon using a palmaris longus interposition graft. (D) Subluxation of the reconstructed FDP tendon over the transverse carpal ligament and hook of hamate during wrist flexion.

Table 1. Summary of the present cases

Case	Age/Sex	Symptoms	Postoperative Symptom Onset	Intraoperative Findings	Revision Procedure
1	74/female	Persistent pain along with fourth and fifth fingers	Immediately	Low-grade attritional tear and subluxation of fourth and fifth FDS over hamate	Excision of hamate hook
2	38/female	Persistent pain along with fourth and fifth fingers on bilateral wrists	Three months	Low-grade attritional tear and subluxation of fourth and fifth FDS over hamate	Excision of hamate hook
3	58/female	Gradual palm pain and loss of 5th DIP flexion	Three months	5 cm gap rupture with attritional degeneration Subluxation of reconstructed FDP tendon during wrist flexion	FDP reconstruction using a palmaris longus graft + hamate hook excision

FDP, flexor digitorum profundus tendon; FDS, flexor digitorum superficialis tendon

References

1. Itsubo T, Uchiyama S, Takahara K, Nakagawa H, Kamimura M, Miyasaka T. Snapping wrist after surgery for carpal tunnel syndrome and trigger digit: a case report. J Hand Surg Am. 2004;29:384-6.
2. Ceran F, Basat SO, Surmeli M, Bozkurt M. Flexor Tendon Laceration Due to Carpal Tunnel Release Surgery: An Impossible Complication. J Hand Microsurg. 2016;8:63-4.
3. Cline JA, Rogers JT, Merritt CH, Behzadpour V, Hearon BF. Snapping Wrist From Bowstringing of the Digital Flexors After Carpal Tunnel Release: A Case Report. Hand (N Y). 2025;20:Np7-np11.

Surgical Management of Advanced Pachydermodactyly: A Case report

[1]Plast Reconstr Surg. Saeson Hosp. [2]Orthop Surg. Saeson Hosp.
Hyun Rok Lee[1], Yeongsik Yoon[2], Jae In Chung[1]

Introduction : Pachydermodactyly (PDD) is a rare, benign condition characterized by bilateral soft tissue thickening around the proximal interphalangeal (PIP) joints of the fingers. PDD typically occurs without joint damage and is often a result of factors like finger cracking and overuse. Most cases are managed conservatively; however, surgical intervention may be necessary when conservative treatments fail. In this study, we reported a case of PDD that did not improve with lifestyle modifications and was successfully treated with surgical excision, along with insights gained during the treatment process.

Case report : A 17-year-old boy presented with a thickening of the second finger on his right hand. Approximately five years prior, thickening of the PIP joint on the radial and ulnar sides had developed without any significant trauma. He reported no pain during movement or tenderness at the joint site (Fig. 1). The patient had no family history of similar symptoms. He reported a habit of finger cracking but exhibited no psychiatric symptoms. Laboratory tests showed normal findings. MRI confirmed an infiltrative soft-tissue lesion on both sides of the PIP joint, while radiological assessments showed no joint abnormalities.. The joint spaces, bones, and ligaments remained intact. In the axial view of the T1-weighted images, the lesion was distinct from the neurovascular bundle and was positioned on the dorsal side of the neurovascular bundle (Fig 2).

Due to the lack of effectiveness of conservative treatment through behavioral modification over the course of eight months following the diagnosis, the patient opted for surgical excision due to aesthetic concerns as he approached university admission. A bilateral mid-axial incision was performed to excise the thickened tissue while preserving surrounding neurovascular structures (Fig. 3). Intraoperatively, the thickened tissue was dissected without significant adhesion to surrounding structures, and the procedure was completed without neurovascular damage (Fig. 4).

Histopathological examination revealed thickening of the dermal layer due to collagen fibers deposition, with fibrosis extending to the deep dermis and subcutaneous tissue (Fig. 5A). Thickened collagen fibers with intervening mucin accumulation were observed (Fig. 5B). Additionally, epidermal acanthosis and minimal

perivascular lymphocytic infiltration in the upper dermis were observed. One year after surgery, the patient reported satisfaction with the appearance and function of his fingers, showing no signs of recurrence (Fig 6).

Discussion : PDD primarily occurs in young men and is characterized by finger enlargement on the ulnar and radial sides of the PIP joints without significant symptoms. It rarely affects the distal interphalangeal (DIP) or metacarpophalangeal (MCP) joint. This condition typically presents bilaterally and commonly affects the second, third, and fourth fingers, with no reported cases involving the thumb. Typically, patients with PDD have normal laboratory test results. Plain radiography and MRI imaging reveal soft tissue swelling without abnormalities in the joint structures. Histopathological examination demonstrates findings such as orthokeratotic or parakeratotic hyperkeratosis, acanthosis, and increased fibroblast numbers in the dermis. PDD can be misdiagnosed as conditions such as pseudo-knuckle pads or juvenile idiopathic arthritis (JIA), and therefore accurate differential diagnosis is essential. Discussions regarding the treatment methods for PDD remain limited. Conservative treatment approaches, including lifestyle modifications and lesional corticosteroid injections, have shown reasonable results in many cases. The existing literature on PDD consists mainly of case reports focusing on conservative treatment, with very few reports addressing surgical intervention. This is likely because most case reports have been published by nonsurgical departments such as rheumatology and dermatology. In cases such as the one presented in this study, where the patient has failed conservative treatment or seeks a more predictable and definitive outcome within a short timeframe, surgical intervention may be considered a viable treatment option. This case highlights that surgical management can be an effective option for PDD in cases where conservative approaches are insufficient, and rapid improvement in finger appearance is desired. Increased awareness among surgeons about surgical intervention for PDD may lead to expanded treatment options for affected patients.

Figure 1. Preoperative clinical photographs reveal both sides thickening of the right second finger, particularly at the proximal interphalangeal (PIP) joints.

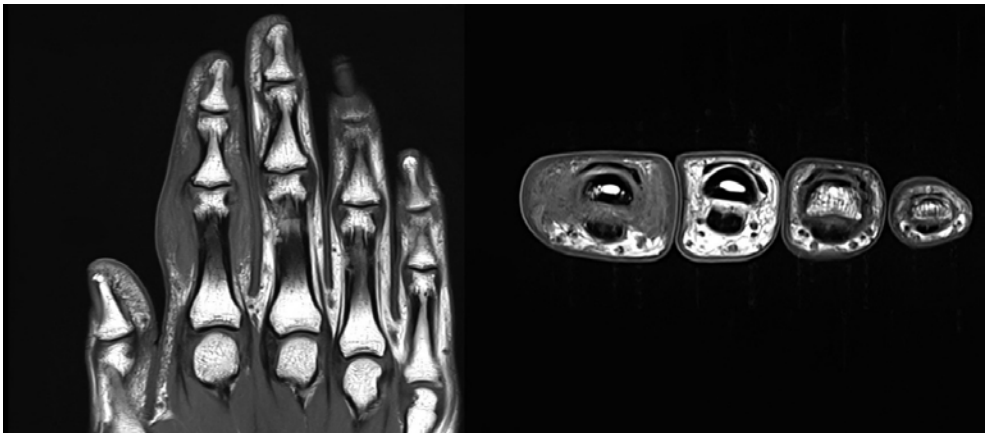

Figure 2. In magnetic resonance imaging, an infiltrative soft tissue lesion was observed on the radial and ulnar sides of the proximal interphalangeal (PIP) joint of the right second finger. On T1-weighted images, the lesion demonstrated homogeneous isointensity relative to muscle.

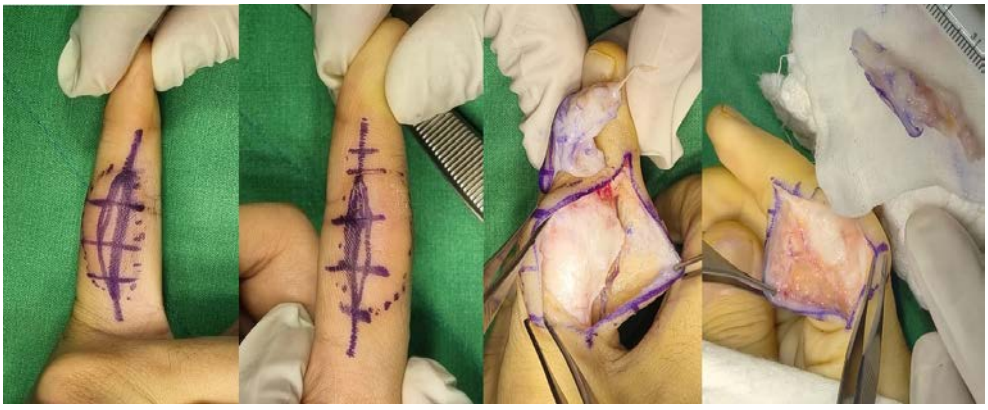

Figure 3. Intraoperative photographs illustrating the excision of tissue through a mid-axial incision, performed successfully without compromising the surrounding critical structures.

Figure 4. Postoperative images showing the excised tissue and the appearance of the fingers immediately after the procedure.

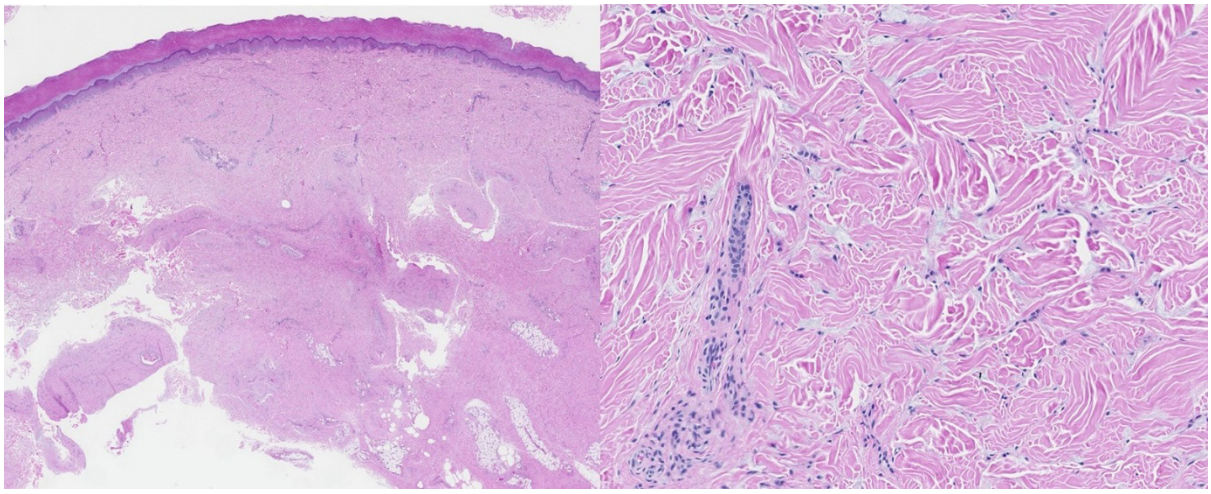

Figure 5. Histopathological examination revealed thickening of the dermal layer due to the deposition of collagen fibers, with fibrosis extending to the deep dermis and subcutaneous tissue (A). Collagen fibers showed thickening, and mucin accumulation was observed between the fibers (B).

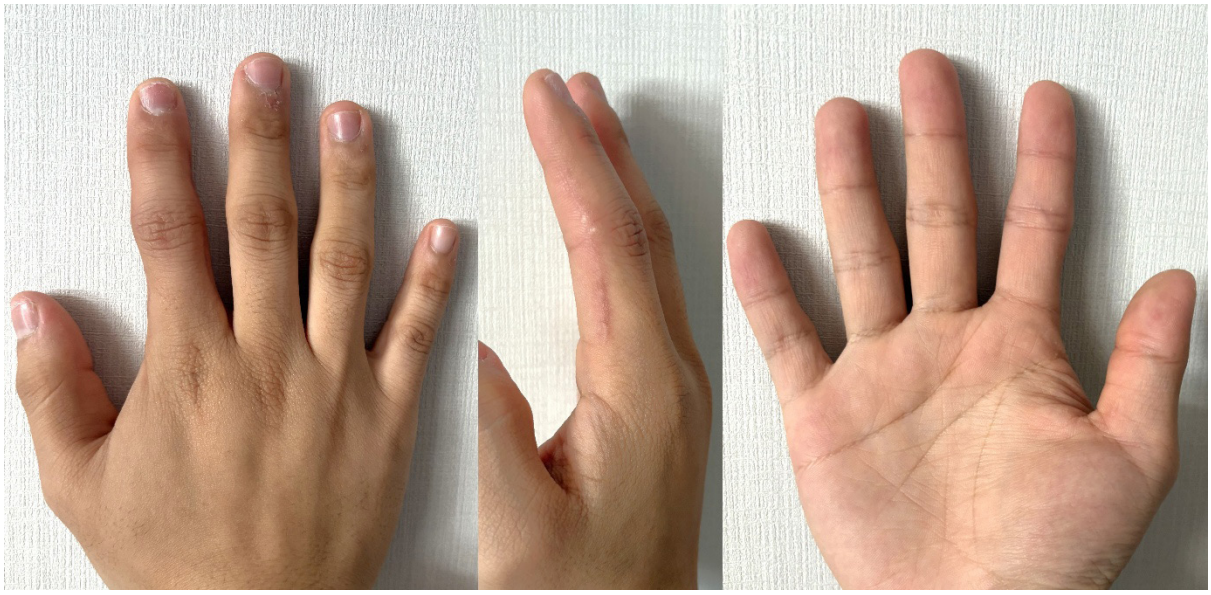

Figure 6. Clinical photographs one year postoperatively. There was no recurrence, no notable symptoms, and the patient was satisfied with the appearance of the fingers.

Keywords: pachydermodactyly, Finger Phalanges, hand joint

Giant Lipoma of the Hand Located Between the Digital Nerves of the Thumb: A case report

[1]Plast Reconstr Surg. Saeson Hosp. [2]Orthop Surg. Theson Hosp.
Hyun Rok Lee[1], Jaehoon Kang[1], Jeewoong Kim[2]

Introduction: While lipomas are common soft-tissue masses, giant lipomas (>5 cm) of the hand are rare. Previously reported cases mostly involved the palm area, occasionally causing displacement and symptoms related to digital nerves other than the thumb. However, giant lipomas positioned radially between the digital nerves of the thumb remains undocumented. This report presents a unique case, reviewing its clinical presentation, diagnosis, and treatment considerations.

Case report: A 45-year-old woman presented with a progressively enlarging, soft, non-tender mass in her left hand, present for 3 years (Fig. 1). The mass extended from the palm to the first web space, causing pain, functional impairment, and cosmetic concerns, prompting surgical removal. Preoperative MRI revealed a well-encapsulated, lipid-rich tumor (6×4×3 cm) near the median nerve, with the radial digital nerve of the thumb positioned between the tumor and the skin (Fig. 2). A marginal excision was performed without nerve injury (Fig. 3). Histopathology confirmed a benign lipoma. The patient remained symptom-free postoperatively, with no recurrence at 1-year follow-up.

Discussion: Lipomas, which are composed of mature fat cells, can occur in various locations, including the subcutaneous, intermuscular, and intramuscular layers. Although they are common in the trunk, shoulders, neck, and arms, they occur less frequently in the hands and feet. Giant lipomas (>5 cm) are exceptionally rare in the hand and are mostly asymptomatic, although they can occasionally cause pain or neurological symptoms. Imaging modalities such as CT, ultrasonography, and particularly high-resolution 3.0T MRI are essential for accurate diagnosis and preoperative planning, facilitating assessment of the tumor's relationship with neurovascular structures and potential malignancy. The typical location of such lipomas is central in the palm, and their anatomical orientation can allow expansion between digital nerves, especially in the thumb, increasing the risk of iatrogenic nerve injury during surgery. Features suggestive of malignancy on MRI include non-adipose nodular areas, thickened septa, and reduced fat content, warranting careful differential diagnosis from liposarcomas. While marginal excision usually suffices for benign giant lipomas, preoperative MRI is vital for

minimizing neurovascular injury, guiding surgical approach, and ensuring complete removal. Given their rarity, surgical intervention for giant lipomas is primarily indicated for cosmetic and functional reasons, emphasizing the importance of detailed preoperative assessment to optimize outcomes.

Fig. 1. An approximately 6×4 cm tumor located from the palm to the 1st web space.

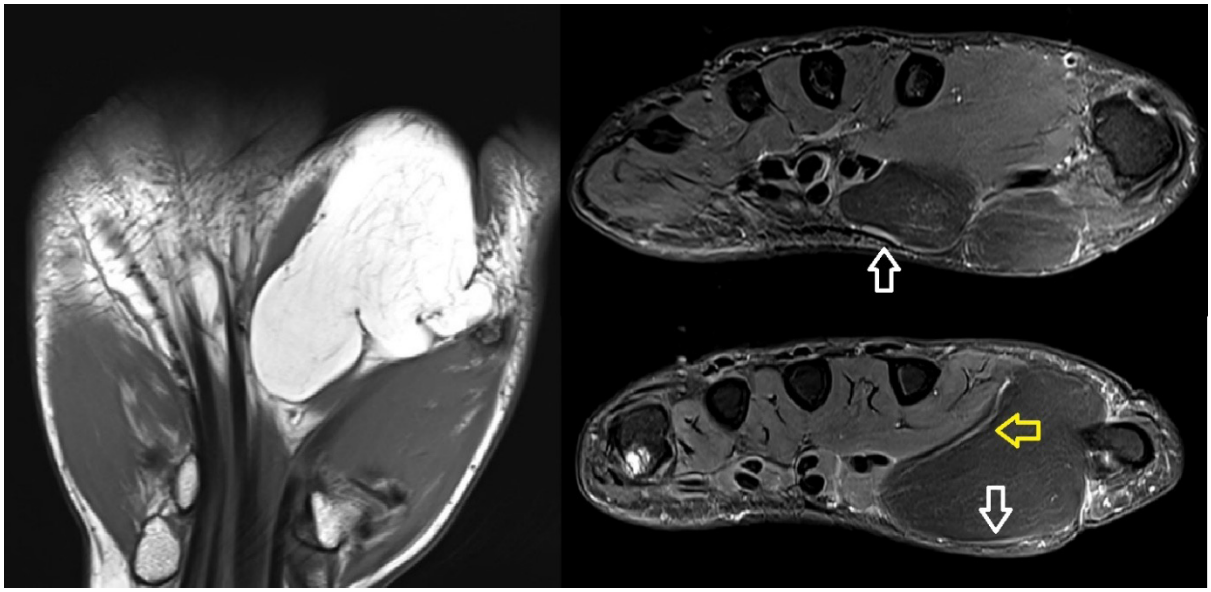

Fig. 2. Preoperative MRI findings. A 6×4×3 cm tumor, appearing as a lipoma, is situated on the radial side of the palm. The tumor is located between the ulnar digital nerve (yellow arrow) and the radial digital nerve (white arrow) of the thumb.

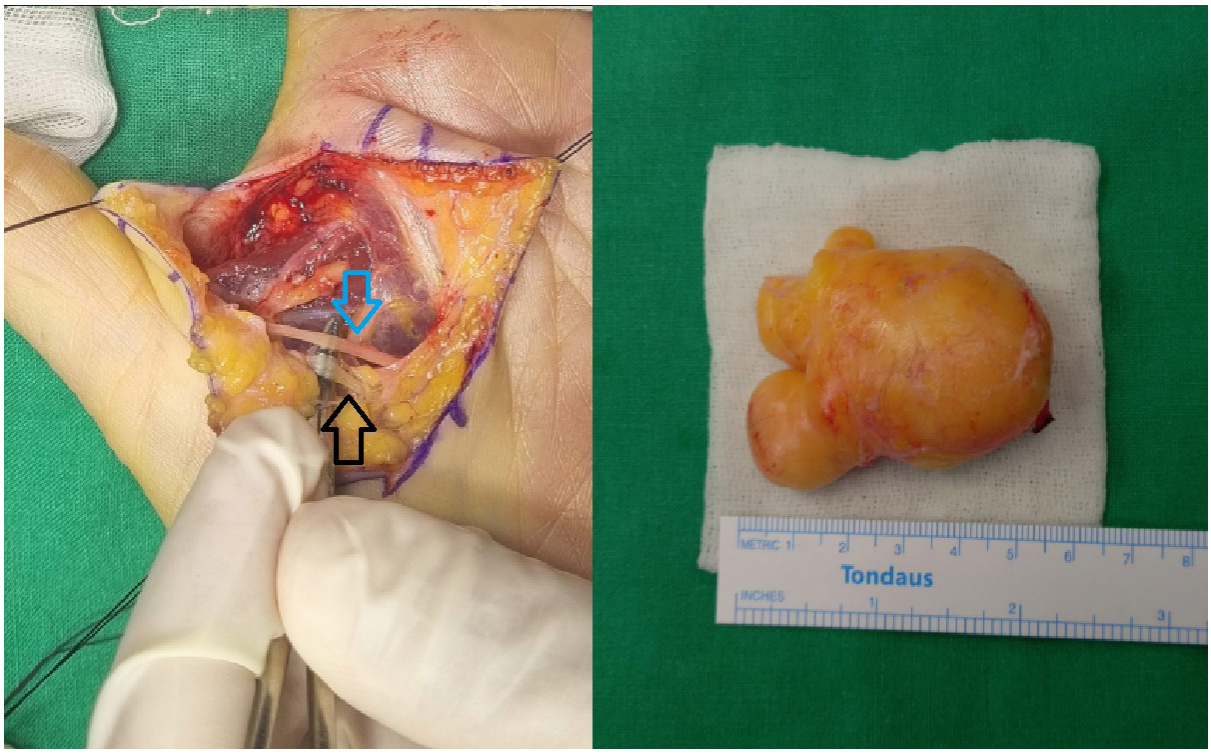

Fig. 3. Intraoperative findings. The tumor was removed with minimal damage to surrounding normal tissue. An attenuated radial digital nerve of the thumb (blue arrow) and the ulnar digital nerve of the thumb (black arrow) closely adhered at the posterior aspect, were observed.

Keywords: Lipoma, Lipomas, Fatty tumor

Surgical management of delayed mallet finger fractures using combined two-extension block Kirschner wire and dorsal counterforce techniques

[1]Orthop Surg. Chungnam National Univ., [2]Orthop Surg. Seoul National Univ.
Seung Hoo Lee[1], Min Bom Kim[2], Young Ho Lee[2]

Purpose: This study assessed the efficacy of combining the "two-extension block Kirschner wire (K-wire) technique" and "dorsal counterforce technique" for treating delayed bony mallet fractures (≥4 weeks), previously introduced to prevent fracture fragment rotation in axial and sagittal planes in acute cases.

Method: Twenty-nine patients with delayed bony mallet fractures were treated using percutaneous curettage followed by the two-extension block K-wire technique, incorporating the dorsal counterforce technique for cases of inadequate reduction. If satisfactory reduction could not be achieved, we converted to an open procedure. Outcomes were evaluated over a 6-month postoperative period, focusing on healing time, range of motion, complications, and Crawford functional outcomes.

Results: Of the 29 patients with delayed bony mallet fractures, 13 were treated using percutaneous curettage combined with the two-extension block K-wire technique, while 15 required additional dorsal counterforce technique. One patient required conversion to open procedure due to failure to restore a congruent joint surface and was excluded from the outcome assessment. All 28 fractures treated using our suggested method healed within 8 weeks, with 24 patients (85.7%) achieving healing within 6 weeks. According to Crawford's evaluation system, the outcomes were excellent, good, fair, and poor in 19, 6, 1, and 2 patients, respectively.

Conclusion: Two-extension block K-wire technique combined with the dorsal counterforce technique appears to be a feasible option for delayed bony mallet fractures, achieving congruent joint surface and satisfactory outcomes in most cases.

Level of evidence: IV

The concentric circles method to define and assess anterior subluxation in bony mallet finger

[1]Orthop Surg. Chungnam National Univ., [2]Orthop Surg. Seoul National Univ.
Seung Hoo Lee[1], Min Bom Kim[2], Soo Min Cha[1], Young Ho Lee[2]

We have described and validated the concentric circles method for assessing anterior subluxation in the bony mallet finger. We retrospectively analysed 114 radiographs from cases of bony mallet finger assessed by four hand surgeons and one radiologist using three approaches: subjective visual inspection, the concentric circles method and the malalignment method. The concentric circles method defines subluxation as a disruption of the normal concentric annulus between the middle phalangeal head and distal phalangeal articular surface on true lateral radiographs. It showed improved accuracy (94%), higher sensitivity (91%) and specificity (97%) compared with the other methods, with excellent inter- and intra-observer reliabilities.

Level of evidence: III

Keywords: Anterior subluxation, bony mallet finger, concentric circles method, radiographic assessment, surgical decision-making

Published in Journal of Hand Surgery, European Vol. 2025

Extensor Tendon Joint Anchorage: A Novel Technique for Surgical Repair of Sagittal Band Rupture

Soo Hosp.
Soonwon Chung, Jae-Won Kim, Byung Ho Lee, Jun-Mo Lee

Introduction: The sagittal band is an essential component of the extensor hood, functioning as the primary stabilizer of the extensor digitorum communis (EDC) tendon at the metacarpophalangeal (MCP) joint. Sagittal band injuries typically result in swelling, pain, and instability of the extensor tendon, with ulnar-sided subluxation being the most frequent presentation. Conservative management remains the first-line option in acute injuries, often involving splinting in neutral or hyperextension for several weeks. However, outcomes are inconsistent, particularly in delayed presentations or chronic cases, where persistent subluxation, extensor lag, or pain may remain. Numerous surgical approaches have been described for refractory cases, including direct repair of the ruptured band, tendon slip procedures, or reconstruction using tendon grafts. Despite advances, consensus on the optimal surgical method remains lacking. Direct repair may fail in cases with attenuated tissue, and reconstruction methods may restrict tendon gliding, leading to stiffness. To overcome these limitations, we developed a novel method—the Extensor Tendon Joint Anchorage (ETJA) technique—that directly secures the EDC tendon to the MCP joint capsule with multiple sutures. Although fixation of tendon to joint may appear restrictive, intraoperative and postoperative observations demonstrate that the tendon and joint surface rotate synchronously, thereby preserving full finger range of motion while providing a secure and durable repair.

Methods: We conducted a retrospective review of patients who underwent surgical repair for sagittal band rupture using the Joint Extensor Anchoring Technique (JEAT) at Jeonju Soo Hospital between January 2024 and December 2024. A total of 24 patients were included in the study. Exclusion criteria included concomitant fractures, open lacerations, rheumatoid arthritis, and connective tissue disease.

All procedures were performed under regional anesthesia with brachial plexus block. The Joint Extensor Anchoring Technique fixate the volar layer of the extensor tendon to the dorsal layer of the periarticular capsule of the MCP joint using 3–4 interrupted 3-0 Vicryl sutures, effectively coupling the tendon with the joint itself. Following fixation of the extensor tendon to the joint using the JEAT technique, passive range of motion was performed. The area marked with a pen on the joint can be seen gliding together with the tendon

during flexion and extension. Because the joint moves synchronously with the tendon, fixation does not restrict range of motion while providing stronger stabilization. (Fig.) All patients were immobilized in a functional splint maintaining the MCP joint in extension for the first 3 weeks. Progressive active range of motion exercises began at 3 weeks postoperatively, and sustained for 3 weeks.. Standardized rehabilitation protocols were supervised by specialized hand therapists. Patient demographic and clinical data were collected from medical records. Variables included: Mechanism of injury, Time from injury to surgery, Rehabilitation duration, Follow-up period, Range of motion recovery, Extensor tendon stability, Reoperation or failure rate. At the final follow-up, the Visual Analog Scale (VAS) score was assessed.

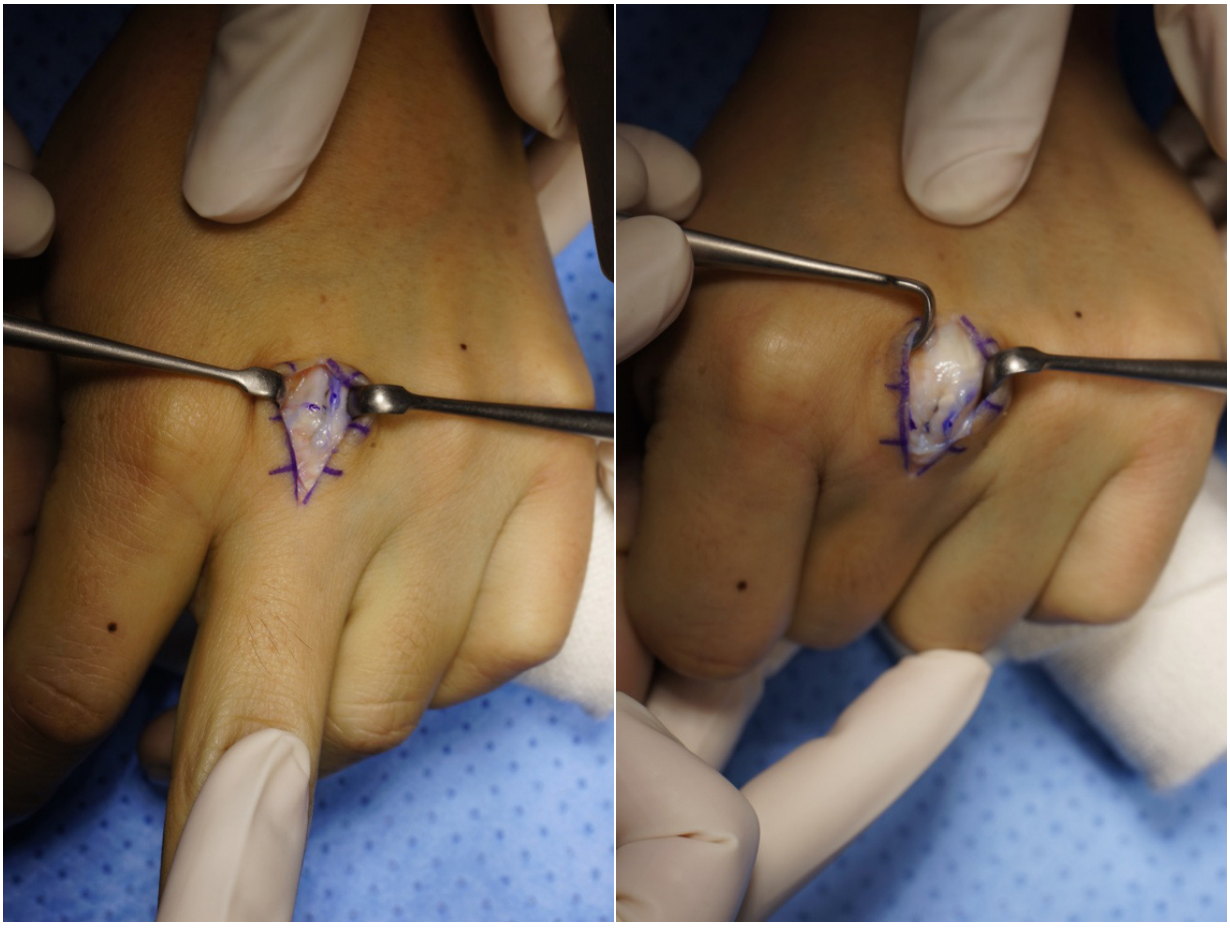

Fig. The mark placed on the joint remains visible in extension (Left) and shifts with the tendon during flexion (Right), demonstrating synchronous gliding.

Results: A total of 24 patients underwent surgical repair of sagittal band rupture using the Extensor Tendon Joint Anchorage (ETJA) technique between January 2024 and December 2024. The mechanisms of injury included traumatic causes in 19 patients (79.2%) and spontaneous ruptures in 5 patients (20.8%). At final follow-up, the mean range of motion of the metacarpophalangeal joint was fully recovered, indicating complete

recovery compared with the contralateral side. No patients demonstrated recurrent tendon subluxation or dislocation. Functional outcomes were favorable across both traumatic and spontaneous subgroups, with no significant difference in ROM recovery or complication rate. At the final follow-up, the mean Visual Analog Scale (VAS) score for pain was 1.9, indicating minimal residual discomfort.

Conclusion: The Extensor Tendon Joint Anchorage (ETJA) technique provided secure stabilization of the extensor tendon while preserving full metacarpophalangeal joint motion. These results indicate that ETJA is a reliable alternative to conventional repair methods for sagittal band injuries, offering durable fixation and favorable functional recovery.

equential Ulnar and Radial Stress Fractures in a Neurofibromatosis Patient with Upper Limb Weight-Bearing Ambulation

[1]Orthop Surg. National Health Insurance Service Ilsan Hosp., [2]Orthop Surg. Wonkwang Univ.
Hyun-Tak Kang[1], Hong-Je Kang[2]

Stress fractures of the forearm are rare and typically associated with athletes or crutch users. Sequential fractures involving both the ulna and radius have been only sporadically reported. We report a 60-year-old female patient with neurofibromatosis and paraplegia who ambulated with crutches and by crawling, and subsequently developed sequential stress fractures of the ipsilateral ulna and radius. Both fractures were treated conservatively with cast immobilization and healed uneventfully. In the absence of bisphosphonate therapy or metabolic bone disease, these injuries were considered stress fractures resulting from repetitive upper limb weight-bearing. We present this case with a brief review of the literature.

Negative Pressure Wound Therapy (NPWT)-Assisted Dermatotraction for Compartment Syndrome in a Toddler: A Case Report

Plast Reconstr Surg. The Catholic Univ. of Korea
Su Ram Kim, Rah Yoon Kim, Hye Ju Han, Sang Oon Baek, Gyeol Yoo, Jun Yong Lee

Purpose: Extravasation injuries in toddlers can cause severe soft tissue damage and compartment syndrome, requiring prompt surgical intervention. We report a case of right forearm and hand compartment syndrome in a toddler, successfully managed with NPWT-assisted dermatotraction and staged wound closure.

Methods: A 13-month-old toddler admitted for acute gastroenteritis developed an extravasation injury on the right forearm during intravenous fluid administration. Physical examination revealed pallor on the palm, volar wrist, and radial dorsum of the hand, with erythema and multiple bullae on the dorsal wrist and proximal radial forearm. Emergency fasciotomy was performed, including carpal tunnel release and extended incisions to the cubital fossa for complete decompression. Additional incisions were made on the dorsal hand and radial thenar area. Reperfusion of the affected tissues was confirmed intraoperatively, followed by warm saline irrigation and daily wound care. On postoperative day 3, NPWT-assisted dermatotraction using vessel loops was applied. Delayed wound closure was performed on postoperative day 7.

Results: The wound showed progressive healing with reduced edema and healthy granulation tissue. From postoperative week 5, the patient began scar management with laser therapy and occupational rehabilitation, which has continued through the 5-month follow-up. Nerve conduction studies revealed partial median and ulnar sensory neuropathy, showing improvement compared to initial studies.

Conclusion: Prompt surgical decompression with confirmed reperfusion, followed by NPWT-assisted dermatotraction and staged closure, can be an effective strategy for managing extravasation-related compartment syndrome in toddlers, contributing to both wound recovery and neurological improvement.

Fix Rather Than Excise? Headless Screw Treatment of Hook of the Hamate in Ten Consecutive Patients

Soo Hosp.
Soonwon Chung, Jae-Won Kim, Byung Ho Lee, Jun-Mo Lee

Introduction: Hook of hamate fractures are uncommon carpal injuries, about 2–4% of carpal fractures, clustered in impact sports (golf, baseball, racket sports) and in falls with ulnar sided loading, where patients present with hypothenar pain, painful grip, and sometimes neuritic or flexor tendon symptoms. Standard PA and lateral radiographs miss a sizeable fraction; carpal tunnel views and, most reliably, CT reduce false negatives and accelerate treatment decisions. Delayed diagnosis increases the risks of nonunion, persistent pain, ulnarnnerve irritation, and tendon attrition, so definitive management is often recommended once the diagnosis is secure.

Excision is widely used in athletes for its predictable and rapid return-to-play (RTP) timetable, typically from 4 to 7 weeks, though transient ulnar nerve symptoms are reported more often than previously appreciated. ORIF preserves the pulley complex and native biomechanics; modern minimally invasive techniques (volar, percutaneous, Carm guided) report universal union with very low complication rates in acute, structurally favorable fractures. Evidence syntheses agree that both strategies work, but head to head data remain sparse, heterogeneous, and likely athletes, which is limiting generalizability to mixed real world cohorts.

Notably, several series indicate that carefully selected early presenters can succeed with conservative immobilization, reminding surgeons to individualize care rather than default to a single algorithm. Meanwhile, contemporary athlete cohorts expand external validity. professional and collegiate baseball populations resume hitting by 4.5 weeks and full activities by 7 weeks after surgery, with high RTP rates but non zero neuropathic complications to discuss during consent. Against this backdrop, we conducted a single center, consecutive case analysis of ORIF (screw) from 2022 to 2024, emphasizing pragmatic descriptors mechanism mix, injury to surgery timing, and short term clinical endpoints to guide everyday practice beyond elite athlete settings.

Methods: We conducted a retrospective, single center case series of consecutive headless screw fixations for hook of hamate fractures performed between January 2022 and September 2024 at our institution. Case identification used the operative logbook and electronic health record cross checks to maximize capture and reduce selection drift.

Inclusion criteria were (1) radiographic or CT diagnosis of hook of hamate fracture and (2) operative treatment with headless screw fixation as the index procedure; patients treated by excision or plate were excluded from the analytic cohort a priori to avoid technique mixing. From 23 surgical cases, 10 screw fixation cases met criteria.

We abstracted age, sex, injury mechanism, injury to surgery interval (ITS), follow up (f/u) duration, pain at last visit (routine VAS scale), ROM limitation (yes/no), sensory symptoms (yes/no), and union (radiograph or CT documented by the treating surgeon). Because timing units varied in charts, ITS was normalized to weeks, a convention also used in technique series analyzing continuous timing variables. Follow up was normalized to months.

All cases underwent volar approach with protection of the ulnar neurovascular bundle, anatomic reduction under fluoroscopy, and fixation using a headless compression screw across the hook fragment; closure and early protected motion followed surgeon judgment on stability. Early mobilization focused on edema control and pain.

The primary outcome was union at last follow-up, secondary outcomes were pain score (VAS), ROM limitation, and sensory symptoms at last follow up. We selected these endpoints to align with recent systematic work (union, pain/function) to facilitate external comparability across fixation vs excision literature, even though the present report is technique specific.

Continuous data are reported as mean ± SD and median, categorical data as n (%). Given small n and pragmatic heterogeneity, we present descriptive statistics only without hypothesis testing, a reporting posture common to focused surgical case series of the hamate.

Results: Ten patients (9 men; mean age 31.4 ± 13.1 years) underwent headless screw fixation; mechanisms were predominantly falls, which accounts for 7 out of 10 with sports in the remainder (golf 2, kendo 1). Median injury-to-surgery interval (ITS) was 1.5 weeks [1.0–3.8], with two delayed presentations at 16 weeks; median follow-up was 4.5 months [3.0–9.8]. These timing and mechanism patterns align with mixed real-world cohorts rather than strictly athlete-only samples, supporting generalizability beyond elite sports settings.

Union was achieved in 9 out of 10 (90%) at last follow up. This rate is within the broad range reported for headless screw fixation in acute or subacute fractures, which is often 90–100%, in small series employing modern reduction and stable compression, while acknowledging that chronicity and fragment biology modulate risk. The single nonunion occurred despite standard technique and routine rehabilitation. No patient in this series demonstrated ROM limitation or sensory symptoms at last follow up, suggesting low morbidity in the short term even when union is not confirmed.

Pain at last follow up had a median 1.5 (mean 1.8), consistent with favorable early symptom control expected

after stable fixation in nonelite cohorts. ROM limitation and sensory symptoms did not exist at the last visit.

Taken together, these ten cases reinforce three practical points. Early fixation yields predictable comfort and motion with high union probability and short-term morbidity after modern headless screw fixation is low in mixed populations when neurovascular handling is meticulous and early motion is encouraged. These findings also highlight the need for standardized timing and prospective future work to refine selection between fixation and excision in everyday practice.

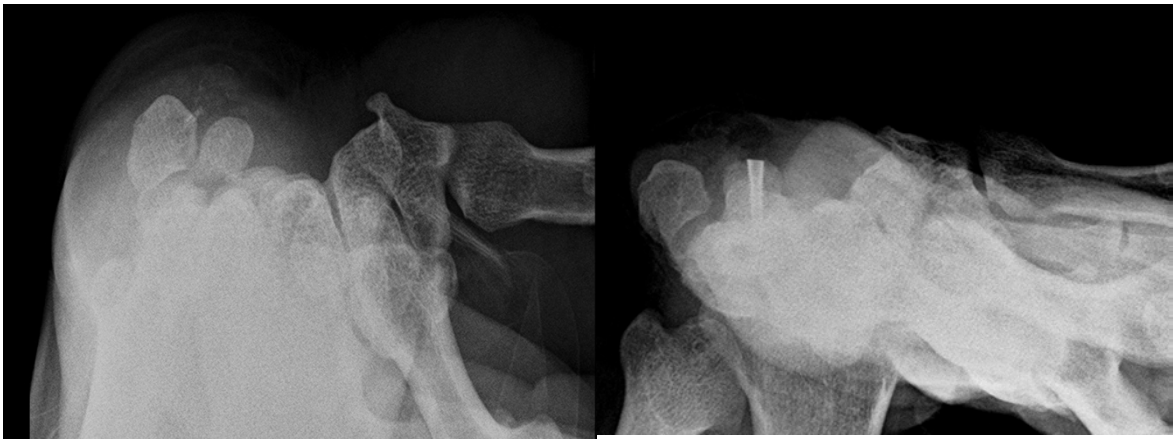

Fig. Preoperative image of hamate hook fracture (Left), 19 months after postoperative image, union state (Right)

Lipoma of the Third Web Space of the Hand: A Rare Case with Dorsal and Palmar Extension

Plast Reconstr Surg. The Catholic Univ. of Korea
Su Ram Kim, Gyeol Yoo, Jun Yong Lee, Sang Oon Baek, Rah Yoon Kim, Hye Ju Han

Purpose: Lipoma is a common benign tumor, but occurrence in the interdigital web space of the hand is rare. We report a case of lipoma in the third web space with dorsal and palmar extension and discuss its clinical implications.

Methods: A 47-year-old woman presented with a 2×2 cm fixed, round mass on the dorsal aspect of the left third web space, causing discomfort without neurological symptoms (Figure 1). CT showed a larger and deeper lesion than expected, extending between the third and fourth metacarpals to the palmar aspect (Figure 2). Excision was performed through two vertical incisions at dorsal and palmar aspects. Dissection was carefully carried out between interosseous and lumbrical muscles while preserving adjacent digital nerves and vessels, and the mass was removed dorsally (Figure 3).

Results: The mass was well encapsulated and excised completely without complications. Histopathology confirmed lipoma. Symptoms resolved after surgery, and no sensory deficit or recurrence was observed (Figure 4).

Conclusion: Although lipoma in the hand is not uncommon, its occurrence in the interdigital web space, particularly the third web space, is unusual and may mimic ganglion or neuroma. Such lesions often appear smaller and more superficial on examination but can extend deeply, underscoring the importance of preoperative imaging. Combined dorsal and palmar approaches enable complete excision while protecting neurovascular structures. Careful surgical planning and meticulous dissection are essential for favorable outcomes and prevention of recurrence.

Fig. 1. Clinical findings of the mass

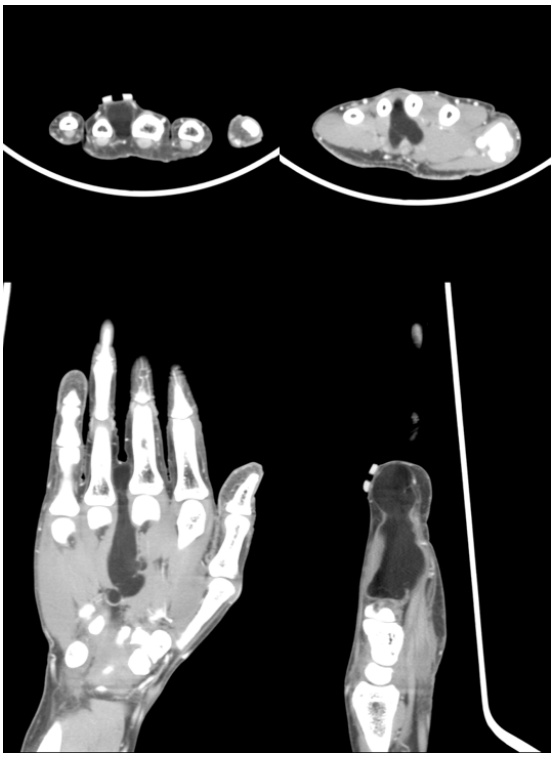

Fig. 2. Radiological findings of the mass

Fig. 3. Intraoperative findings following total excision of the mass

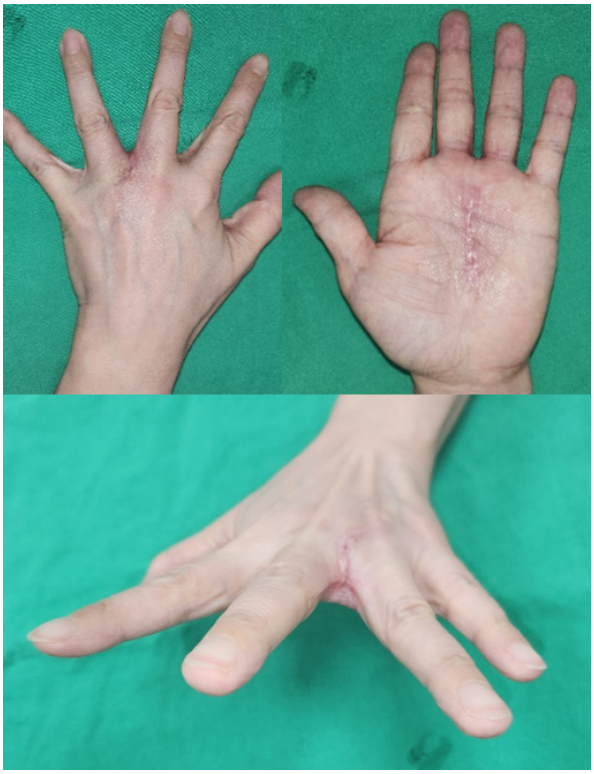

Fig. 4. Postoperative clinical findings

Pediatric Digital Ischemic Necrosis from Constrictive Finger dressing: A Case Report of Hypothenar Muscle Perforator Flap Reconstruction

Gwangmyeong Sungae General Hosp.
Dong Chul Lee, Jong Ju Park, Kyung Jin Lee

Purpose: Digital ischemic necrosis due to constrictive dressings such as Coban is a rare but serious complication, particularly in pediatric patients or post-traumatic settings. We report a unique case of ischemic necrosis following Coban dressing applied after a hinge crush injury to the finger, ultimately requiring distal amputation and soft tissue coverage with a hypothenar muscle perforator flap.

Method: A pediatric patient sustained a hinge crush injury to the finger and was subsequently treated with Coban dressing. The patient presented with progressive signs of digital ischemia, including discoloration and necrosis of the distal phalanx. Clinical assessment and imaging confirmed compromised perfusion. Surgical intervention was performed in two stages: initial debridement and distal phalanx amputation, followed by coverage using a hypothenar muscle perforator flap.

Result: Postoperative recovery was uneventful, with flap survival and preserved finger function. The patient achieved satisfactory aesthetic and functional outcomes at follow-up. The case illustrates the risk of secondary ischemic injury from improperly monitored circumferential dressings, especially following trauma.

Conclusion: This case highlights the potential for severe ischemic complications from compressive dressings applied after digital trauma. Prompt recognition and timely surgical management, including the use of perforator flaps for reconstruction, can lead to favorable outcomes. Caregiver and clinical staff education is crucial in preventing such avoidable complications.

Atypical Proximal Ulnar Fracture Induced by Chronic Mechanical Overload in the Absence of Antiresorptive Therapy: A Case Report

[1]Orthop Surg. Kangdong Sacred Heart Hosp., [2]Seoul Jump Orthopedic Clin., [3]Orthop Surg. National Medical Center
Sanglim Lee[1], Ji Yeong Kim[2], Suk Ha Jeon[3]

Atypical fractures are most often linked to long-term antiresorptive therapy and usually occur in the femur. Atypical ulnar fractures are rare, mostly reported with bisphosphonate or denosumab use. However, repetitive mechanical stress in osteoporotic patients may also induce such fractures.

We present the case of an 84-year-old woman with severe osteoporosis (T-score: −3.2 lumbar, −3.7 femoral neck) and prior vertebroplasty. She habitually leaned on desks to support ambulation due to back pain. After striking her left forearm on a desk, she developed pain. She had no history of bisphosphonate use, and denosumab had been discontinued after a single injection three years earlier. Examination showed hyperkeratotic changes on both forearms. Imaging revealed a transverse fracture of the proximal ulna with sclerotic margins, posterior cortical thickening, and volar hypertrophy. Intraoperatively, atrophic nonunion with sclerotic bone and absent callus was confirmed. Histology demonstrated fibrosis, chronic inflammation, and necrotic bone.

The patient underwent curettage, open reduction and internal fixation with plating, and allogeneic bone grafting. Pain resolved by four weeks, union was achieved at seven weeks, and at 18 months she had functional recovery with nearly full motion.

This case highlights that atypical ulnar fractures may occur in osteoporotic patients under chronic mechanical overload, even without prolonged antiresorptive therapy. Recognition of atypical radiographic features outside the femur is essential. Early surgical debridement with grafting is effective for union and functional restoration.

Keywords: Atypical ulnar fracture, osteoporosis, mechanical overload, antiresorptive therapy, nonunion

Figures:

Fig. 1. Preoperative radiograph (A) and CT (B).

Fig. 2. Immediate postoperative radiograph.

Fig. 3. Radiograph at 18 months postoperatively.

Clinical Outcomes and Demographic Characteristics of Surgical Treatment for Transcondylar Fractures of the Distal Humerus in Elderly Patients (Orthogonal and Parallel Plating)

[1]Gohyeon Seoul Samsung Orthopaedic Clin., [2]Orthop Surg. Inje Univ., [3]Gayang Samsung Orthopaedic Clin.
Dong Suk Kim[1], Seung Joo Kim[2], Sang Hoon Chae[3], Hyoung Keun Oh[2], Hyun Il Lee[2]

Background: Transcondylar fractures of the distal humerus in elderly patients present significant challenges due to osteoporotic bone quality and short bone stock in distal fragment. Open reduction and internal fixation (ORIF) is crucial for restoring functional elbow range of motion, with dual plating techniques, including 90-90 (orthogonal) and Parallel plating, being primary methods for stable fixation. This study aims to compare the clinical outcomes and demographic characteristics of 90-90 and Parallel plating techniques for transcondylar fractures of the distal humerus in elderly patients.

Methods: A retrospective analysis was conducted on patients aged 65 years or older who underwent ORIF for transcondylar fractures of the distal humerus using either 90-90 or Parallel plating. Patient demographic information (age, sex, comorbidities, injury mechanism) and clinical outcomes (fracture union rate, time to union, elbow range of motion (extension, flexion), and complication rates) were collected. Statistical comparisons were performed to identify significant differences between the two plating groups.

Results: A total of 32 elderly patients were included in the study, with a mean age of 82.1 ± 6.2 years. The majority were female (27 patients, 84.4%), and the most common injury mechanism was 'slip down from the gorund level' (28 patients, 87.5%). The 90-90 plating group comprised 19 patients, and the Parallel plating group had 13 patients. No statistically significant differences were observed between the two groups in terms of demographic characteristics (age, sex, comorbidities, fracture morphology), indicating comparability at baseline. In clinical outcome analysis, the final union rate was 100% for both the 90-90 plating group (12/12 confirmed unions, 7 lost to follow-up) and the Parallel plating group (8/8 confirmed unions, 5 lost to follow-up). The mean time to union was 4.8 ± 3.8 months for the 90-90 group and 3.1 ± 2.4 months for the Parallel group. Mean extension deficit was -11.7 ± 10.4 degrees and mean flexion was 115.8 ± 14.5 degrees for the 90-90 group. For the Parallel group, mean extension deficit was -16.9 ± 9.6 degrees and mean flexion was 108.5 ± 19.3 degrees. The overall complication rate (for exmaple, nerve irritation) was 10.5% (2/19 patients) in the 90-90 group and 7.7% (1/13 patients) in the Parallel group.

Conclusion: This study demonstrates that both 90-90 and Parallel plating techniques are effective in achieving fracture union and restoring functional joint motion in elderly patients with transcondylar fractures of the distal humerus. While overall complication rates were comparable, further large-scale prospective studies are warranted to comprehensively compare long-term clinical outcomes and complication profiles of these surgical methods.

Functional Impairment of Chopsticks associated with Motor Function of Ulnar nerve in Cubital Tunnel Syndrome

[1]Soo Hosp., [2]Seojinyoung Neurology Clin.
Soonwon Chung[1], Byung Ho Lee[1], Han A Lee[1], Jun-Mo Lee[1], Jin Young Seo[2]

Background: The purpose of this clinical study was to identify preoperative and postoperative ability to use Chopsticks and its relationship with the motor function of the ulnar nerve in cubital tunnel syndrome.

Methods: Fifty eight patients(42 men, 16 women) with cubital tunnel syndrome underwent surgery from September 2019 to July 2024. 12 cases(21%) were followed up. The average age at the time of surgery was 69.4 years(range 47-89). The right elbow was involved in 11 cases(92%) and the left in 1(8%). There were no bilateral cases. 1 case was coincidentally involved with carpal tunnel syndrome(8%). All cases complained motor weakness when using chopsticks(McGowan GradeI IIB for 3 cases, GradeI III 9 for cases) at their first visit and motor tests(Egawa sign and confrontation test) were positive. Before surgery all cases had radiologic pictures to find bony spur and bony abnormality and nerve conduction study of the ulnar nerve to localize accurate compression site and degree(Nerve Conduction Velocity(NCV) and Compound Muscle Action Potential(CMAP) and an ultrasonography to discover the presence of compression structures in the cubital tunnel and to measure the largest diameter of the ulnar nerve at the level of medial epicondyle. Surgical procedures to release and/or remove compressive structures associated with minimal medial epicondylectomy performed.

Results: Surgically compression sites were medial epicondyle in 2 cases(17%), bony spur in the cubital tunnel in 1 case(8%), anconeus epitrochlearis in 1 case (8%), ganglion in 2 cases(17%), cubital tunnel retinaculum in 3 cases(25%), Osborne's fascia in 3 cases(25%). Preoperative ulltrasonography was reliable modality to find out the presence of bony spur, ganglion and anomalous anconeus epitrochlearis in the cubital tunnel. Over an average follow-up period of 2.8 years, chopsticks function were improved in 12 cases(100%). The average value of nerve conduction study in the elbow segment increased from 19.5 m/s before surgery to 53.3 m/s after surgery and the amplitude of the compound muscle action potential recovered from 30.5% before surgery to 69.5% after surgery compared to the contralateral ulnar nerve of the patient.

Conclusions: A preoperative motor function study of the ulnar nerve in the cubital tunnel syndrome was must be to confirm functional impairment when using chopsticks. Preoperative ultrasonography was valuable tool to find

any compressive structures in the cubital tunnel. Release and/or removal of compressive structures with minimal medial epicondylectomy were the best procedures to fulfill the excellent results.

신경초종 수술 후 저린 증상 발생의 위험인자: MRI상 감각신경다발 침범의 역할

[1]Gohyeon Seoul Samsung Orthopaedic Clin., [2]Orthop Surg. Sungkyunkwan Univ.
Dong Suk Kim[1], Jae Woo Shim

Numbness can occur frequently after resection of a schwannoma. This study aimed to evaluate risk factors for numbness after schwannoma surgery and, in particular, to analyze the association between the intraneural location of the schwannoma observed on MRI and numbness.

Patients who underwent schwannoma resection at our hospital between 2020 and 2024 were included only if they had schwannomas in the upper extremity. Lesions too proximal or distal were excluded due to difficulties in accurately assessing the location of the schwannoma on MRI. Ultimately, the analysis focused solely on schwannomas from the proximal humerus to the wrist joint. Postoperative numbness was defined as numbness lasting more than one month during outpatient follow-up and the use of medications such as analgesics. Sensory nerve bundle involvement was assessed by tracing the relevant nerve on axial MRI sections and assessing the location of the schwannoma within the nerve. If the location of the schwannoma corresponded to a sensory nerve bundle on nerve topography, it was defined as sensory bundle involvement. Furthermore, if the lesion occurred distally in a region already branching into a sensory nerve branch, it was also considered sensory bundle involvement. Patient medical records and MRI images were reviewed to determine basic demographic information, the type of nerve involved, and whether the sensory bundle was involved. Risk factors for the development of numbness were assessed using multivariable logistic regression analysis.

A total of 33 patients were ultimately included: 20 men and 13 women, with a mean age of 33 years (range: 18–86). The affected nerves included the radial nerve in 14 cases, the ulnar nerve in 10 cases, and the median nerve in 9 cases. Fifteen patients (46%) received medication for postoperative numbness. Patient age, sex, symptom duration, involved nerve, presence of multiple lesions, and proximal involvement were not significantly associated with the development of numbness. Meanwhile, sensory fascicle involvement was observed in 16 patients (49%) on MRI. Sensory fascicle involvement was significantly associated with a higher incidence of numbness (80% vs. 22%, p=0.004), and multivariable logistic regression analysis confirmed sensory fascicle involvement as an independent risk factor.

In conclusion, MRI findings during schwannoma resection suggest that patients with sensory fascicle involvement are more likely to develop postoperative numbness. This finding can be used as a guideline for surgical planning.

Keywords: Schwannoma, MRI, Risk factors, Sensory nerve

Restricted thumb extension due to flexor pollicis longus tendon adhesion following volar plate fixation with bone substitute use for distal radius fracture: A case report and literature review

[1]H Plus Yangji Hosp., [2]Orthop Surg. The Catholic Univ. of Korea
Youn-Tae Roh, Il-Jung Park

Tendon adhesion after distal radius fracture surgery is relatively rare complication. A 51-year-old female patient underwent open reduction and volar plate fixation for a distal radius fracture at another hospital approximately 4 weeks ago. The chief complaint at the time of her visit to our hospital was limited extension of the thumb, which was diagnosed as adhesion of the flexor pollicis longus tendon. During the surgery, the flexor pollicis longus tendon was severely adhered, and the demineralized bone matrix (DBM) and hydroxyapatite complex used at another hospital remained around the volar plate, which was removed. Caution is required when using bone graft substitutes such as DBM or bone morphogenetic proteins (BMPs), as they can cause adhesion when exposed to soft tissue.

Forearm Pleomorphic Rhabdomyosarcoma in the Lateral Cubital Fossa: Surgical Management and Adjuvant Radiotherapy

Plast Reconstr Surg. The Catholic Univ. of Korea
Su Ram Kim, Gyeol Yoo, Jun Yong Lee, Sang Oon Baek, Rah Yoon Kim, Hye Ju Han

Purpose: Pleomorphic rhabdomyosarcoma of the forearm is extremely rare. We report a case in the lateral cubital fossa treated with surgical excision followed by adjuvant radiotherapy, emphasizing clinical, diagnostic, and surgical considerations.

Methods: A 67-year-old man presented with a 5×5 cm hard mass on the lateral right forearm, growing rapidly over 1 year, without neurological symptoms. CT and MRI revealed a hypervascular tumor within the brachioradialis muscle, suspicious for soft tissue sarcoma, with no distant metastasis on CT and PET-CT. Surgery was performed via an incision along the medial brachioradialis border. Cephalic vein, radial vessels, and radial nerve were preserved. The tumor and adjacent skin were excised with clear margins; lateral antebrachial cutaneous nerve was sacrificed. Frozen section confirmed negative skin margins.

Results: Histopathology confirmed pleomorphic rhabdomyosarcoma, grade 2/3 (FNCLCC), 4.3×4.2×4.0 cm, with negative resection margins. Adjuvant radiotherapy was administered. At 6-month follow-up, the patient had lateral forearm hypesthesia corresponding to the sacrificed nerve, but no other functional deficits or recurrence.

Conclusion: Forearm pleomorphic rhabdomyosarcoma is rare and may mimic benign lesions. Preoperative imaging is crucial to assess depth, vascularity, and invasion. Complete excision with adequate margins while preserving major neurovascular structures is essential. Minor sensory deficits may occur if small nerves are sacrificed. Adjuvant radiotherapy and multidisciplinary management are important for preventing recurrence and optimizing oncologic and functional outcomes. Early recognition and careful surgical planning are key to balancing tumor control with limb function.

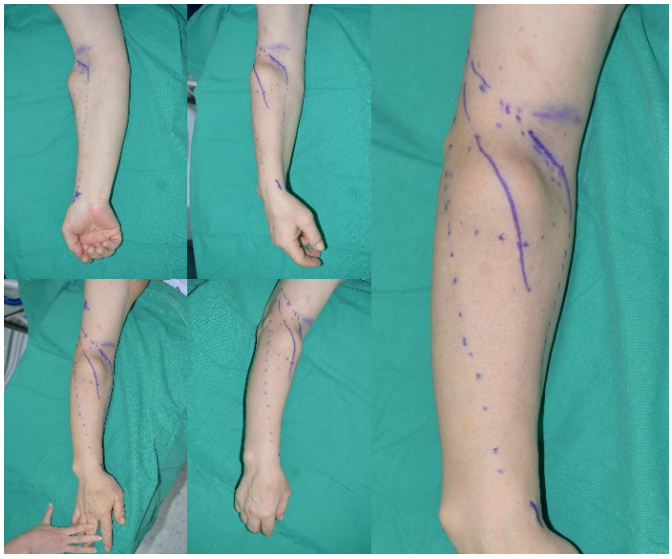

Fig. 1. Clinical findings of the mass

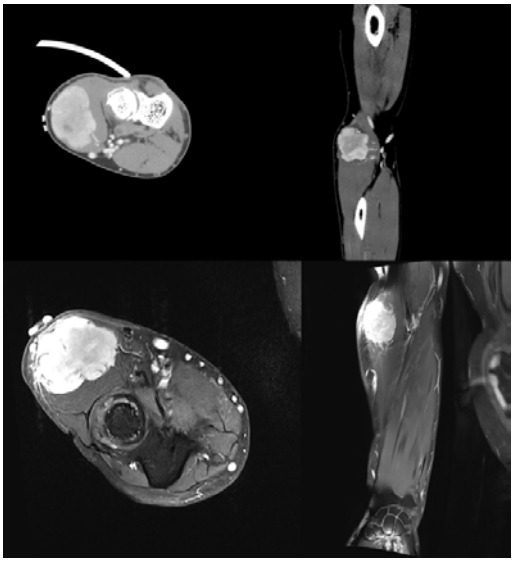

Fig. 2. Radiological findings of the mass

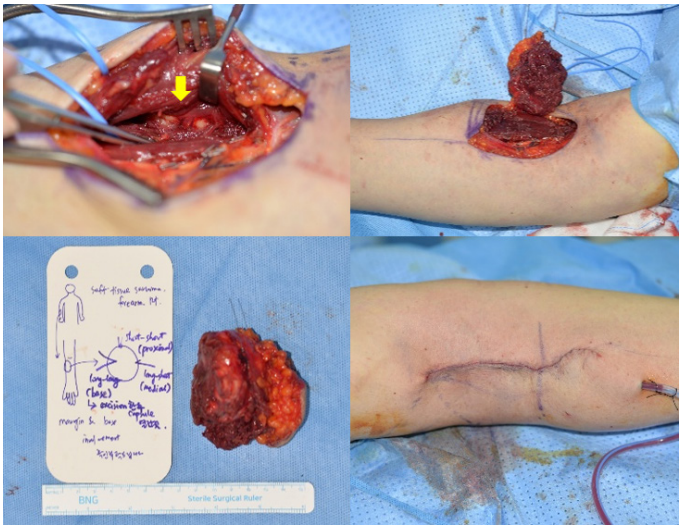

Fig. 3. Intraoperative findings following total excision of the mass

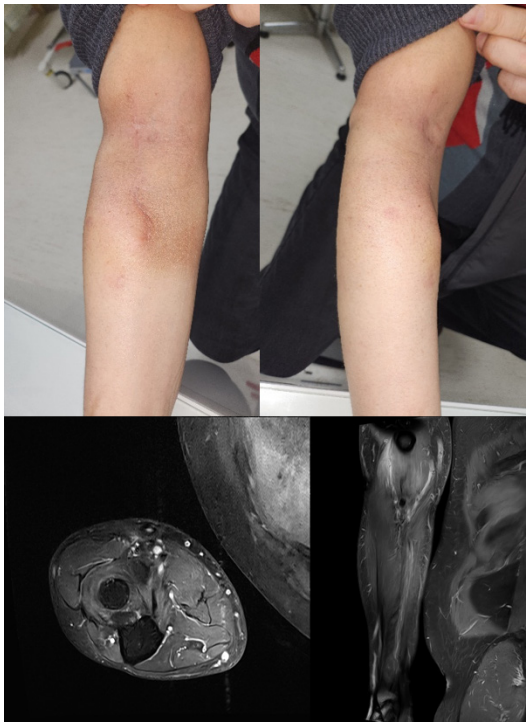

Fig. 4. 6-months postoperative clinical and radiological findings

Multiple Schwannomas on digital nerves : a case of segmental schwannomatosis

[1]Plast Reconstr Surg. Saeson Hosp., [2]Orthop Surg. Saeson Hosp.
Jaehoon Kang[1], Hyun Rok Lee[1], Jae In Chung[1], Yeong Sik Yoon[2]

Keywords: Schwannoma, Digital nerve, Schwannomatosis

Introduction: Schwannomas are the most common benign tumors affecting the peripheral nervous system. They represent a benign proliferation of Schwann cells. Schwannomas and other peripheral nerve sheath tumors are common in the head and neck, thorax, abdominal wall, and retroperitoneum.

These tumors are rarely found in the hands, particularly the fingers. It accounts for about 5% of benign soft tissue neoplasm, and among them incidence in the upper limb ranges from 3% to 19% of all neurilemmomas. Schwannomatosis is characterized by multiple schwannomas without diagnosis of neurofibromatosis type 2. There are two types of schwannomatosis, sporadic and familial type. Segmental Schwannomatosis is defined as multiple schwannomas limited to one limb or five or fewer contiguous segments of the spine.

In this case we present a 43-years-old male patient with sporadic segmental schwannomatosis of the digital nerves, and share our experience in diagnosis and clinical features, treatment options, which may be contributive.

Case report: The 43-year-old male patient visited our department in April 2025, complained of the growing multiple masses over both dorsal and volar side of right ring finger. There was no history of significant trauma or inflammation of the right hand.

The tumor has been present for several years and has begun to grow last year. The patient reported pain that increased when pressure was applied on the noduled and finger movements.

Physical examination revealed total 4 masses on radial side of right ring finger, volar PIP and DIP, dorsal 3rd web space and middle phalanx (Fig 1). The size varied, but dorsal masses were larger than volar masses, firm, mobile, painless, and percussion in the volar region gave a positive Tinel sign. In the masses on the dorsal side, Tinel sign was negative, and there was no paresthesia on both sides.

Based on the clinical picture and ultrasonography findings, masses arising from a nerve were suspected, the ultrasound findings showed that the masses were attached to the nerve but had a distinct border, so it seemed more likely to be a schwannoma (Fig 2).

The surgical procedure was performed under brachial plexus block and the total 4 masses of the dorsal and volar digital nerves in the right ring finger of the radial side were removed, using tourniquet and microscope (Fig 3).

Irregular in shape, pearly white in color in cross section with significant adhesions for the surrounding tissues, so external and internal neurolysis were performed and all shown fascicles were preserved. At the time of postoperative period, the patient was neurologically intact and discharged on second postoperative day.

On postoperative histopathological examination confirmed diagnosis of schwannomas, all tumors had the same histopathological pattern, nuclear palisading (verocay bodies) with Antoni A, which characterized as compact bundles of schwann cells (Fig 4). After 3 months, the patient is without symptoms, neurological deficit and with no signs of tumor recurrence.

Discussion: Schwannomas are typically benign slow growing nerve sheath tumors, which usually arise on the flexor aspect of the extremities. They present as solitary tumors, although there are reports of patients with multiple tumors in the literature.

In material presented by Rockwell et al. schwannomas located in the hand and wrist constituted 7.5% of all schwannomas. The most frequent site of origin in material presented by authors mentioned above were proper digital nerves (52%) and common digital nerves (19%). Cases of multiple schwannomas in this region are of great rarity.

Pain and swelling are the usual presentations in general clinical physical examinations. Sharing similar features with other soft tissue tumors causes difficulties in diagnosis and may be misdiagnosed as neurofibroma, lipoma and ganglion. Wide spectrum of clinical symptoms such as paresthesia, hypoesthesia, tingling, motor deficit, and positive Tinel's sign contribute to almost impossible clinical distinction between schwannomas and other peripheral nerve tumors or other soft-tissue tumors.

Additional diagnostic procedures are usually required. Ultrasonography (USG) and MRI are useful for the differential diagnosis of soft tissue mass. On ultrasonography, a schwannoma is a homogeneous, hypoechoic mass with enhanced transmission, target appearance, and pseudocystic appearance. In our case, USG shows well-defined schwannoma with peripheral hypoechogenicity and central hyperechogenicity, also direct contact with adjacent peripheral digital nerve. Considering the ultrasound findings and clinical features above, the possibility of schwannomas is higher than that of other cystic masses.

Although magnetic resonance imaging (MRI) has proven to be the most effective imaging modality, ultrasonog-

raphy has become more widely used due to its relatively lower cost. With the development of higher resolution techniques, the use of ultrasonography in diagnose of hand diseases has increased, and now it is the primary diagnostic tool for a mass lesion of the hand.

Treatment for schwannoma is determined by the location of the tumor, any symptoms such as pain or paresthesia, and how rapidly it grows. Sometimes observation is indicated, but surgical treatment is needed if symptoms occur. Main goal is enucleating the tumor while avoiding nerve damage with internal neurolysis, so usage of operative microscope is essential.

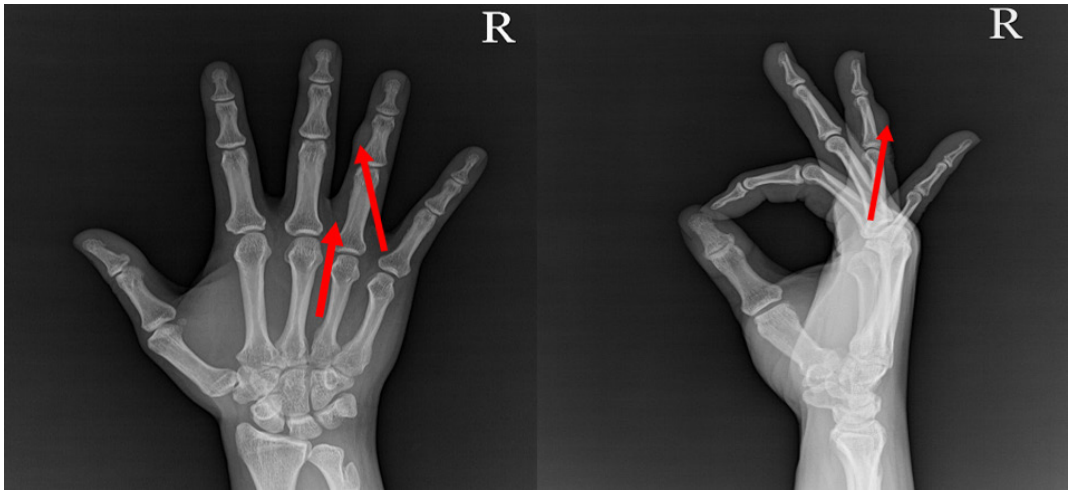

Fig 1. The anteroposterior and lateral radiograph of right hand. Shows noncalcified soft tissue nodular thickening with similar density on dorsal surface of right ring finger (Red arrows). The volar masses are too small and not appear to protrude on an x-ray.

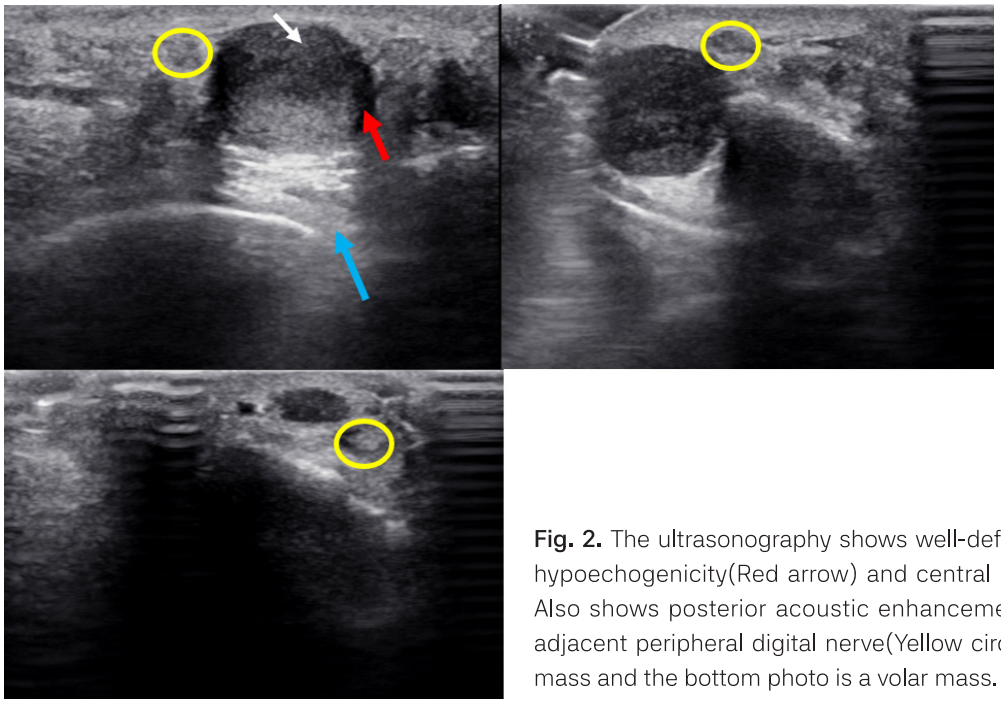

Fig. 2. The ultrasonography shows well-defined schwannoma with peripheral hypoechogenicity(Red arrow) and central hyperechogenicity (White arrow). Also shows posterior acoustic enhancement(Blue arrow) and contact with adjacent peripheral digital nerve(Yellow circle). Above two photos are dorsal mass and the bottom photo is a volar mass.

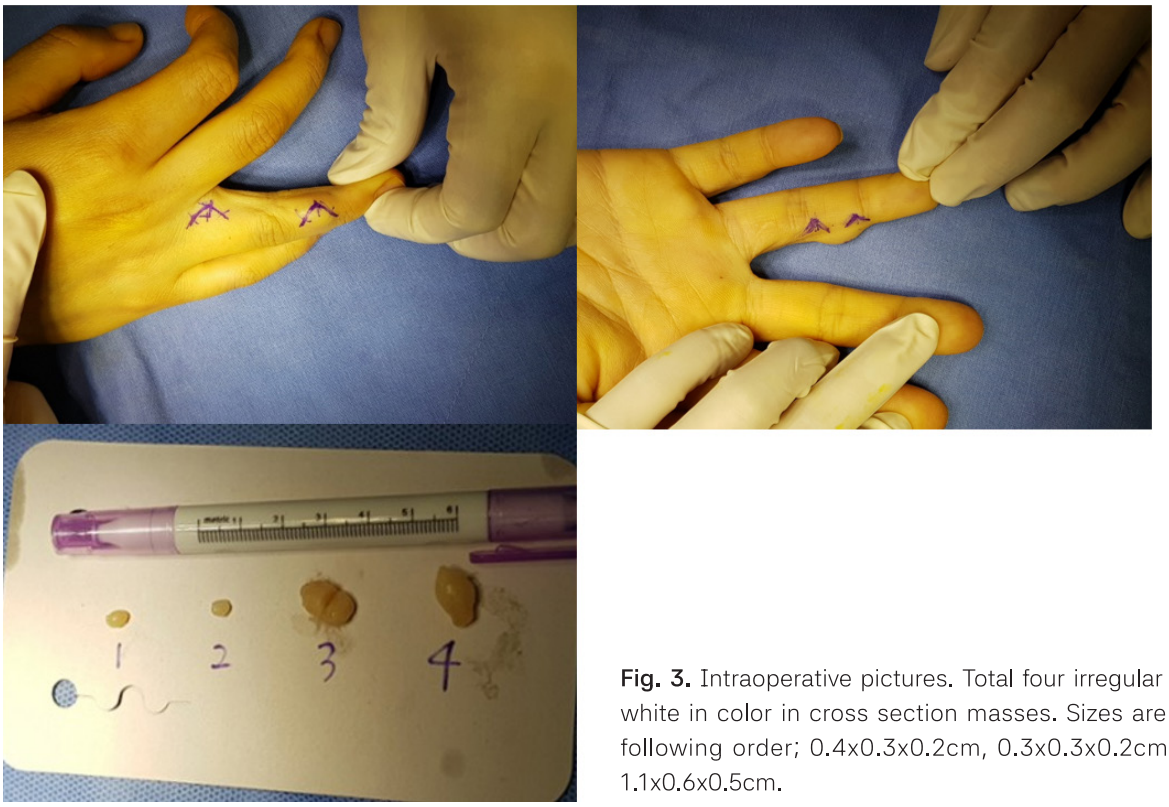

Fig. 3. Intraoperative pictures. Total four irregular in shapes, pearly white in color in cross section masses. Sizes are measured in the following order; 0.4x0.3x0.2cm, 0.3x0.3x0.2cm, 1.3x0.7x0.5cm, 1.1x0.6x0.5cm.

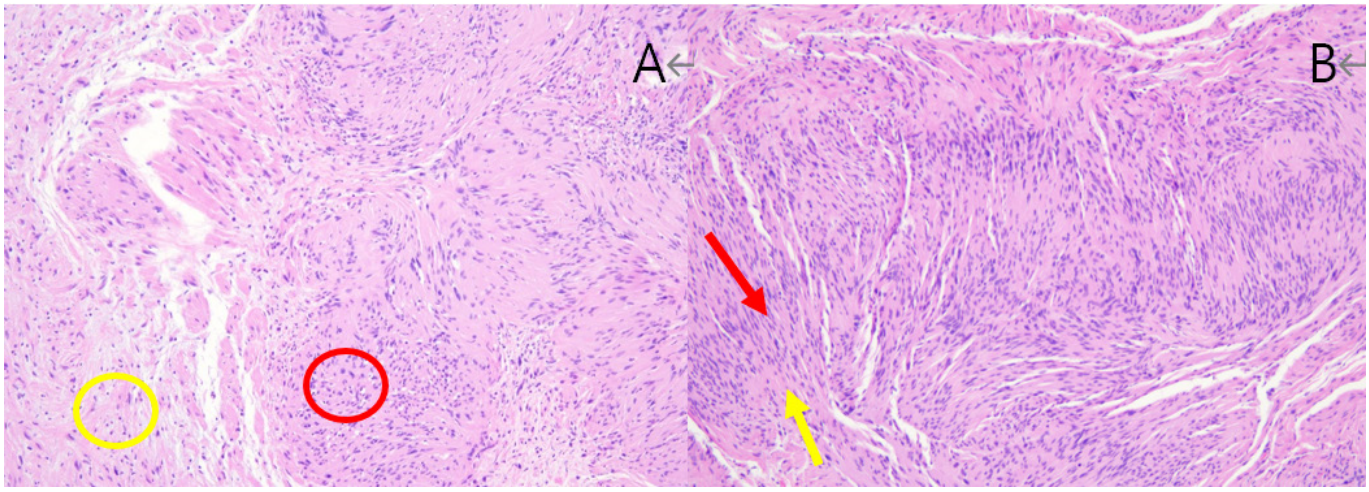

Fig. 4. Histopathological examination results show nuclear palisading (arrangement of elongated nuclei in parallel row) with verocay bodies (nuclear free zones), Antoni A&B(comprised spindle cells with wavy or buckled nuclei arranged in dense and loose areas): A) Atoni A(Red circle) and Atoni B(Yellow circle); B) nuclear palisading (Red arrow) and verocay body(Yellow arrow). H-E stain, x100 magnification.

Early diagnosis and multidisciplinary management of mycobacterial hand and wrist infections: case series

[1]Plast Reconstr Surg. Saeson Hosp., [2]Plast Reconstr Surg. The FRAU Hosp.
Jaehoon Kang[1], Sangho Oh[2]

Keywords: Tuberculous, Nontuberculous, Mycobacterial, Tenosinovitis

Introduction: Atypical hand infections differ from typical hand infections in that they often present with uncommon and non-specific clinical features, making diagnosis and treatment more challenging. Among these, mycobacterial infections are extremely rare compared to those caused by more common pathogens. Mycobacterial infections can be broadly classified into tuberculous mycobacterial infections (MTB) and nontuberculous mycobacterial infections (NTM).

Mycobacteria are difficult to identify in wound or tissue culture due to their unique growth characteristics, particularly in the case of atypical mycobacteria, which require special culture conditions. Furthermore, there are relatively few reported cases in the literature, and clinical information is limited. As a result, their atypical presentations often mimic other diseases, leading to delayed diagnosis, incorrect treatment, and prolonged therapeutic courses.

In this report, we present three cases of mycobacterial infection of hand that were successfully treated. Through these cases, we aim to provide a practical, step-by-step approach for the early diagnosis and appropriate management of mycobacterial infections in the hand, to improve clinical outcomes and reduce diagnostic delays.

Case report:

Case1

A 60-year-old female presented with persistent swelling and limited flexion of the third digit extending to the palm, which had not improved despite multiple prior interventions over a 2-year period. The patient had a 10-year history of trigger finger involving the third digit and had received repeated triamcinolone injections. She had undergone several tenosynovectomies at another institution within the past two years for similar symptoms, but

each resulted in recurrence.

On examination, the patient reported pain during flexion of the third digit. Swelling was noted from the PIP joint level to the A1 pulley region in the palm, accompanied by mild flexion limitation. Given the chronic course, history of repeated triamcinolone injections, and recurrent tenosynovitis, mycobacterial infection was suspected. Plain radiographs revealed no abnormalities, but ultrasonography and MRI demonstrated multiple rice bodies and severe flexor tenosynovitis extending from the distal flexor tendon region to the carpal tunnel(Fig. 1).

Surgical flexor tendon tenosynovectomy and en-bloc excision of inflamed tissue were performed under suspicion of MTB or NTM tenosynovitis. Intraoperatively, numerous rice bodies were observed around the A1 pulley(Fig. 2). Infection-related changes were also seen involving the A2 pulley and the flexor digitorum superficialis (FDS) tendon. Therefore, complete excision of all inflamed tissues was performed, including FDS tendon and A2 pulley resection. Tissue samples were sent for AFB stain, MTB/NTM PCR, and culture.

Although AFB stain and PCR were negative, the clinical and intraoperative findings were highly suggestive of mycobacterial infection. Given the recurrent nature and extent of disease, empirical antimycobacterial chemotherapy was initiated prior to culture confirmation, in consultation with the infectious disease department. The patient tolerated the regimen well without complications.

Case2

A 74-year-old female presented with progressive swelling of the left second digit, which had initially developed three years prior. Two years earlier, the patient had undergone surgery under the impression of an epidermal inclusion cyst, but recurrence was noted postoperatively, and the swelling gradually worsened over time.

The patient's past medical history was notable only for pulmonary tuberculosis diagnosed 20 years ago. At presentation, she exhibited painful swelling and instability of the PIP joint of the second digit. Preoperative imaging, including plain radiographs and MRI, revealed destructive pan-arthritis of the PIP joint without evidence of a discrete mass such as a giant cell tumor(Fig. 3).

Surgical intervention under brachial plexus block was planned as PIP joint ostectomy with possible insertion of an antibiotic-loaded cement spacer if intraoperative findings suggested infection. No rice bodies were identified intraoperatively(Fig. 4).

Tissue samples were submitted for AFB staining, MTB/NTM PCR, histopathology, and culture. AFB stain and PCR were negative. However, histopathology performed at 1 week postoperatively revealed chronic granulomatous inflammation with fibrinoid necrosis. Although the intraoperative findings were not specific to mycobacterial infection, and both first and second mycobacterial cultures were negative, the presence of granulomatous inflammation combined with the patient's history of previous pulmonary tuberculosis raised the clinical suspicion for latent or reactivated mycobacterial disease. Therefore, empirical antimycobacterial chemotherapy

was initiated on postoperative day 14.

The patient completed a 9-month course of chemotherapy without complications. No recurrence was observed during the first 6 months postoperatively.

CASE 3

An 80-year-old female presented with progressive swelling of the left thumb carpometacarpal (CMC) joint, which had developed one month prior(Fig 5). She had a history of multiple corticosteroid injections over the past year for CMC joint pain and arthritis. Her past medical history was notable only for hypertension; she had no history of tuberculosis or other relevant systemic illness.

Intraoperatively, the CMC joint cartilage was completely destroyed, and inflammatory spread was observed extending into the first and second extensor compartments. Notably, multiple rice bodies were found in the synovium surrounding the second extensor compartment tendons(Fig. 6). Following the principle of en-bloc excision, all affected tissues were excised, including resection of the involved abductor pollicis longus tendon. A CMC joint ostectomy and insertion of an antibiotic-loaded cement spacer were performed, along with extensive tenosynovectomy of the first and second extensor compartments, synovectomy around the CMC joint, and massive irrigation.

Tissue samples were sent for histopathological examination, MTB/NTM PCR, AFB stain, and culture. One week postoperatively, AFB staining was negative, but MTB PCR was positive. Histopathology revealed chronic granulomatous inflammation with necrosis, consistent with tuberculous infection. Consequently, antituberculous chemotherapy was initiated. At 4 weeks, M. tuberculosis was identified on culture.

Three weeks postoperatively, the patient experienced a localized recurrence of abscess, requiring an additional tenosynovectomy and cement spacer exchange. The patient completed a 9-month course of chemotherapy without complications. Follow-up over 2 years revealed no recurrence, and no other treatment-related adverse events were observed.

Discussion: Hand infections can result in severe disabilities, including stiffness, contracture, and functional disability. atypical infections such as Mycobacterium, viruses, and fungi may have a slow progressing, indolent course and may be delayed in diagnosis. Therefore, atypical hand infections are commonly misdiagnosed or diagnosed in a delayed fashion and may not respond to the standard antibiotic therapy. Surgical debridement is often required to eliminate the offending organism or lower the disease burden.

Mycobacterial hand infections usually have an indolent course, marked by variable and nonspecific presentations. Pain, presence of swelling mass or neurological signs like median nerve compression are most likely symptoms and signs to be encountered, and there are even asymptomatic.

Early diagnosis may be made based on a history of exposure, occupational risk, clinical examination, surgical findings (rice bodies), and histopathologic findings of granulomatous inflammation, this can help reduce recurrence and provide a good prognosis

Gold standard of diagnosis is a biopsy of suspected infection and the result from these tissue culture. Histopathology examination of the biopsy specimens revealed, fragments dense inflammatory infiltrate containing T-lymphocytes, plasma cells, macrophages, appearance of proliferative synovitis with synovial cell hyperplasia and hypertrophy, and lymphoplasmacytic infiltrate. In addition, blood vessel hyperplasia, epithelioid granulomas with multinucleated giant cells, some of them Langhans cell-like, fibrin organized in the form of rice bodies with amorphous acidophilic core surrounded by a thin fibrous layer.

If findings such as granulomatous inflammation (with/without caseating) and rice bodies are observed, mycobacterial infection should be considered primarily.

In conclusion, mycobacterial infection of the hand is very rare and difficult to diagnose, and it is a disease that requires a multidisciplinary approach with a team for hand surgeons to reduce recurrence and complications along with rapid diagnosis. Biopsy and culture are very important as confirmatory tests, and if bone or tissue reconstruction is necessary after surgery due to extensive infection, a delayed procedure should be performed after drug treatment.

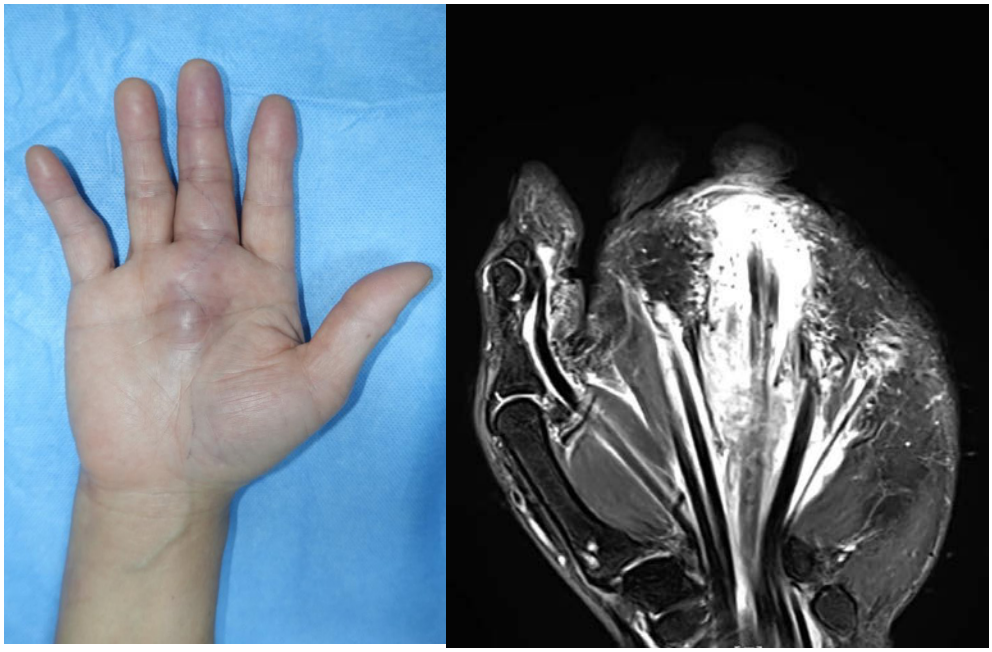

Fig 1. Swelling over midpalmar are of Rt long finger and previous operation scars. Pre-operative magnetic resonance imaging shows prominent tenosynovial thichkening and fluid collections(Red arrow).

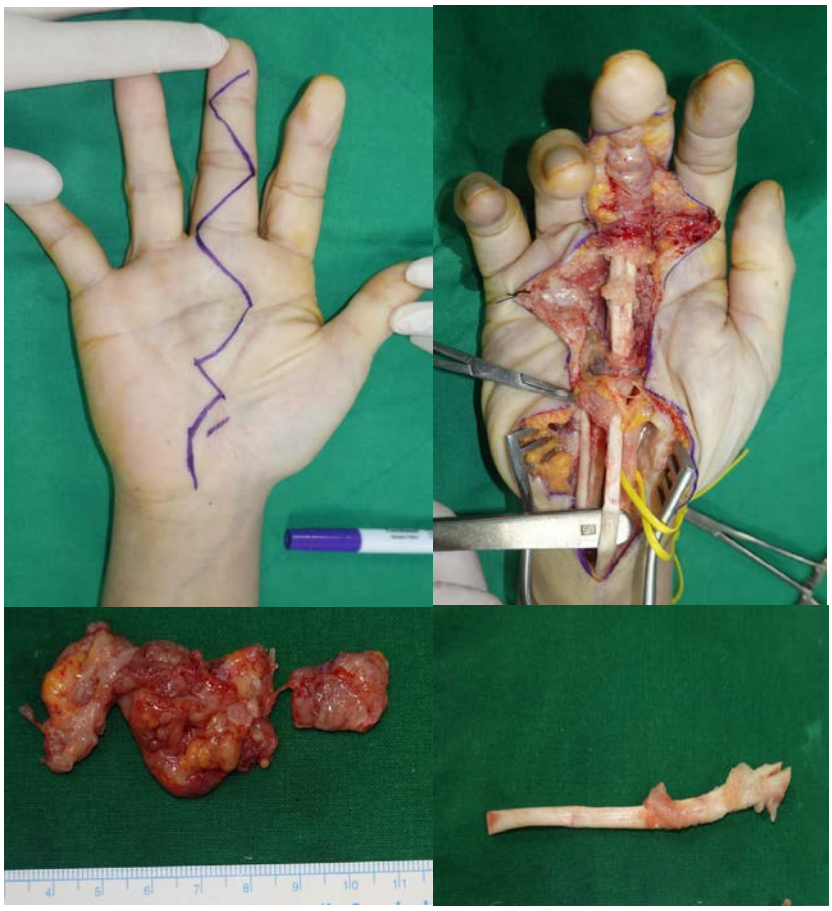

Fig 2. Intraoperative pictures. Extensive tenosynovectomy was performed with biopsy. Affected FDS was removed to reduce recurrence

Fig 3. A 74-year-old female patient. showing prominent bone destruction around Lt index proximal interphalangeal joint. Pre-operative magnetic resonance imaging hows Osteomyelitis and increased joint effusion and synovitis with hyperplasia.

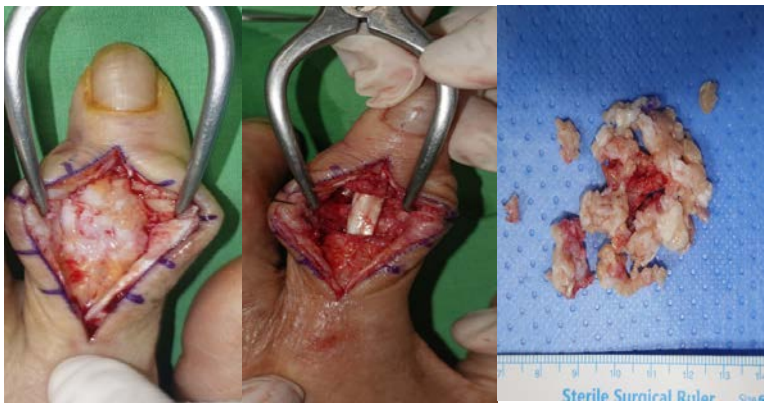

Fig 4. Intraoperative pictures. Tenosynovectomy was performed with biopsy.

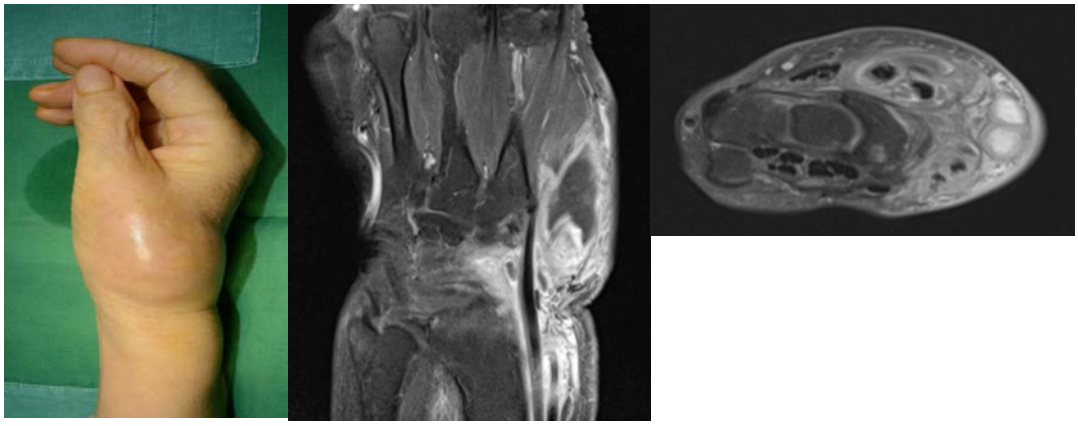

Fig 5. 80-year-old female patient. 1st carpometacarpal joint (CMC) swelling and redness were observed. Pre-operative magnetic resonance imaging shows large cavitary lesion with thin peripheral rim enhancement along EPL & EPB tendons and marked enlargement of ECRL, ECRB and APL, suggest infectious tenosynovitis. Bone marrow edema and osteomyelitis with joint involvement.

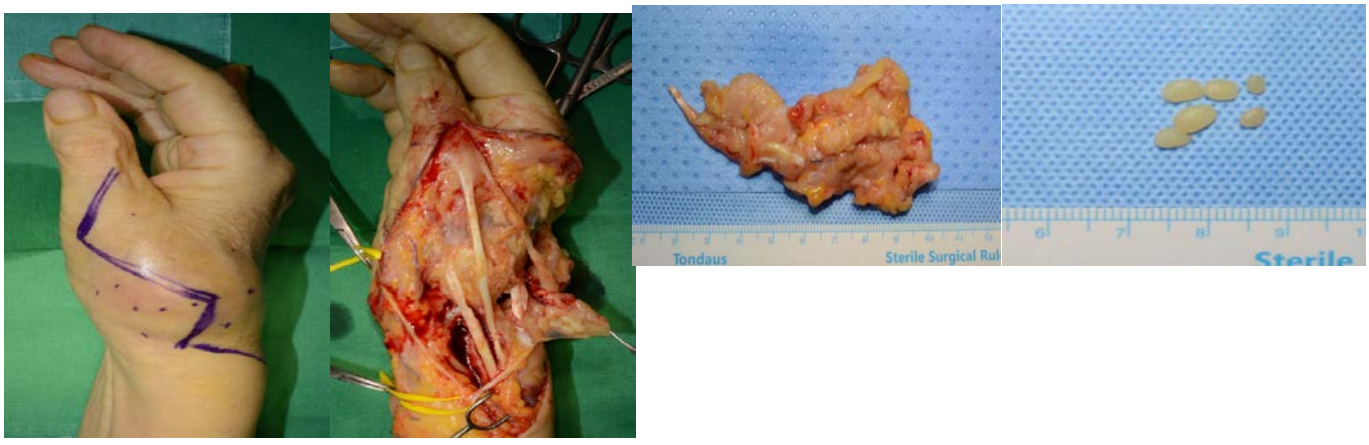

Fig 6. Intraoperative pictures. Radical Tenosynovectomy was performed with biopsy. Affected trapezium bone were removed. Rice bodies were observed within mass.

Delayed Digital Flexor Tendon Rupture Outcomes of Direct Repair: A Clinical Review

Plast Reconstr Surg. Gwang Myeong Sung Ae General Hosp.
Ji Song Yoon, Dong Chul Lee, Sung Hoon Koh, Jin Soo Kim, Si Young Roh, Kyung Jin Lee

Purpose: Conventional recommendations advise repairing flexor tendon injuries within four weeks to prevent myostatic muscle shortening. This study examines the clinical outcomes of direct flexor tendon repair in a series of patients who presented more than four weeks after injury.

Patients and methods: We retrospectively reviewed the medical records of 142 patients with flexor tendon injuries treated at our institution between January 2017 and May 2020. Patients who underwent primary repair within four weeks of injury were excluded. Four patients who underwent direct repair despite a delayed presentation met the inclusion criteria. We analyzed their complications and final range of motion outcomes.

Results: Of the 142 patients, four were included in this review. Three were male, and the mean age was 36.2 years. The time from injury to surgery was 6.1, 10.6, 11.9, and 70.6 weeks. The mean follow-up was 76.9 weeks. Postoperatively, the average range of motion improved by 6.25° at the MP joint, 5.0° at the PIP joint, and 20.0° at the DIP joint. No re-ruptures were reported. The heterogeneity of cases, including one patient with a complex wrist injury, was a notable finding.

Conclusion: Our findings suggest that direct repair can provide meaningful functional recovery even in delayed flexor tendon injuries. Despite myostatic muscle shortening, which can make direct repair challenging, the functional gains were most significant at the DIP joint. With an appropriate surgical technique and dedicated rehabilitation, this approach may be a viable option for some patients, although the small, heterogeneous sample size limits the generalizability of these findings. Further research is warranted to validate these results.

Patient no.	Sex/Age	Interval (weeks)	Mode of injury	Tendon	Level	OPD FU (weeks)	Pre-op ROM	Post-op ROM	ROM improvement	Re-rupture
1	M/54	11.9	Twisting	FDP, FDS	Lt. 4F / Wrist	0	45,60,20	60,80,45	15,20,25	X
2	M/31	6.1	Glass	FDP	Rt. 5F / DIPJ	44.9	75,35,10	75,35,20	0,0,10	X
3	F/41	70.6	Knife	FDP	Lt. 3F / Wrist	31.1	70,70,0	80,75,0	10,5,0	X
4	M/19	10.6	Knife	FDP	Lt. 5F / DIPJ	0.9	80,90,0	80,90,45	0,0,45	X

Figure 1: Patients demographics (n=4) (ROM is stated in order of MPJ, PIPJ and DIPJ)

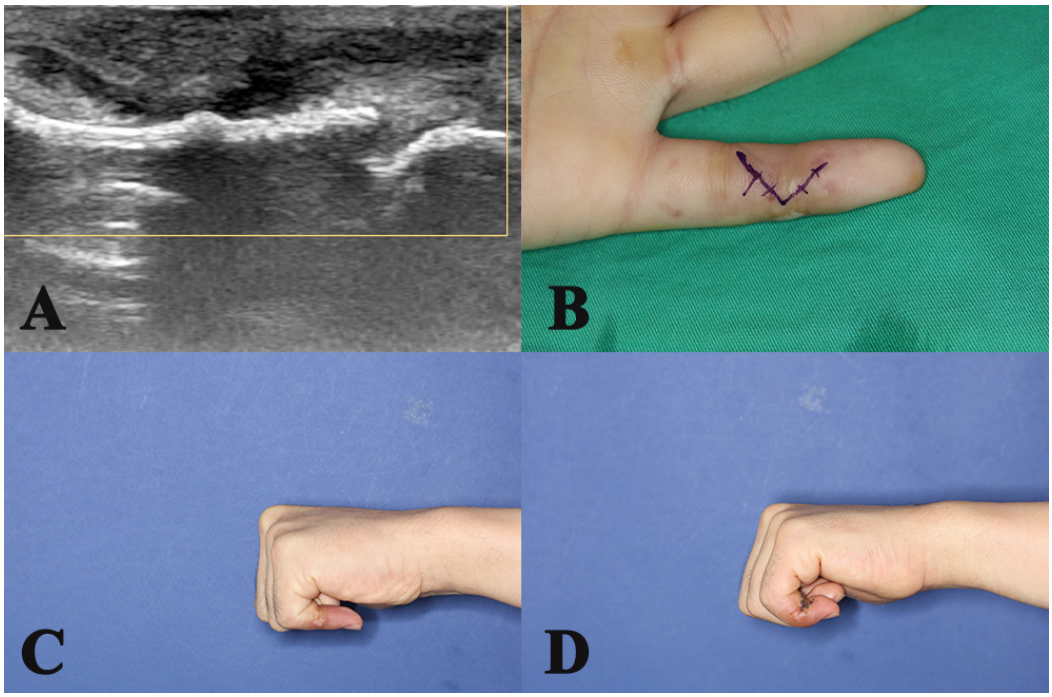

Figure 2: A) Pre-operative ultrasonography (chronic rupture of FDP at middle phalangeal shaft with soft tissue mass-like lesion in gap of the ruptured and retracted tendon is noted), B) Pre-operative view of the completely healed little finger, C) Pre-operative range of motion, D) Post-operative range of motion (Patient no.4, Little finger)

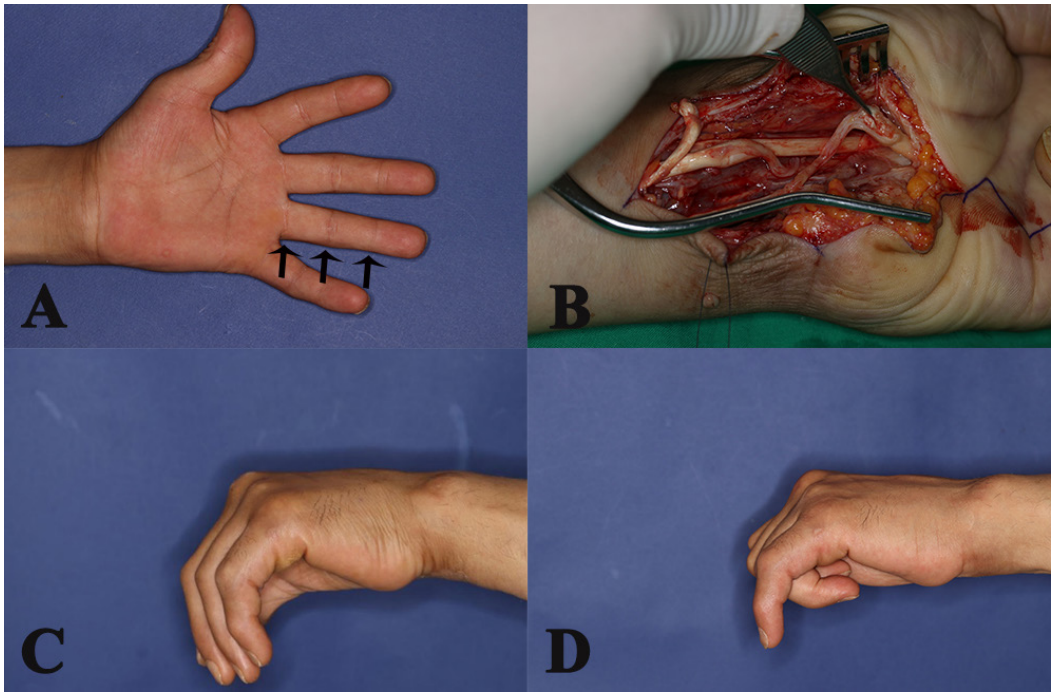

Figure 3: A) Pre-operative photography (Note that interphalangeal creases were disappearing due to flexion failure), B) Intra-operative view of completely ruptured FDP and FDS C) Pre-operative range of motion, D) Post-operative range of motion (Patient no.1, Ring finger)

Skin Necrosis over the Iliac Crest: A Case Report

Plast Reconstr Surg. Gwang Myeong Sung Ae General Hosp.
Tae Hee Kim, Si Young Roh, Sung Hoon Koh

Background: Local anesthetics with epinephrine, such as lidocaine–epinephrine or articaine–epinephrine, are widely used to reduce pain and bleeding during surgery. Their safety has been confirmed in the face and extremities, but ischemic complications like dermal necrosis in the trunk are extremely rare. This report describes a unique case of iliac crest skin necrosis after articaine–epinephrine infiltration for bone graft harvesting.

Case Presentation: A 32-year-old healthy woman underwent iliac bone grafting to treat nonunion of the left index finger. At the donor site, 8.5 mL of articaine with epinephrine was injected subcutaneously for hemostasis. Although the intraoperative course was uneventful, epidermal demarcation and pain developed on postoperative day 1, followed by bullae and localized necrosis on day 2. The lesion remained stable under conservative management with antibiotics and dressings. At two months, debridement and secondary closure were performed, and complete wound healing without sequelae was achieved at six months.

Fig.1 Postoperative findings in the iliac crest resgion. (A) No significant inflammatory signs on day 1. (B) Bulla formation on day 2 (C) Week 2 findings

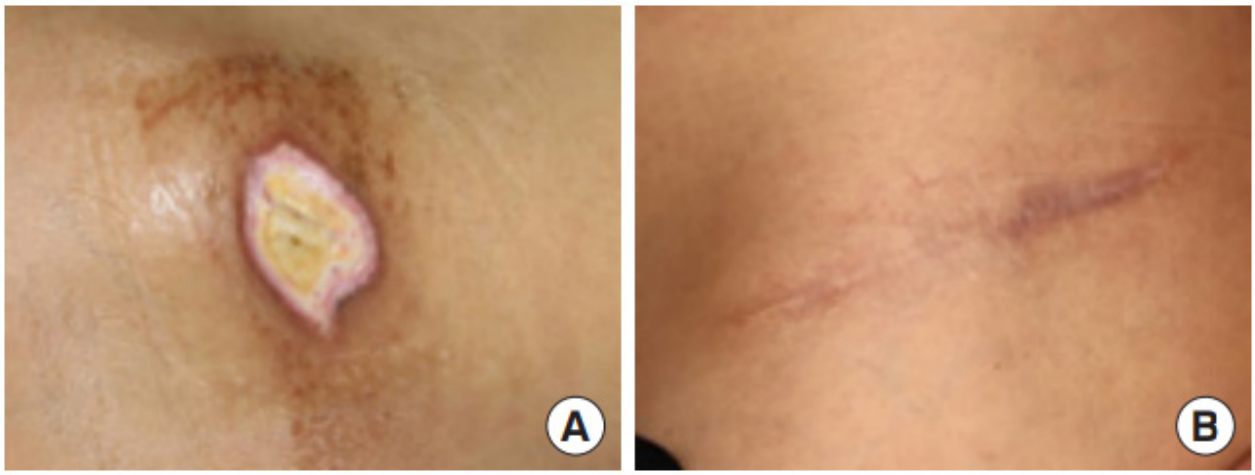

Fig.2 Follow- up monitoring at 2 and 6 months. (A) Wound dehiscence on follow-up monitoring at 2 months. (B) Healed state on 6-month follow-up.

Discussion: Despite the rich vascularity of the iliac crest, dermal necrosis occurred. Likely mechanisms include vasospasm, vascular irritation, or sympathetic-mediated constriction. Excessive infiltration, traction injury, and infection were considered unlikely. The absence of immediate circulation monitoring delayed early recognition, and reversal therapy such as phentolamine was not administered.

Conclusion: Although rare, dermal necrosis after articaine–epinephrine injection in the trunk is clinically important. Surgeons should closely monitor skin circulation following iliac crest anesthesia and consider timely interventions to improve patient safety.

Central Nail Bed Defect Repair Using a Subcutaneous Flap and Nail Bed Graft

Plast Reconstr Surg. Gwang Myeong Sung Ae General Hosp.
서현지

Purpose: Full-thickness nail bed defects with distal phalanx exposure pose reconstructive challenges due to limited vascularized tissue for graft uptake. This study presents a case of successful central-type nail bed reconstruction using a subcutaneous flap combined with subsequent split-thickness nail bed grafting.

Methods: A 59-year-old woman sustained a 1.2×0.6 cm central nail bed defect of the right middle finger after a blender injury, with associated bone exposure. Both lateral and proximal nail folds were intact. A subcutaneous flap involving the digital artery was elevated from the volar pulp, transposed dorsally through a tunnel beneath the intact nail bed and lateral fold to cover the defect. After confirming flap survival at 3 weeks, a split-thickness nail bed graft harvested from the great toe was applied.

Results: The flap survived without complications, and the nail bed graft successfully took. At 12 months postoperatively, the nail demonstrated good regrowth with preserved eponychial folds and minimal deformity. According to Zook's criteria, the outcome was graded as "very good." No donor site morbidity was noted, and the patient reported satisfaction with both functional and aesthetic results.

Conclusions: A subcutaneous flap provides a reliable vascularized bed for subsequent nail bed grafting in central-type nail bed defects with bone exposure. This technique preserves intact nail fold structures, facilitates favorable nail regrowth, and offers a straightforward alternative to complex microsurgical options.

Fig1. Case presentation : Full thickness nail bed defect with intact lateral and proximal nail fold

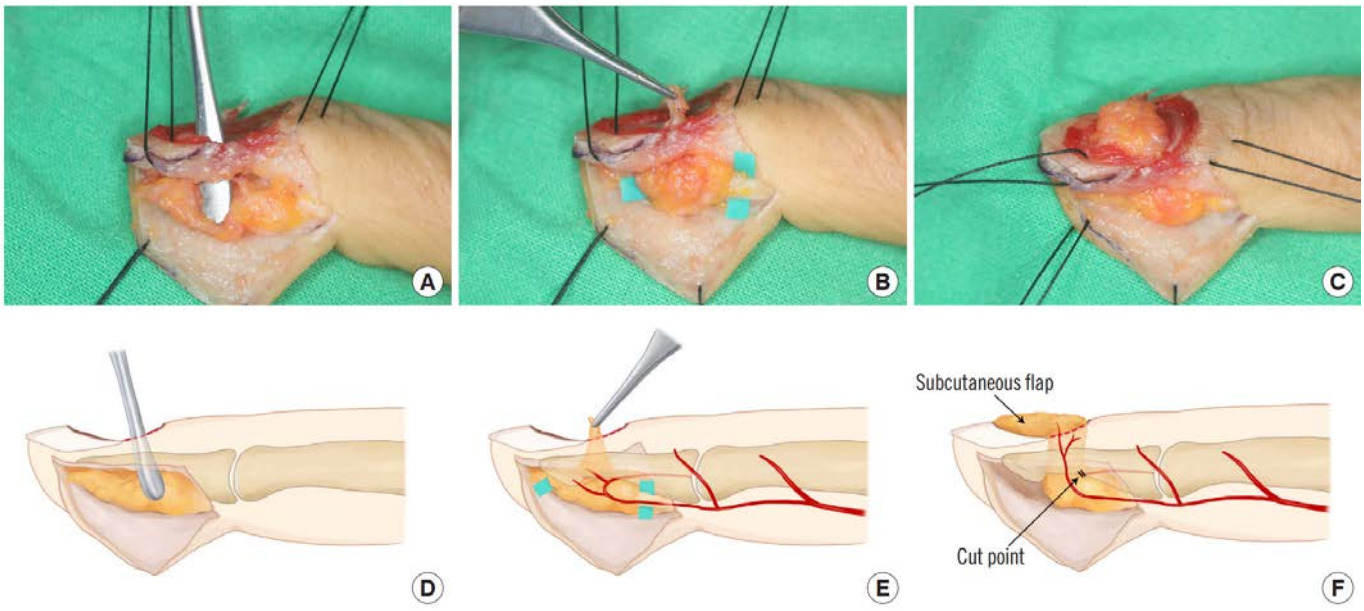

Fig 2. Schematic image of subcutaneous flap elevation and transposition

Fig 3. Split thickness nailbed graft performed after 3weeks

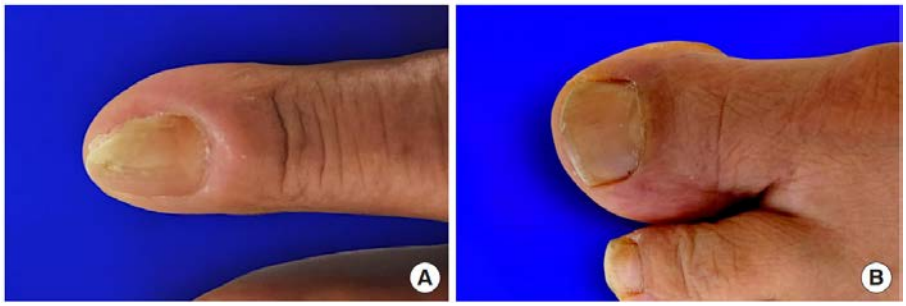

Fig 4. Postoperative result of 12months follow up

Thumb Tip Reconstruction by Modified Moberg flap

Plast Reconstr Surg. Gwang Myeong Sung Ae General Hosp.
Joowan Son, Sung Hoon Koh, Jin Soo Kim, Dong Chul Lee, Si Young Roh, Kyung Jin Lee

Purpose : The Moberg flap is a common solution for thumb pulp defects up to 1.5 cm, maintaining both length and sensation. Larger or oblique wounds, however, may leave distal areas exposed, raising the need for grafting or risking scar contracture. This report introduces a "flap-in-flap" technique, where excess tissue of the Moberg flap is converted into a small propeller flap to enhance distal coverage and reduce complications.

Methods : A 50-year-old man sustained a 2 × 1.5 cm volar pulp loss of the thumb after a chainsaw accident. Conventional Moberg advancement left a 0.5 × 0.5 cm raw area uncovered. Instead of grafting or proximal extension, redundant flap tissue was divided, raised as a neurovascular island, and rotated 180° to cover the defect. The donor site was closed primarily.

Results: Healing was uneventful with no wound problems. At three-year follow-up, the thumb showed durable coverage, preserved contour, and excellent sensory recovery. The modification eliminated the need for grafts, limited scarring to the thumb, and lowered the risk of interphalangeal contracture.

Conclusions: This "flap-in-flap" variation broadens the usefulness of the Moberg flap by repurposing redundant tissue for distal coverage. It is simple, reliable, and preserves the sensory and functional benefits of the original method while minimizing morbidity. The technique offers a valuable alternative when standard Moberg advancement is insufficient.

Nail reconstruction using composite graft

Plast Reconstr Surg. Gwang Myeong Sung Ae General Hosp.
Je Hyun Lee, Kyung Jin Lee, Jin Soo Kim, Sung Hoon Goh, Dong Chul Lee, Si Young Roh

Background: Conventional techniques for nailbed graft often neglect the damage to surrounding structures, leading to potential deformities. We describe a novel method of nail bed defect reconstruction using "Matched Composite Graft for Fingernail", aimed at preventing such outcomes by grafting not only the nailbed but also the adjacent skin structures.

Methods: We retrospectively reviewed 98 patients who underwent nailbed grafts using the big toe as the donor site between August 2011 and October 2023. Among these, 63 patients had concurrent defects in other nail apparatus structures and were treated using the matched composite graft technique. 22 patients were followed until the new nail plate fully grew. Outcomes were evaluated using Zook's criteria and patient questionnaires.

Results: All grafts successfully integrated without adverse events. New nail plate growth was completed between 6 to 12 months post-surgery. No significant deformities, such as changes in nail shape, variations in the eponychium, or split nails, were observed. Adherence was well maintained in all cases. The 18 patients (82%) achieved an 'Excellent' grade, three were 'Very Good' (14%), and one 'Fair' (4%). Their subjective evaluations indicated high satisfaction levels with an average score of 4.95. The donor sites exhibited minimal deformities without significant complications.

Conclusions: The matched composite graft for the fingernail allows for nearly complete restoration of the nail apparatus without increasing donor site morbidity, achieving outstanding functional and aesthetic results.

Figure 1. Procedures of Matched Composite Graft for the Finger Nail

Single-Stage Reconstruction of a Devastating Osteochondral and Ligamentous Elbow Injury Using a Costal Autograft and Tendon Graft: A Case Report

Orthop Surg. Kyungpook National Univ.
Won-Seok Chae, Hyun-Joo Lee

Purpose: Massive osteochondral and ligamentous elbow injuries present a significant reconstructive challenge. We report a case involving loss of the capitellum and lateral collateral ligament complex, which was successfully managed with a single-stage autologous graft reconstruction.

Materials and Methods: A 59-year-old male presented with a severe open left elbow injury from a traffic accident. The injury included posterior capitellum loss, lateral ligamentous complex rupture, and a brachial artery tear. Following emergency vascular repair and negative pressure wound therapy, a single-stage reconstruction was performed two weeks later. The capitellum was reconstructed using an ipsilateral costal osteochondral autograft, and the lateral ulnar collateral ligament (LUCL) was reconstructed with a contralateral palmaris longus tendon graft.

Results: The single-stage reconstruction successfully restored the articular surface and stabilized the elbow joint. The costal graft provided excellent anatomical restoration, and the tendon graft ensured joint stability. Postoperatively, the patient's elbow was stable, and he began a structured rehabilitation program.

Conclusion: A single-stage reconstruction using a costal osteochondral autograft and a palmaris longus tendon graft is an effective solution for severe, complex elbow trauma. This approach is a viable option for salvaging a severely damaged elbow by restoring both stability and anatomical integrity.

2025년
대한수부외과학회 추계학술대회

발행일 2024년 11월 1일

발행처 대한수부외과학회

제작처 (주)우리의학사
Tel: 02) 2266–2752
E–mail: uri@urimed.co.kr